

THE α -HYDROXYALKYL DIAZENES AND THE α -HYDROPEROXYALKYL
DIAZENES AS SOURCES OF RADICALS FOR THE KINETIC STUDIES OF SOME
RADICAL-MOLECULE REACTIONS IN SOLUTION

BY

Lukose K. Mathew, M.Sc.

A Thesis

Submitted to the School of Graduate Studies
in Partial Fulfilment of the Requirement for the
Degree

Doctor of Philosophy

McMaster University

**KINETIC STUDIES OF SOME
RADICAL-MOLECULE REACTIONS IN SOLUTION**

TO
MY WIFE, SUJA
AND
TO
OUR CHILDREN
ANDREW, JOSEPH, AND BENJAMIN

DOCTOR OF PHILOSOPHY (1990)

McMASTER UNIVERSITY

HAMILTON, ONTARIO

TITLE: THE α -HYDROXYALKYL DIAZENES AND THE
 α -HYDROPEROXYALKYL DIAZENES AS SOURCES OF
RADICALS FOR THE KINETIC STUDIES OF SOME
RADICAL-MOLECULE REACTIONS IN SOLUTION

AUTHOR: LUKOSE K. MATHEW, B.Sc. (KERALA UNIVERSITY, INDIA),
M.Sc. (CALICUT UNIVERSITY, INDIA), M.Sc. (McMASTER
UNIVERSITY, CANADA)

SUPERVISOR: PROFESSOR JOHN WARKENTIN

Number of Pages: xiv, 218

ABSTRACT

α -Hydroxyalkyl diazenes and α -hydroperoxyalkyl diazenes are known for a long time as initiators for free radical polymerization. Their application as suitable radical precursors for kinetic studies such as the radical-molecule and radical-radical reactions are not well-exploited. This thesis deals mainly with the rate constants for a number of radical-molecule reactions studied by generating radicals in solution from suitable radical precursors mentioned above. The initiation mechanism for the decomposition of α -hydroxyalkyl diazenes was also investigated.

Alkyl(1-hydroperoxy-1-methylethyl)diazenes (154) $[(CH_3)_2C(OOH)N=NR]$: a, R = n -C₃H₇-CH₂; b, R = n -C₃H₇-CD₂; c, R = CH₂=CH-(CH₂)₃-CH₂; d, R = CH₃(CH₂)₂-CH₂ and phenyl(1-hydroperoxy-1-methylethyl)diazene (154e) were prepared in solution by autoxidation of the corresponding hydrazones of acetone. They (154a-e) were converted to the corresponding alkyl(1-hydroxy-1-methylethyl)diazene (155a-d) and phenyl(1-hydroxy-1-methylethyl)diazene (155e) by reduction with triphenyl phosphine.

The radical chain decomposition of 5-hexenyl(1-hydroxy-1-methylethyl)diazene (155c) in carbon tetrachloride and product analysis gave the rate constant (k_{Cl}) for chlorine abstraction by the 5-hexenyl radical. The rate constant was calculated from the product composition and the known rate constant for the cyclization of the 5-hexenyl radical. For the temperature range 274-353 K, the rate constant is given by $\log(k_{Cl}/M^{-1} s^{-1}) = (8.4 \pm 0.3) - (6.2 \pm 0.4)/\theta$, where $\theta = 2.3$ kcal/mol, which leads to $k_{Cl}(25^\circ C) = 7.2 \times 10^3 M^{-1} s^{-1}$.

Rearrangement of cyclopropylmethyl radical to the but-3-enyl radical was used to clock bromine and iodine abstraction reactions from a number of substrates. Cyclopropylmethyl(1-hydroxy-1-methylethyl)diazene (155a) was used as the source for cyclopropylmethyl radical.

Decomposition of 155a in hexafluorobenzene or in dichloromethane containing bromotrichloromethane, and product analysis enabled the calculation of the rate constant (k_{Br}) for bromine abstraction by cyclopropylmethyl radicals from bromotrichloromethane.

The rate constant was calculated from the product composition and from the known rate constant for the isomerization of the cyclopropylmethyl radical. For the temperature range 253-341 K, the rate constant is given by $\log(k_{Br}/M^{-1} s^{-1}) = 9.75 - 2.11/\theta$, where $\theta = 2.3 RT$ kcal/mol, which gives $k_{Br} = 2 \times 10^8 M^{-1} s^{-1}$ at 25°C.

Rate constants (k_{Br}) for bromine abstractions and the rate constants (k_I) for iodine abstractions from various substrates were also determined by the use of the cyclopropylmethyl clock. The rate constants (in $M^{-1} s^{-1}$ units) at 80°C are: $k_{Br}(CHBr_3) = 2.86 \times 10^7$; $k_{Br}(CHCl_2Br) = 1.07 \times 10^7$; $k_I(CH_2I_2) = 2.63 \times 10^7$; $k_I(CH_3I) = 3.9 \times 10^6$; $k_I(C_6H_5CH_2I) = 1.2 \times 10^8$; $k_I((CH_3)_2CHI) = 1.4 \times 10^7$; $k_I(CF_3CH_2I) = 6.6 \times 10^6$; $k_I((CH_3)_3CI) = 6.5 \times 10^7$.

Non-chain decomposition of 155d and 155e in solutions containing bromotrichloromethane and 1,1,3,3-tetramethylisindolin-2-yloxyl (86) afforded butyl bromide and bromobenzene, in yields determined by the concentrations of 86 and $BrCCl_3$. From product yields and from the known rate constants for coupling of radicals with 86, the rate constants for the attack (at 80°C) of butyl ($k_{Br(Bu)} = 0.26 \times 10^9 M^{-1} s^{-1}$) and phenyl ($k_{Br(Ph)} = 1.55 \times 10^9 M^{-1} s^{-1}$) radicals were determined.

Generation of the deuterium-labelled cyclopropylmethyl radical ($c\text{-}C_3H_5\text{-}CD_2$) from 155b in a solution containing the spin trap, 1-methyl-4-nitroso-3,5-diphenylpyrazole (123), resulted in the formation of the spin adducts, [1-methyl-3,5-diphenyl]-4-pyrazolyl-[1'-cyclopropyl-1',1'-dideuterio]methyl nitroxyl (190) and [1-methyl-3,5-diphenyl]-4-pyrazolyl-[4',4'-dideuterio-but-3-enyl] nitroxyl (191) radicals. From the relative concentrations of the two spin adducts determined from esr spectral measurements, the rate constant (k_T) for spin trapping was determined. For the temperature range 283-333 K, the rate constant was calculated as $\log(k_T) = (10.4 \pm 0.4) - (3.6 \pm 0.5)/\theta$, where $\theta = 2.3 RT$ kcal/mol, which gives $k_T = 7.7 \times 10^7 M^{-1} s^{-1}$ at 40°C.

The initiation mechanism for the decomposition of α -hydroxyalkyl diazene was investigated using phenyl(1-hydroxy-1-methylethyl)diazene (155e). The results of various kinetic studies strongly suggested that azocarinols decompose by the reversible formation of acetone and the 1-substituted-1-H diazene (197).

ACKNOWLEDGEMENT

First of all, I would like to thank my supervisor, Professor John Warkentin for his continued assistance, encouragement, and eternal optimism throughout the entire course of this work. He was the man who placed a lot of confidence in me, and I am very grateful to him for his extreme patience, kindness, and understanding. I thank him from the bottom of my heart.

I would like to acknowledge McMaster University for the much needed financial support in the form of research scholarships and teaching assistantship.

I am deeply indebted to my wife, Suja, for her never-ending love, patience, and understanding that helped me to work long hours, even at night, for the success and completion of this research. She also helped me by typing part of this thesis, and by patiently listening to my successes as well as my failures in the research.

My sincere thanks goes to Mr. Brian Sayer, and Ian Thompson, and Dr. Don Hughes for obtaining several NMR spectra and also for helping me to learn and master the use of several instruments such as NMR, UV, IR, and ESR spectrometers. Thanks are also due to Mr. Fadjar Ramelan, and Mr. Jim Kapron for obtaining most of the mass spectra.

I would like to thank Dr. Emmanuel Osei-Twum, and Dr. Prabhakar Risbood for helping me to get started in the lab. I am indebted to Dr. Osei-Twum for the time that he spent with me in fruitful discussions and for teaching me how to use the GC and HPLC instruments.

Thanks are also due to all my co-workers who shared Room 358 with me for their co-operation and help in several ways. Special thanks goes to Debbie Jewell who allowed me to use some of the compound 153c, which she had synthesized. I would also like to thank Adrian Schwan, with whom I enjoyed working together and sharing ideas for over four years. Special thanks also go to Michel Zoghbi and Elizabeth Jefferson who helped me in several ways, including proof reading part of the thesis.

TABLE OF CONTENTS

ABSTRACT	iii
ACKNOWLEDGEMENTS	v
TABLE OF CONTENTS	vii
LIST OF TABLES	xi
LIST OF FIGURES	xiv
Chapter 1. INTRODUCTION	1
1.0.0. FREE RADICALS: A BRIEF HISTORY	1
1.1.0. DETECTION OF FREE RADICALS BY ESR SPECTROSCOPY	4
Basic Principles	4
The g-Factor	6
Hyperfine Splitting Constants	6
Spin Trapping	7
1.2.0. INTRAMOLECULAR RADICAL REACTIONS - RADICAL REARRANGEMENTS	8
1.2.1. Neophyl and Related Radical Rearrangements	9
1.2.2. 1,2-Vinyl Migration	11
1.2.3. The 5-Hexenyl and Related Radical Cyclizations	13
Substituent Effects	15
Stereoselectivity	15
1.2.4. Cyclopropyl and Related Radical Rearrangements	20
1.2.5. Rearrangements of Cyclopropylmethyl and Related Radicals	21
1.3.0. FREE RADICAL CLOCKS	24
1.3.1. Calibration of "Clocks" for Solution Kinetics	25
1.3.2. The 5-Hexenyl Radical Clock	27
1.3.3. The Cyclopropylmethyl Radical Clock	29

1.4.0.	INTERMOLECULAR RADICAL REACTIONS	35
1.4.1.	Radical Substitution Reactions	36
	(i) Determination of Rate Constants for substitution	
	(S _H 2) reactions	36
	(ii) Temperature Dependence of Rate Constants	39
	(iii) Solution Phase Data for Some S _H 2	
	Processes	43
	(iv) Polar Effect in S _H 2 Processes	46
1.4.2.	Radical Additions to Multiple Bonds	47
	(i) Stereospecificity in Radical Additions	48
	(ii) Radical Additions to Some Cyclic Diene..	50
	(iii) Radical Additions to Some Nitroso and..	53
1.4.3.	Radical-Radical Reactions and	55
1.5.0.	DIAZENES AS RADICAL SOURCE	58
1.5.1.	Monosubstituted Diazenes	58
1.5.2.	α-Hydroxyalkyl Diazenes	60
1.5.3.	α-Hydroperoxyalkyl Diazenes	66
Chapter 2.	METHODS, RESULTS, AND DISCUSSION	70
2.1.0.	SYNTHESIS AND PROPERTIES OF RADICAL SOURCES: THE α-HYDROPEROXYALKYL DIAZENES AND THE α-HYDROXYALKYL DIAZENES	70
2.1.1.	Synthesis of 1,1,3,3-Tetramethylisindolin-2- -yloxyl	78
2.2.0.	RATE CONSTANTS FOR SOME RADICAL-MOLECULE REACTIONS IN SOLUTIONS	79
2.2.1.	Rate Constants for Cl Abstraction From CCl ₄	

2.2.2.	Rate Constants for Bromine Abstractions from a Few Bromo Compounds by Carbon Centered Radicals	89
	(i) Reactions of BrCCl_3 with Radicals	89
	a. Rate constants for the reaction of cyclopropylmethyl radicals with bromotrichloromethane	91
	b. Rate constants for bromine abstraction from BrCCl_3 by n-butyl radicals	102
	c. Rate constants for bromine abstraction from BrCCl_3 by phenyl radicals	107
	(ii) Cyclopropylmethyl Radical Attack on Bromoform and its Rate Constant (50°C)	111
	(iii) Rate Constants for the attack of Cyclopropylmethyl radicals on Dibromochloromethane	112
2.2.3.	Rate Constants for Iodine Abstraction from Iodo Compounds by a Primary Alkyl Radical using the Cyclopropylmethyl Radical Clock	115
	(i) Rate Constants for Methylene Iodide	118
	(ii) Rate Constants for Methyl Iodide	122
	(iii) Rate Constants for Benzyl Iodide	126
	(iv) Rate Constants for 1-Methylethyl Iodide	129
	(v) Rate Constants for 2,2,2-Trifluoroethyl Iodide	133
	(vi) Rate Constants for 1,1-Dimethylethyl (t-Butyl) Iodide	135
2.2.4.	Rate Constants for a Primary Alkyl Radical Attack on 1-Methyl-4-Nitroso-3,5-Diphenyl Pyrazole	136

2.3.0.	MECHANISTIC INVESTIGATIONS OF THE DECOMPOSITION OF AZOCARBINOLS	146
2.3.1.	UV Kinetics	152
2.3.2.	NMR Kinetics	156
	(i) Exchange of Acetone-D ₆ with 155e	156
	(ii) The influence of aldehydes on the decomposition of 155e	161
	(iii) The influence of acids on the rate of decomposition of 155e	169
2.3.3.	ESR Kinetics	171
2.4.0.	CONCLUSION	174
Chapter 3. EXPERIMENTAL		
3.0.0.	GENERAL	175
3.1.0.	SYNTHESIS	176
3.2.0.	THERMOLYSIS	185
3.3.0.	PHOTOLYSIS	187
3.4.0.	PRODUCT ANALYSIS	187
3.5.0.	NMR KINETICS	189
3.6.0.	UV KINETICS	190
3.7.0.	SPIN TRAPPING	190
4.0.0.	APPENDIX	191
5.0.0.	REFERENCES	204

LIST OF TABLE

1.	Splitting constants for representative nitroxides, $R^1R^2NO\cdot$	8
2.	Rate constants for neophyl and some related radical rearrangements	10
3.	Effects of substituents on the modes of cyclization of 5-hexenyl radical	16
4.	Effects of substituents on the stereoselectivity of the 5-hexenyl radical cyclization	17
5.	Rate constants for the 5-hexenyl radical rearrangement calculated using different Arrhenius expressions	29
6.	Estimated rate constants for the cyclocholesteryl radical rearrangement using the latest published data	31
7.	Gas-phase data for the activation energy of some hydrogen transfer reactions of methyl radicals	43
8.	Rate constants (k_H) for the reaction of n-octyl radical with various substrates (RH)	46
9.	Rate constants for <i>t</i> -butoxyl radical attack on some nitron spin trap	53
10.	Rate constants for primary and secondary radical attacks on some nitroso and nitron traps	54
11.	Rate constants for some radical coupling reactions with nitroxides at 20°C	57
12.	Calculation of entropy change for reaction [98]	62

13a.	Spectral data for 155a, and 154a, and 153a	72
13b.	Spectral data for 154b, and its precursor 153b	73
13c.	Spectral data for 155c, and 154c, and 153c	74
13d.	Spectral data for 155d, and 154d, and 153d	75
13e.	Spectral data for 155e, and 154e, and 153e	76
14.	Rate constants for the attack of some alkyl radicals on CCl_4	80
15.	Photolysis/thermolysis of 155c in CCl_4 : product ratios and rate constants	87
16.	Product ratios and rate constants for Br abstraction from BrCCl_3 by cyclopropylmethyl radicals	98
17.	Product ratios and rate constants for 1-butyl radical attack on BrCCl_3 (80°C) Product ratios and rate constants for phenyl radical attack on BrCCl_3	118. 105
19.	Product ratios and rate constants for iodine abstraction from CH_2I_2 by cyclopropylmethyl radicals	119
20.	Data used for linear regrassion yielding eq.135	120
21.	Rate constants for iodine abstraction from CH_3I by cyclopropylmethyl radicals	125
22.	Rate constants for iodine abstraction from benzyl iodide by cyclopropylmethyl radicals	128
23.	Data used to calculate the Arrhenius expression in eq.140	128
24.	Rate constants for iodine abstraction from isopropyl iodide by cyclopropylmethyl radicals	132

25.	Rate constants for iodine abstraction from 2,2,2-trifluoroethyl iodide by cyclopropylmethyl radicals	134
27.	Change in product ratio [190]/[191] with time	142
28.	Extinction coefficients of 123 in benzene at 40°C and at 23°C at $\lambda = 738$ nm	143
29.	Rate constants for the disappearance of 155e in CH ₃ CN at 80°C	153
30.	NMR kinetic data on the rate constants for decomposition and exchange reactions	159
31.	Influence of benzaldehyde on the rate constants for exchange and decomposition reactions of the azocarbinol, 155e.	164
32.	Half-life for the disappearance of TEMPO esr signal by the decomposition of 155e in the presence and absence of benzaldehyde	171

LIST OF FIGURES

1.	Splitting of Electron Energy Levels as a Function of Field Strength, H	5
2.	Energy Level Diagram Showing the Transition for an Electron Interacting with a Proton at a Field, H	6
3.	Arrhenius Plot for the Data in Table 15	88
4.	Arrhenius Plot for the Data in Table 16	100
5.	Arrhenius Plot for the Data in Table 20	121
6.	Arrhenius Plot for the Data in Table 28	130
7.	ESR Spectrum Obtained while Thermolyzing 154b in the Presence of MNDP	139
8.	Arrhenius Plot for the Data in Table 28	144
9.	UV Kinetics of Unimolecular Decomposition of 155e in CH ₃ CN at 80°C	154
10.	NMR Kinetics of Dissociation of 155e in Acetone-D ₆	160
11.	NMR kinetics of the Effect of Benzaldehyde on the Dissociation of 155e in Acetone-D ₆	165
12.	Kinetics of the Disappearance of TEMPO ESR Signal by Decomposition of 155e in Acetone-D ₆ in the Presence and in the Absence of Benzaldehyde	172

CHAPTER 1

INTRODUCTION

This Section of the thesis is intended to introduce a few selected free-radical processes that are relevant for a proper evaluation of the small, but significant, contribution that the author has made in the mechanistic and kinetic areas of free radical chemistry. First of all, a brief survey of the evolution of free radical chemistry over the century will be presented (Section 1.0) with emphasis on the recent, rapid development in the application of free radicals in synthesis, and with the suggestion that the availability of the rate constants for a number of radical processes has contributed to the design and execution of several synthetic projects. However, it should be emphasized that for a larger number of key reactions in free radical synthesis, the rate constants have yet to be determined.

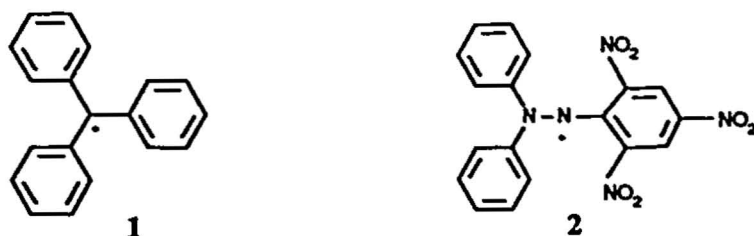
The objective of this thesis project was to fill in some gaps in the available kinetic data for a number of radical-molecule reactions in solution such as halogen atom abstractions and addition to the nitroso group (See Section 2) and also to explore the potential of some α -hydroxydiazenes (Section 1.5.2) as convenient sources of radicals for the kinetic studies. The sections that follow are arranged in such a way as to familiarize a new researcher with the significance of some intramolecular radical reactions (Section 1.2) which can be used as 'clocks' (Section 1.3) for measuring the absolute rate constants for a variety of radical-molecule reactions (Section 1.4). The importance of some diazenes, especially the α -hydroxy and α -hydroperoxy diazenes which are used as the source of free radicals for the kinetic and mechanistic studies reported in this thesis, is discussed in Section 1.5.

1.0.0. FREE RADICALS: A BRIEF HISTORY

Free radicals have a long standing history, dating back to 1900, when Gomberg¹ discovered the first free radical, the triphenylmethyl radical, 1. Now the term free radical or simply radical refers to species with one or more unpaired electrons associated with non

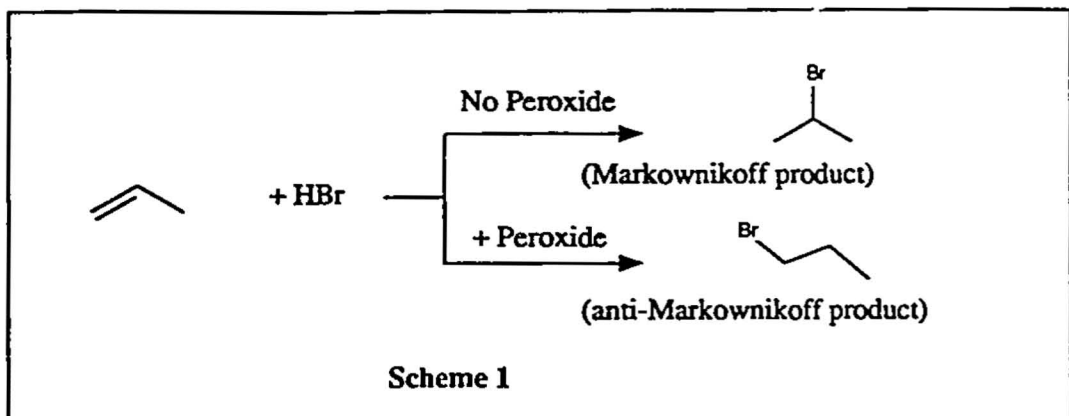
metals like carbon, halogen, oxygen, nitrogen, phosphorous, sulphur or a few metal atoms such as silicon, tin, or germanium bearing organic groups. The most extensively studied free radicals are the carbon-centered radicals and this thesis deals mainly with them. There are a number of reviews² that deal with the fundamentals of various free radical processes, and they can serve as resource materials for an overall understanding of this subject.

The initial growth in the field of free radical chemistry was very slow, probably because of the lack of understanding of the subject and also because of the fact that radical reactions are extremely fast and therefore their study was not easy. There had been considerable effort, in the beginning, in obtaining stable free radicals such as triarylmethyl (eg. triphenylmethyl, 1)^{3,4} radicals and diphenylpicrylhydrazyl (DPPH, 2)^{5,6} radicals. Apart



from that, the knowledge about radicals was scattered and studies of free radicals were isolated incidences in the early stages of free radical chemistry. The formation of methyl radicals as transient intermediates in the decomposition of tetramethyl lead was demonstrated by Paneth⁷ as early as 1929. Rice and Herzfeld⁸ appear to be the first to report the involvement of free radicals in many gas-phase pyrolysis reactions. A few years later, the first comprehensive report about free radical chemistry was published by Hey and Waters.⁹ Many unanswered mechanistic problems, which existed at that time were interpreted in terms of free radical processes. The anti-Markownikoff addition of hydrogen bromide to olefins in the presence of peroxides (Scheme 1) was explained by Kharasch¹⁰ as being the result of a free radical chain process.

The importance of free radicals in vinyl polymerization had been recognized by Flory,¹¹ and that led him to the publication of one of the most significant papers on the



kinetics of the first free radical polymerization reaction.¹²

Even though the new ideas proposed and propagated in the early publications did not get enough recognition or immediate acceptance, they formed the basis for much significant research in many laboratories. The last two decades especially witnessed a tremendous accelerating growth in the chemistry of free radicals. A deeper understanding of the mechanistic and kinetic aspects of free radical chemistry has been made possible through a number of text books written by Walling^{2d} Pryor^{2g} and Huyser²ⁱ and a collection of monographs edited by Kochi.^{2k} "*Advances in Free Radical Chemistry*" is a series published on selected topics in this field.

Over the years, several processes have been developed for generating radicals in solution.¹³ Thermal or photochemical decomposition of peroxides¹⁴ and azo compounds (see Section 1.5) are still the most convenient and widely used procedures for generating radicals.

Of all the different types of radical reactions, radical rearrangements (Section 1.2) as well as various inter-molecular radical reactions (Section 1.4) are of special interest not only to physical-organic chemists but also to synthetic chemists for various reasons. The availability of rate constants for many of the above-mentioned radical processes¹⁵ has opened a wider horizon for the application of radicals, especially in synthesis.¹⁶

Until recently, the practical application of free radical chemistry was mainly confined to one of the world's largest chemical industries, namely the plastic and polymer industry. The wide application, in the last few years, of free radicals in the synthesis of target

molecules,¹⁶⁻³⁰ including many natural products,²⁰⁻²⁶ has triggered the growth of many research projects in different laboratories. There has also been a tremendous growth in the mechanistic and kinetic areas of radical chemistry as well.^{15,31-33} The potential for application of free radicals in synthesis has been greatly increased as a result of kinetic data available for various free radical processes.¹⁵⁻¹⁹ A balanced interplay of rate constants and concentrations of reactants are necessary for the development of a useful free radical process in synthesis.¹⁶

Due to the development of various experimental procedures in conjunction with modern technology, it has been possible for detailed studies on many radicals and radical processes. Electron spin resonance (esr) spectroscopy (see Section 1.1) is a very powerful and sensitive technique for detecting radicals.³⁴ Concentrations of radicals as low as 10^{-7} M can be detected by the esr spectroscopy. *Kinetic esr spectroscopy* is a powerful technique used to measure rate constants for many free radical reactions.^{35,36}

1.1.0. DETECTION OF FREE RADICALS BY ESR SPECTROSCOPY

Of all the available techniques,³⁷⁻⁴⁰ electron spin resonance (esr) spectroscopy⁴¹ is the most powerful and extensively used method for the detection of free radicals in solution. For a detailed treatment of the subject of esr spectroscopy and its applications, reference can be made to a number of recent reviews.⁴¹ This section deals only with the most basic principles with a view to highlight a few terms which are usually encountered in esr spectral analysis.

Basic Principles

Spinning of a charged species such as an electron produces a magnetic moment. The total magnetic moment produced by the spin of an electron in a radical is the result of two contributions; (a) the spin of the electron about its own orbital axis (spin magnetic moment) and (b) the motion of the orbit about the nucleus of the atom (orbital magnetic moment). The orbital contribution to the total magnetic moment in most cases is very small when compared to the spin magnetic moment.

When placed in a magnetic field of strength H , the radical may orient itself in the two possible energy states ($m_s = \pm 1/2$) due to the interaction of the electronic magnetic moment with the applied field. Electrons with magnetic moments in the direction of the applied field have lower energy than those with opposing magnetic moments. The separation of the energy states, ΔE , increases with the increasing magnetic field, H , according to the eq 1.

$$[1] \quad \Delta E = g\beta H$$

In eq.1, g is the gyromagnetic ratio (called the g -factor), a spectroscopic constant, and β is the Bohr magneton, a constant given by $\beta = e\hbar/2\pi mc = 9.27 \times 10^{-21} \text{ erg Gauss}^{-1}$, where e

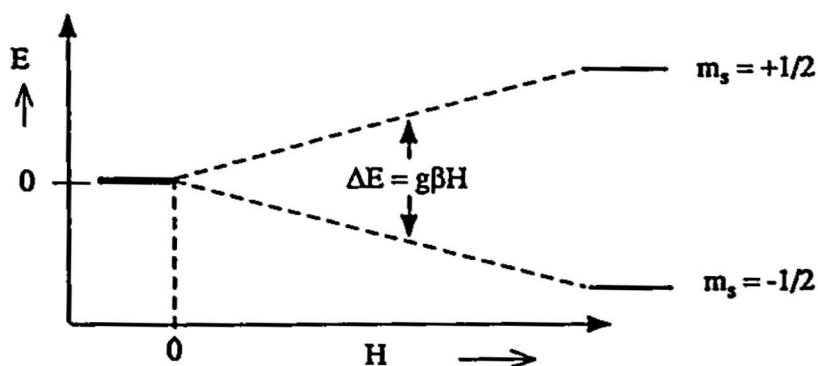


Fig. 1 : Splitting of electron energy levels as a function of field strength, H

is the charge on the electron, \hbar is Planck's constant, m is the electronic mass, and c is the speed of light. Resonance absorption of radiation (of frequency ν) promoting an electron from the lower to the upper spin state occurs when the energy of the radiation ($\hbar\nu$) equals the energy difference between the two states, that is when $\hbar\nu = g\beta H$. The splitting of the single energy level for an electron as a function of the applied field H is given in Fig. 1.

The two most important fundamental quantities that are necessary for the interpretation of an esr spectrum are (1) the g -factor and, (2) the hyperfine splitting constants.

The g-Factor

In an ESR spectrum, the g-factor has the same significance as that of the chemical shift in NMR spectra. For a free electron, the g-factor is 2.00232. Because of the difference in spin-orbit coupling, the g-factors for different radicals vary slightly from that of the free electron. For example, a few radicals with their g-factors in brackets are: $\text{CH}_3\cdot$ (2.00255), $\text{CH}_3\text{-CH}_2\cdot$ (2.00260), $(\text{CH}_3)_3\text{C}\cdot$ (2.00260), $\text{CH}_2\text{F}\cdot$ (2.0045), $\text{CF}_3\cdot$ (2.0031), $\text{CHCl}_2\cdot$ (2.0083), $\text{CCl}_3\cdot$ (2.0091).^{41c} The g-factor for a N-centered radical in $\text{R}_2\text{N}\cdot$ is 2.0032; for the O-centered radical in $\text{RO}\cdot$ it is 2.015, and for nitroxides it is 2.006 G.

Hyperfine Splitting Constants

When the unpaired electron in a radical is adjacent to other magnetic nuclei (eg. ^1H , ^{13}C , ^{14}N) in the molecule, the magnetic field produced by the nuclei induce small additional fields which add to or subtract from the external magnetic field. This is known as the hyperfine interaction which results in the splitting of resonance lines into two or more components. Thus the presence of a proton adjacent to a radical center splits the resonance

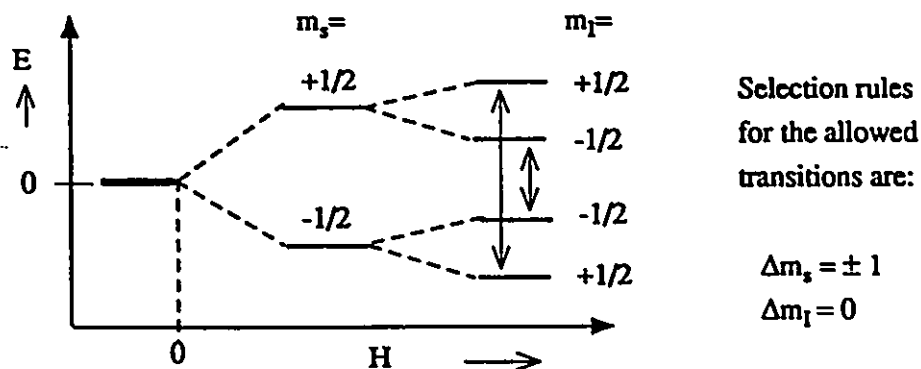


Fig. 2 : Energy level diagram showing the transitions for an electron interacting with a proton at a field, H

line into two components; the schematic presentation of such a state is given in Fig. 2. The phenomenon is similar to the nuclear coupling in NMR spectroscopy.

In general, a nucleus of spin I interacts with an electron ($s = \pm 1/2$) to result in a splitting of the resonance line into $2nI + 1$ components where n stands for the number of the equivalent interacting nuclei. The separation between the lines, usually expressed in field units (Gauss) is known as the hyperfine coupling constant denoted by the symbol a .

For technical reasons, esr spectra are usually presented as first derivative curves rather than the normal plot of absorption against magnetic field at a constant frequency.

Spin Trapping

Most organic radicals undergo bimolecular self reactions at rates close to the diffusion controlled limit; consequently their steady state concentrations are very low. Therefore, the detection of such radicals even by the most powerful esr technique requires conditions under which radical concentrations can be raised to the detection limit ($10^{-7}M$ or more) of the esr instrument. The most commonly used procedures for raising the radical concentration in solution involve (a) the use of low temperatures, (b) intense in-situ irradiation,⁴² (c) the use of flow cells,⁴³ and most importantly (d) the use of spin traps.⁴⁴

Spin trapping is a technique by which very short lived radical intermediates are trapped by suitable diamagnetic species called "spin traps" to form relatively long-lived paramagnetic species. The secondary radicals thus obtained (which are called the "spin adducts") are then easily characterized by esr spectroscopy.

Nitrones (3) and nitroso compounds (4) are the most commonly used spin traps. Both 3 and 4 react with radicals ($R\cdot$) to form the nitroxyl radicals 5 and 6 respectively.⁴⁴

The esr spectra of nitroxides $R_1R_2NO\cdot$ are relatively simple. The interaction of the nitrogen with the electron produces a triplet ($2nI + 1 = 3$) with intensities in the ratios 1:1:1. The actual magnitude of the hfc depends on a variety of factors such as delocalization of the unpaired electron into the nitrogen and also on the substituents. For normal carbon centered substituents, R^1 and R^2 , the a_N values range from 10-17 Gauss. Additional splitting of the triplet can also arise from hyperfine interactions of protons on the α -carbon atoms. A few

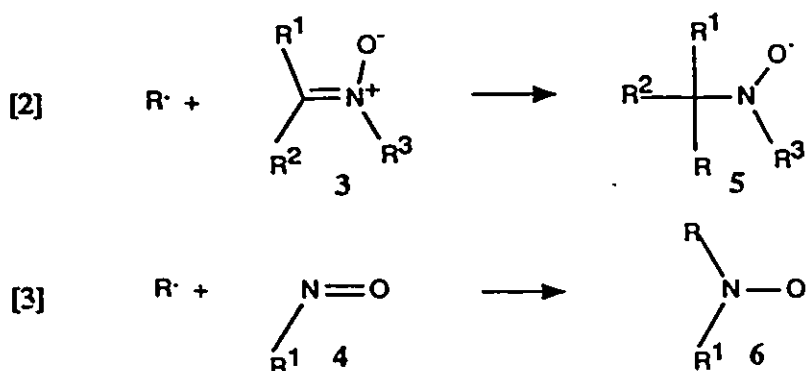
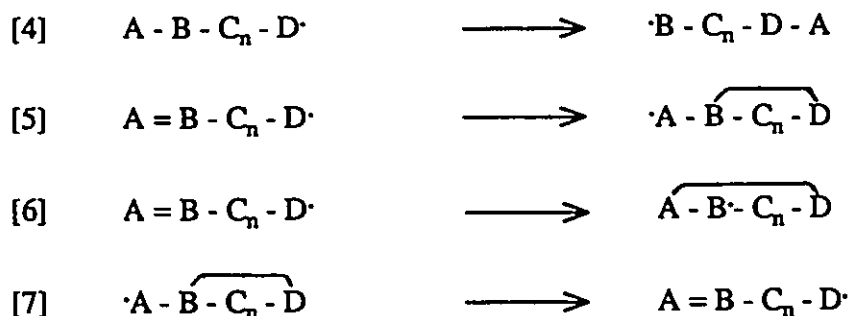


Table 1. Splitting Constants for Representative Nitroxides, $R^1R^2NO^{\cdot}$ ⁴⁵				
R^1	R^2	a_N	$a_{\beta(H)}$	$a_{(other)}$
C_6H_5	C_6H_5	10.9		2.0(o,p), 0.8(m)
C_6H_5	$(CH_3)_3C$	13.4		1.7(o,p), 0.8(m)
CH_3	$(CH_3)_3C$	15.2	11.3	
CH_3CH_2	$(CH_3)_3C$	15.2	10.4	
$(CH_3)_2CH$	$(CH_3)_3C$	16.8	1.8	
$(CH_3)_3C$	$(CH_3)_3C$	17.0		
$(CH_3)_2CH$	$(CH_3)_2CH$	15.0	4.4	
$C_6H_5CH_2$	$(CH_3)_3C$	14.6	7.4	

examples are given in Table 1. For more examples of the esr spectral data of nitroxyls and numerous other radicals reference may be made to a text by Beilski and Gebicki.⁴⁵

1.2.0. INTRAMOLECULAR RADICAL REACTIONS (REARRANGEMENTS)

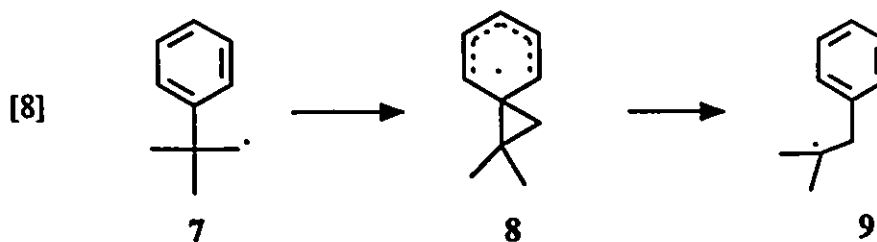
The subject of free radical rearrangement has been a topic of extensive reviews⁴⁶⁻⁵¹ in the last few years. According to Beckwith and Ingold⁴⁹ free radical rearrangements can be classified into group transfer (eq.4), ring closure (eq.5, 6), and ring opening (eq.7) reactions.



In eq. 4-7, the subscript n represents the number of C atoms separating the sites B and D.

1.2.1. Neophyl and related radical rearrangements

Group transfer reactions, which can be generally represented by eq.4, involve migrations of a group from one atom to another in a molecule. The most common among them are the 1,2 shifts ($n=0$). More remote group transfers are also known, for example, the 1,4-shifts and the 1,5-shifts. The first free radical rearrangement to be recognized, namely the neophyl rearrangement (eq.8),⁵² is a classical example of a group transfer reaction in which a

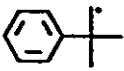
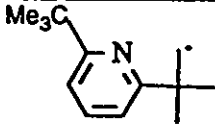
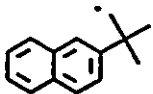
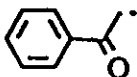
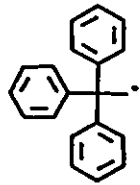


phenyl group is migrated from one carbon atom to another by a 1,2-shift.

The mechanism of this rearrangement has been extensively investigated by several workers^{53,54} and is known to involve an intramolecular radical addition to the aromatic ring to form an intermediate radical 8 which undergoes a ring-opening in the more exothermic sense to form the tertiary radical 9, instead of the less exothermic path to form the primary radical 7.

The neophyl rearrangement and similar rearrangements in which a 1,2-shift of an aryl

group occurs have been the subject of extensive quantitative kinetic studies.⁵⁵⁻⁵⁹ The rate

Table 2. Rate constants (k) for neophyl and some related radical rearrangements				
Unrearranged radicals	log(A/s ⁻¹)	E, kcal/mol	k(s ⁻¹) at 20 °C	Ref.
	10.98 ^a	10.83	1.1 x 10 ³	59
	11.7	12.0	8.0 x 10 ²	55
	11.75 ^b	11.3	2.9 x 10 ³	55
	11.8 ^b	14.7	10	56
	11.8 ^b	8.5	3.6 x 10 ⁵	58

^a Recalculated from data given in ref. 59 using the latest value for the H-abstraction from Bu₃SnH by neophyl radical⁶⁰

^b The pre-exponential factors are assumed,⁵⁵ and probably require minor corrections based on the revised value for the neophyl rearrangement itself.⁵⁹

constants for a number of similar radical rearrangements are known.⁵⁵⁻⁵⁹ Some representative rearrangements and their absolute rate constants are given in Table 2.

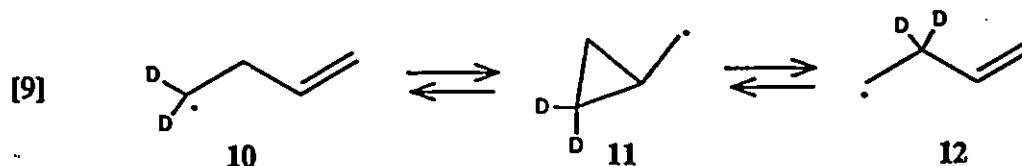
The neophyl rearrangement, which has been used as a "free radical clock"⁶¹ for many kinetic studies, is relevant to some discussions in a future section of this thesis. Its rate

constant has been determined both by direct measurement using the esr technique⁵⁵ and also by indirect ways.⁵⁹ The latest value reported for this rearrangement (764 s^{-1} at 25°C)⁵⁹ can be recalculated, by the procedure used by Ingold et.al.⁶¹ using the latest value for the rate constant ($k_H = 3.6 \times 10^6 \text{ M}^{-1}\text{s}^{-1}$, at 25°C) for H-abstraction from Bu_3SnH by neopentyl radical, as $1.1 \times 10^3 \text{ s}^{-1}$ at 25°C .

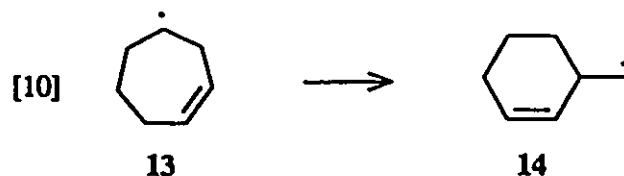
The effect of substituents on the rapidity of the neophyl-like rearrangements has also been investigated.⁶²⁻⁶⁵ The stabilization of the intermediate spiro(2-5)octadienyl radical (similar to 8) by delocalization, the stabilization of the intermediate (eg.8) by the gem-dimethyl group (Thorpe-Ingold effect), and the stability of the rearranged radical (eg.9) relative to the unrearranged radical (eg.7) are major contributors to the increased rate constants for rearrangements of a number of substituted neophyl radicals.⁶⁶

1.2.2. 1,2-Vinyl migration⁶⁷

This is similar to the 1,2-phenyl migration in the neophyl rearrangement, where the

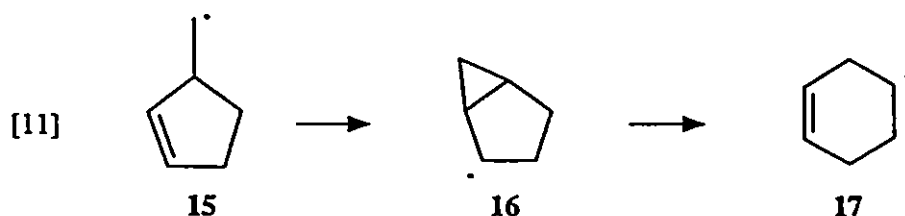


group transfer occurs by the intramolecular radical addition to an unsaturated group followed by a β -scission of the intermediate radical to form the isomeric product. The 1,2-vinyl shift in allyl carbonyl radical (such as that in eq.9) is known to be a facile process.⁶⁷⁻⁷⁶ The involvement of cyclopropylmethyl radicals as discrete intermediates in these processes has been established by various observations.^{67-69,76} Some typical examples of 1,2-vinyl

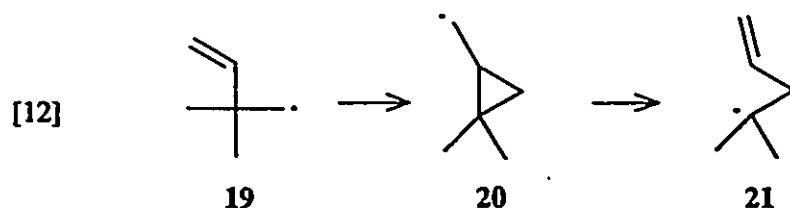


migrations can be seen in the rearrangements of 13 to 14⁷² and 15 to 17.^{71,75}

The vinyl migrations are faster than the 1,2 aryl shifts. However, only a limited

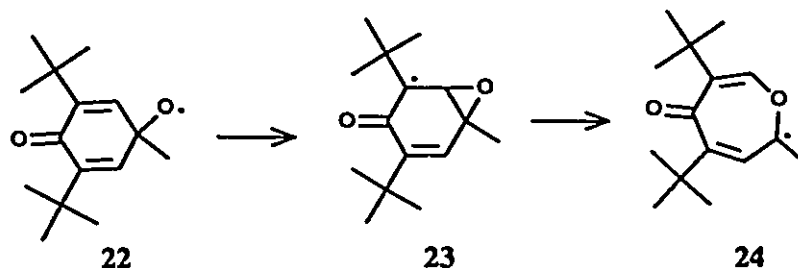


number of absolute rate constants for vinyl migrations are available. The overall rate constant for the vinyl migration (eq.9) is estimated as $4.9 \times 10^3 \text{ s}^{-1}$ at 25°C .⁷³ For the rearrangement of 13 to 14, the estimated rate constant⁴⁹ lies between $1 \times 10^4 \text{ s}^{-1}$ and $5 \times 10^4 \text{ s}^{-1}$.⁷¹ The rate constant for the overall rearrangement of 2,2-dimethyl-3-buten-1-yl radical (19) to

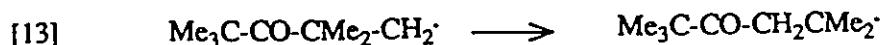


1,1-dimethyl-3-buten-1-yl radical (21, eq.12) has been reported recently by Warkentin and Ingold⁷⁴ as $4.3 \times 10^7 \text{ s}^{-1}$ at 25°C . The extreme facility of the above rearrangement was explained on the basis of the Thorpe-Ingold effect.⁷⁴

A similar 1,2-vinyl migration from carbon to oxygen has been reported by



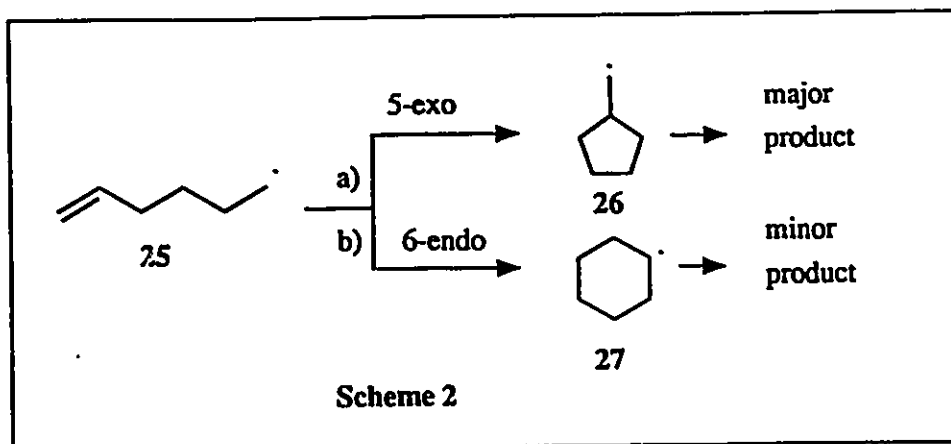
Nishinaga,⁷⁷ who observed rearrangement of 22 to 24. 1,2-Migrations of other unsaturated groups such as $\text{C}\equiv\text{N}$, $\text{C}=\text{N}$, and $\text{C}=\text{O}$, even though possible, are less frequently encountered in free-radical rearrangements. Lindsay, Luszyk, and Ingold⁶¹ have shown that the 1,2-migration of a carbonyl function, eq.13, is faster than phenyl migration in the neophyl rearrangement. Similar rearrangement involving the migration of a $\text{C}\equiv\text{N}$ group (eq.14) is



reported to be very slow. The rate constants for reactions [13] and [14] have been estimated at 25°C as $1.7 \times 10^5 \text{ s}^{-1}$ and 0.9 s^{-1} , respectively.⁶¹

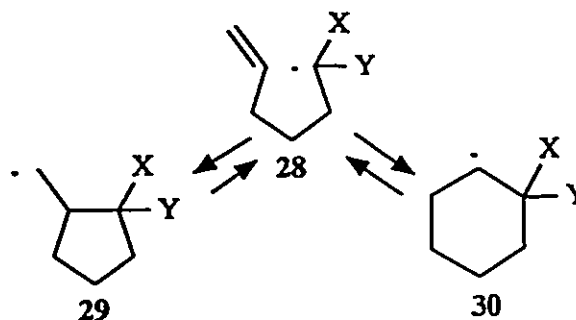
1.2.3. The 5-hexenyl and related radical cyclizations

By far the most extensively studied free-radical rearrangements are those related to the 5-hexenyl radical. It has been well established that the 5-hexenyl radical (25) undergoes cyclization by intramolecular addition to form the thermodynamically less stable cyclopentylmethyl radical (26) instead of the more stable cyclohexyl radical (27) presumably by a kinetically controlled process (Scheme 2).^{78,79} It has also been demonstrated that in the



case of unsubstituted 5-hexenyl radical, each mode of cyclization is irreversible.^{80,81} However, Julia and his co-workers^{82,83} have shown that in cases where the radical cyclizations are reversible, six-membered rings are predominantly formed, probably in a thermodynamically controlled process (eq.15).⁸⁴

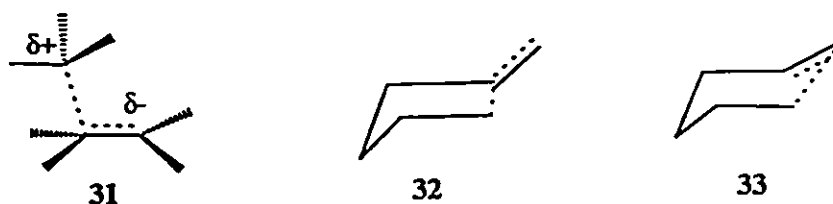
[15]



a) X=H, Y=H	>98%	<2%
b) X=H, Y=CN	>98%	<2%
c) X=H, Y=COCH ₃	72%	28%
d) X=H, Y=COOC ₂ H ₅	56%	44%
e) X=Y=COOC ₂ H ₅	70%	30%
f) X=CN, Y=COOC ₂ H ₅	16%	84%

One explanation for the regioselectivity in the cyclization of the unsubstituted 5-hexenyl and related radicals to form the 5-exo product is based on the differences in the entropies of activation for the two modes of cyclization.^{85,86} The entropy change associated with the 5-exo cyclization is more favourable than that for the 6-endo mode.⁸⁷

The most widely accepted explanation for the preferred exo-cyclization of various ω -alkenyl radicals is based on the stereo-electronic hypothesis first proposed by Beckwith⁸⁸ and later supported by various theoretical calculations.⁸⁹ According to this hypothesis, the transition state is attained by the overlap of the semi-occupied 2-p orbital with one lobe of the vacant π^* orbital. Consequently, the transition state is dipolar and the incoming radical behaves as a nucleophile and assumes a partial positive charge while the receptor site becomes partially negative. The position of the three participating atoms in the transition state for the attack of a methyl radical to an olefin is shown to be as that in 31,⁸⁹ where the partially formed CH₃-C bond makes an obtuse angle with the partially broken C=C bond. This type of a transition state is more easily attained for the 5-exo cyclization (32) than for the 6-endo case (33).⁹⁰



Substituent effects

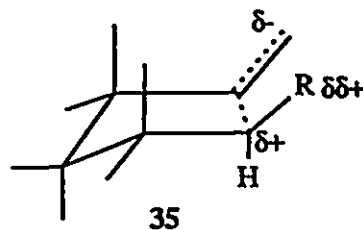
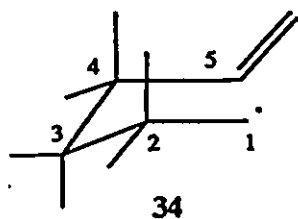
The effects of substituents on the ratio of products formed from the two different modes of cyclizations have been well established by Walling,⁹¹ Beckwith,⁹² and Julia.⁹³ For substituted 5-hexenyl radicals, the ratios of products (5-exo/6-endo) depend mainly on the substituents at the olefinic bond. A methyl group at the receptor site reduces the attack at that carbon due to the steric effects.^{92,93} Methyl groups at the radical center have only a small effect.⁹¹⁻⁹³ A few examples (eq.16-19) and the ratio of products from the two modes of cyclization are given in Table 3.

Stereoselectivity

Exocyclic ring closure of hexenyl and related systems, mono-substituted at C-1, C-2, C-3, or C-4 gives rise to a mixture of *cis*- and *trans*-disubstituted products in which one of the isomers predominates. Predictions regarding the major stereoisomer can be made from the rules formulated by Beckwith.⁹⁴ According to those rules 1- or 3- substituted radicals preferentially give *cis*-disubstituted cyclopentyl products and 2- or 4- substituted radicals give mainly *trans*-disubstituted products. The above rules has been explained in terms of the transition state structure 35. The more favourable conformer is that in which the substituents occupy an equatorial position at C-2, C-3, or C-4. The preferred formation of *cis*-product from a 1- substituted system is more difficult to explain. A dipolar interaction between the partial positive charge developed at the radical site (which is inductively dispersed into the alkyl substituent), and the partial negative charge developed at the receptor site (as shown in structure 35) is believed to be a reason for the above stereoselectivity.^{94,95} Numerous


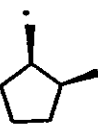
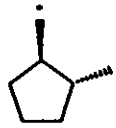
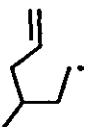
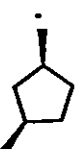
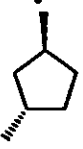
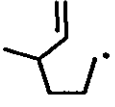
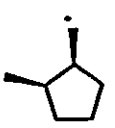
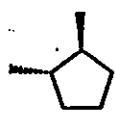
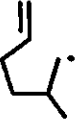

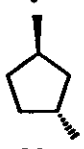
Table 3. Effects of substituent on the modes of cyclization of 5-hexenyl radical.

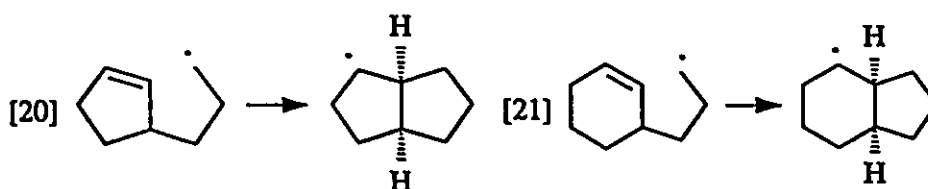
	Radical	5-exo product	6-endo product	product ratio 5-exo : 6-endo
[16]				98 : 2
[17]				99 : 1
[18]				99 : 1
[19]				33 : 66



examples are available from recent literature⁹¹⁻⁹⁶ to illustrate the rules governing stereoselectivity in the 5-exo ring closure of substituted 5-hexenyl radicals. A few of them are given in Table 4.

The stereoselectivities in the 5-hexenyl cyclizations are even more pronounced in cyclizations involving cyclic alkenes.⁹⁷ Formation of a cis-junction, which can be illustrated by eqs.20, 21, is the main reaction.

Table 4. Effects of substituents on the stereoselectivity of the 5-hexenyl radical cyclization			
Position of substituent	Radical	<i>Cis</i> -product	<i>Trans</i> -product
C-1		 73	 27
C-3		 75	 25
C-4		 35	 65
C-2		 17	 83

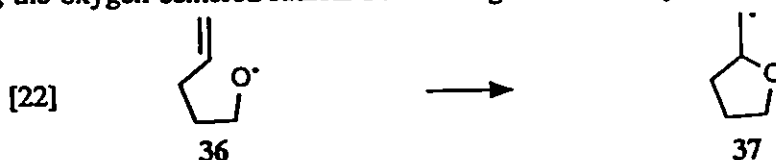


The regioselectivity and stereoselectivity in the 5-hexenyl radical cyclizations find extensive applications in the synthesis of target molecules. In the last few years there has been a tremendous expansion in the field of organic synthesis making use of radical cyclization reactions for the synthesis of many cyclic systems including several natural products.¹⁶

Most of the new developments in this area of free radical chemistry have been made

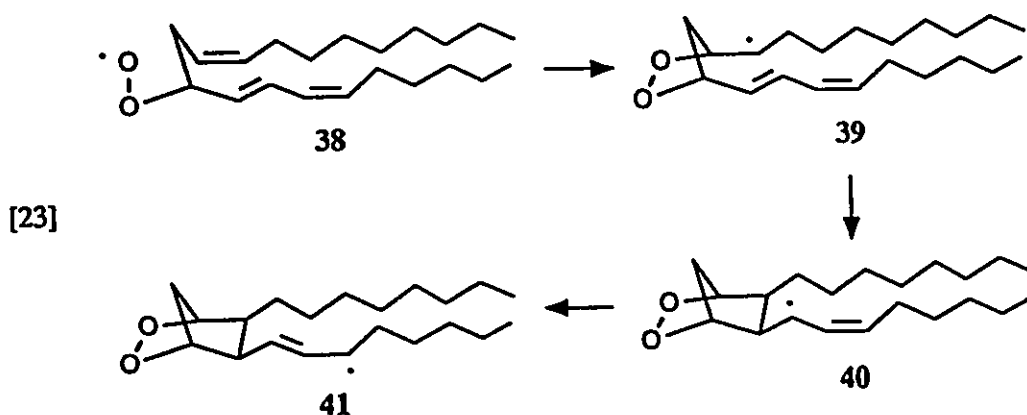
possible through the pioneering efforts of physical organic chemists such as Ingold and Beckwith who were instrumental in determining rate constants for many radical cyclizations and related radical processes. A properly designed synthetic scheme involving radical cyclizations requires the knowledge of how fast the desired radical reaction is compared to other radical destroying processes such as radical coupling and radical-molecule reactions, that can compete in a particular chemical environment.

A number of rearrangements similar to the 5-hexenyl radical rearrangement in which the unrearranged radical center is a hetero atom (O, N, or S), have also been studied. For example, the oxygen-centered radical 36 rearranged exclusively to the radical 37 in a 5-exo

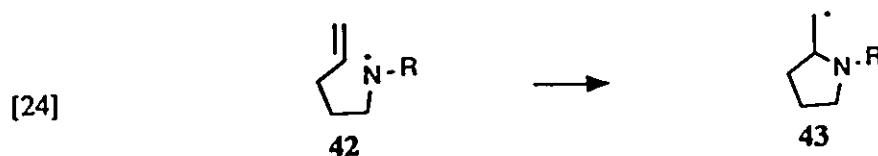


mode of cyclization.⁹⁸ The rate constant for this rearrangement is not known accurately, but the epr data⁹⁹ suggests that it is much higher ($\approx 10^8 \text{ s}^{-1}$) than that for the 5-hexenyl radical itself ($2 \times 10^5 \text{ s}^{-1}$) at room temperature.

The postulated mechanism for the biosynthesis of prostaglandins involves the cyclization of the peroxy radical 38 in the 5-exo sense.¹⁰⁰ The intermediate carbon-centered radical 39 cyclizes again to give radical 40 (eq.23).

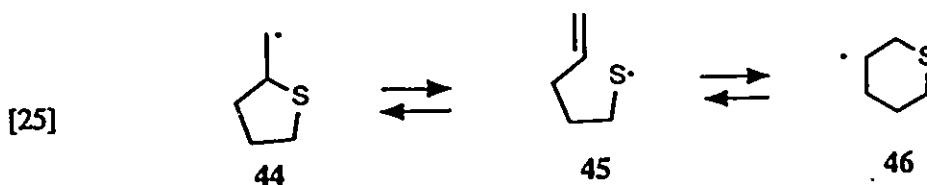


Several examples are known of 5-exo cyclization of N-centered radicals of the 5-hexenyl type (eq.24).^{32,101} The rate constant for the above rearrangement is known to be

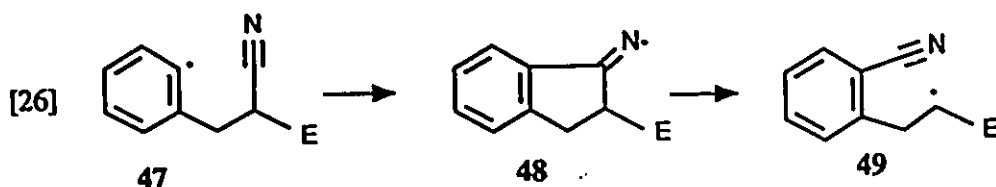


much smaller ($< 10^3 \text{ s}^{-1}$, at 25°C)¹⁰² than that for the corresponding carbon-centered radicals ($\approx 10^5 \text{ s}^{-1}$).

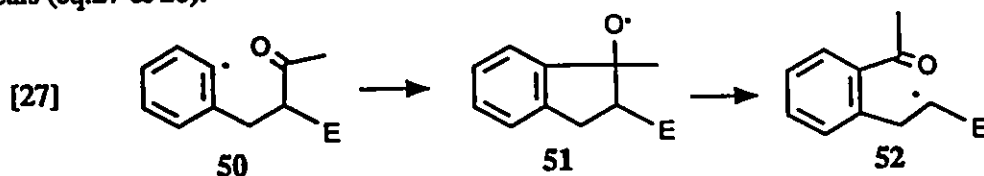
Similar cyclization reactions of sulfur-centered (thiyl) radicals are more complicated because of the reversibility of these reactions. Both exo- and endo-cyclization products are observed (eq.25).¹⁰³



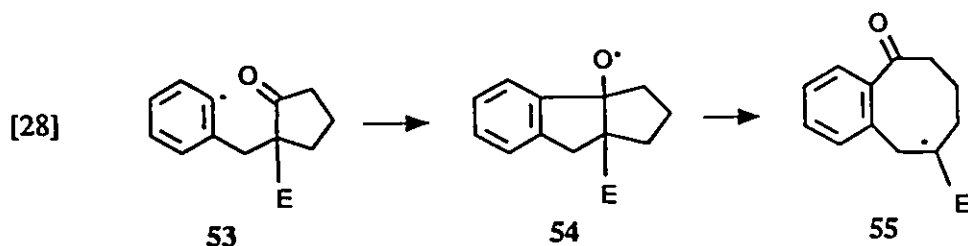
A large number of radical rearrangements, similar to 5-hexenyl cyclizations, involve intramolecular addition onto multiple bonds such as $\text{C}=\text{O}$, $\text{C}\equiv\text{N}$, $\text{C}=\text{S}$, and $\text{N}=\text{N}$. Examples of these can be found in the reviews by Surzur³² and Beckwith and Ingold³¹ and from the references therein. A few recent examples (eq.26-28, where $\text{E} = \text{COOC}_2\text{H}_5$) involving such processes are reported by Beckwith et al.¹⁰⁴ The rearrangement of 47 to 49 involves the



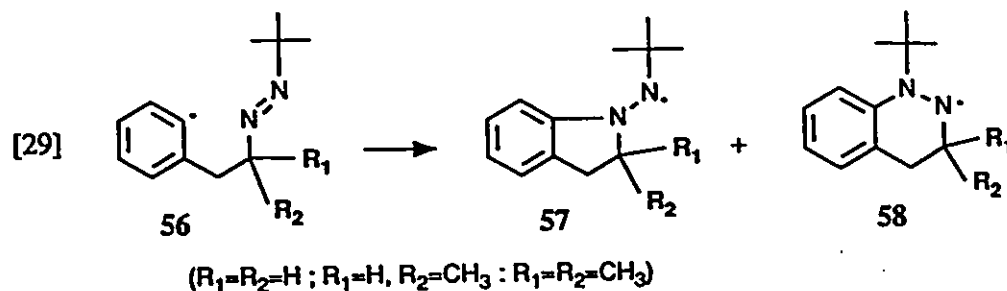
initial radical attack on the cyano ($\text{C}\equiv\text{N}$) function to form the intermediate 48, which ring-opens to form the more stable radical 49. Similarly the rearrangement of 50 to 52, and 53 to 55 both involve intramolecular additions to $\text{C}=\text{O}$ bonds followed by β -scission of the oxy radicals (eq.27 & 28).¹⁰⁴



Several examples of cyclizations of aryl radicals onto the azo function ($\text{N}=\text{N}$) in a

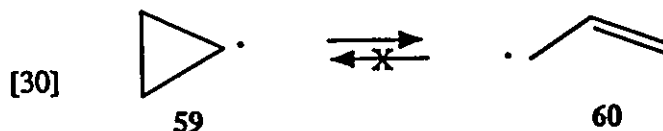


5-exo/6-endo competition system have been reported very recently by Warkentin et.al.¹⁰⁵ They isolated products resulting from both exo- and endo-cyclizations, eq.29.



1.2.4. Cyclopropyl and related radical rearrangements

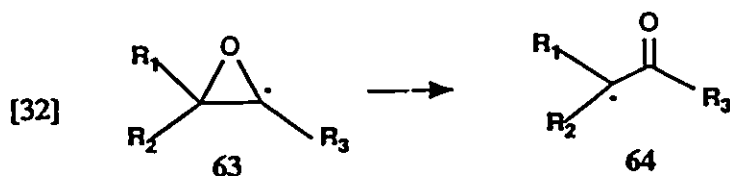
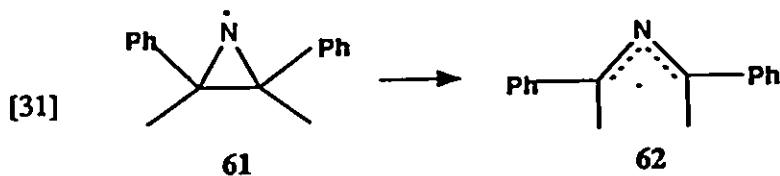
The rearrangement of cyclopropyl radical 59 to the allyl radical 60 is known to be highly exothermic (25-30 kcal/mol),^{106,107} and therefore the reverse reaction (60 to 59, involving a 3-endo cyclization) is practically impossible.



In spite of the fact that the rearrangement (eq.30) is thermodynamically very facile, it is observed that, in many cases, only small amounts of products from the rearrangement of substituted cyclopropyl radicals are formed in solution.^{108,109} The relatively small rate constant for the ring-opening of the cyclopropyl radical in solution is probably the result of a very high activation energy. Indeed it has been shown by gas-phase kinetic studies that the ring-openings of cyclopropyl radicals have activation energies in the range 20-30 kcal/mol.^{110,111}

Ring-opening of three-membered heterocyclic radicals containing O and N atoms are

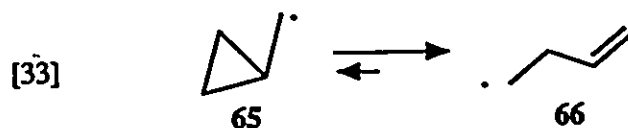
also known. For example, the aziridinyl radical **61** rearranges to **62** (eq.31)¹¹² and the oxiranyl radical **63** rearranges to the α -ketoalkyl radical **64** (eq.32).^{113,114}



Itzel and Fischer¹¹³ have determined the absolute rate constants for a number of substituted oxiranyl radicals. For the unsubstituted oxiranyl radical (**63**, $R_1 = R_2 = R_3 = H$) the rate constant for the isomerization is found to be $<10^3 \text{ s}^{-1}$ at room temperature:

1.2.5. Rearrangements of cyclopropylmethyl and related radicals

The rearrangement of cyclopropylmethyl radical (**65**) to the 3-butenyl radical (**66**) is one of the fastest radical isomerization reactions (eq.33). This thesis deals mainly with one of

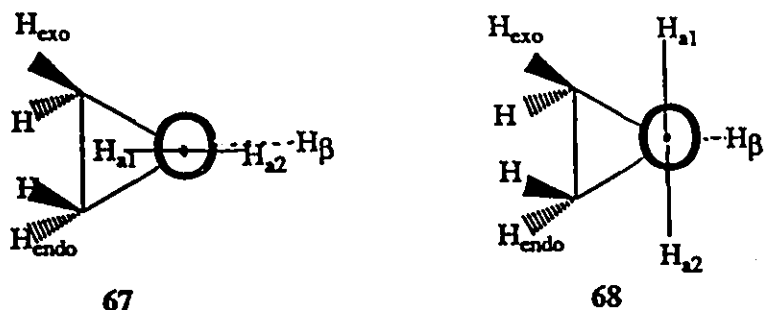


the most important kinetic applications of this rearrangement, namely its use as a 'clock' for measuring the absolute rate constants for some fast radical molecule reactions. Therefore, a detailed discussion about its isomerization rate constant and some potential applications are given under a separate section.

Kochi, Krusic, and Eaton¹¹⁵ were the first to observe the esr spectra of the rearranged radical **66** and the unrearranged radical **65** at very low temperatures. They found that the rearrangement (eq.33) was extremely fast and that, when cyclopropylmethyl radicals were generated at temperatures above -100°C , the esr signals from only the rearranged radicals

could be detected. At temperatures between -100°C and -140°C , both rearranged and unrearranged radicals could be detected while below -140°C the esr signals consisted mainly of those of cyclopropylmethyl radicals.^{115,116}

The two extreme conformations that are possible for the cyclopropylmethyl radicals are given by 67 and 68, in Newman projection. Kochi et.al.¹¹⁵ have shown that the preferred conformation of the cyclopropylmethyl radical is 68, based on the esr spectral studies. They

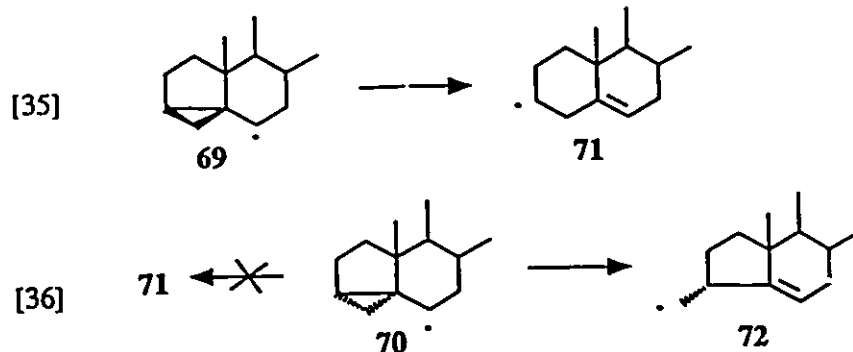


found that the hyperfine coupling constant (hfc) for the β -hydrogen in cyclopropylmethyl radical was unusually small (2.5 G) when compared with those for other alkyl radicals (20-25 G). Therefore a conformation (68) in which the β -hydrogen lies on the nodal plane of the p-orbital bearing the unpaired electron has been proposed for the cyclopropylmethyl radicals under the esr experimental conditions. The preference for the above conformation has also been supported by results from semi-empirical INDO calculations,^{117,118} which predicted 67 to be of lowest energy and also predicted the hfc for the β -hydrogen in 68 as 1.3 G - 1.7 G, which is close to the experimental value (2.5 G).

The reversibility of the reaction represented by eq.33 has already been mentioned in connection with the vinyl group migration (Section 1.2.2). The reverse reaction is known to be very slow ($k_{(-33)} = 4 \times 10^3 \text{ s}^{-1}$ at 25°C)¹¹⁹ when compared with the forward reaction ($k_{33} = 2 \times 10^8 \text{ s}^{-1}$).¹²⁰ This explains the inability of the esr technique to detect any signals from the cyclopropylmethyl radical when 3-butenyl radicals are generated in the cavity of the esr instrument even at temperatures below -140°C .

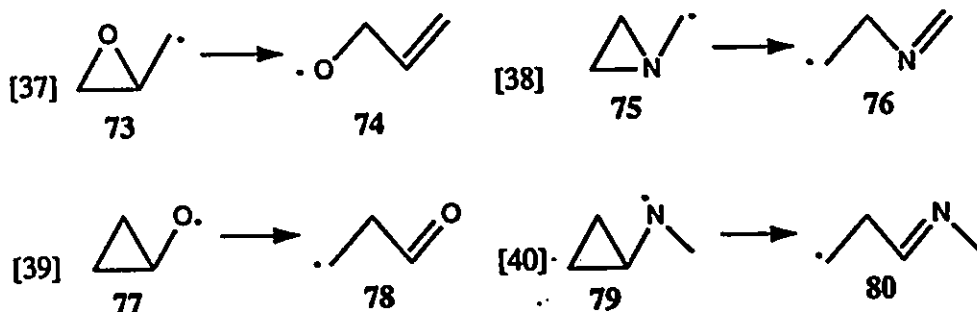
The cyclopropylmethyl and related radical rearrangements are sensitive to

stereoelectronic effects.¹²¹ The ring opening occurs by the preferential fission of the β,γ -bond which lies closest to the semi-occupied p-orbital. For example, the isomeric steroid radicals **69** and **70** rearrange specifically to **71** and **72**, respectively.¹²¹



It is observed from eq.36 that, of the two possible modes of ring-opening, the less stable primary radical **72** is formed in preference to the more stable secondary radical **71**. A similar stereo-electronic effect has already been mentioned for the cyclization of the 5-hexenyl radical (Scheme 2), where the less stable primary radical is formed in preference to the secondary radical.

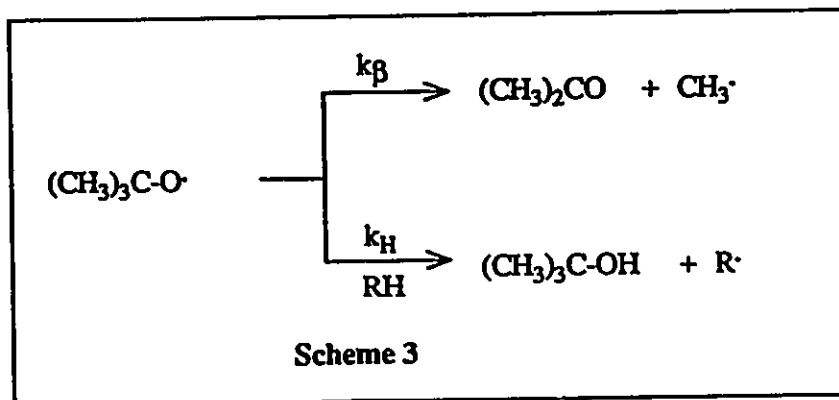
A number of radicals related in structure to the cyclopropylmethyl system are known to undergo ring-opening reactions. For example, heterocyclic radicals like **73**¹²² and **75**¹²³ and hetero-atom centered radicals like **77**¹²⁴ and **79**¹²⁵ are known to rearrange to the corresponding ring-opened products (eq.37-40).



1.3.0 FREE RADICAL CLOCKS

The absolute rate constants for many radical reactions have been extensively used to quantitate the rate constants for other radical processes. The term "free radical clock" has been introduced first by Griller and Ingold¹²⁶ to describe any unimolecular radical reaction or a radical molecule reaction for which the absolute rate constant is known. The importance and many practical applications of free radical "clocks" were clearly demonstrated by the above authors in the article, "*Free-Radical Clocks*".¹²⁶ This is one of the most extensively quoted reviews in radical kinetics, ever since its publication in 1980. Over 30 unimolecular reactions and their absolute rate constants together with their Arrhenius parameters are given in this article.

The β -scission of t-butoxy radical is a classical example of a simple radical clock used to measure relative rates of hydrogen abstraction from various substrates. The reaction of the t-butoxy radical with a hydrogen donor, RH, involves the following competition kinetics (Scheme 3).



At low conversions of RH, when the concentration of RH remains approximately constant, the ratio of rate constants expressed by eq.41 can be calculated simply from the relative concentrations of the products, t-butyl alcohol and acetone.¹²⁶

$$[41] \quad \frac{(\text{CH}_3)_2\text{CO}}{(\text{CH}_3)_3\text{COH}} = \frac{k_\beta}{k_H [\text{RH}]}$$

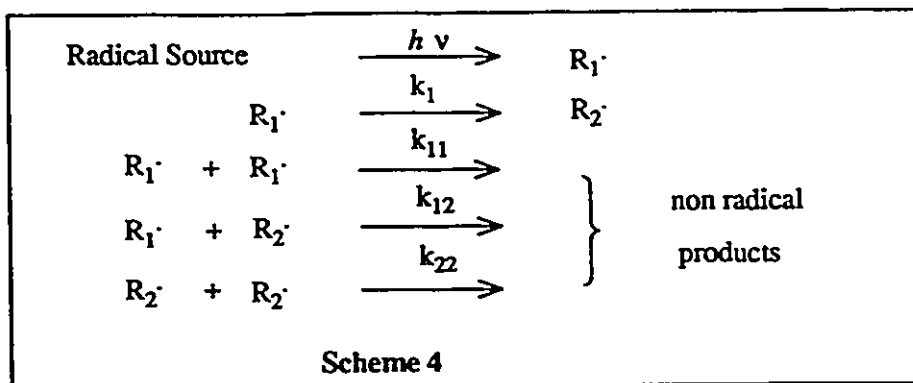
If the rate constant (k_β) for the β -scission is known, it is possible to calculate the rate constant for the hydrogen abstraction, k_H . Here the β -scission of t-butoxy radical acts as a timing device for measuring the rate constant for hydrogen abstraction. But if a separate experiment is done with another substrate, $R'H$, under conditions of the same temperature and solvent, the ratio of rate constants k_H/k'_H can be obtained from the product ratios and the substrate concentrations, since the rate constant for β -scission, k_β , being constant, cancels out.

1.3.1 Calibration of "clocks" for solution kinetics

A large amount of kinetic data is available for unimolecular reactions in the gas phase.¹²⁷ Since they are not transferable to solution phase kinetics, new techniques have been developed for measuring the rate constants in solution. A general and most extensively used procedure for the determination of rate constants for unimolecular radical reactions in solution is the kinetic esr method developed by Ingold and co-workers.¹²⁸

The principle is very simple. A radical $R_1\cdot$, whose rate constant for rearrangement to $R_2\cdot$ has to be determined, is generated in the cavity of an esr spectrometer by suitable photochemical techniques. The temperature of the sample is adjusted so as to observe the spectra of both $R_1\cdot$ and $R_2\cdot$, and their absolute concentrations are determined by integration and calibration of their signals against standard DPPH (2) using conventional techniques.^{129,130} Assuming that the radicals undergo reactions according to Scheme 4, the following rate laws were derived¹⁴² for steady state photolysis condition.

Using eq.42, the ratio of rate constants k_1/k_{22} can be obtained from the absolute concentrations of the unrearranged ($R_1\cdot$) and the rearranged ($R_2\cdot$) radicals. The diffusion controlled rate constant¹³¹ for the radical coupling can be determined experimentally¹³² or can be calculated from the viscosity of the reaction medium¹³³ and therefore k_1 can be estimated.



$$\frac{d [R_2^\cdot]}{d t} = 0 = k_1 [R_1^\cdot] - 2 k_{12} [R_1^\cdot] [R_2^\cdot] - 2 k_{22} [R_2^\cdot]^2$$

$$\text{or, } \frac{1}{[R_2^\cdot]} = \frac{2 k_{12}}{k_1} + \frac{2 k_{22} [R_2^\cdot]}{k_1 [R_2^\cdot]}$$

$$\text{if } k_{12} = k_{22} = k_{\text{diffusion}}, \text{ then :}$$

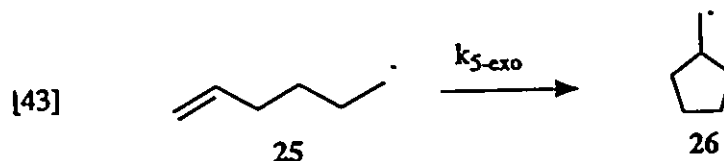
$$[42] \quad \frac{k_1}{2 k_{22}} = [R_2^\cdot] \left\{ 1 + \frac{[R_2^\cdot]}{[R_1^\cdot]} \right\}$$

The esr technique enables one to determine the rate constant for radical isomerization reactions at various temperatures, provided the signals of both R_1^\cdot and R_2^\cdot can be measured and quantitated. To reduce experimental error, the concentrations of radicals are measured under conditions where $[R_1^\cdot]/[R_2^\cdot] = 0.2$ to 5. The usual concentrations of radicals, which undergo self reactions at diffusion controlled rates (k_{diff} is in the range 10^9 - $10^{10} \text{ M}^{-1}\text{s}^{-1}$ at 25°C for most common solvents), that can be generated by conventional methods are in the range 10^{-6} - 10^{-8} M in solution.^{132,134} Therefore, the rearrangement rate constants that can be measured conveniently using the kinetic esr technique lie between 10^2 to 10^4 s^{-1} .¹²⁶ Thus, for fast radical isomerization reactions such as the 5-hexenyl or the cyclopropylmethyl rearrangement, the esr technique requires very low temperatures so as to observe both rearranged and the unrearranged radicals.

The most important use of the free radical clocks is for the determination of rate constants for radical-molecule reactions which are otherwise difficult to measure experimentally. Detailed discussion about the relevant clocks and the methodologies for rate constant studies will be presented under appropriate sections below.

1.3.2 The 5-hexenyl radical clock

The cyclization of the 5-hexenyl radical to the cyclopentylmethyl radical (eq.43) is



the most extensively studied and used free radical clock reaction.

The rate constant ($k_{5\text{-exo}}$) for this reaction has been estimated by Carlsson and Ingold¹³⁴ as early as 1968. They used the literature data¹³⁵ for the ratio of rate constants for the isomerization ($k_{5\text{-exo}}$) to the rate constant for H-abstraction (k_H) from Bu_3SnH by the 5-hexenyl radical. From the rate constant ratio ($k_{5\text{-exo}}/k_H = 0.1$)¹³⁵ and their experimental value, for $k_H = 1 \times 10^6 \text{ M}^{-1}\text{sec}^{-1}$ at 25°C ,¹³⁴ the rate constant for the 5-hexenyl radical cyclization was estimated as $1 \times 10^5 \text{ M}^{-1}\text{s}^{-1}$ at 25°C .

Ever since the rate constant was first estimated, the 5-hexenyl radical rearrangement has been used to 'clock' other radical-molecule reactions in solution.¹³⁶⁻¹⁴⁰ Since the rate constant for this clock was available only for 25°C , its initial application was limited to studies at or near room temperature.

In 1974 Ingold et al¹⁴¹ published the temperature dependence of this rate constant over a range of temperatures from 188 to 228 K using the kinetic esr technique. The Arrhenius expression for the rate constant was given by eq.44, where $\Theta = 2.3 \text{ RT kcal/mol}$.

$$[44] \quad \log(k_{5\text{-exo}}/\text{s}^{-1}) = (10.7 \pm 1.0) - (7.8 \pm 1.0)/\Theta$$

Extrapolation with this equation to room temperature gives a value for the cyclization rate

constant at 25°C as $k_{5\text{-exo}} = 9.58 \times 10^4 \text{ s}^{-1}$. This estimated value¹³⁴ is about a factor of two less than the most recent value reported viz. $2.2 \times 10^5 \text{ s}^{-1}$ at 25°C,^{143,139} and the discrepancy probably means nothing more than that extrapolations of Arrhenius plots to calculate rate constants at a temperature far away from those at which they are actually determined can lead to errors. This Arrhenius expression had been used very extensively to calculate rate constants at and above room temperature to exploit the potential of the 5-hexenyl clock as a powerful kinetic probe in many radical-molecule reactions.¹³⁶⁻¹³⁸

Schmid, Griller and Ingold¹⁴² have reported a slightly modified Arrhenius expression (eq.45) for this rearrangement in 1979.

$$[45] \log (k_{5\text{-exo}}/\text{s}^{-1}) = (9.5 \pm 1.0) - (6.1 \pm 1.0)/\Theta$$

The most recent estimate of the rate constant for the 5-hexenyl rearrangement comes from the latest value for the rate constant for H- abstraction from Bu_3SnH by 1° alkyl radicals.¹⁴³ The Arrhenius expression for the rate constant (k_H) for the reaction $n\text{Bu}^\cdot + \text{Bu}_3\text{SnH} \rightarrow n\text{BuH} + \text{Bu}_3\text{Sn}^\cdot$ has been reported as eq.46, where $\Theta = 2.3 \text{ RT kcal/mol}$. By

$$[46] \quad \log (k_H/\text{M}^{-1}\text{s}^{-1}) = (9.07 \pm 0.24) - (3.69 \pm 0.32)/\Theta$$

substituting this value into the expression for the relative pre-exponential factor ($\log A_{5\text{-exo}}/A_H = 1.30 \pm .08$) and the relative activation energy ($E_{5\text{-exo}} - E_H = 3.16 \pm .10 \text{ kcal mol}^{-1}$) for the two competing reactions, they calculated the latest Arrhenius expression for the 5-hexenyl cyclization rate constant, eq. 47.¹⁴³

$$[47] \quad \log k_{5\text{-exo}}(\text{s}^{-1}) = (10.42 \pm .32) - (6.85 \pm .42)/\Theta$$

The following table is illustrative of the rate constants for the 5-hexenyl cyclization using the various reported Arrhenius expressions for this reaction. It is clear from Table 5

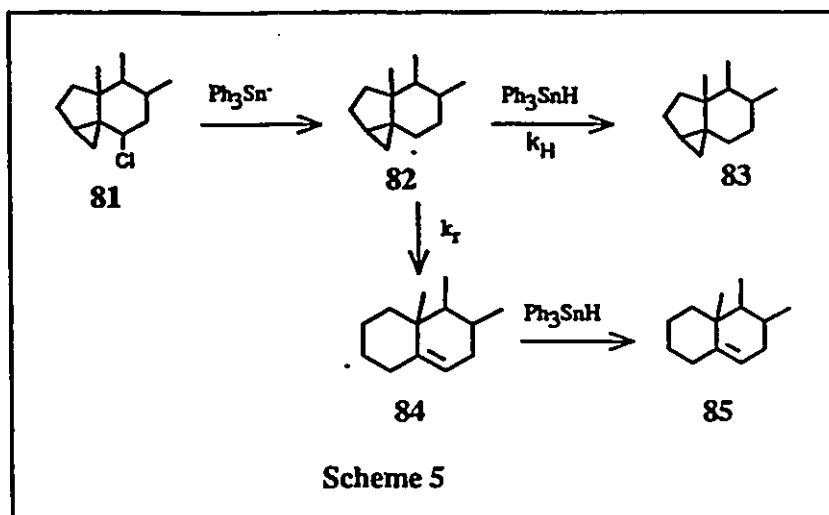
Table 5. Rate Constants for the 5-Hexenyl Radical Rearrangement Calculated using Different Arrhenius Expressions ¹⁴¹⁻¹⁴³					
Arrhenius Expression (log k =)	Rate constants ($k_{5\text{-exo}}$, sec ⁻¹)				Reference
	0°C	25°C	50°C	100°C	
10.7 - 7.7/θ	2.9×10^4	9.8×10^4	2.7×10^5	1.4×10^6	141
9.5 - 6.1/θ	4.2×10^4	1.1×10^5	2.4×10^5	8.5×10^5	142
10.4 - 6.9/θ	7.5×10^4	2.2×10^5	5.4×10^5	2.2×10^6	143

that even though these different sets of expressions come from very different experimental techniques, the rate constants calculated from these equations span only a very narrow range at a given temperature. This simply means that there is no major revision needed for the literature kinetic data which are derived from the previous Arrhenius expressions for the 5-hexenyl radical clock.

1.3.3. The cyclopropylmethyl radical clock

The cyclopropylmethyl to 3-butenyl radical isomerization (eq.33) is one of the fastest free radical clocks. The first reported rate constant for this type of a rearrangement seems to be that estimated by Carlsson and Ingold¹³⁴ based on Cristol and Barbour's¹⁴⁴ experimental data on the reduction of 6β-chloro-3α,5α-cyclocholestane (cyclocholesteryl chloride, 81) with triphenyltin hydride. The reaction is given in Scheme 5. The attack of triphenyltin radical on the chloride 81 yields 82. The rearrangement of 82 to 84 competes with the H-abstraction from Ph₃SnH to form 83.

The rate constants for this rearrangement (82 → 84) were calculated using the



expression $k_r = k_H [\text{Ph}_3\text{SnH}] [83/85]$. The data given in Table XIV of ref.134 can be recalculated based on the recent estimate of the rate constant for H-abstraction by cyclohexyl radical from Bu_3SnH ($\log k_H = 9.24 - 3.97 \theta$, where $\theta = 2.3 \text{ RT kcal mol}^{-1}$).¹⁴³ The calculated results based on an estimated 5-fold increased reactivity of triphenyltin hydride¹³⁴ relative to the tributyltin hydride are given in Table 6.

In order to use the cyclopropylmethyl radical rearrangement as a kinetic standard, Maillard, Forrest, and Ingold¹⁴⁵ determined its rate constant in 1976. They used the well-established kinetic esr method as a tool for its determination, over the temperature range 128 - 153 K. The Arrhenius expression for this rate constant was given as:

$$[49] \log(k/s^{-1}) = (12.48 \pm 0.85) - (5.94 \pm 0.57)/\theta$$

where $\theta = 2.3 \text{ RT kcal mol}^{-1}$. This expression, after correction for a minor arithmetical error¹⁴⁶ in the derivation, becomes expression [50] for the rate constant.

$$[50] \log(k/s^{-1}) = (11.34 \pm 0.85) - (5.94 \pm 0.57)/\theta$$

Table 6. Estimated rate constants for the cyclocholesteryl radical rearrangement (see text) using the latest published data^{143,144}

T (°C)	k_H (Bu ₃ SnH) ^a	k_H (Ph ₃ SnH) ^b	[83]/[85]	[Ph ₃ SnH] (M)	k_r (M ⁻¹ sec ⁻¹)
30	2.38×10^6	11.92×10^6	6.3	~ 4.0	2.56×10^8
15	1.69×10^6	8.46×10^6	25	0.4	8.46×10^7
15	1.69×10^6	8.46×10^6	100	0.04	3.38×10^7
-15	7.55×10^5	3.78×10^6	2.3	1.0	8.69×10^6
-20	6.48×10^5	3.24×10^6	4.5	0.08	1.17×10^6

^acalculated for cyclohexyl radical from ref.144

^bbased on estimated 5-fold excess reactivity for triphenyltin hydride relative to tributyl system (see text)

From this expression the rate constant at 25°C can be calculated as $k_i = 9.7 \times 10^6 \text{ s}^{-1}$. This value is an order of magnitude less than that calculated from the faulty equation [49] viz. $1.3 \times 10^8 \text{ s}^{-1}$. Eq.50 gives a rate constant at 30°C as $1.14 \times 10^7 \text{ s}^{-1}$, which is an order of magnitude less than that for the similar rearrangement of cyclocholesteryl radical 82 (see Table 6). According to theoretical predictions¹⁴⁵ the pre-exponential factor for the cyclopropylmethyl radical rearrangement is expected to be close to 10^{13} s^{-1} , which is substantially larger than the experimental value ($10^{11.34}$). This situation necessitated a re-calibration of this fast radical clock at and near room temperature.

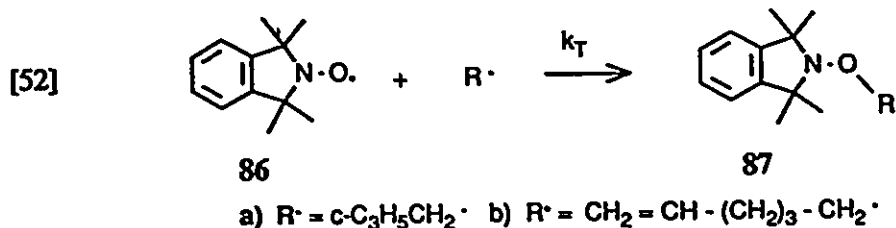
In 1986 Mathew and Warkentin¹⁴⁷ determined the rate constant for the cyclopropylmethyl radical rearrangement over the range 30-89°C. Competition kinetics involving the rearrangement and the diffusion controlled capture by a stable nitroxyl radical

was employed for the calibration of the isomerization rate constant.

It was really pleasing to observe that an Arrhenius plot ($\log k_i$ vs. $1/T$) for our own experimental points¹⁴⁷ passed through the majority of points from the low temperature kinetic epr data by Ingold.¹⁴⁵ This result indicated that both sets of experimental data should be combined to derive an Arrhenius expression for the cyclopropylmethyl radical rearrangement covering a wide range of temperatures (128-362 K). The least squares treatment of the combined data gives the following rate expression (eq.51) for the cyclopropylmethyl radical rearrangement. This expression yields the rate constant at 25°C as $2.1 \times 10^8 \text{ s}^{-1}$.

$$[51] \quad \log(k/\text{s}^{-1}) = (13.9 \pm 0.4) - (7.6 \pm 0.2)/\theta$$

The derivation of eq.51 involved the assumption that the rate constant for the reaction between the nitroxyl radical 86 and cyclopropylmethyl radical (eq.52,a) is diffusion-controlled. However Beckwith, Bowry, and Moad were able to determine the rate



$$[53] \quad \log(k_T) = 9.7 - 0.9/\Theta, \text{ where } \Theta = 2.3 \text{ RT kcal/mol}$$

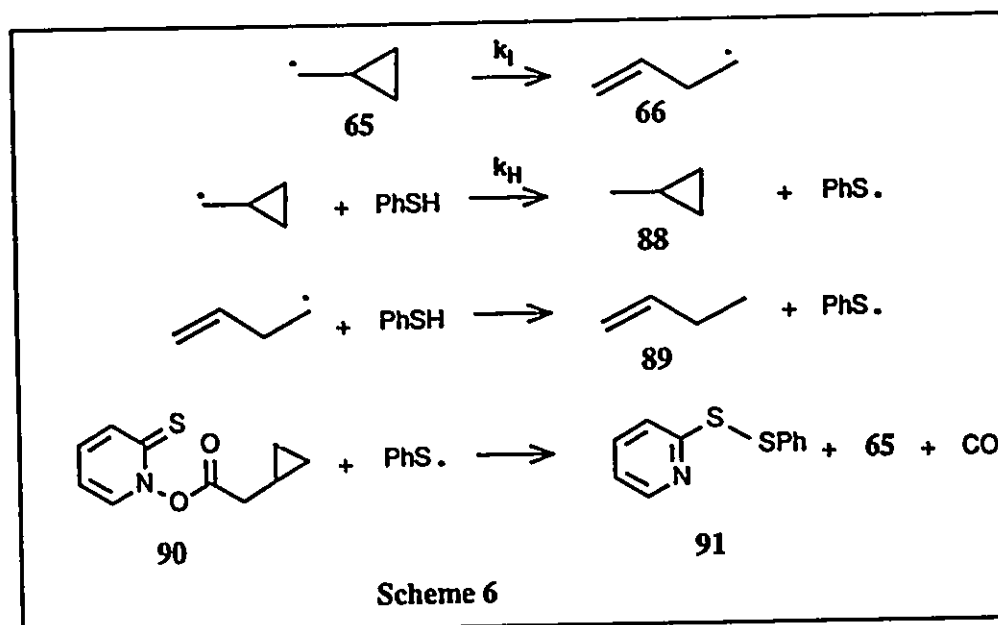
constant for a primary radical combination with 86 using the 5-hexenyl radical clock.¹⁴⁸ The temperature dependence of the 5-hexenyl radical attack (eq.52, b) on 86 is given as eq.53,¹⁴⁸ which gives the rate constant at 25°C as $1.1 \times 10^9 \text{ M}^{-1} \text{ s}^{-1}$. The above rate constant is a factor of two smaller than that which we assumed, based on a diffusion-controlled reaction. Recalculation of our data,¹⁴⁷ using the new coupling rate constants calculated from eq.53, give values which are in excellent agreement with those reported by Beckwith¹⁴⁸ and by

Newcomb.¹⁴⁹

Beckwith, Bowry, and Moad¹⁴⁸ did an independent estimate of the rate constant, using the same competition system that we used. They obtained the rate constant for the cyclopropylmethyl radical rearrangement in the temperature range 40-130°C as eq.54, where $\theta = 2.3 RT$ kcal/mol. From this equation, the rate constant at 25°C becomes $7.5 \times 10^7 \text{ s}^{-1}$.

$$[54] \quad \log (k/s^{-1}) = 13.3 - 7.4/\theta$$

Probably the most recent estimate of the rate constant for the cyclopropylmethyl radical rearrangement is by Newcomb and Glenn.¹⁴⁹ They employed a kinetic procedure, involving the ring opening of cyclopropylmethyl radical in competition with the H-abstraction from thiophenol by cyclopropylmethyl radical, according to Scheme 6. This elegant and



unique approach for the study of fast radical rearrangements deserves special mention. In this experiment the pyridothione ester 90 was employed as the cyclopropylmethyl radical source. Developed by Barton,¹⁵⁰ the pyridothione esters find increasing application as excellent

radical precursors for many kinetic studies requiring the formation of radicals in a chain reaction.^{149,151-153} Thiophenol is used as the trapping reagent which transfers the H-atom to cyclopropylmethyl radical in competition with the isomerization reaction.

The rate constant for the rearrangement was calculated using eq.55, where k_H is the rate constant for the H-atom transfer, and $[\text{PhSH}]_m$ is the average concentration of thiophenol over the course of reaction. The rate constants (k_H) for H-abstraction from PhSH by primary,

$$[55] \quad k_i = k_H[\text{PhSH}]_m[89]/[88]$$

secondary, and tertiary radicals were reported recently by Franz et.al¹⁵⁴ and, therefore, by substituting the appropriate value for k_H in eq.55, the rate constant for the cyclopropylmethyl radical rearrangement was calculated. The temperature dependence of the rate constant in the range -37 to 50°C is given as eq.56, where $\Theta = 2.3RT$ kcal/mol. Eq.56 gives the rate constant

$$[56] \quad \log (k/s^{-1}) = (13.0 \pm 0.14) - (6.8 \pm 0.2)/\Theta$$

at 25°C as $1.0 \times 10^8 \text{ s}^{-1}$, which is slightly higher than the value ($7.5 \times 10^7 \text{ s}^{-1}$) reported by Beckwith,¹⁴⁸ and a factor of two less than that ($2.1 \times 10^8 \text{ s}^{-1}$) reported by us.¹⁴⁷

Combining the data (in the range -145 to -120°C) by Ingold¹⁴⁵ and that (in the range 40 to 130°C) by Beckwith¹⁴⁸ with their own (in the range -37 to 50°C), Newcomb and Glenn obtained eq.57 for the rate constant for cyclopropylmethyl radical clock,¹⁴⁹ which leads to $k_i^{25^\circ\text{C}} = 9.6 \times 10^7 \text{ s}^{-1}$.

$$[57] \quad \log (k/s^{-1}) = 13.15 - 7.05/\Theta, \text{ where } \Theta = 2.3RT \text{ kcal/mol.}$$

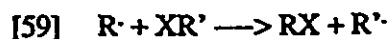
Finally, the latest rate constant for this rearrangement is the one reported by Beckwith and Bowry (eq.58).¹⁵⁵ In addition to the data used by Newcomb to derive eq.57, the authors combined the data from our laboratory as well to derive eq.58 which gives the rate constant at 25°C as $9.7 \times 10^7 \text{ s}^{-1}$.

$$[58] \quad \log (k/s^{-1}) = 13.31 - 7.26/\Theta$$

1.4.0. INTERMOLECULAR RADICAL REACTIONS

Intermolecular radical reactions can be broadly classified into radical-molecule (viz. substitution and addition) reactions and radical-radical (viz. coupling and disproportionation) reactions. In this section we deal only with the former class of reactions.

The main classes of radical-molecule reactions are the atom abstraction or substitution reactions, eq.59 (which are generally called S_H2 : substitution, homolytic, bimolecular processes), and radical additions to multiple bonds. S_H2 processes can occur either by a direct displacement of an atom such as hydrogen or halogen (eq.59), or by an addition followed by an elimination reaction (eq.60).



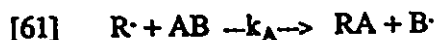
One of the most extensively studied S_H2 reactions is the H-abstraction from a variety of trialkyl and aryl-tin hydrides by a number of carbon-centered radicals.^{134,143} A great amount of kinetic data is also available for reactions at various C-H bonds.¹⁵⁶ Hydrogen atoms attached to other atoms like oxygen^{157,158} and sulfur¹⁵⁴ are also known to undergo homolytic substitution reactions. The rate constants for some of these processes are known,¹⁵ but for a larger number of reactions the absolute rate constants are yet to be determined. A class of S_H2 processes for which there exists only a limited number of rate constant data in the literature are the halogen abstractions by alkyl radicals from halo compounds. For example, polyhalo compounds such as CCl_4 , CBr_4 , CCl_3Br , CHI_3 are known for a long time to undergo radical substitution at the halogen. Until recently, the absolute rate constants for many of these reactions were only "guesstimates". Radical additions to multiple bonds are among the most significant and extensively investigated free radical-molecule reactions,

probably because of their well-exploited applications in the polymer industry. The different classes of radical-molecule reactions and their rate constants will be considered in a little more detail in the next few subsections. This section is intended to introduce to the new reader how the rate constants for some important radical-molecule reactions are determined experimentally.

1.4.1. Radical substitution reactions

(i) Determination of rate constants for substitution (S_H2) reactions

There is no simple and direct method for determining the rate constants for radical substitution reactions.^{15b,126} For a reaction such as eq.61, where a radical $R\cdot$ reacts with a substrate molecule AB to form RA and $B\cdot$, the rate of the reaction can be expressed in terms of the rate constant k_A and the concentrations of the radical $[R\cdot]$ and of the substrate $[AB]$ (eq.62)



$$[62] \quad -d[AB]/dt = d[RA]/dt = k_A[R\cdot][AB]$$

In order to calculate the rate constant (k_A) for this reaction, the concentrations of the radical $[R\cdot]$ and the substrate $[AB]$ should be accurately known. Because of the very high reactivity of most radicals, their steady state concentrations in solutions are very low ($\sim 10^{-7}M$ for carbon centered radicals in non-polar solvents)¹³⁴ and in fact the accurate measurements of radical concentrations are often difficult. Therefore, it is a common practice to express the relative rate constants for two chemically similar reactions. For example, if the radical $R\cdot$ is allowed to compete for AB and another substrate CD in a mixture, the rate of the competing reaction (eq.63) can be given as eq.64.



$$[64] \quad -d[CD]/dt = d[RC]/dt = k_C [R\cdot] [CD]$$

By dividing [62] by [64], the relative rate constant k_A/k_C can be expressed as eq.65.

$$[65] \quad \frac{-d[AB]/dt}{-d[CD]/dt} = \frac{d[RA]/dt}{d[RC]/dt} = \frac{k_A \times [AB]}{k_C \times [CD]}$$

Under conditions where the concentrations of AB and CD remain constant during reaction, integration and rearrangement of eq.65 leads to eq.66.

$$[66] \quad k_A/k_C = [RA]/[RC] \times [CD]/[AB]$$

From the product ratio, $[RA]/[RC]$, and from the concentrations of the substrates, $[AB]$ and $[CD]$, the relative rate constant (k_A/k_C) can be readily calculated. For this reason, the literature data are much more numerous for relative rate constants than for the absolute rate constants for radical- molecule reactions.¹⁵

An illustration of this can be given from the work of Danen and Saunders.¹⁵⁹ They determined the rate constants for the abstraction of iodine (k_I) from aromatic iodides relative to the rate constant of chlorine abstraction (k_{Cl}) from CCl_4 by phenyl radicals. Thus for iodine abstraction from o-nitroiodobenzene the relative rate constant $k_I/k_{Cl} \approx 186$.

The rate constants for iodine abstractions by phenyl radicals from a variety of aliphatic iodides, relative to the bromine abstraction rate constant (k_{Br}) from $BrCCl_3$, were also reported.¹⁶⁰ For ethyl iodide, the relative rate constant reported is $k_I/k_{Br} = 0.33$.

It follows from eq.66 that if the absolute rate constant for one of these reactions, say k_C , is known, then from the measured relative rate constant, k_A/k_C , the rate constant k_A for

the competing reaction can be calculated. Thus for the two specific examples given in the previous paragraphs, the absolute rate constant k_I for the abstraction of iodine by phenyl radicals could be calculated if the rate constants for the competing reactions k_{Cl} and k_{Br} were known.

Measurements of the rate constants for radical-molecule reactions are now possible by the use of radical clocks. A variety of 'clocks' with a wide range of rate constants (10^3 - 10^9 s^{-1}) are available as kinetic standards,¹²⁶ as already explained in Section 1.3. The principle is very simple. Suppose in reaction [59] the radical $R\cdot$ undergoes a rearrangement ($R\cdot \rightarrow R'\cdot$) to the isomeric radical $R'\cdot$ with a known rate constant say k_i , and also suppose that k_i is of the right order of magnitude so as to compete effectively with the radical molecule reaction represented by [59]. Now, both $R\cdot$ and $R'\cdot$ will react with AB to form RA and R'A, respectively. The ratio, $[RA]/[R'A]$, of the product concentrations can now be expressed in terms of the ratio of rate constants (k_A/k_i) according to eq.67, under pseudo first order conditions.

$$[67] \quad [RA]/[R'A] = k_A/k_i [AB]$$

The reliability of rate constants calculated using radical clocks depends mostly on the accuracy of the 'clock' itself. Because of its extensive calibration over a wide range of temperatures, and also because of the agreement in the rate constants and Arrhenius parameters determined using different experimental techniques, the 5-hexenyl radical cyclization (Section 1.3.1) is one of the most extensively used free radical clocks. Another reason for its versatility can be attributed to its isomerization rate constant (2×10^5 s^{-1} at 25 °C) which is of the same order of magnitude as those of many radical-molecule reactions of interest.¹²⁶ However, its use is limited to reactions having rate constants in the range of 10^3 - 10^7 $M^{-1} s^{-1}$.

In order to determine rate constants in the range 10^7 - 10^{10} $M^{-1} s^{-1}$, the

cyclopropylmethyl radical rearrangement (Section 1.3.2) can serve as an excellent clock since the Arrhenius parameters are known over a wider range (-145 °C to 130 °C) of temperatures including values at and around room temperature.¹⁵⁵ The rate constant for isomerization of cyclopropylmethyl radical at room temperature is $1 \times 10^8 \text{ s}^{-1}$. The 5-hexenyl and the cyclopropylmethyl radical clocks together cover almost the entire range of rate constants for most radical-molecule reactions that can be studied experimentally.

It should also be emphasized that in competition kinetic studies for the determination of absolute rate constants, a proper choice of a 'clock' reaction is very important. The most common analytical techniques for rate constant measurements rely on determination of the relative rates of formation of the products or the consumption of the reagents. The greater the difference between the rates of the two reactions, the greater the error in the estimation of the relative rate constants.

(ii) Temperature dependence of rate constants

There are two general forms of representing the variation of rate constants for any reaction as a function of temperature. One is called the Arrhenius expression [68], where k is

$$[68] \quad k = A e^{-E_a/RT}$$

the rate constant for a particular reaction at any temperature, T . A is called the pre-exponential factor and E_a is the activation energy. By taking logarithms on both sides of the eq.68, and by rearranging, the most common form of the Arrhenius expression (eq.10) is obtained. The units of A are the same as those of the rate constant k . For a unimolecular

$$[69] \quad \log k = \log A - E_a/2.3 RT$$

process the unit is sec^{-1} (or s^{-1}) and for a bimolecular process it is $\text{M}^{-1}\text{s}^{-1}$. E_a has the same units as that of the gas constant R , and is usually expressed in kcal mol^{-1} .

The second form of the expression, commonly known as the Eyring equation (eq.70),

where k is the Boltzman constant and h is the Planck's constant), comes from the transition

$$[70] \quad k = \frac{(ekT/h)}{e^{\Delta S^\ddagger/R}} e^{-\Delta H^\ddagger/RT}$$

state theory.¹⁶¹ In this form, the rate constant k is expressed in terms of the thermodynamic quantities such as entropy of activation ΔS^\ddagger and the enthalpy of activation ΔH^\ddagger .

Comparing eq.69 and eq.70, the pre-exponential factor A and the activation energy E_a can be identified in terms of the enthalpy and entropy of activation as is given in eq.71 and eq.72.

$$[71] \quad A = (ekT/h) e^{\Delta S^\ddagger/R}$$

$$[72] \quad E_a = \Delta H^\ddagger + RT$$

At 298 K, (ekT/h) becomes $10^{13.2}$, and therefore A is simplified to $A = 10^{13.2} e^{\Delta S^\ddagger/R}$ at room temperature.

So far the majority of thermodynamic data available are for reactions in the gas phase.¹⁶¹ Entropies of activation for many gas-phase reactions are known from experimental data. These results are, for a limited number of reactions, in good agreement with theoretical predictions.¹⁶² However, since there is no way of knowing the exact geometry of the transition state, there have been instances where theoretical results differ widely from the experimental data.

It is generally observed that for a bimolecular reaction $\log(A/M^{-1} s^{-1})$ values range from 7 to 12, and for the majority of reactions it is about 8.5 ± 0.5 . This corresponds to an entropy of activation of 20 ± 5 gibbs/mol. Usually the entropy change in the transition state reflects the changes in the internal rotational and vibrational degrees of freedom in the transition complex, relative to the ground state. For relatively bigger transition complexes, the pre-exponential factors are small. For example, for the reaction between H atom and CH_4 to give H_2 and CH_3 the pre-exponential factor is $10^{11 \pm 0.5}$ whereas for H-abstraction by

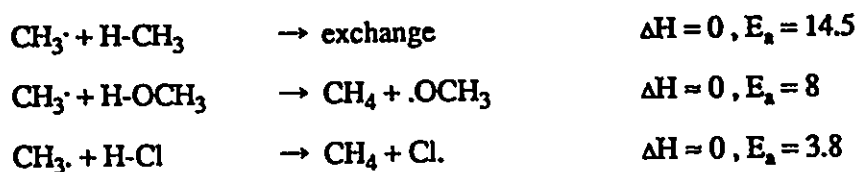
methyl radical from CH_4 , C_2H_6 or $\text{HC}(\text{CH}_3)_3$ it is $10^{8.5 \pm 0.5} \text{ M}^{-1} \text{ s}^{-1}$.¹⁶²

Due to the development of new and improved mathematical calculations, it has been possible to predict some of these thermochemical quantities by the logical assumption of the transition states.¹⁶¹

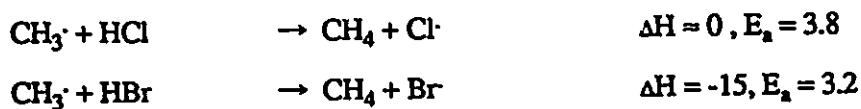
As has been explained by Ingold¹⁶² there is no simple and general rule for predicting the activation energies for radical-molecule reactions. One of the earliest predictions by Polanyi¹⁶³ (eq.73) met with only little success. For exothermic reactions the activation

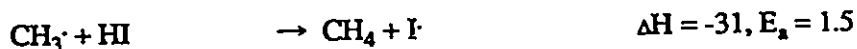
$$[73] \quad E_a = E_0 + \alpha(\Delta H)$$

energy E_a was given as the sum of the intrinsic energy E_0 and a fraction of the heat of reaction ΔH (eq 73). For a homologous series E_0 and α were assumed to be constant and for many gas phase reactions $E_0 \approx 11.5 \text{ kcal/mol}$ and $\alpha \approx 0.25$.¹⁶⁴ Even though this relation gives satisfactory results for H-abstraction reactions by methyl radicals from alkanes, for other homologous series these crude predictions are unsuccessful. The inadequacy of the above equation has been elegantly demonstrated by Benson and DeMore¹⁶⁵ by considering the following thermoneutral reactions, where ΔH and E_a are in kcal/mol.



It is obvious that even though the reactions are almost thermoneutral the activation energies range from 3.8 to 14.5 kcal/mol. Another example illustrated is the insensitivity of E_a to ΔH , which is reflected in the following equations, where ΔH and E_a are all in kcal/mol.





Benson and DeMore's review¹⁶⁵ also mentions some other empirical equations^{166,167} for the calculation of activation energies. As the above authors have pointed out, the majority of gas phase radical-molecule reactions have activation energies of 8 ± 3 kcal/mol, and the empirical relations in the most ideal cases are accurate only to about ± 2 kcal/mol. Because of the similarities of activation energies for many reactions and the uncertainties in the theoretical values, the empirical relations have only little practical importance.

A more accurate and comprehensive method for determining activation energies has been developed by Zavitsas.¹⁶⁸ The activation energy for H atom transfer reactions such as eq.74 has been expressed as the sum of two terms, the first being the bonding energy of the



$$[75] \quad E_a = 0.5 ({}^1E_{\text{XH}} + {}^1E_{\text{HY}}) + {}^3E_{\text{XY}}$$

triatomic transition state, which is the average of the sum of the bond energies $\{0.5[{}^1E_{\text{XH}} + {}^1E_{\text{HY}}]\}$ and the second term is the antibonding energy (${}^3E_{\text{XY}}$) between X and Y (eq.75), where 1E and 3E are given by the Morse function¹⁶⁹ (eq. 76, 77), where D_e is the

$$[76] \quad {}^1E = D_e \{ (1 - e^{-a(r-r_e)})^2 - 1 \}$$

$$[77] \quad {}^3E = f D_e \{ (1 + e^{-a(r-r_e)})^2 - 1 \}$$

observed dissociation energy (D_0) plus the zero point energy ($0.001431 w_0$), and 'r' is the internuclear distance, ' r_e ' the equilibrium distance between the nuclei, 'f' is a constant and 'a' is a spectroscopic constant given by eq.78, where w_0 is the equilibrium vibrational frequency of the bond in cm^{-1} , and μ is the reduced mass in atomic mass units.

$$[78] \quad a = 0.1218 w_0 \{ \mu/350 D_0 \}^{1/2}$$

Table 7 represents some of the reactions and their rate constants calculated using [75].¹⁶⁸ The Table is just a demonstration of how theoretical predictions can compliment the

Table 7. Gas-phase data for the activation energy of some hydrogen transfer reactions of methyl radicals: $\text{RH} + \text{CH}_3\cdot \rightarrow \text{R}\cdot + \text{CH}_4$		
R-H	Activation Energy, E_a (kcal/mol)	
	Calculated	Experimental
H-H	11.7	10 - 13
$\text{CH}_3\text{-H}$	13.7	13.8 - 14.8
$\text{CH}_3\text{CH}_2\text{-H}$	11.0	11 - 12
$(\text{CH}_3)_2\text{CH-H}$	10.3	9 - 10.5
$(\text{CH}_3)_3\text{C-H}$	7.6	6.6 - 9
$n\text{-C}_6\text{H}_{11}\text{-H}$	9.3	8.3 - 9.5
$\text{CH}_3\text{-O-CH}_2\text{-H}$	8.9	8.3 - 9.5
$\text{CH}_3\text{-O-H}$	10.0	6.5 - 9
$\text{HOCH}_2\text{-H}$	8.9	8 - 10
Br-H	1.7	1 - 2
$\text{CCl}_3\text{-H}$	6.4	5.8 - 6.8

experimental observations in many gas phase reactions. This is not the case with solution phase kinetics. Polar effects of the solvent, in many cases, can affect the activation energies of solution phase reactions. But it has been suggested by Ingold¹⁶² that for radical reactions in non-polar, non-polarizable solvents which do not have any complexing effect on the radicals, the data from gas-phase calculations can provide useful approximations.

(iii) Solution phase kinetic data for some $\text{S}_{\text{H}}2$ processes

H-abstraction from Bu_3SnH by alkyl radicals.

One of the the most synthetically as well as kinetically useful $\text{S}_{\text{H}}2$ reactions is the H-atom abstraction from alkyl and aryl tin hydrides by a variety of carbon centered radicals.

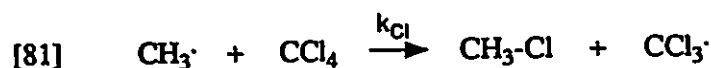
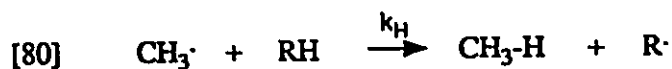
The rate constants for radical attack on tributyltin hydride ($n\text{-Bu}_3\text{SnH}$) is reported to range between $1.5 \times 10^5 \text{ M}^{-1}\text{s}^{-1}$ and $5.9 \times 10^7 \text{ M}^{-1}\text{s}^{-1}$ at 27°C , depending on the radical.^{143,170} An important application, as a kinetic standard for the above reaction, has already been discussed in connection with *free radical clocks* (Section 1.3).

H-abstraction from hydrocarbons and some rate constants

The H-atom abstractions from hydrocarbons by radicals and atoms (for example halogen, eq.79) are well known. The polar nature of the transition state and its influence on the reactivity and selectivity in these processes have been reviewed by Russell.¹⁵⁶



Even though the absolute values for many of these hydrogen abstraction processes are not known, the relative reactivities of a variety of C-H bonds toward radical attack are known. One of the earlier estimates of the relative reactivities of various hydrocarbons toward methyl radical is based on competition kinetics. Methyl radical was allowed to compete for H-abstraction (eq.80) from the alkane, and Cl-abstraction (eq.81) from carbon tetrachloride. The relative rate constant $k_{\text{H}}/k_{\text{Cl}}$ was then calculated from the ratio of the concentrations of the products and the reactants (eq.82).¹⁷¹

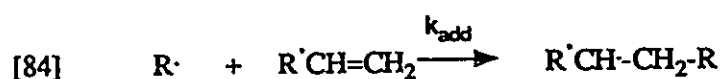


$$[82] \quad k_{\text{H}}/k_{\text{Cl}} = [\text{CH}_4]/[\text{CH}_3\text{Cl}] \times [\text{CCl}_4]/[\text{RH}]$$

Since k_{Cl} is a constant and does not depend on the hydrocarbon, by comparing the relative rate constants, $k_{\text{H}}/k_{\text{Cl}}$, of two different hydrocarbons, it is possible to get the relative

reactivities of the two hydrocarbons toward methyl radical. Several similar competition studies using phenyl and substituted phenyl radicals are also known.¹⁷²

Another type of competition kinetics involves the reaction of the radical in a mixture of the substrate hydrocarbon and an alkene (eq. 83, 84). For simple radicals ($R\cdot$), the determination of k_H/k_{add} is very difficult. However, in a radical polymerization, where $R\cdot$ represents the polymer radical, the above ratio is the chain transfer constant (see Section 1.4.2) for the substrate RH and can be easily calculated from the degree of polymerization.



For example, the observed chain transfer constant for toluene in the vinyl acetate polymerization ($R' = \text{CH}_3\text{COO}$) is $\approx 2 \times 10^{-3} \text{ M}^{-1} \text{ s}^{-1}$ at 60 °C and the propagation rate constant (k_{add}) is $1.01 \times 10^3 \text{ M}^{-1} \text{ s}^{-1}$ at 25 °C ($\approx 2 \times 10^3$ at 60 °C).¹⁷³ Therefore, the rate constant for H-abstraction by the polyvinyl acetate radical can be calculated as $(2 \times 10^{-3}) \times (2 \times 10^3) = 4 \text{ M}^{-1} \text{ s}^{-1}$ at 60 °C.

The rate constants for hydrogen abstraction by *sec*-octyl radicals from various substrates have been reported by Afanas'ev et al.¹⁷⁴ The rate constants (k_H) for H-abstraction are reported relative to the rate constant (k_I) for iodine abstraction by the same radical from ethyl iodide. The rate constants for H-transfer from acetone, toluene, and anisole relative to k_I are 0.0031, 0.031, and 0.0035 at 100 °C.¹⁷⁴ The same type of competition kinetics have also been employed by the above authors¹⁷⁵ to calculate rate constants for H-abstractions from CH_2Cl_2 , CHCl_3 , $\text{C}_2\text{H}_5\text{I}$, and 1-hexene (allylic hydrogen). The rate constants (k_H) relative to the rate constant (k_I) for iodine abstraction from ethyl iodide by the *sec*-octyl radical, $\text{CH}_3\text{CH}_2\text{CH}_2\text{CH}(\text{CH}_2)_3\text{CH}_3$, are: .0062, .24, 0.019, and 0.013, respectively. The absolute rate constants for some H-abstraction reactions, calculated from the chain transfer constants in various polymerization and competition studies have also been reported.¹⁷⁶ The rate

constants for H-abstraction (k_H) reactions for a few substrates, relative to the rate constant for iodine abstraction (k_I) from *n*-heptyl iodide, are given in Table 8.¹⁷⁶

Table 8. Rate constants (k_H) for the reaction of $n\text{-C}_9\text{H}_{19}\cdot$ with various substrates (R-H) relative to its k_I (<i>n</i> -heptyl iodide)			
R-H	k_H/k_I	Ct ^a	k_H^b ($\text{M}^{-1} \text{s}^{-1}$)
$\text{HCOOCH}_2\text{-H}$	0.376×10^{-3}	0.0037	6.70
$\text{NCCH}_2\text{-H}$	2.86×10^{-3}	0.0283	51.5
$\text{CH}_3\text{COCH}_2\text{-H}$	2.98×10^{-3}	0.0295	53.6
$\text{C}_6\text{H}_5\text{CH}_2\text{-H}$	2.56×10^{-3}	0.0254	46.2
$(\text{HOOC})_2\text{CH-H}$	9.90×10^{-2}	0.0980	178
HOOCCHCl-H	1.23×10^{-2}	0.1230	224

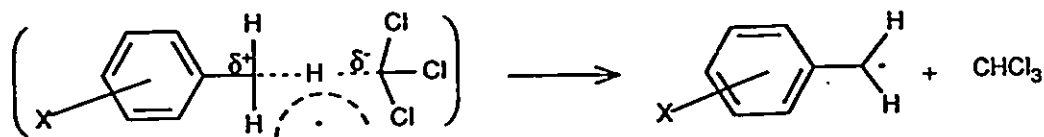
^a The chain transfer constant for the substrate, RX

^b Ct multiplied by the polymer chain propagation rate constant, $k_p = 1820 \text{ M}^{-1} \text{s}^{-1}$, at 110°C

(iv) Polar effects in S_H2 processes

Polar effects in the H-abstraction reactions have been well studied for both aliphatic and aromatic systems.¹⁷⁷ It has been observed that alkyl radicals attack at the α -position of propionic acid¹⁷⁸ whereas chlorination takes place predominantly at the β -carbon.¹⁵⁶ This has been attributed to the fact that alkyls are donor radicals. The transition states for H-abstractions by alkyl radicals from the α -carbon are more stabilized by the electron withdrawing COOH group. A chlorine atom is electrophilic and as a result the COOH group destabilizes the transition state for the attack of Cl atom at the α -hydrogen.

The H-abstractions from substituted toluenes by a variety of radicals have been subjected to the Hammett-type correlation¹⁷⁹ and it is observed that the ρ -values are always negative for attack of electrophilic radicals like Cl, Br, peroxy, *t*-butoxy, or trichloromethyl radicals when σ^+ constants¹⁸⁰ (since they give the best fit line) for substituents are used.¹⁸¹⁻¹⁸⁵ This is indicative of a positive charge developed at the benzylic carbon in the transition state.¹⁸¹ Groups which stabilize positive charge are known to increase the rate of



Scheme 7

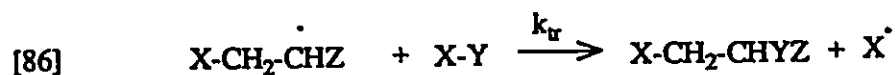
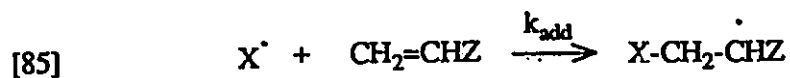
reaction. For the attack of $\text{CCl}_3\cdot$ radical on substituted toluene, the transition state can be represented as shown in Scheme 7.

1.4.2. Radical addition to multiple bonds

We have already seen a number of examples of radical addition reactions in connection with radical rearrangements (Section 1.2). This section deals only with some intermolecular radical addition reactions.

Several reagents XY are known to add to carbon-carbon (and other) multiple bonds by a radical chain mechanism.¹⁸⁶ Radical additions are probably the most extensively studied and exploited radical reactions, probably because of their versatile applications in the synthesis of small molecules (1:1 addition products) as well as large (polymeric) molecules.^{186,187} Because of its relevance to this thesis, a few addition reactions of radicals to carbon-carbon double bonds to yield small molecules are considered in this section. The following discussion is mostly a repetition of what has been covered in the reviews¹⁸⁶ mentioned earlier.

The important propagation steps involved in the radical chain addition of a reagent XY to an unsaturated compound $\text{CH}_2=\text{CHZ}$ are the radical addition (eq.85) and the chain transfer step (eq.86), where k_{add} is the rate constant for the addition of $\text{X}\cdot$ to the double bond



and k_{tr} is the rate constant for chain transfer. When the transfer step is very slow compared to

the radical addition to the olefin, the intermediate radicals may undergo further addition with other molecules of the alkene to form telomers or polymers, represented by eq.87, where k_p is the rate constant for propagation in a polymer forming chain reaction.



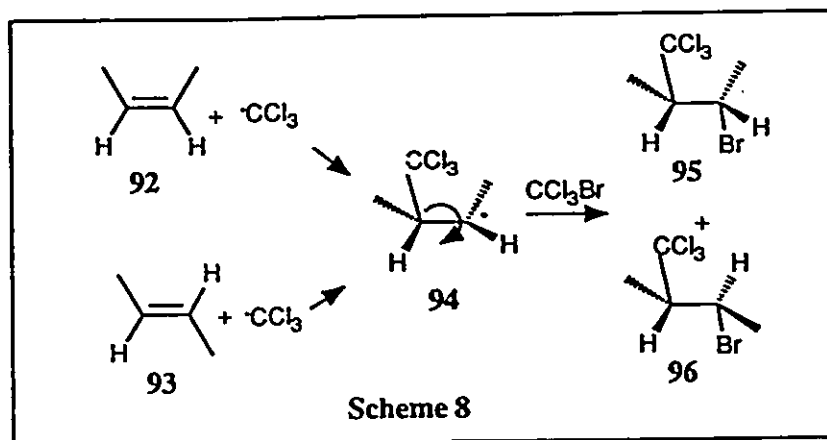
The efficiency of a radical process to form 1:1 addition products depends on the efficiency of the chain transfer step. For example, very high yields of 1:1 addition products have been reported for radical chain additions of reagents like polyhalomethanes and various thiols to double bonds.¹⁸⁸ The chain transfer constants (defined as k_{tr}/k_p , see eq.86 & eq.87), for the above reagents are expected to be very high.

For various classes of reagents X-Y such as hydrocarbons, halo compounds, thiols, aldehydes etc., the chain transfer constants vary widely in their magnitude. The different factors that influence chain transfer are bond strengths, steric effects, resonance stabilizations, and polar effects.¹⁸⁹

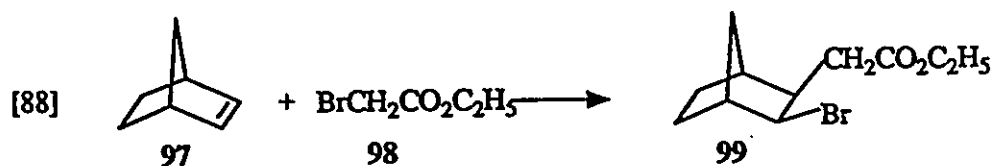
(i) Stereospecificity in radical additions

Radical addition reactions in general are non-stereospecific. However, the addition of HBr to olefins in the presence of a peroxide at low temperature occurs stereospecifically in an anti addition mode.¹⁹⁰ A certain degree of stereoselectivity observed in some intermolecular and intramolecular addition reactions is known to be the result of special steric or conformational preferences.

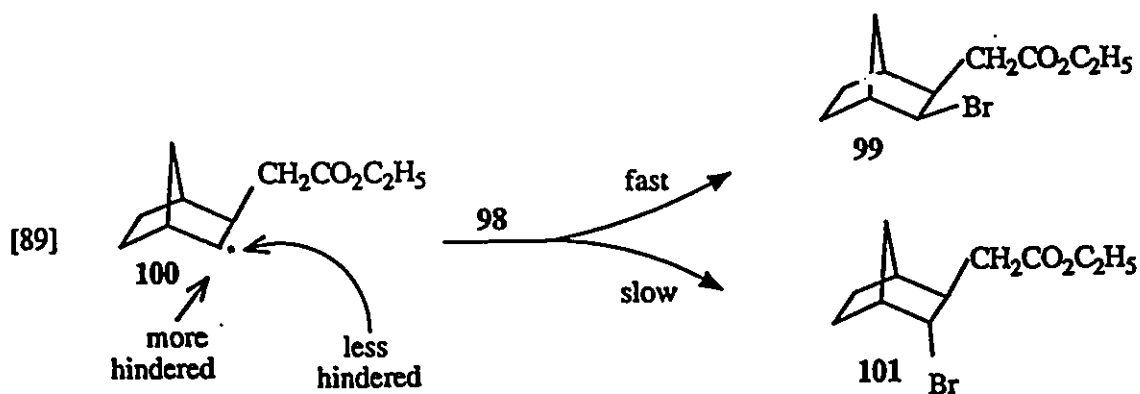
A classical example of the lack of stereospecificity in intermolecular radical addition processes is given in eq.88. Addition of bromotrichloromethane to cis-2-butene 92 and trans-2-butene 93 under free radical conditions yielded the same mixture of erythro product 95 and threo product 96.¹⁹¹ The results indicate that 92 and 93 react with $CCl_3\cdot$ to give radicals which undergo rapid conformational equilibration to give 94 before the bromine transfer with bromotrichloromethane can occur (Scheme 8).



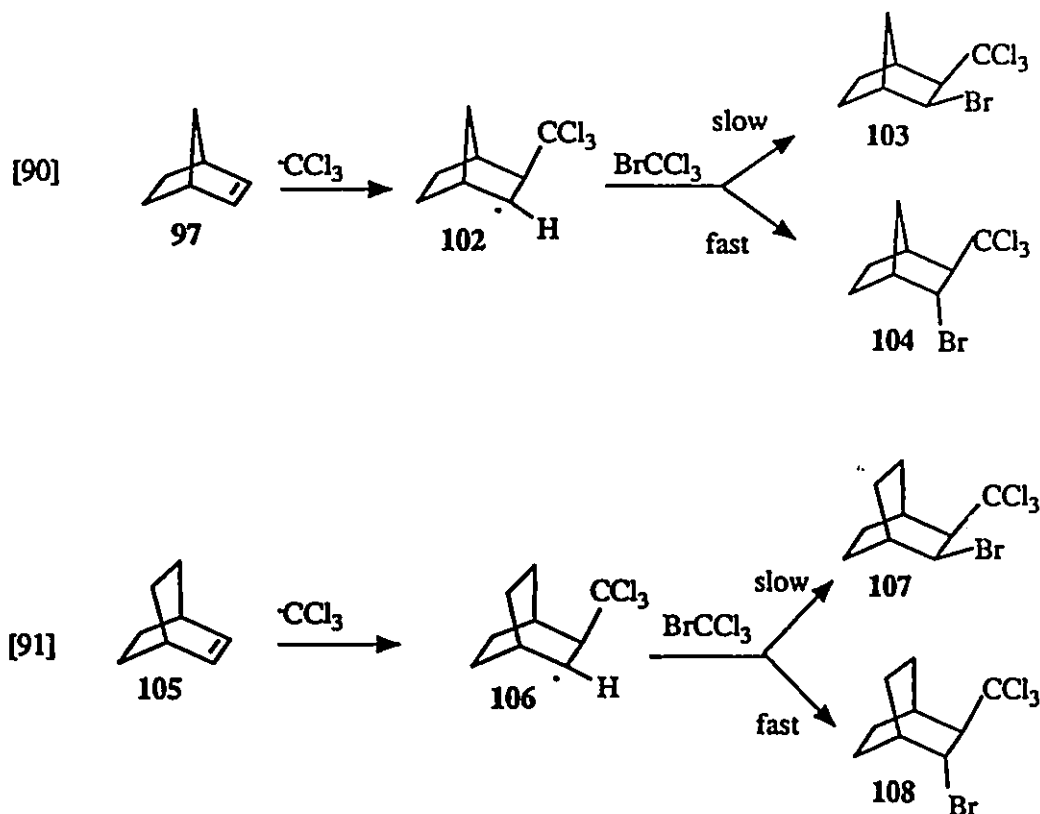
A high degree of stereoselectivity is observed in the radical chain additions of certain reagents to norbornene and related systems. The addition is known to take place on the same side of the double bond in an *exo-exo* addition mode, since the *exo* approach is less hindered than the *endo* approach.¹⁹² For example, the addition of ethyl bromoacetate 98 to norbornene



97 gives product 99 by a highly stereoselective *exo* addition. The explanation for the stereoselectivity is illustrated in eq.88, where the intermediate radical (100) formed by the initial radical attack on 97 undergoes Br atom transfer at the less hindered *exo* site leading to 99 as the major product.



In contrast to the addition of ethyl bromoacetate, the free radical addition of BrCCl_3 to norbornene (97) and bicyclo[2.2.2]octene (105) gave the stereoselective trans addition



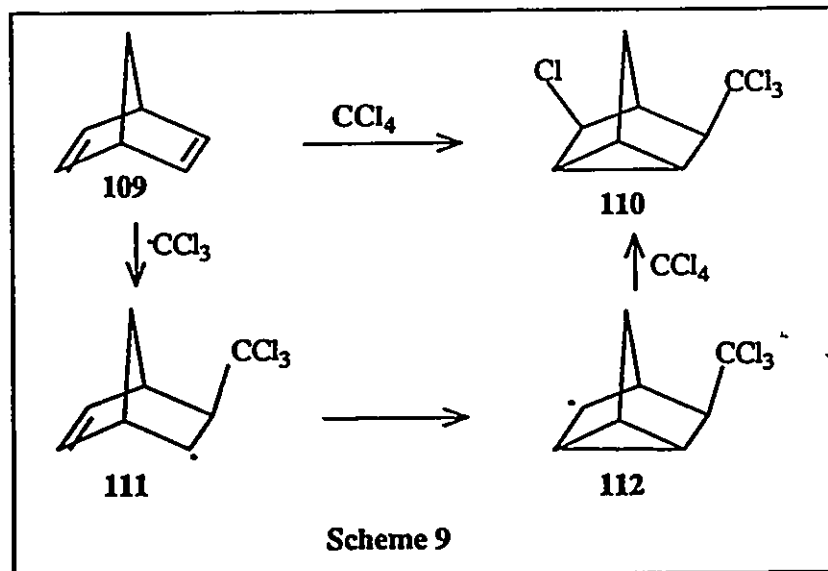
products 104 and 108, respectively.¹⁹⁴

The high stereoselectivity observed in the addition of BrCCl_3 to the above bicyclic systems probably is the result of steric effects. The bulky trichloromethyl groups in the intermediate radicals 102 and 106 hinder the bromine transfer at the exo-positions leading to the exclusive formation of trans addition products.

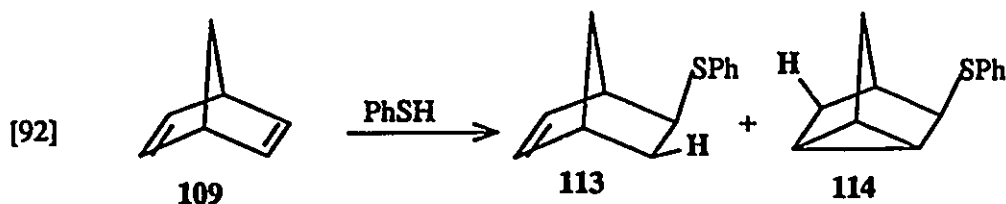
(ii) Radical additions to some cyclic diene systems

Radical additions to dienes give different products depending on the position of the double bonds in the molecule. Isolated double bonds usually give the normal 1,2- addition products while conjugated dienes yield both 1,2- and 1,4- addition products. If the

intermediate radical formed by the initial radical attack on one of the double bonds is suitably oriented for an intramolecular addition to the second double bond in the diene system, cyclic products can also be made. Moreover, if such a suitably placed diene system is part of a ring then polycyclic compounds are formed. For example, the addition of CCl_4 to norbornadiene 109 gives the tricyclene product 110 in very good yield.¹⁹⁵ In this reaction (Scheme 9) the

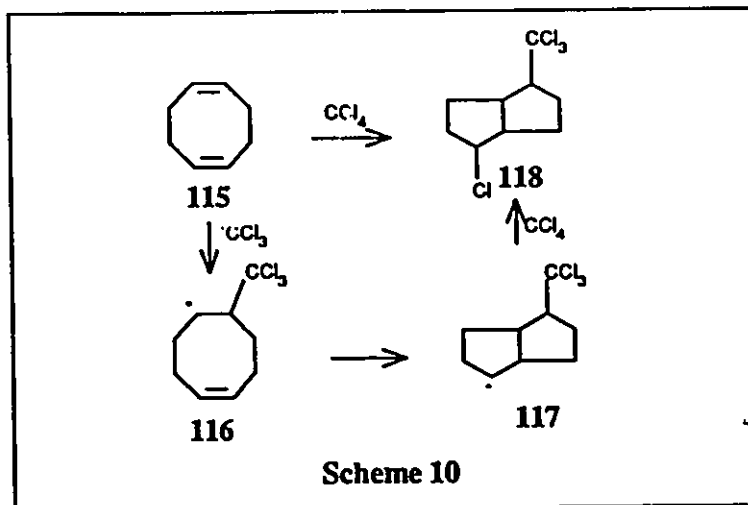


intermediate 111 formed by the addition of trichloromethyl radical on one of the double bonds undergoes an intramolecular addition in the 3-exo sense to form the isomeric radical 112 before the chain transfer occurs. A number of other reagents such as CHCl_3 , $\text{C}_3\text{H}_7\text{CHO}$, and $\text{C}_6\text{H}_5\text{CHO}$ were also found to add to norbornadiene in a similar manner.¹⁹⁵ However, for reagents such as thiophenol, for which the chain transfer constant is very high, addition to the above diene resulted in the formation of some of the normal 1,2- addition product (eq.92).¹⁹⁶

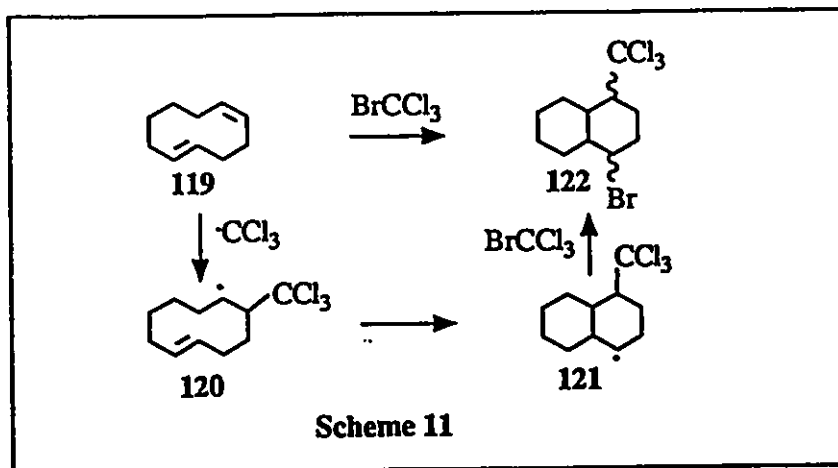


Dowbenko¹⁹⁷ has shown that a variety of substrates RX with low chain transfer constants, such as CCl_4 , CHCl_3 , and some aldehydes, on free radical addition to

1,5-cyclooctadiene **115** yield transannular cyclization products. For example, the addition of CCl_4 to **115** yields **118** (Scheme 10) presumably by way of 5-exo cyclization of the intermediate radical **116**.



Traynham and Hsieh¹⁹⁸ have shown that even with one of the fastest chain transfer agents, BrCCl_3 , excellent yields of the transannulation product **122** could be obtained from *cis,trans*-1,5-cyclodecadiene (**119**, Scheme 11) when neat ($\sim 9\text{M}$) BrCCl_3 was used. The intermediate radical **120** undergoes a 6-endo cyclization fast enough to compete effectively with Br abstraction from bromotrichloromethane.

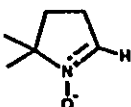
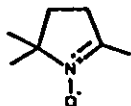


(iii) Radical additions to nitroso and nitron groups

The addition of carbon-centered radicals to nitron (eq.2) and nitroso (eq.3) compounds have already been mentioned in connection with spin trapping (Section 1.1). The efficiency of a few spin-traps measured by their spin-trapping rate constants will be discussed in this Section.

Spin trapping has been used qualitatively for several years for detecting and identifying transient free radicals. But the quantitative aspect of radical reactions with spin traps has not been exploited until recently.⁴⁴

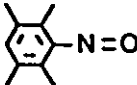
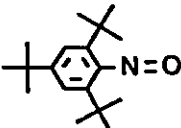
Janzen and Evans^{199,201} seem to be the first to report quantitative kinetic data on the rate constants for radical attack on spin traps. Their first report¹⁹⁹ involved the *t*-butoxy

Table 9. Rate constants for <i>t</i> -butoxyl radical attack on some nitron spin traps ¹⁹⁹	
Trap	Rate Constant (k_T , $M^{-1}sec^{-1}$)
$CH_2=N^+(O^-)-CMe_3$	3.5×10^8
$C_6H_5CH=N^+(O^-)-CMe_3$ (PBN)	5.5×10^6
<i>p</i> -NO ₂ -PBN	9.0×10^6
<i>p</i> -Cl-PBN	6.5×10^6
<i>p</i> -MeO-PBN	5.5×10^6
	5.0×10^8
	9.0×10^6

radical attack on some nitrones and on 2-methyl-2-nitroso propane (NtB). The rate constants (k_T) reported for a few spin traps are given in Table 9. In their second report,²⁰⁰ the above authors have given the rate constant for the attack of phenyl radicals on phenyl-*t*-butyl nitron (PBN). The reported rate constant ($k_T = 10^7 M^{-1} s^{-1}$) is a factor of 2 lower than that

for the t-butoxy radical attack on the same trap. The above rate constants give a quantitative measure of the efficiency of a spin trap; the larger the rate constant the more efficient a spin trap is.

Schmid and Ingold^{201,202} were the first to report the rate constant for the attack of primary alkyl radicals on some commonly used nitroso and nitron spin traps. They used the

Table 10. Rate constants for primary and secondary radical attacks on some nitroso and nitron traps		
Spin Trap	Rate Constant, ^a $k_T(\text{M}^{-1}\text{s}^{-1})$	
	Primary ^b	Secondary ^c
$(\text{CH}_3)_3\text{CNO}$	9.0×10^6	6.1×10^6
	3.9×10^7	4.0×10^7
$\text{CH}_2=\text{N}(\text{O})\text{C}(\text{CH}_3)_3$	3.1×10^6	1.3×10^6
$\text{C}_6\text{H}_5\text{CH}=\text{N}(\text{O})\text{C}(\text{CH}_3)_3$	1.3×10^5	6.8×10^4
	4.7×10^6	1.8×10^4

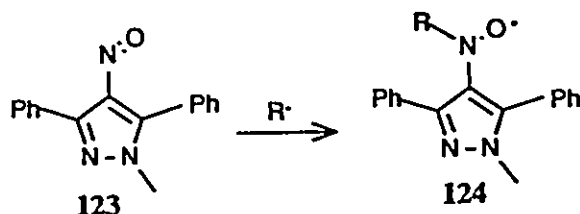
^a) The numbers are abstracted from ref.202 and ref.203, and are uncorrected. However, they need minor corrections based on the revised values for the 5-hexenyl radical clock (see Section 1.3)

^b) The values are taken from ref.202. ^c) The values are taken from ref.203.

5-hexenyl radical cyclization as the clock for the estimation of spin-trapping rate constants. It was observed by Maeda and Ingold²⁰³ that the rate constants for trapping of secondary radicals are similar in magnitude to those of the primary alkyl²⁰² radicals. Rate constants for

the attack of primary and secondary alkyl radicals on some commonly used spin traps are given in Table 10.

Kaur and Perkins²⁰⁴ have recently reported an extremely efficient nitroso spin trap, 1-methyl-4-nitroso-3,5-diphenyl pyrazole (MNDP, 123), which is shown to react with a

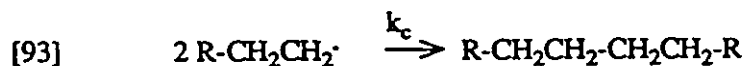


variety of radicals to form relatively stable nitroxyl radicals, whose esr spectra are simple and are easily characterized.²⁰⁵ The kinetic utility of MNDP comes from its monomeric nature (compared to those in Table 10, which are associated) in solution and its high rate constant. The absolute rate constant for the attack of undecyl radicals on 5 has been estimated as $1.5 (\pm 1) \times 10^7 \text{ M}^{-1} \text{ s}^{-1}$ at 40°C . Our attempt to determine the rate constant for attack of a primary alkyl radical on this spin trap (123) at different temperatures, around room temperature, so as to obtain an Arrhenius expression and thereby to extend the applicability of this trap as a kinetic standard will be presented in the Results and Discussion Section (Section 2.3).

1.4.3. Radical-radical reactions and some rate constants

Because of their high reactivity, organic radicals undergo reactions with themselves or other radicals in solution forming closed shell molecules. There are two ways in which bimolecular reactions between radicals can take place; (a) radical combination or coupling (eq.93), and (b) radical disproportionation (eq.94), where k_c and k_{dis} are their respective bimolecular rate constants. The latter reaction is limited to reactions in which at least one of the radical species contains an H-atom adjacent to the radical site.

The subject of radical coupling and disproportion reactions has been extensively reviewed.²⁰⁶ The most important aspect about radical coupling (and also disproportionation)



reactions is that their rate constants approach the diffusion-controlled limit. When two species react with one another, a chemical reaction can take place only as fast as the reactants can collide with each other by way of diffusion. Such a process is called a 'diffusion controlled' reaction. The second order rate constant for such a reaction can be calculated from a combination of the laws of diffusion²⁰⁷ and the modified form of the Stokes-Einstein equation.²⁰⁸ The final form of the diffusion-controlled rate constant has been given as eq.95,

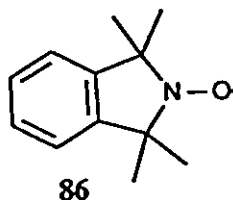
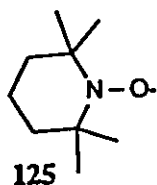
$$[95] \quad k_{diff} = 1/4 (2 + d_1/d_2 + d_2/d_1)(8RT/3 \times 10^3 \eta) \text{ M}^{-1}\text{s}^{-1}$$

where d_1 and d_2 are the diameters of the reacting radicals, R is the Gas Constant, and η is the viscosity (in poise) of the medium.²⁰⁹ In radical reactions where the radicals involved have the same radii (ie. $d_1 = d_2$, as for identical radicals), the diffusion controlled rate equation reduces to eq.96.²¹⁰ For common solvents like cyclohexane, benzene, carbon tetrachloride,

$$[96] \quad k_{diff} = 8RT/(3 \times 10^3 \eta) \text{ M}^{-1}\text{s}^{-1}$$

water, etc., the rate constants calculated using the above equation come approximately to $8 \times 10^9 \text{ M}^{-1} \text{ s}^{-1}$ at 25°C .^{209,210} The experimental values for the bimolecular rate constants (usually quoted as $2k_t$, where k_t is the sum of the recombination and disproportionation reactions) for the disappearance of most carbon- and tin-centered radicals in solution are in the range 10^9 - $10^{10} \text{ M}^{-1} \text{ s}^{-1}$. For the majority of carbon-centered radicals the value is close to $2 \times 10^9 \text{ M}^{-1} \text{ s}^{-1}$, which is a factor of four lower than that for a diffusion-controlled reaction.²¹¹

The coupling of carbon-centered radicals with a variety of aminoxyl radicals ($>\text{N}-\text{O}^\bullet + \text{R}^\bullet \rightarrow >\text{N}-\text{O}-\text{R}$) are known to have rate constants in the range 10^8 - $10^9 \text{ M}^{-1} \text{ s}^{-1}$.²¹² For example, the rate constants for the reaction of a variety of radicals with 2,2,6,6-tetramethylpiperidine-N-oxyl (TEMPO, 125) and with 1,1,3,3-tetramethyl-



isoindolin-N-oxyl (86) have been reported by Ingold et al.^{212,213} Some representative reactions and their rate constants²¹³ are given in Table 11. The rate constant for the reaction

Reaction #	Radicals (R $^\bullet$)	Nitroxide	Rate Constants $k_c \times 10^{-8} (\text{M}^{-1}\text{s}^{-1})$
1	$\text{CH}_3(\text{CH}_2)_7\text{CH}_2$	125	12.3
2	$(\text{CH}_3)_3\text{CCH}_2$	125	9.6
3	$(\text{CH}_3)_3\text{C}$	125	7.6
4	$\text{C}_6\text{H}_5\text{CH}_2$	125	4.9
5	$(\text{CH}_3)_3\text{C}$	86	8.8
6	$\text{C}_6\text{H}_5\text{CH}_2$	86	5.5
7	$\text{CH}_2=\text{CH}-(\text{CH}_2)_3-\text{CH}_2$	86	10.7

of a primary alkyl radical with 86, reported by Beckwith et.al,¹⁴⁸ has already been mentioned in Section 1.3.3.

1.5.0. DIAZENES AS RADICAL SOURCE

Compounds with an N=N function are called diazenes; the parent compound being diazene, $\text{HN}=\text{NH}$. Substitution of both hydrogens of diazene by alkyl (or aryl) groups results in dialkyl (or diaryl) diazenes, which are commonly known as azo compounds. Azobenzene, $\text{C}_6\text{H}_5\text{-N}=\text{N-C}_6\text{H}_5$, should therefore be named systematically as 1,2-diphenyl diazene.²¹⁵ Disubstituted diazenes are much more stable than the monosubstituted or unsubstituted diazenes. As a class, diazenes are known to be the most convenient sources of radicals and biradicals. Several recent reviews on the chemistry of diazenes, especially the disubstituted diazenes, are available.²¹⁶ The following sections deal only with a few specific classes of diazenes such as monosubstituted diazenes, α -hydroxyalkyl diazenes (azocarinols), and α -hydroperoxyalkyl diazenes (azohydroperoxides). The latter two are the main sources of radicals for the kinetic studies presented in the Results and Discussion Section, and the former one is believed to be involved in the decomposition of α -hydroxyalkyl diazenes. For simplicity the terms α -hydroxy diazene (or, azocarinol) and α -hydroperoxyalkyl diazene (or, azohydroperoxide) will be used hereafter to designate the appropriate α -substituted alkyl diazene.

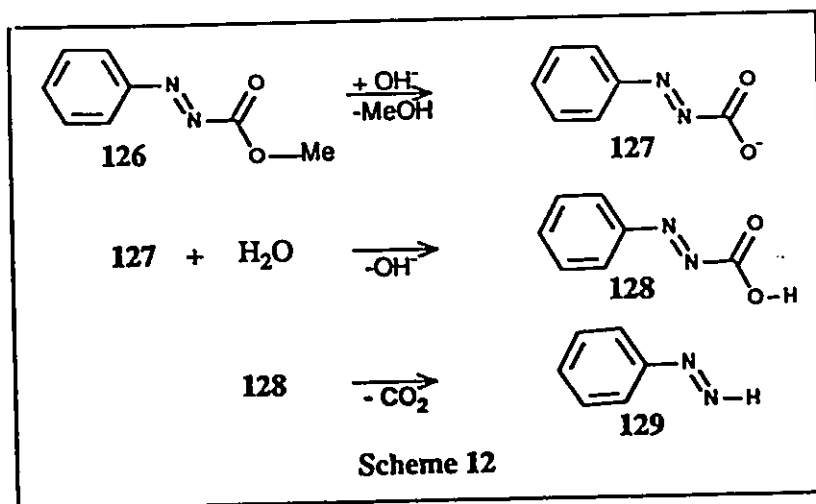
1.5.1. Monosubstituted diazenes

Until recently,²¹⁷ monosubstituted diazenes ($\text{R-N}=\text{NH}$) have only been postulated as possible intermediates in some chemical reactions. The possibility that aryl diazenes ($\text{Ar-N}=\text{NH}$) are intermediates in the decarboxylation of phenyldiazene carboxylic acids ($\text{Ar-N}=\text{N-COOH}$) and that they lead to the formation of Ar-H, nitrogen, and carbon dioxide had been proposed by Widman²¹⁸ as early as 1895. The formation of benzene and nitrogen from the oxidation of phenylhydrazine was reported by Chattaway²¹⁹ to involve phenyl diazene ($\text{Ph-N}=\text{N-Ph}$) as an intermediate

In 1965 Huang and Kosower²¹⁷ were able to prepare and characterize phenyldiazene,

the first monosubstituted diazene to be observed and studied directly. Several aryl-^{215,220}, alkyl-²²¹, and alkenyl-²²² diazenes were prepared and studied by Kosower and co-workers in the subsequent years. The monosubstituted diazenes, prepared and studied by Kosower, were shown to have *trans* geometries. However, a scheme for the synthesis of *cis*-phenyldiazene have been reported very recently by Smith and Hillhouse.²²³

The preparation of phenyldiazene^{220a} involves a straightforward hydrolysis of the

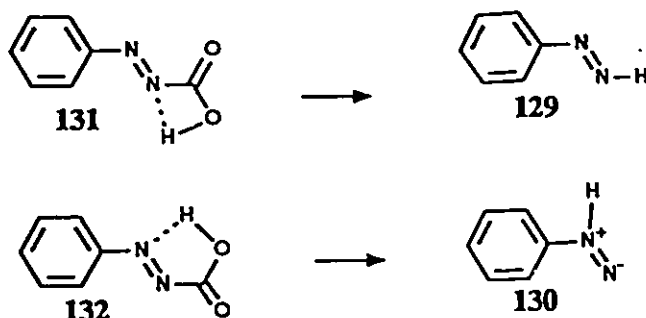


diazene carboxylic ester 126 to the corresponding salt 127 and hydrolysis of the salt with aqueous buffer solutions ($\text{pH}=7$) to form the unstable carboxylic acid 128, which decarboxylates to form the diazene 129 (Scheme 12).

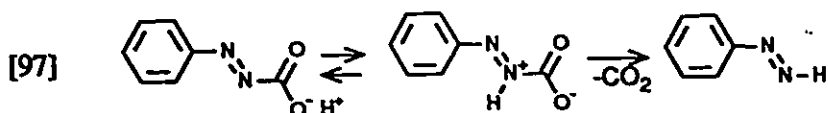
There are two possible structures (129 and 130) for monosubstituted diazenes. Structure 129 is called a 1,2-diazene, and 130 is a 1,1-diazene. From spectroscopic and other



evidence, Kosower was able to assign the structure of phenyl diazene as 129. However, it was proposed that 130 could be a possible intermediate in the formation of 129 from the decarboxylation of phenyl diazene carboxylic acid, 128. It is possible that 130 is formed



through the transition state 132, which is more easily attained than the transition state (131) for the formation of 129. A zwitterionic pathway (eq.97) has also been proposed^{220a} for the decarboxylation.

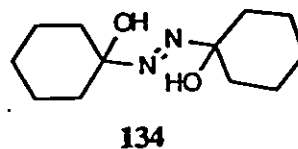
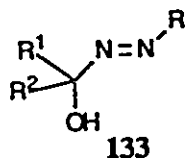


The most important characteristics of the reactions of phenyldiazene are: (1) the radical chain oxidation of phenyl diazene to give benzene and biphenyl, (2) the bimolecular disappearance, whose mechanism probably is very complex, and (3) the inability to undergo nucleophilic attack at reactive electrophiles such as benzenesulfonyl chloride and methyl chloroformate.

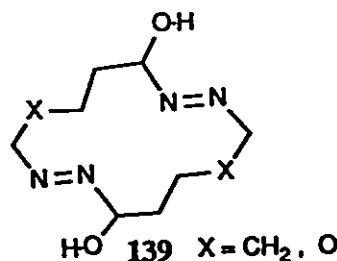
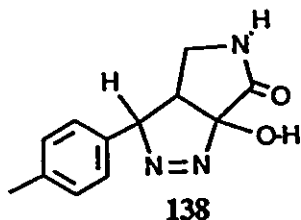
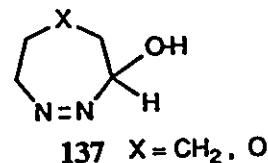
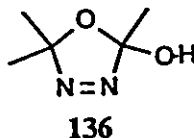
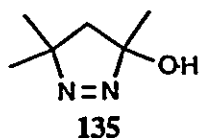
Monosubstituted diazenes have also been proposed as intermediates in the decomposition of α -hydroxy diazenes. Details of this are discussed in the following section.

1.5.2 α -Hydroxyalkyl diazenes (azocarinols)

Compounds of the type 133 with a hydroxy group alpha to an azo function have received much attention since the first compound of this type, 1,1-dihydroxyazo cyclohexane, 134, was reported by Schmitz and co-workers²²⁴ in 1963. Over the years several azocarinols of the type 133 have been synthesised and characterized by several workers. In addition to the acyclic azocarinols 133 and 134, a few systems in which the azo function is part of a ring are also known. Compounds 135,²²⁵ 136,²²⁶ 137,²²⁷ 138,²²⁸ and



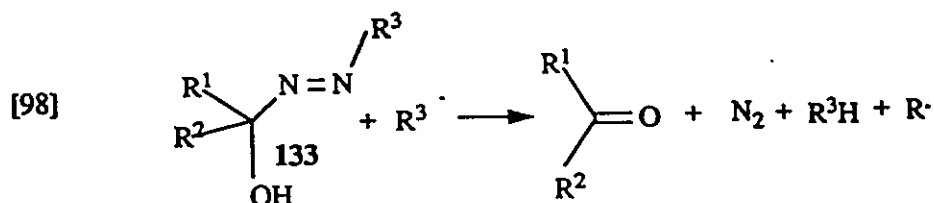
139²²⁹ are examples.



Azo compounds in general have been known for years as free radical sources. The chemistry of α -azocarbonols is somewhat different from that of normal azo compounds (1,2-dialkyl diazenes) of the type $R-N=N-R$. There is a remarkable difference in the thermal stabilities of azo compounds relative to that of azocarbonols; the latter compounds, especially the acyclic ones (133), are highly unstable and undergo thermal decomposition to generate radicals in solution even at or near room temperature.²³⁰ However, some cyclic azocarbonols such as the substituted hydroxy pyrazole (135) are known to have stability similar to that of the 1,2-dialkyl diazenes.²²⁵

α -Hydroxyalkyl diazines are excellent sources of radicals in solution. Because of their usefulness as initiators for polymerization processes, MacLeay²³¹ synthesized and patented a number of these compounds in 1978.

Our own interest in α -hydroxyalkyl diazines comes from the fact that 133 are convenient sources of alkyl radicals in solution at and near room temperature. A radical chain mechanism (eq.98) for the decomposition of 133 in neutral media has been proposed and proven by Warkentin and co-workers.^{230,232,233} The overall reaction represented by eq.98 is



exothermic by about 62 kcal/mol as is given in Table 12.

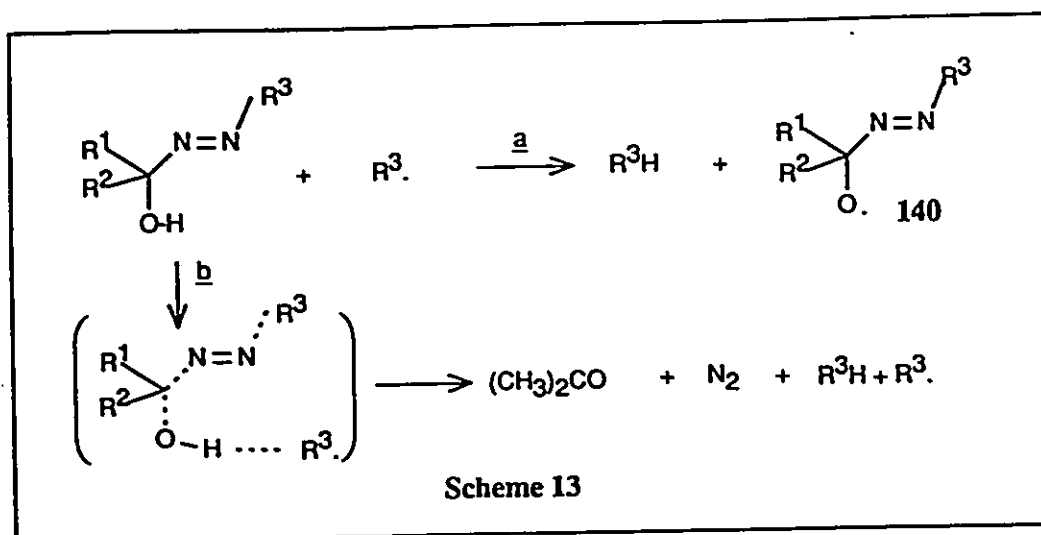
Table 12. Calculation of enthalpy change for reaction [98]

Energy lost ^a		Energy gained ^a		Enthalpy change ^a
H-O	110	C-H	99	-504
C-O	86	C=O	179	+442
2x C-N	146	N=N	226	-62
N=N	100		504	
	<u>442</u>			

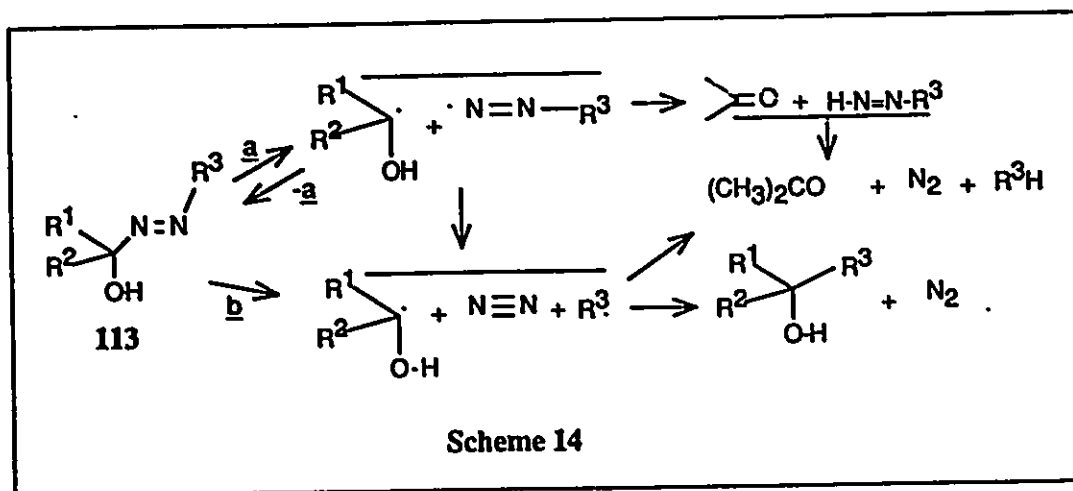
^a)all energies are in kcal mol⁻¹

Several lines of evidence exist for a chain mechanism (eq.98) in which a radical-chain induced decomposition of 133 occurs by the attack of a radical at the hydroxyl hydrogen. Evidence such as (a) hydroalkylation of olefins²³³ using 133, (b) characterization by spin trapping of several of the alkyl radicals (R₃·) generated from 133,²³⁴ (c) lower rate constants observed for the decomposition of azocarinols in the presence of "inhibitors";²³²⁻²³⁴ all well fit for such a radical chain mechanism.

There are two pathways for the induced, radical chain decomposition of azocarinols (Scheme 13). Path a involves the hydrogen abstraction by R₃· to form the intermediate 140, which decomposes rapidly to give N₂, acetone and R₃·, or path b where a concerted process operates. The latter mechanism have been proven by Warkentin and Nazran.²³² The driving force for a concerted mechanism (path b) could be due to the simultaneous formation of acetone and nitrogen in the decomposition process.

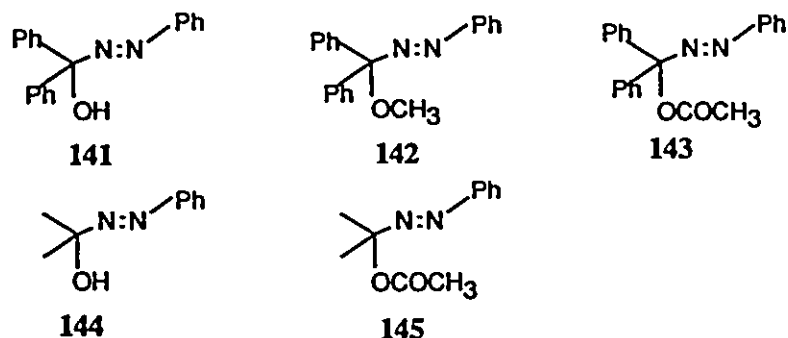


A second mechanism for the decomposition of azocarinols involves the unimolecular decomposition of 133 to produce the ketyl radical $R^1R^2\dot{C}OH$, and a diazenyl radical which then can undergo further reactions (Scheme 14).



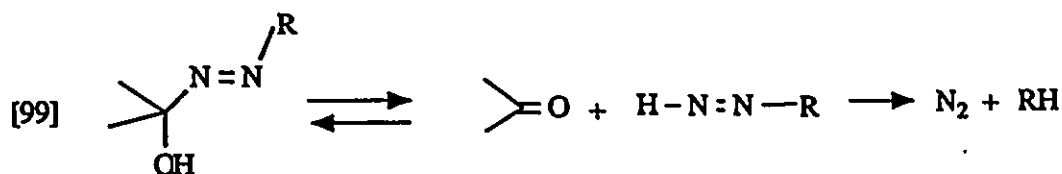
Warkentin and co-workers were able to disprove such a mechanism based on kinetic data.²³³ They found that methylated and acetylated azocarinols (142, 143 & 145) decompose with rate constants much smaller than those of the azocarinols (141, 144)

themselves.



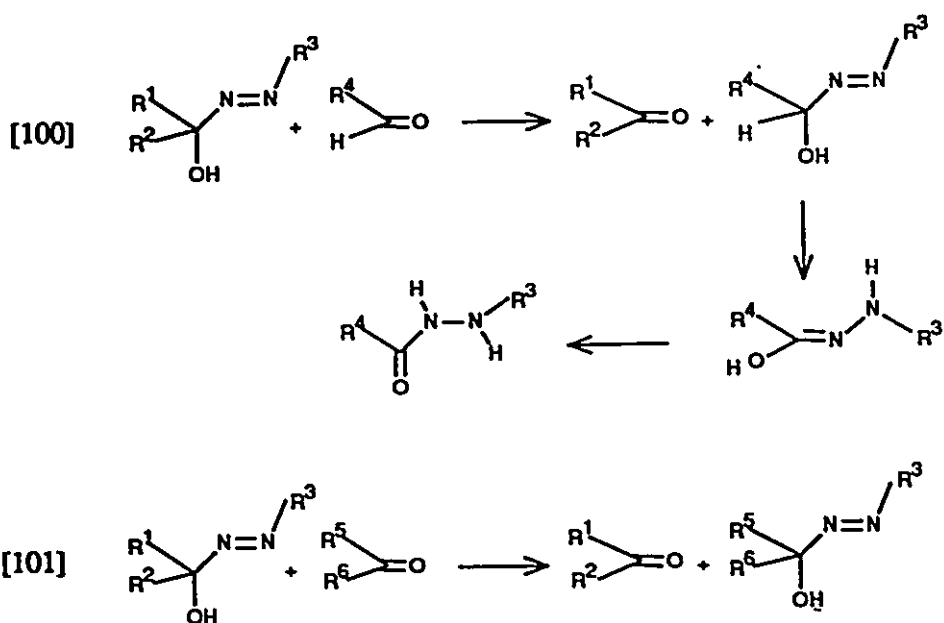
Compounds 142, 143 & 145 decompose in CCl_4 at 80°C with rate constants (k/s^{-1}) $= 3.6 \times 10^{-6}$, 1.2×10^{-6} , and 3×10^{-8} respectively; whereas the azocarbinoles 141 and 144 decompose with rate constants $2.5 \times 10^{-4} \text{ s}^{-1}$ and $4.0 \times 10^{-6} \text{ s}^{-1}$, respectively. The addition of thiophenol to the reaction mixture greatly enhanced the rate constant ($k = 3 \times 10^{-3} \text{ s}^{-1}$) for the decomposition of 144 even at 35°C . These observations are inconsistent with the mechanism proposed in Scheme 14.

A third mechanism for the decomposition of 133 in basic media has been proposed by Hünig and co-workers.²³⁵ This mechanism involves a reversible decomposition of 133 to the ketone and a mono substituted diazene as given in eq.99.



The above mechanism is based on the observation of Hünig and Buttner,²³⁵ and also by Schulz and Missol,²³⁶ that azocarbinoles react with aldehydes to form hydrazides via new azo alcohols (eq.100), and with ketones to form new azocarbinoles (eq.101).

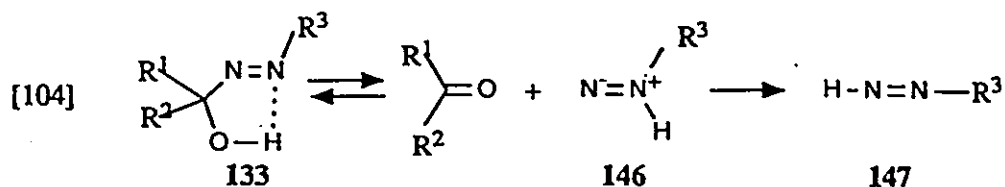
There is no direct evidence for the involvement of monosubstituted diazenes as intermediates in the decomposition of azocarbinoles. The mechanism hinges only on the evidence that diazenes react with aldehydes to form hydrazides. So far there is no report in



the literature regarding reactions of monosubstituted diazenes with ketones, even though the results of Schulz and Missol²³⁶ could only be explained on the logical assumption of such a diazene intermediate. However, phenyl diazene (129), prepared and extensively studied by Kosower and Huang,^{220b} did not react with reactive electrophiles such as methyl chloroformate and benzenesulfonyl chloride (eq.102,103). According to Kosower and Huang "The nitrogens of the diazene group are non-nucleophilic toward methylchloroformate and benzenesulfonylchloride, as would be expected of azo compounds". The reaction of H-N=N-R or H-N=N-Ar with any aldehyde and ketone can hardly be expected since phenyl diazene does not react with much more electrophilic species.



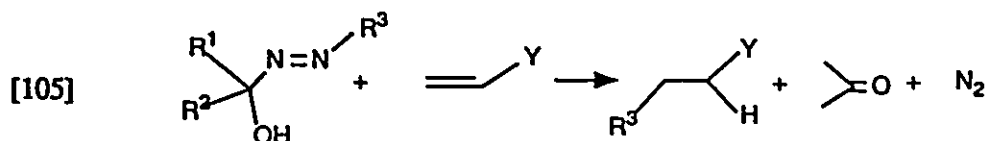
Warkentin and co-workers²³³ suggested that a 1,1-diazene (146) could be an intermediate, which then rearranges to the 1,2-diazene (147, eq.104). This appears to be more



reasonable, based on the earlier observations that intramolecular H-bonding such as that shown in eq.104 exists in azocarinols.²³⁵ The direct formation of 1,2-diazene would be rather difficult because of the 4-membered transition state involved in that process. However, the mechanism (eq.104) did not get enough experimental support.²³³

Azocarinols as hydroalkylating agents

Thermal decomposition of azocarinols in the presence of alkenes results in the formation of hydroalkylation products (eq.105). Because of its potential synthetic value,

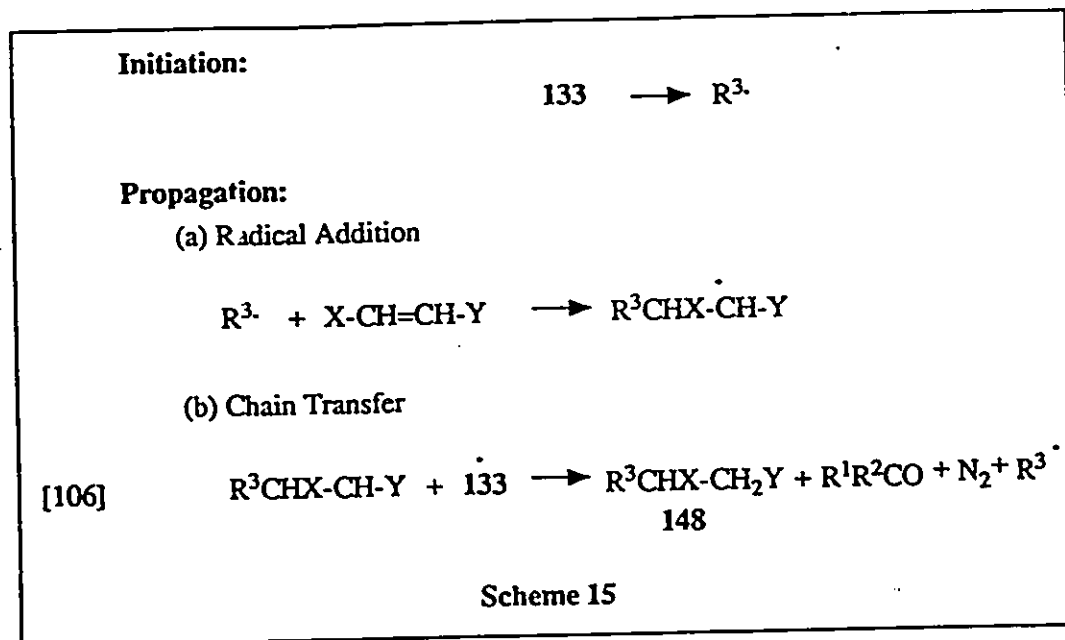


hydroalkylation of alkenes (and also azobenzene) by azocarinols has been explored by Warkentin et al.^{230a,233,234} The general sequence of reactions, known to be a radical chain process, is given in Scheme 15.

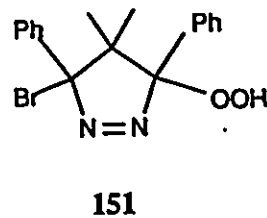
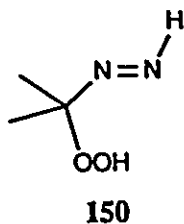
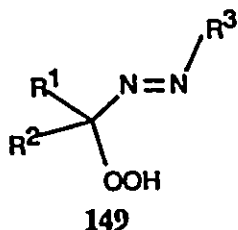
Several compounds of the type 148 have been synthesized by the above workers using this method. The success of such reactions in synthesis depends on the efficiency of the chain transfer step (eq.106), which involves the induced decomposition mentioned earlier in this section.

1.5.3 α -Hydroperoxy diazenes

Compounds of the type 149 with a hydroperoxy group alpha to an azo function are generally called α -hydroperoxydiazenes or α -azohydroperoxides. The above compounds were recognized as good radical initiators for polymerization reactions, and because of that



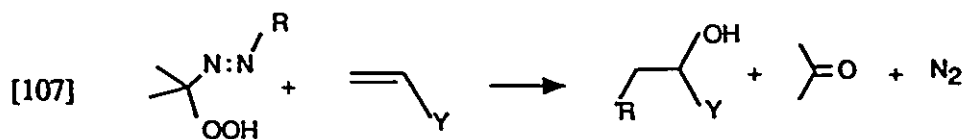
several of these compounds and their alkaline and alkaline earth metal salts were synthesized and patented by MacLeay and associates.²³⁷ Hydroperoxides of the type 150 were unknown until very recently, when Dixon and Barbush²³⁸ were able to generate them by photooxygenation of acetone hydrazone at -78°C and to assign their structure from their nmr spectra. Cyclic azohydroperoxides such as 151 are also known.²³⁹



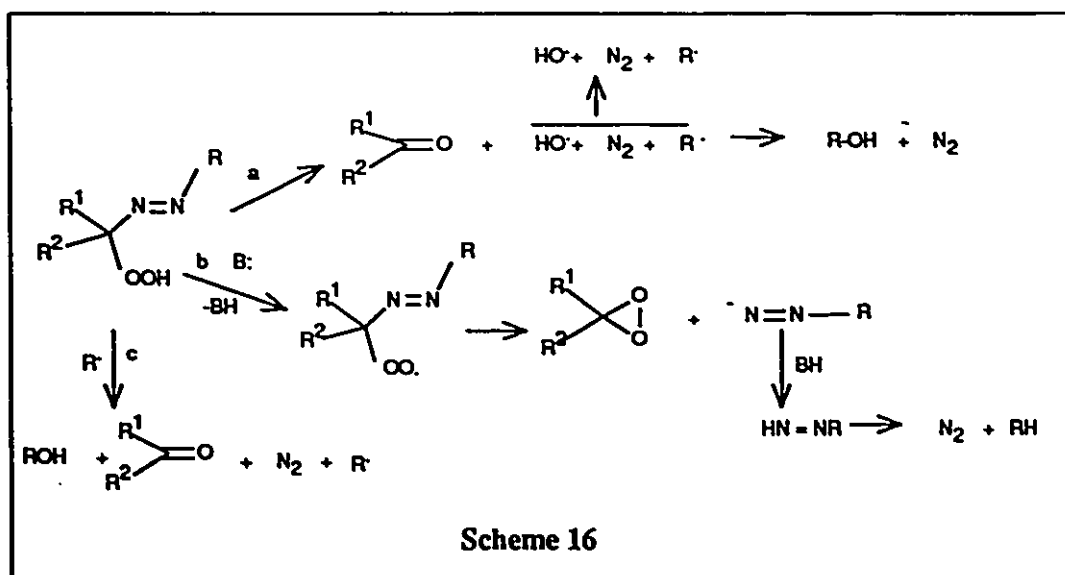
In addition to their use as radical initiators, α -azohydroperoxides have been used as oxidizing agents²⁴⁰ in the oxidation of olefins to epoxides,^{239b,241} sulfides to sulfoxides,²⁴² and phosphines to phosphoxides.^{233,236} They are also known to be good sources of hydroxyl radicals in non-aqueous media.²⁴³

Azohydroperoxides have been used by Warkentin and co-workers²⁴⁴ as

hydroxyalkylating agents, i.e., for the addition of a hydroxyl group and an alkyl group across double bonds (eq.107).



Several mechanisms have been proposed for the decomposition of α -azohydroperoxides. They are summarized in Scheme 16.

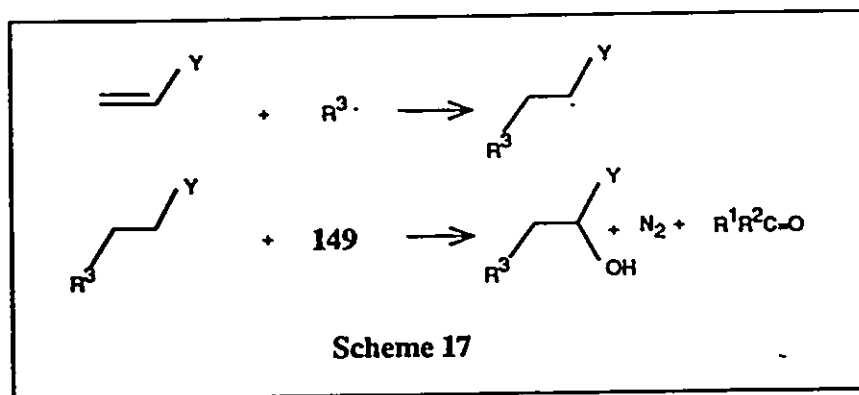


Mechanism a has been proposed by Tezuka and co-workers^{243a} to account for the formation of hydroxyl radicals and alkyl (or aryl) radicals from the thermal decomposition of azohydroperoxides.

Mechanism b has also been proposed by Tezuka and Iwaki^{241a} to account for the base catalyzed decomposition of α -azohydroperoxides. This mechanism however lacks any sort of strong evidence to support it, because none of the intermediates have been proven to exist in the reaction medium. Moreover, their experimental results could well be explained by an alternate mechanism such as the one proposed by Baumstark²⁴² to account for epoxidation of

olefins in basic media and conversion of pyridine to pyridine N-oxide.

Mechanism c has been proposed by Warkentin and co-workers²⁴⁴ to account for the radical chain addition of azohydroperoxides to olefins to form hydroxyalkylation products (Scheme 17). Small amounts of epoxides and hydroalkylation products were also observed



during the reaction of α -azohydroperoxides with olefins.²⁴⁴ A detailed discussion of the results of hydroxyalkylation as well as other competing reactions of the α -azohydroperoxides with olefins can be found in ref.244.

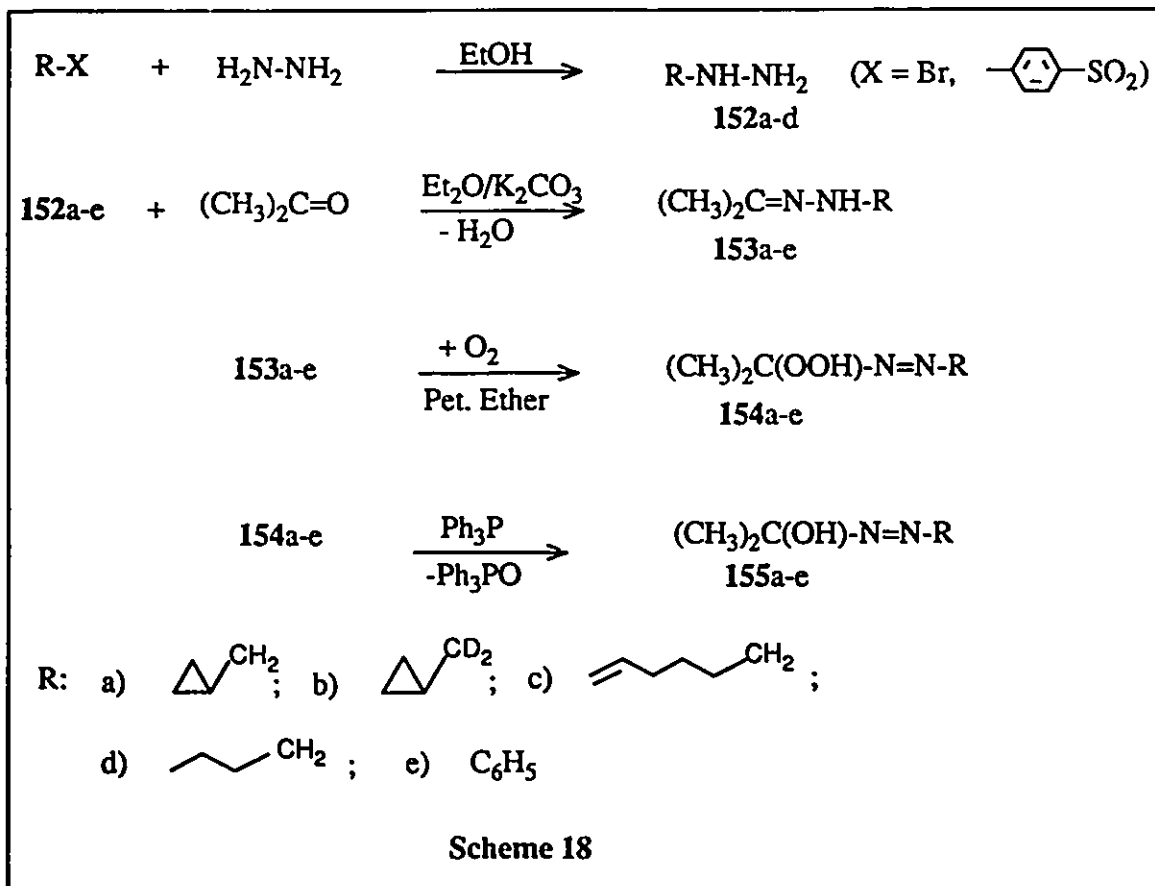
CHAPTER 2

METHODS, RESULTS, AND DISCUSSION

2.1.0. SYNTHESIS AND PROPERTIES OF RADICAL SOURCES: THE α -HYDROPEROXYALKYL DIAZENES AND THE α -HYDROXYALKYL DIAZENES

The main sources of radicals for the present kinetic studies were the α -hydroxyalkyl diazenes, **155**, which were synthesized according to Scheme 18. The first step in the synthesis involved the preparation of the alkyl hydrazine, **152**, by reacting either an alkyl tosylate or an alkyl bromide with hydrazine hydrate. The alkyl hydrazine was then condensed with acetone to produce the corresponding hydrazone, **153**. Autoxidation of the hydrazone gave the α -hydroperoxy diazene, **154**, which was then reduced by triphenylphosphine to the α -hydroxy diazene, **155**. The spectroscopic data for the radical sources and their precursors are given (separately according to the substituents, a-e) in Tables 13a - 13e.

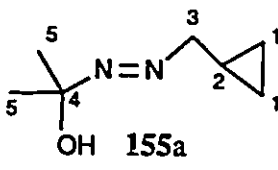
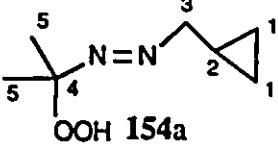
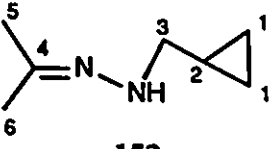
The alkyl tosylates for the syntheses of the hydrazines, **152a-c**, were prepared from the corresponding alcohols and p-toluenesulphonyl chloride using standard procedures.²⁴⁵ The yields of the tosylates ranged between 60% and 96% of the starting alcohol. It was observed that the best yields were obtained when the solvent (pyridine) used was extremely dry, and when the initial temperature of the reaction was kept constant at or around 0°C for at least 3-4 hours. Traces of moisture in the solvent was found to decrease the yield of the product, considerably. Treatment of the crude tosylates with hydrazine monohydrate in absolute ethanol gave very good yields (70%-92%) of the hydrazines.



152a-c. Treatment of n-butyl bromide with hydrazine hydrate in ethanol produced the butylhydrazine **155d** in 83% yield (See Experimental Section for details).

Condensation of the alkyl hydrazines, **152a-e**, with acetone resulted in the formation of the corresponding hydrazones, **153a-e**. The yields of distilled hydrazones ranged between 28% and 95%; the lower yields in some cases are apparently due to losses involved in distilling small quantities of fairly volatile compounds such as the low molecular weight hydrazones (**153a,b,&d**). Since hydrazones are sensitive to oxygen, the compounds were stored under an atmosphere of nitrogen in air-tight, amber-coloured bottles at low ($\sim -10^\circ C$) temperatures.

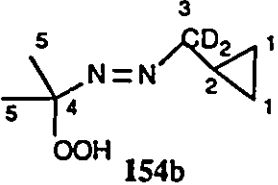
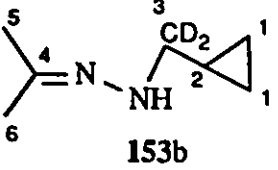
Oxidation of the hydrazones, **153a-e**, to the α -hydroperoxyalkyl diazenes, **154a-e**,

Table 13a. Spectral data for 155a, and its precursors, 154a, and 153a				
Compound	^1H nmr ^a δ (ppm)	^{13}C nmr ^b δ (ppm)	UV(hexane) λ_{max} (ϵ)	IR(neat) (cm^{-1})
 155a	0.07-0.63(m,4H) 0.97-1.33(m,1H) 1.34(s,6H) 3.68(d,2H) 4.73(s,1H)	3.30(C_1) 9.01(C_2) 26.90(C_5) 71.39(C_3) 93.60(C_4)	290 (9.8) 338 (19.2)	3410 3080 2982 2933 1685 1215
 154a	0.17-0.77(m,4H) 1.03-1.40(m,1H) 1.47(s,6H) 3.67(d,2H) 9.47(s,br,1H)	3.51(C_1) 9.20(C_2) 21.84(C_5) 73.60(C_3) 102.89(C_4)	292 (10.2) 358 (21.9)	3320 3080 2988 2936 1680 1179 847
 153a	0.08-0.63(m,4H) 0.77-1.27(m,1H) 1.75(s,3H) 1.93(s,3H) 3.01(d,2H) 4.20(s,br,1H)	2.80(C_1) 10.26(C_2) 15.21(C_6) 24.81(C_5) 55.88(C_3) 145.36(C_4)	290 (16.1) 358 (2.7)	3420 3240 3080 2992 2904 2842 1660

^a In CDCl_3 , with Me_4Si (TMS) as internal standard. The chemical shifts (δ -values) are followed, in parenthesis, by the multiplicity (s = singlet, d = doublet, m = multiplet etc.), and the signal intensity.

^b In CDCl_3 , with the solvent signal as the internal reference..

using molecular oxygen was done either in petroleum ether or in benzene at 5-10°C. A gas burette fitted with a mercury manometer was used to measure the volume of oxygen taken

Table 13b. Spectral data for 154b, and its precursor 153b			
Compound	^1H nmr ^a δ (ppm)	^{13}C nmr ^b δ (ppm)	UV(hexane) λ_{max} (ϵ)
 <p>154b</p>	0.18-0.82(m,4H) 1.10-1.40(m,1H) 1.48(s,6H) 9.50(s,br,1H)	3.35(C ₁) 8.98(C ₂) 21.79(C ₅) ? (C ₃) 102.89(C ₄)	292 (10.4) 358 (22.2)
 <p>153b</p>	0.08-0.63(m,4H) 0.77-1.27(m,1H) 1.75(s,3H) 1.93(s,3H) 4.20(s,br,1H)	2.74(C ₁) 10.18(C ₂) 15.16(C ₆) 24.73(C ₅) ? (C ₃) 145.36(C ₄)	290 (16.4) 358 (3.0)

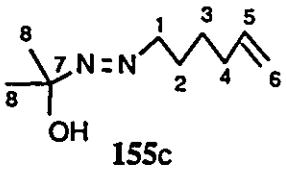
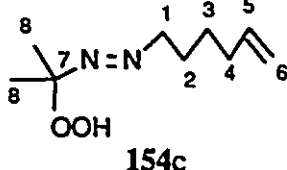
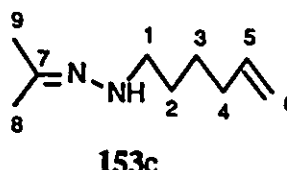
^a In CDCl_3 , with Me_4Si (TMS) as internal standard. The chemical shifts (δ -values) are followed, in paranthesis, by the multiplicity (s = singlet, d = doublet, m = multiplet etc.), and the signal intensity.

^b In CDCl_3 , with the solvent signal as the internal reference..

up. The completion of the reaction was inferred from the steady oxygen level in the burette for more than two hours, and was confirmed by taking the NMR spectrum of the solvent free material, which gave a singlet peak of the gem-dimethyl group of 154 in place of the two separate methyl singlets for the hydrazone 153 (refer to Table 13a-e). The purity of the hydroperoxy diazene was estimated by iodometric titration.

Reductions of the α -hydroperoxy diazenes, 154a-e, to the corresponding α -hydroxy diazenes using triphenylphosphine (Ph_3P) were done in petroleum ether (b.p.

Table 13c. Spectral data for 155c and its precursors, 154c and 153c

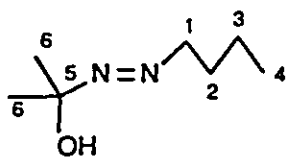
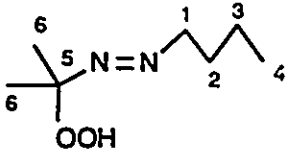
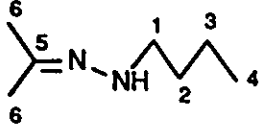
Compound	^1H nmr ^a $\delta(\text{ppm})$	^{13}C nmr ^b $\delta(\text{ppm})$	UV(hexane) $\lambda_{(\text{max})}$ (ϵ)
 <p>155c</p>	1.26(s,6H) 1.34-2.15(m,6H) 3.75(t,2H) 4.30(s,br,1H) 4.85(m,2H) 5.63(m,1H)	26.50(C ₃ orC ₂) 26.95(C ₈) 27.04(C ₂ orC ₃) 33.36(C ₄) 66.57(C ₁) 93.61(C ₇) 114.80(C ₆) 138.30(C ₅)	232 (93.3) 328 (21.3)
 <p>154c</p>	1.32(s,6H) 1.32-2.25(m,6H) 3.81(t,2H) 4.97(m,2H) 5.73(m,1H) 9.35(s,1H)	21.63(C ₈) 26.53(C ₃ orC ₂) 26.96(C ₂ orC ₃) 33.35(C ₄) 68.69(C ₁) 102.73(C ₇) 128.34(C ₆) 138.24(C ₅)	222 (94.9) 362 (22.4)
 <p>153c</p>	1.30-1.48(m,4H) 1.68(s,3H) 1.91(s,3H) 3.05(s,br,1H) 4.10(s,br,1H) 4.85(m,2H) 5.65(m,1H)	15.24(C ₈) 25.00(C ₉) 26.27(C ₃ orC ₂) 28.97(C ₂ orC ₃) 33.48(C ₄) 50.85(C ₁) 114.30(C ₆) 138.56(C ₅)	224 (84.2) 246 (92.2) 364 (7.6)

^a In CCl_3 with Me_4Si (TMS) as internal standard. The chemical shifts (δ -values) are followed, in paranthesis, by the multiplicity (s = singlet, d = doublet, m = multiplet etc.), and the signal intensity.

^b In CDCl_3 , with the solvent signal as the internal reference..

30-60°C) at around 0°C. The use of Ph_3P as the reducing agent has several advantages.

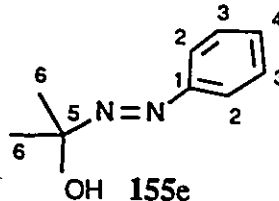
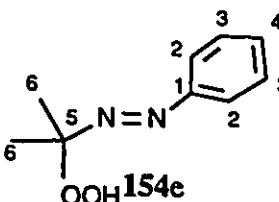
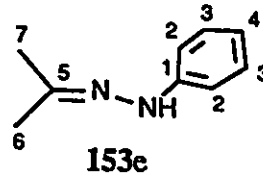
Table 13d. Spectral data for 155d and its precursors, 154d and 153d

Compound	^1H nmr ^a $\delta(\text{ppm})$	^{13}C nmr ^b $\delta(\text{ppm})$	UV(hexane) $\lambda_{(\text{max})}$ (ϵ)
 155d	0.93(t,3H) 1.15-1.58(m) + 1.42(s); 8H 1.70-1.88(m,2H) 3.92(t,2H) 4.80(s,br,1H)	13.80(C ₄) 20.38(C ₃) 26.95(C ₆) 29.66(C ₂) 66.48(C ₁) 93.55(C ₅)	292 (9.4) 340 (19.5)
 154d	0.97(t,3H) 1.12-1.61(m) + 1.45(s); 8H 1.65-1.93(m,2H) 3.87(t,2H) 9.40(s,br,1H)	13.95(C ₄) 20.38(C ₃) 21.80(C ₆) 29.79(C ₂) 68.82(C ₁) 102.86(C ₅)	292(10.4) 360(22.1)
 153d	0.93(t,3H) 1.19-1.63(m,4H) 1.75(s,3H) 1.95(s,3H) 3.14(t,2H) 4.08(s,br,1H)		

^a In CDCl_3 , with Me_4Si (TMS) as internal standard. The chemical shifts (δ -values) are followed, in paranthesis, by the multiplicity (s = singlet, d = doublet, m = multiplet etc.), and the signal intensity.

^b In CDCl_3 , with the solvent signal as the internal reference..

First of all, the reaction is very fast even at 0°C and an almost quantitative yield of the azocarbinol is formed regardless of the substituents on the azohydroperoxide. Secondly, triphenylphosphine oxide (Ph_3PO) formed as a product of the reaction is a crystalline solid

Compound	^1H nmr ^a $\delta(\text{ppm})$	^{13}C nmr ^b $\delta(\text{ppm})$	UV $\lambda_{(\text{max})}$ (ϵ)
 155e	1.48 (s,6H) 4.91 (s,br,1H) 7.30-7.90(m,5H)	26.97(C_6) 94.20(C_5) 122.63(C_3) 129.02(C_4) 130.96(C_2) 149.77(C_1)	$\left\{ \begin{array}{l} 258^{\text{c,d}} \\ 378 (135.1)^{\text{d}} \end{array} \right.$ $\left\{ \begin{array}{l} 260^{\text{f,e}} \\ 384 (121.2)^{\text{e}} \end{array} \right.$
 154e	1.52(s,6H) 7.32-7.75(m,5H) 9.15(s,br,1H)	21.96(C_6) 103.98(C_5) 122.68(C_3) 127.24(C_4) 131.44(C_2) 151.21(C_1)	260 ^{c,d} 406 ^{c,d}
 153e	1.65(s,3H) 1.92(s,3H) 6.55-7.40(m,6H)	14.96(C_6) 24.75(C_7) 112.74(C_2) 119.17(C_4) 128.85(C_2) 143.75(C_1) 145.85(C_5)	

^a In CDCl_3 , with Me_4Si (TMS) as internal standard. The chemical shifts (δ -values) are followed, in paranthesis, by the multiplicity (s = singlet, d = doublet, m = multiplet etc.), and the signal intensity.

^b In CDCl_3 , with the solvent signal as the internal reference..

^c The extinction coefficient not determined. ^d Measurements made in petroleum ether. ^e In acetone.

and is practically insoluble in petroleum ether at low temperatures; therefore it could be easily removed by filtration. Finally, since Ph_3P and Ph_3PO are non-volatile solids having very high boiling points, the azocarinols could be easily purified by bulb to bulb distillation (See Experimental Section for details) under reduced pressure.

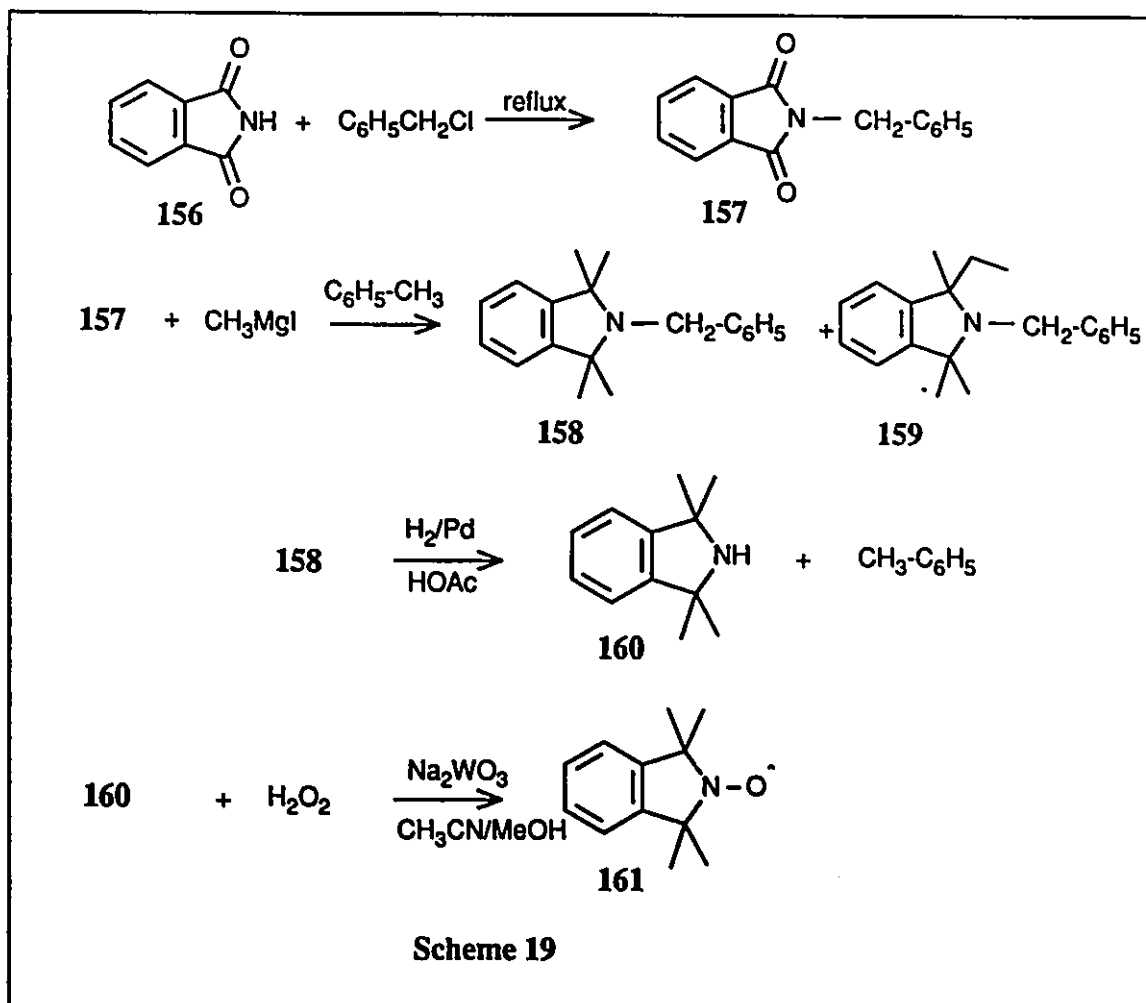
As mentioned earlier, characteristic changes in the ^1H NMR spectra are observed when the hydrazone (153) is converted to the hydroperoxide (154). Two separate methyl signals (at around δ 1.7 and δ 1.9 ppm) of the hydrazone give way to a singlet (at around δ 1.4 ppm) when it is oxidized to the peroxide. The azohydroperoxides can be easily distinguished from the corresponding azocarinols. The gem-dimethyl signal of the hydroperoxide appears slightly downfield from that of the azocarinol. Moreover, the peroxide has a characteristic -OOH (δ 9.2 ppm) signal, while the -OH group of the azocarinol appears at around δ 4.5 ppm.

^{13}C NMR spectra of the hydrazones show two separate methyl signals at around 15 ppm and 25 ppm, while for the peroxide the methyl groups are equivalent and the signal appears at around 22 ppm. Upon oxidation, the imine-like carbon, at around 145 ppm, of the hydrazone is converted to an sp^3 carbon, at around 103 ppm, of the hydroperoxide. The main difference in the ^{13}C NMR spectrum of the peroxide and the azocarinol is in the carbon atoms bearing the hydroperoxy and the hydroxy groups. The former one appears around 103 ppm and the latter one is around 93 ppm.

All the compounds listed in Tables 13a-e are liquids, soluble in petroleum ether and in benzene. The hydrazones are stable and can be stored in the absence of air for months, without any problem. On the other hand, the azohydroperoxides and the azocarinols are thermally (and also photochemically) unstable and therefore should be stored at low temperatures preferably in bottles wrapped with aluminum foil. **Warning!!:** Because of the explosive nature of the azohydroperoxides and of the azocarinols, they should be handled with great care and with adequate protection.

2.1.1 Synthesis of 1,1,3,3-Tetramethylisindolin-2-ylloxyl radical (161)

The procedure developed by Solomon and co-workers²⁴⁶ was used for the synthesis of this powerful radical scavenger. Modifying the procedure reported by Heidenbluth et.al.,²⁴⁷ Solomon and co-workers²⁴⁶ used N-benzyl phthalimide (157) in the place of N-methyl phthalimide as the precursor for its synthesis. The various steps involved in the synthesis are summarized in Scheme 19.



Initial attempts to make 158 using the Grignard reaction in Step 2 (Scheme 19) gave only low yields (<15%) of the product. However, by reducing the volume of the

solvent and increasing the reaction time (see Experimental Section) it was possible to increase the yield of **158** to 42%, which is slightly higher than the reported (37%)²⁴⁶ yield. The only major difference observed was in the ratio of the products **158** and **159** formed in the Grignard reaction. The product **159** was obtained in a relative yield of 18.5% in the unrecrystallised product, whereas Solomon et al²⁴⁶ reported the contaminant **159** to be 2-3% in their unrecrystallised product.

2.2.0 DETERMINATION OF RATE CONSTANTS FOR SOME RADICAL-MOLECULE REACTIONS IN SOLUTION

2.2.1 Rate constants for Cl abstraction from CCl₄ by the 5-hexenyl radicals

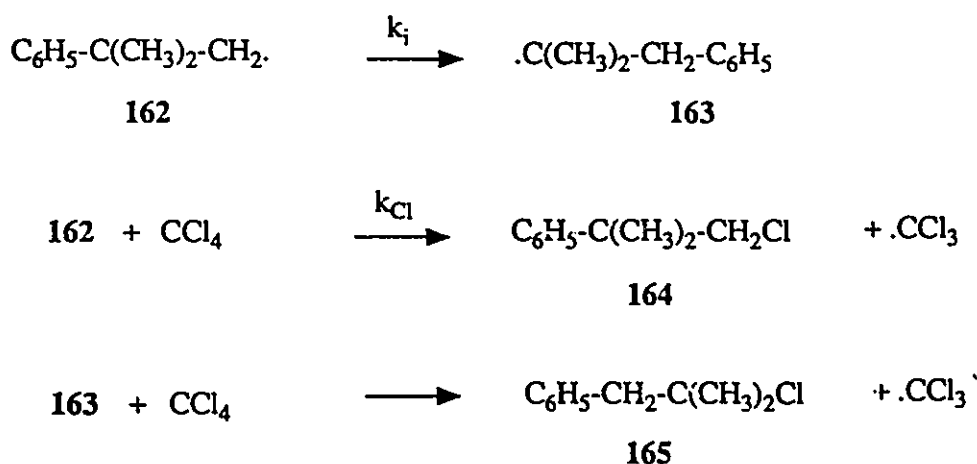
There are a number of reports in the literature regarding the facile Cl abstraction from CCl₄ by a variety of alkyl radicals.²⁴⁷⁻²⁵⁵ The absolute rate constants for the Cl atom transfer, determined using different experimental techniques, for various radicals differ very widely in their magnitudes (10²-10⁵ M⁻¹sec⁻¹). The available kinetic data (from both solution-phase and gas-phase studies) are summarized in Table 14. Even for similar radicals, the gas-phase and solution-phase rate constants differ by orders of magnitude. The following brief introduction deals mainly with the available rate constants for primary alkyl radical attacks on CCl₄, with a view to compare the data from two different experimental procedures (one using the neophyl radical clock²⁵⁴ and the other using the kinetic esr spectroscopy),²⁵⁵ and also to emphasize the need for a re-estimation of the rate constant using the most reliable 5-hexenyl clock.

Ingold et.al²⁵⁴ have estimated the rate constants for chlorine abstraction by neophyl radicals from CCl₄, making use of the neophyl rearrangement (eq.8) as a clock. Generation of neophyl radicals (**162**) in carbon tetrachloride resulted in the formation of the chlorides **164** and **165**, according to the reactions in Scheme 20. The rearrangement

Table 14. Rate constants for the attack of some alkyl radicals on CCl_4

Radicals	Temp.(°C)	Rate Constants ($\text{M}^{-1}\text{s}^{-1}$)	Reference
$n\text{-C}_6\text{H}_{11}\cdot$	25	1.0^a	247
	"	$1.25 \times 10^5^b$	248
$n\text{-C}_5\text{H}_9\cdot$	"	28^a	249
	27	$5.0 \times 10^3^b$	255
$(\text{CH}_3)_3\text{C}\cdot$	37	$4.9 \times 10^4^b$	250
	27	$3.1 \times 10^4^b$	255
$\text{HOCH}_2\cdot$	-40	$2.5 \times 10^5^b$	251
$\text{CH}_3\cdot$	25	24^b	252
	"	69^a	253
$\text{CH}_3\text{CH}_2\cdot$	"	$1.4 \times 10^2^a$	"
$\text{CH}_3\text{CH}_2\text{CH}_2\text{CH}_2\cdot$	27	$5.8 \times 10^4^b$	255
$(\text{CH}_3)_2\text{CH}\cdot$	25	33^a	253
$\text{Ph-C}(\text{CH}_3)_2\text{CH}_2\cdot$	"	$1.2 \times 10^4^b$	254
		$2.0 \times 10^4^{b,c}$	

^a Gas phase data. ^b Solution phase data. ^c For details see text



Scheme 20

(162 to 163) occurred in competition with the Cl-atom abstraction from CCl_4 by 162 (Scheme 20). The relative rate constants (k_i/k_{Cl}) at various temperatures were calculated from measurements of product ratios in the range 60 to 130°C, and from the data the following Arrhenius expression (eq.108, where $\theta = 2.3 \text{ RT kcal/mol}$) was derived.

$$[108] \quad \log(k_i/k_{\text{Cl}}/M) = (3.41 \pm 0.14) - (6.30 \pm 0.23)/\theta$$

Substituting for $\log k_i = (11.55 \pm 0.28) - (11.82 \pm 0.28)/\theta$, derived from the then available kinetic data,²⁵⁴ Ingold et.al obtained the rate constant (k_{Cl}) for chlorine abstraction from CCl_4 by a primary alkyl radical as eq.109, which gives $k_{\text{Cl}} = 1.2 \times 10^4 \text{ M}^{-1} \text{ s}^{-1}$ at 25°C.

$$[109] \quad \log(k_{\text{Cl}}/\text{M}^{-1}\text{s}^{-1}) = (8.14 \pm 0.42) - (5.52 \pm 0.63)/\theta$$

As mentioned before, the rate constants for the neophyl radical rearrangement were calculated by assuming that the rate constant for H-abstraction from Bu_3SnH by neophyl radical is the same as that for ethyl and butyl radicals.²⁵⁴ But a recent estimate by Johnston et.al.⁶⁰ of the rate constants for H-abstraction by neopentyl radicals from

Bu_3SnH probably represents a closer match for the neophyl system. The use of $k_{\text{H}(\text{neopentyl})}$ ⁶⁰ leads to a small revision (see eq.110) for the reported rate constant (k_i) for the neophyl rearrangement. Substitution of eq.110 in eq.108 yields eq.111, which gives

$$[110] \quad \log(k_i/\text{s}^{-1}) = 10.98 - 10.83/\theta$$

$$[111] \quad \log(k_{\text{Cl}(\text{neophyl})}/\text{M}^{-1}\text{s}^{-1}) = 7.6 - 4.5/\theta$$

$k_{\text{Cl}} = 2 \times 10^4 \text{ M}^{-1} \text{ s}^{-1}$ as the rate constant for Cl abstraction from CCl_4 by the neophyl radicals at 25°C.

The most recent estimate for the rate constant (eq.112) for a primary radical attack on CCl_4 is that by Hawari et.al.²⁵⁵ for the *n*-butyl radicals, determined by kinetic esr spectroscopy. Their rate constant ($k_{\text{Cl}(\text{n-bu})} = 5.6 \times 10^4 \text{ M}^{-1} \text{ s}^{-1}$ at 25°C) for butyl radicals is

$$[112] \quad \log(k_{\text{Cl}(\text{n-butyl})}/\text{M}^{-1}\text{s}^{-1}) = 8.6 - 5.3/\theta$$

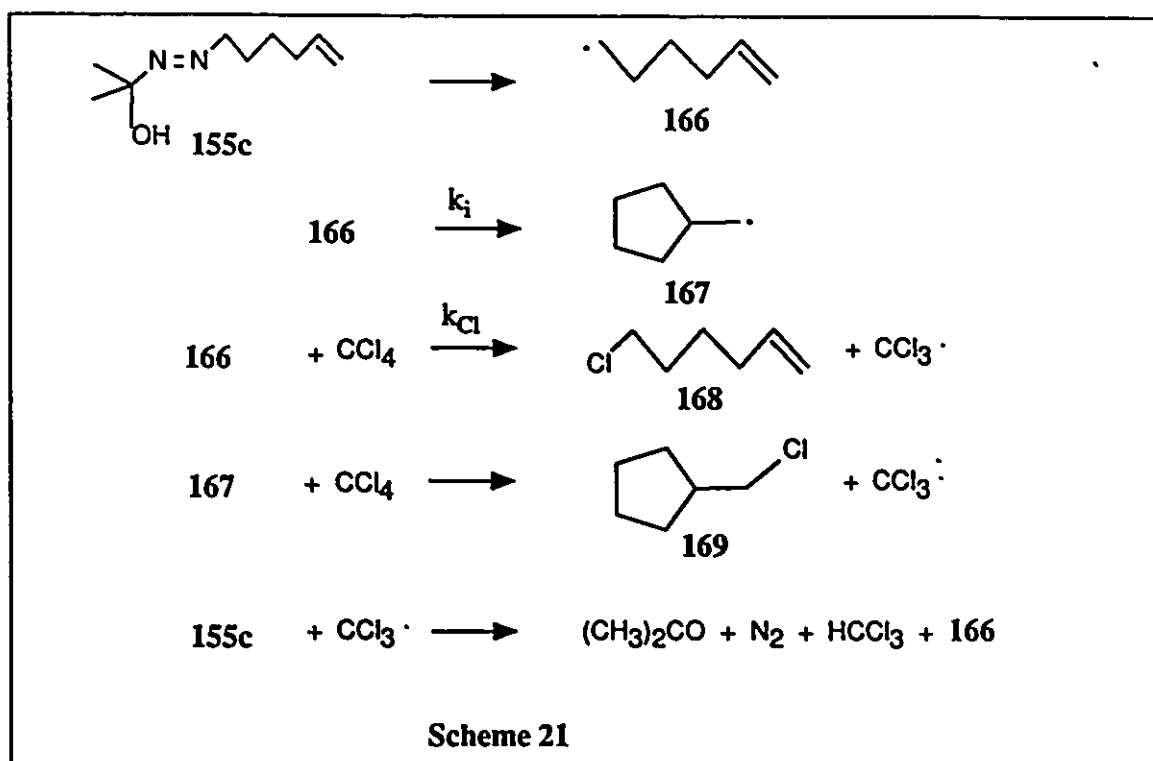
approximately a factor of 3 higher than that for the neophyl radicals at 25°C. In view of the inherent uncertainty in radical concentrations measured by the kinetic esr technique, by which the former rate constant was determined, and of the fact that neophyl is a hindered primary alkyl and therefore not necessarily a good model, it seemed important to determine k_{Cl} by another method.

In an effort to determine k_{Cl} and to answer the question as to whether or not neophyl clock is a good model for estimating reactivities of unbranched 1° alkyl radicals, we have determined the rate constants and Arrhenius expression for attack of the 5-hexenyl radical (5-hex) on CCl_4 . Our results represent an independent check of $k_{\text{Cl}(\text{n-butyl})}$, because *n*-butyl and 5-hexenyl radicals are structurally similar. The introduction of a new source for the 5-hexenyl radical, and the involvement of a radical chain mechanism for the Cl abstraction from CCl_4 by the radical are key elements of the

methodology we have used in this experiment.

Method

The method is based on the competition kinetics involving the ring-closure of the 5-hexenyl radical and the Cl-abstraction by this radical from CCl_4 , according to the reactions given in Scheme 21. The 5-hexenyl radical (166), generated from the radical



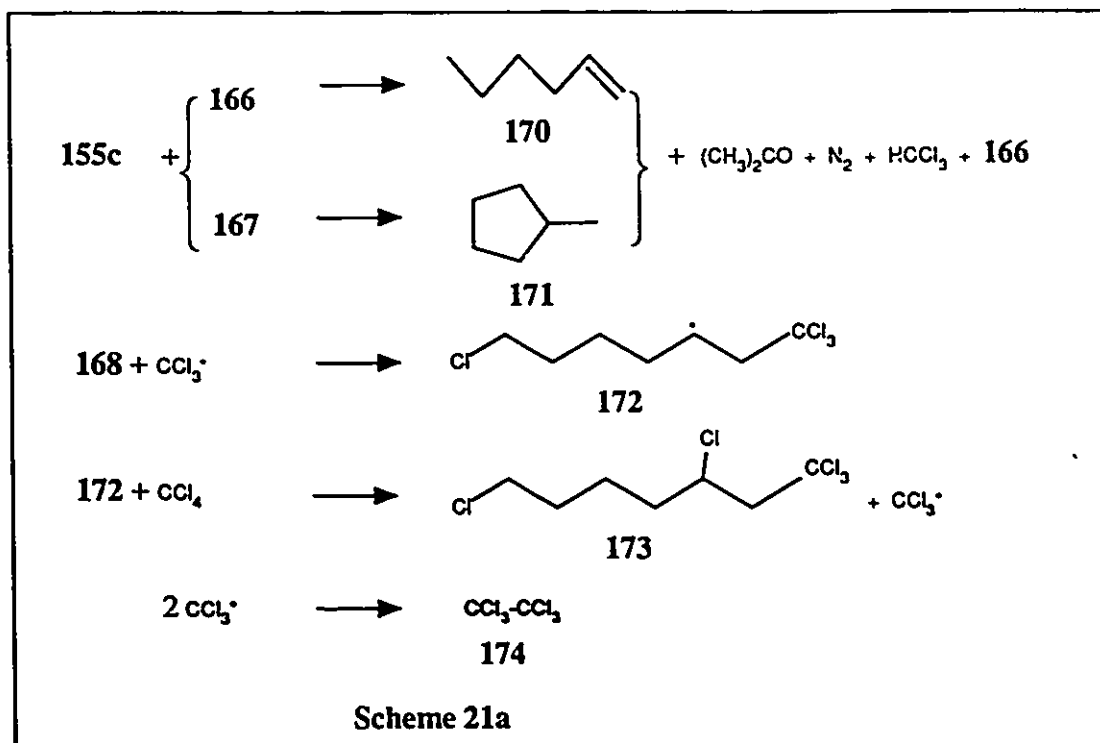
source **155c**, isomerizes (with rate constant k_i) to the cyclopentylmethyl radical **167** in competition with Cl abstraction from CCl_4 (with a rate constant k_{Cl}) to form 5-hexenyl chloride (**168**). Radical **167** also abstracts chlorine from CCl_4 to form cyclopentylmethyl chloride (**169**). The trichloromethyl radicals formed in the above reactions induce the decomposition of the azocarbinoil **155c** to form acetone, nitrogen, chloroform and the radical **166**.

The 5-hexenyl cyclization ($166 \rightarrow 167$) was chosen as the clock for estimating k_{Cl} .

because this rearrangement, having a rate constant $k_i = 2 \times 10^5 \text{ s}^{-1}$ at 25°C , is known to compete effectively with bimolecular reactions having rate constants in the range 10^3 - $10^7 \text{ M}^{-1} \text{ s}^{-1}$. The rate constants (k_{Cl}) for the 5-hexenyl radical attack on CCl_4 are expected to be in the above range since butyl,²⁵⁵ neophyl,²⁵⁴ and phenyl²⁵⁶ radicals are known to react with CCl_4 at 25°C with rate constants $5.6 \times 10^4 \text{ M}^{-1} \text{ s}^{-1}$, $2.0 \times 10^4 \text{ M}^{-1} \text{ s}^{-1}$, and $3.0 \times 10^6 \text{ M}^{-1} \text{ s}^{-1}$, respectively.

α -Hydroxy diazene 155c was chosen as the radical source for various reasons. First of all, it was known that compounds with the following combination of functional groups, $\text{R}^1\text{R}^2\text{C}(\text{OH})\text{-N=N-R}$, undergo induced decomposition by trichloromethyl radicals resulting in the formation of chloroform and other products²³³ in addition to the desired radicals (R^\cdot). Secondly, long kinetic chains are possible for such a source and therefore the product mixture contains only small amounts of products from radical coupling reactions, making the analysis relatively simple and straightforward. The reliability of rate constants determined using competition systems like this largely depends on the accuracy of measurements of the relative amounts of products. The present system makes an excellent example, where the products could be analyzed and quantitated quite reliably using the glc technique.

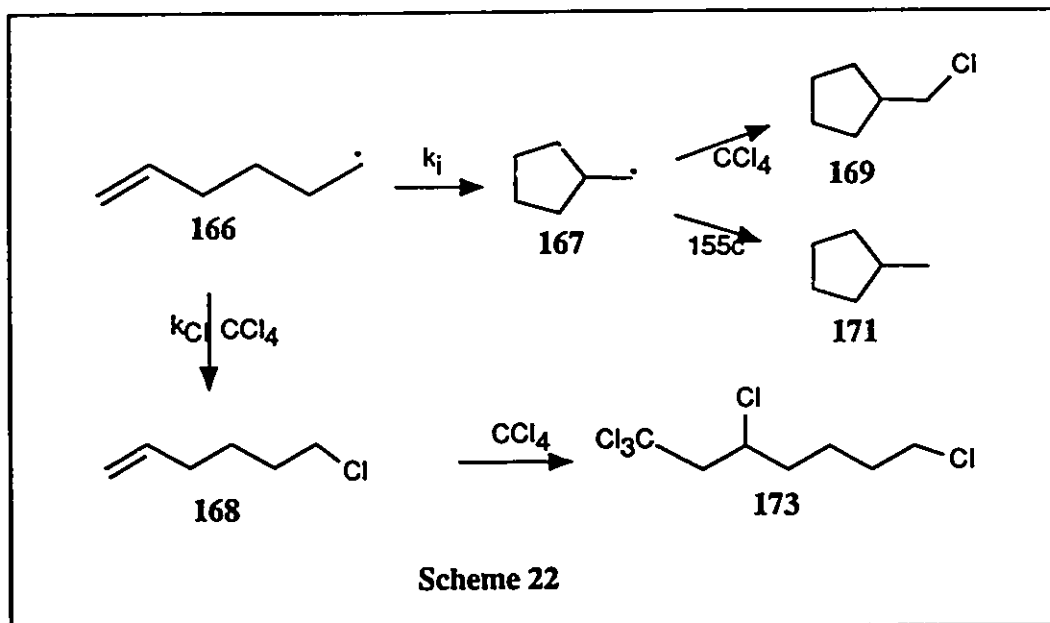
It was observed that thermal as well as photo-initiated decomposition of 155c in CCl_4 resulted in the formation of a few other products in addition to the products presented in Scheme 21. Among the identified products are 1-hexene (170), methyl cyclopentane (171), 1,1,1,3,7-pentachloroheptane (172), hexachloroethane (174), and acetone azine (175). The most probable routes to the formation of products 170-174 are given in Scheme 21a. Induced decomposition of 155c by radicals 166 and 167 results in the formation of the H-abstraction products 170 and 171, respectively. It is reasonable to assume that the attack of trichloromethyl radical on the double bond of 1-chloro-5-hexene (168) results in the formation of the more stable 2° radical 172, which abstracts chlorine



from the solvent (CCl_4) to form the pentachloro compound **173**. Coupling of trichloromethyl radicals results in the formation of **174**.

Calculation of Rate Constants

The relevant reactions (already presented in Schemes 21 & 21a) necessary for the rate constant calculation are summarized in Scheme 22. The sum of the concentrations of the products **169** and **171** should be proportional to the rate of formation ($k_i \times [166]$) of the radical **167**, if one reasonably assumes that **169** and **171** are the only two products formed from the rearranged radical **167**. Similarly, the sum of the concentrations of the chlorine abstraction products ($[168] + [173]$) by **166** should be proportional to the rate of formation ($k_{\text{Cl}} \times [166][\text{CCl}_4]$) of **168**. Therefore, the rate constant (k_{Cl}) can be related to the concentrations ($[169]$, $[171]$, $[168]$, $[173]$) of the products and the concentration ($[\text{CCl}_4]$) of the substrate according to eq.113, where the isomerization rate constant (k_i) at the specific temperature is calculated from eq.47 (Section 1.3.1).



$$[113] \quad k_{Cl} = \frac{k_i([168] + [173])}{([169] + [171])[CCl_4]}$$

The experimental procedure is relatively simple and straightforward. A degassed and sealed (in nmr tube) mixture of 155c (~0.3 M) in CCl₄ (neat, ~10 M) was photolysed (λ250 nm) or thermolysed at a specific temperature, until the starting material (155c) decomposed completely. The completion of the reaction could be inferred from the nmr spectrum by the disappearance of the gem-dimethyl signal of 155c at δ1.26. The products of reaction were analysed both by ¹H nmr spectroscopy and by glc. Details of these are given in the Experimental Section.

It should be pointed out that for the rate constant calculation, the determination of absolute concentrations (which is often difficult for practical reasons) of products is not necessary. The ratio, ([168]+[173])/([169]+[171]), of products can be readily obtained

from the gc counts. Substitution of this ratio in eq.113, along with the values for $[\text{CCl}_4]$ and k_i , gives k_{Cl} . The experimental results obtained for the reaction at 274 K, ²⁵⁷ along with the data for 303 K, 323 K, and 353 K²⁵⁸ are summarized in Table 15.

T(K)	$[\text{CCl}_4]$	Relative Yields ^a				ratio ^b	Mean	$k_i(\text{s}^{-1}) \times 10^{-5}$	$k_{\text{Cl}}(\text{M}^{-1}\text{s}^{-1}) \times 10^{-4}$
		[168]	[173]	[171]	[169]				
274	10.17	0.188	0.237	0.122	1.00	0.382	0.392 ± 0.011	0.791	0.305
		0.268	0.183	0.160	1.00	0.389			
		0.197	0.251	0.110	1.00	0.404			
303	9.81	0.390	0.067	0.128	1.00	0.405	0.401 ± 0.005	2.66	1.11
		0.332	0.127	0.120	1.00	0.410			
		0.418	0.108	0.272	1.00	0.414			
323	9.66	0.355	0.078	0.220	1.00	0.355	0.337 ± 0.017	5.40	1.87
		0.351	0.056	0.210	1.00	0.336			
		0.392	0.054	0.387	1.00	0.332			
353	9.39	0.315	0.055	0.331	1.00	0.278	0.268 ± 0.009	13.5	3.85
		0.305	0.036	0.293	1.00	0.264			
		0.303	0.037	0.298	1.00	0.262			

^a The relative yields calculated from the gc counts, taking the yield of 169 as unity. It is, however, assumed that the detector responses are the same.

^b ratio = $\{[168] + [173]\} / \{[169] + [171]\}$

A least squares treatment of the data given in Table 15 gives eq.114, where $\theta = 2.3$ RT kcal/mol, as the Arrhenius expression for the chlorine abstraction by the 5-hexenyl radical. The Arrhenius plot ($\log k_{\text{Cl}}$ vs. $1/T$) is given in Fig.3. Eq.114 gives $k_{\text{Cl}} = 7.2 \times 10^3 \text{ M}^{-1} \text{ s}^{-1}$, at 25°C, which is a factor of 8 smaller than that reported by Hawari et.al.²⁵⁵ for

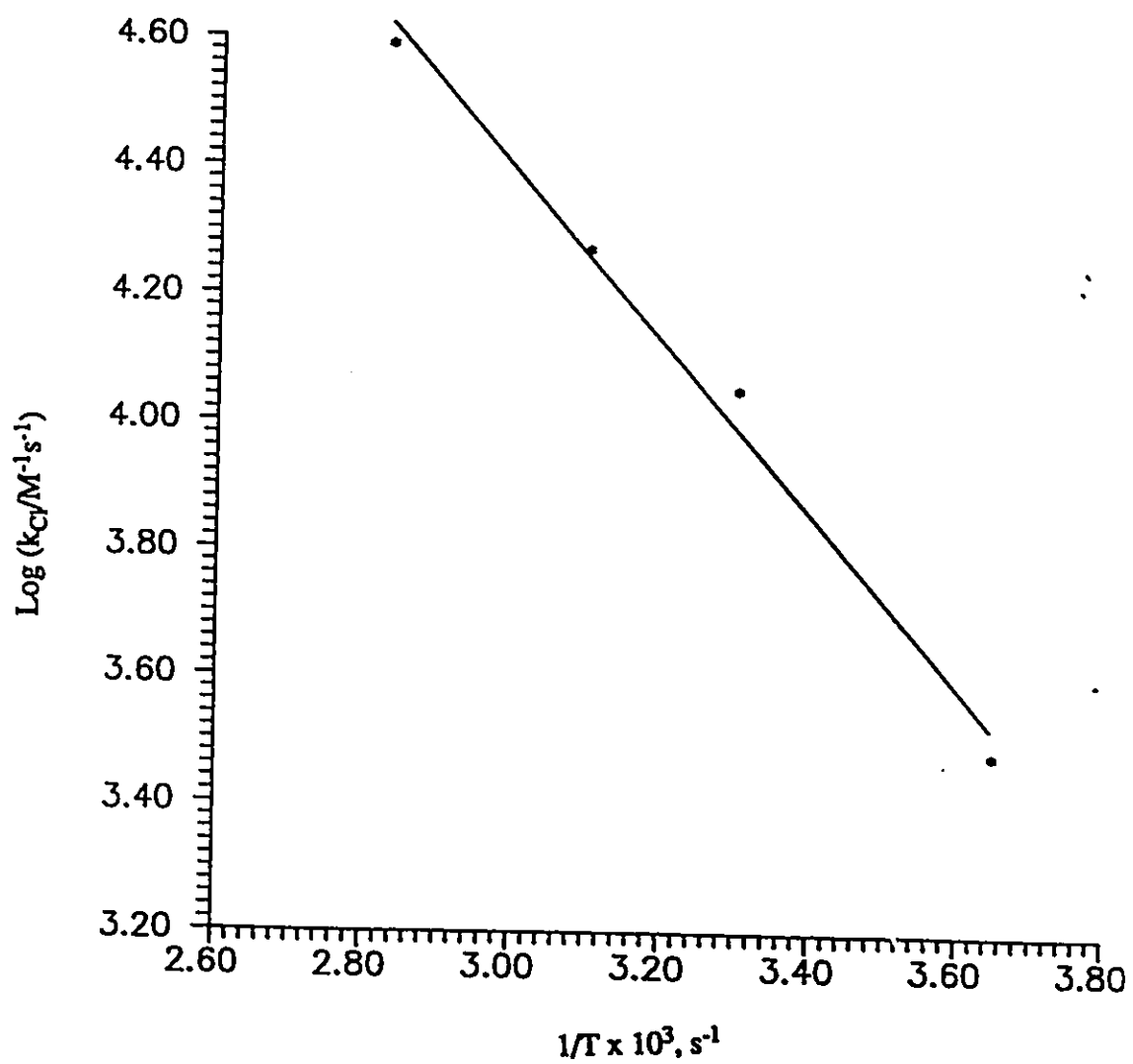


Fig. 3. Arrhenius Plot for the Data in Table 15

$$[114] \quad \log (k_{\text{C}}/\text{M}^{-1}\text{s}^{-1}) = (8.4 \pm 0.3) - (6.2 \pm 0.4)/\Theta$$

the *n*-butyl radical and a factor of ~ 3 smaller than that for the neophyl radical (see Table 14). The considerable disagreement between our results and the results from the esr experiment²⁵⁵ is not very surprising when one recognizes that the kinetic esr technique is prone to large errors. The agreement between our number and that by the use of neophyl radical is quite satisfactory and it seems, therefore, that the neophyl rearrangement can probably be used as a reliable clock for estimating rate constants for radical-molecule reactions such as the chlorine abstraction reaction.

2.2.2. Rate constants for bromine abstractions from a few bromo compounds by carbon-centered radicals

(i) Reactions of BrCCl₃ with cyclopropylmethyl, butyl, and phenyl radicals

Bromotrichloromethane reacts with a large variety of alkyl radicals by the transfer of the bromine atom. There are only a few reports in the literature regarding the absolute rate constants for the attack of primary, secondary or tertiary alkyl radicals on BrCCl₃. An early estimate for the rate constant for the reaction of methyl radicals with bromotrichloromethane comes from the gas-phase studies by Macken and Sidebottom.²⁵² The reported Arrhenius expression for the above reaction is $\log (k_{\text{Br(Me)}}/\text{M}^{-1}\text{s}^{-1}) = 8.1 \pm 0.3 - 3.5/\Theta$, where $\Theta = 2.3 \text{ RT kcal mol}^{-1}$. From the above equation the rate constant at 25°C can be calculated as $k_{\text{Br(Me)}} = 3.4 \times 10^5 \text{ M}^{-1}\text{s}^{-1}$.

For the attack of phenyl radicals on BrCCl₃, the rate constants have been determined in solution by Kryger et al.²⁵⁶ The reported values (calculated using different competition experiments) for the above reaction at 45 °C are $k_{\text{Br(Ph)}} = 1.4 \times 10^9$, $1.93 \times$

10^9 , 1.67×10^9 , and $1.85 \times 10^9 \text{ M}^{-1} \text{ s}^{-1}$. The solvent used was CCl_4 except for the first value, which was obtained in benzene as solvent. The above rate constants, calculated using different competition systems²⁵⁶ are in good agreement with each other and the mean of these values, $1.7 \times 10^9 \text{ M}^{-1} \text{ s}^{-1}$, can be regarded as the rate constant for the phenyl radical attack on bromotrichloromethane.

Rate constants for the reaction of cyclopropyl radicals with BrCCl_3 have been reported by Ingold et al.²⁵⁹ According to their estimate, the rate constant at 25°C is $2.8 \times 10^9 \text{ M}^{-1} \text{ s}^{-1}$.^{259a} 1-Methylcyclopropyl radical reacts with BrCCl_3 with a rate constant, $3.7 \times 10^9 \text{ M}^{-1} \text{ s}^{-1}$ at 25°C ,^{259b} which is slightly larger than that for the cyclopropyl radical itself.

It has been observed by Ingold and co-workers²⁵⁹ that phenyl radicals react with various substrates faster than cyclopropyl radicals while simple alkyl radicals react more slowly. But from the data given in the previous paragraphs it is evident that at least in the case of Br abstraction from BrCCl_3 the cyclopropyl radicals are more reactive than phenyl radicals.

The gas-phase kinetic data²⁵² for methyl radical attack on BrCCl_3 appear to be the only data reported for a primary alkyl radical. A comparison of this rate constant with those of the solution-phase estimations for the phenyl and the cyclopropyl radicals seem, at least to the order of magnitude comparison, to be appropriate. Thus, the relative rate constants (k_{Br}) for cyclopropyl,²⁵⁹ phenyl,²⁵⁶ and methyl²⁵² radicals are $8.6 \times 10^3 : 4.3 \times 10^3 : 1$, respectively at 25°C . Thus, methyl radical appears to be three orders of magnitude less reactive than phenyl radicals.

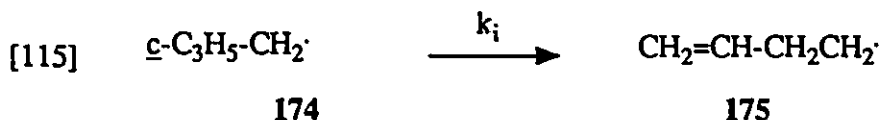
A reliable quantitative assessment of the relative reactivity of a primary alkyl radical and phenyl radical toward BrCCl_3 is possible only if a reliable rate constant for the bromine abstraction from BrCCl_3 by a primary alkyl radical is determined in solution. In this context, we have developed various methods for determining the rate constants for Br abstraction from BrCCl_3 by cyclopropylmethyl, butyl and phenyl radicals in solution.

a. Rate constants for the reaction of cyclopropylmethyl radicals with bromotrichloromethane

Method:

The general experimental procedures that can be used in the determination of rate constants for radical-molecule reactions have already been discussed in the Introduction Sections. The method that has been applied in our laboratory is based on the cyclopropylmethyl radical clock.

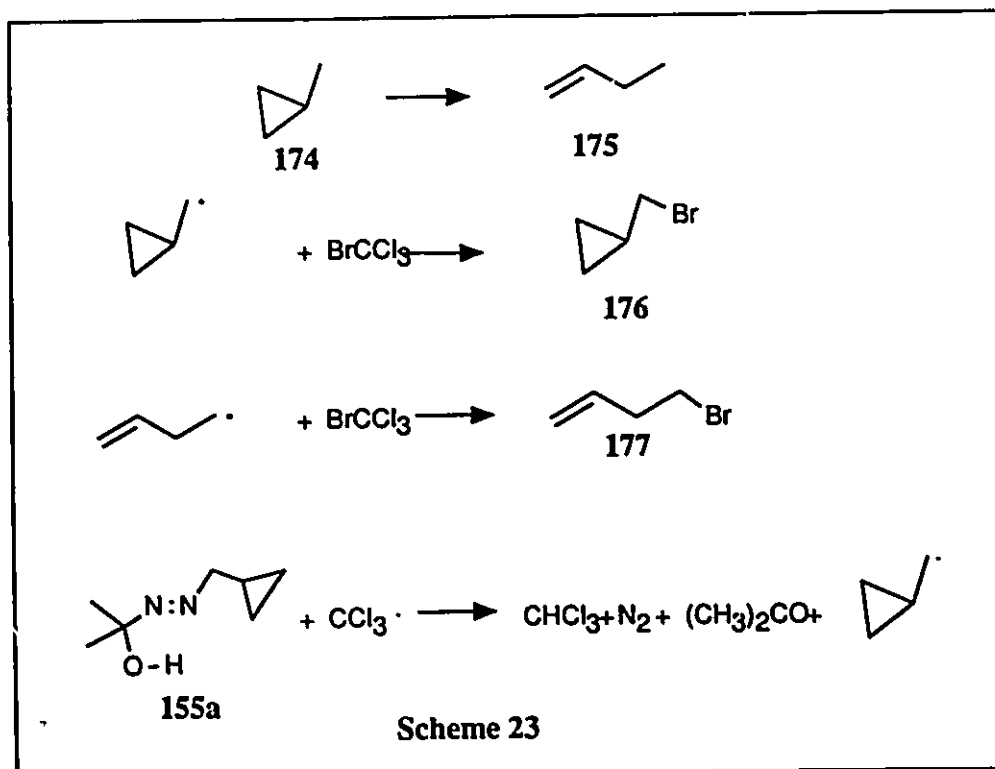
The cyclopropylmethyl radical (174), which undergoes rearrangement to the 3-butenyl radical (175) with a known rate constant k_i (eq.115), has been used as the clock reaction. This reaction was chosen as the most suitable 'clock' because the rearrangement,



with a rate constant, $k_i = 2.1 \times 10^8 \text{ s}^{-1}$ at 25°C, can effectively compete with any radical molecule reactions having rate constants in the range 10^7 - $10^{10} \text{ M}^{-1}\text{s}^{-1}$. This is the range for rate constants expected for radical attack on BrCCl_3 , which is already known to react with phenyl²⁵⁶ and cyclopropyl^{259b} radicals with nearly diffusion- controlled rate constants at or near room temperature. The reverse of the reaction represented by eq.115 is also known;⁷³ but because of its very low rate constant (ca $4.9 \times 10^3 \text{ sec}^{-1}$ at 25 °C),⁷³ this process must be insignificant in the presence of BrCCl_3 .

The source of the cyclopropylmethyl radical was the α -hydroxydiazene 155a, prepared by the sequence of reactions in Scheme 18. α -Hydroxy alkyldiazenes are known to decompose thermally or photochemically to give alkyl radicals in solution (See Section 1.5.2). Because of its facile decomposition at and near room temperature, 155a is a very

convenient source of cyclopropylmethyl radicals for measuring rate constants in this important temperature range. Moreover, the α -hydroxy alkyl diazenes are known to undergo thermal decomposition by a radical chain process, and in the presence of a substrate like BrCCl_3 a chain process represented by Scheme 23 can be expected.



The induced decomposition of the azocarinol, represented by the last reaction in Scheme 23, is a facile process probably because of the exothermicity of this reaction. This reaction enables the radical to be formed in a chain process. For kinetic studies the generation of radicals in a chain process has the additional advantage over other processes such as the decomposition of acyl peroxides, where radical pair chemistry can complicate the quantitation and identification of products. Moreover, the byproducts that are formed in the radical chain process (Scheme 23), namely chloroform and acetone, cause only minor problems during analysis by gas chromatography or by ^1H nmr spectroscopy. It is

also unlikely that chloroform and acetone would undergo any subsequent radical reactions under the experimental conditions.

A brief outline of the experimental procedure follows. Solutions of known concentrations of 155a in hexafluorobenzene or dichloromethane containing a known concentration of BrCCl_3 were degassed and sealed in nmr tubes. The tubes were kept in a constant temperature bath (for thermal runs) or they were irradiated (in low temperature experiments) until the gem-dimethyl signal of 155a could no longer be detected in the ^1H nmr spectrum. The contents of the tubes were then analyzed by the conventional glc technique (see Experimental Section for details).

The initial experiments were conducted in neat bromotrichloromethane and the products were analyzed by ^1H nmr spectroscopy. The major products were cyclopropylmethyl bromide (>90 %), acetone (100%), and chloroform (\approx 90 %). Small quantities (<5 %) of 3-bromobutene (177) were detected by weak signals in the ^1H nmr spectra. However, they could not be integrated with any degree of confidence.

The above results indicated that the bromine abstraction from BrCCl_3 can effectively compete with the ring-opening of cyclopropylmethyl radicals. Since a lower concentration of BrCCl_3 is necessary to give a larger value for $[177]/[176]$, an inert solvent like C_6F_6 , or CH_2Cl_2 was used as diluent for most of the experiments. Indeed, it was observed by ^1H nmr spectroscopy and also by glc analysis that the ratio of the ring opened products to the ring-intact materials increased with decreasing concentrations of BrCCl_3 at a particular temperature. At lower temperatures the above ratio of products was found to decrease. This was expected for cyclopropylmethyl radicals since their ring-opening rate constant decreases rapidly with decreasing temperature (the activation energy for this rearrangement is 7.6 kcal/mol).

Analyses of the reaction mixtures were done both by ^1H nmr and by glc. Because of the insensitivity of the ^1H nmr spectral analysis to detect and quantitate products of

very low concentrations, glc analysis was used for most of the quantitative measurements. Details of the procedure are given in the Experimental Section.

The thermal or photo-initiated reaction of 155a in BrCCl_3 gave the same products. The nmr and glc analyses of spent solutions of 155a indicated a simple mixture of CHCl_3 , $(\text{CH}_3)_2\text{CO}$, $\text{c-C}_3\text{H}_5\text{-CH}_2\text{Br}$ (176), $\text{CH}_2=\text{CH-CH}_2\text{-CH}_2\text{Br}$ (177), hexachloroethane, $\text{Cl}_3\text{C-CH}_2\text{-CHBr-CH}_2\text{-CH}_2\text{Br}$ (179), and acetone azine (181), and a few minor product peaks which are either unidentified or partially identified. The azine which gave ^1H nmr signals at δ 1.7(s) and 1.85(s) in crude reaction mixture, was formed in amounts ranging from up to 8% in thermal runs to ca 3% in the photo-initiated runs. The azine signals were initially thought to originate from the mixed azine $((\text{CH}_3)_2\text{C=N-N=CH-c-C}_3\text{H}_5)$, formed by a formal dehydration of 155a. An authentic sample of the mixed azine, prepared from acetone hydrazone and cyclopropanecarboxaldehyde, gave an entirely different ^1H nmr spectrum as well as a different glc signal, ruling out this possibility. Addition of an authentic sample of the acetone azine to the reaction mixture increased the intensities of the unknown azine signals at δ 1.71 and 1.85. The identity of acetone azine as a product of the reaction was confirmed by the corresponding glc retention times of the authentic acetone azine and those from the reaction mixture.

The formation of acetone azine as a product of reaction is not easy to explain. First of all, the possibility of acetone azine as an impurity in the azocarinol can be ruled out since the ^1H nmr spectrum of different batches of 155a did not show the azine singlets. The signals were eventually formed during thermolysis or photolysis of 155a in the presence of BrCCl_3 and the signal intensities were found to increase during the reaction process. A second possibility to be ruled out was the presence of traces of hydrazine, which if present in the azocarinol could react with the acetone formed during the reaction to form acetone azine. The above possibility could be ruled out from the observation that decomposition of the same azocarinol sample in C_6F_6 in the absence of BrCCl_3 gave no

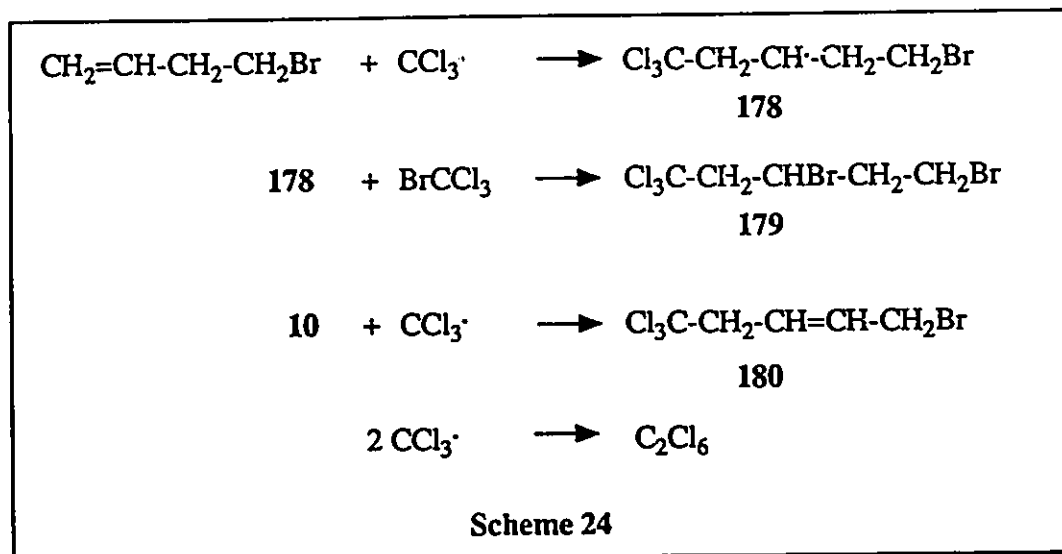
azine signals. Therefore, we assume that the mixed azine is formed as a minor product by the catalyzed dehydration of 155a, and that the mixed azine is subsequently equilibrated with the acetone (formed in excess) to form the acetone azine. Even though acetone azine's concentration is not contained in the kinetic equation (eq.117) for rate constant calculations, its source is of considerable interest mechanistically.

Trace amounts of some additional product signals were also registered by the glc analysis which was sensitive enough to detect products down to 0.2% under ordinary conditions. The total amount of such unidentified products ranged from 3 to 5% of the total identified products. In addition to these, the reaction mixture also contained a material (180) with a long retention time that was eluted just before 179. A careful analysis of the reaction mixture by gas chromatography coupled with mass spectroscopy (gc/ms) gave (for 180) $m/z = 256, 254, 252$, and 250 with intensity ratios appropriate for $C_5H_6BrCl_3$. A comparison of this formula with the molecular formula of 179, $C_5H_7Br_2Cl_3$, indicates that 180 probably is the result of a dehydrobromination of 179. It was also observed that 179 was stable enough to give a sharp and symmetric glc peak on a newly packed column. Partial decomposition of 179 leading to 180 was indicated on old gc columns, in which case two peaks, instead of one, were observed during the analysis.

The most likely structure of 180 is trans-1-bromo-5,5,5-trichloro-2-pentene. A reasonable mechanism for the formation of this compound in $BrCCl_3$ medium seems to be a disproportionation between 1-(2-bromoethyl)-3,3,3-trichloroprop-1-yl radicals (178) and the trichloromethyl radicals (Scheme 24). For the present kinetic studies, it is not critical that the mechanism of formation of 180, or its exact structure, be known. But since 180 is a product resulting from the rearranged radical 175 (see schemes 23 & 24), the concentration of 180 must be counted along with those of 177 and 179 in calculating k_{Br} .

Except for the formation of 3-8% of acetone azine, all the identified products from the decomposition of 155a in $BrCCl_3$ are well accounted for by the reactions given

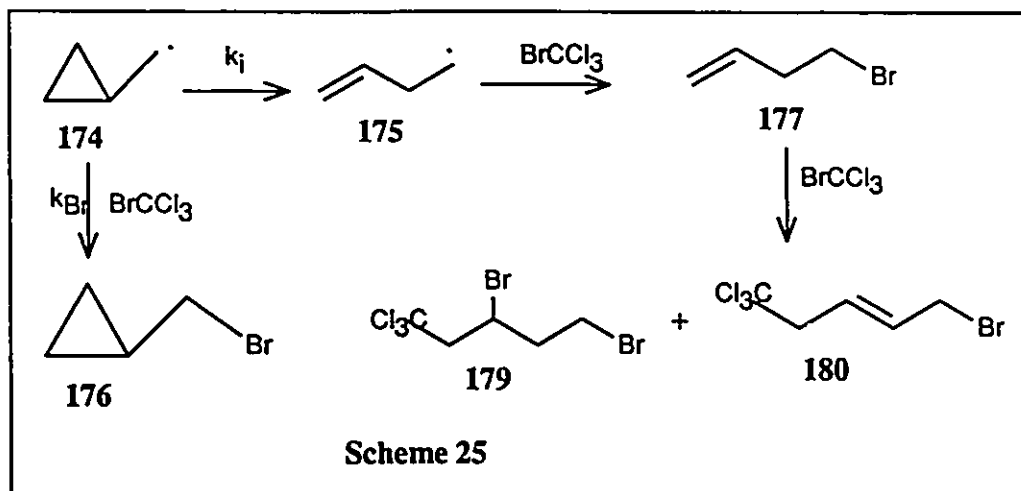
in Scheme 23 and by the subsequent reactions in Scheme 24.



The chain termination product C_2Cl_6 was detected in very small amounts. The ratios of the chain transfer product (CHCl_3) to the chain termination product (C_2Cl_6) in the thermal runs were found to be >70 . The above ratios indicate that 155a undergoes a chain reaction with an average kinetic chain length large enough to minimize competition from radical pair chemistry. For the photo-initiated runs the ratio $[\text{CHCl}_3]/[\text{C}_2\text{Cl}_6]$ were smaller (≈ 30), especially at lower temperatures. An obvious reason for this could be the fact that the activation energies for the H-abstraction by $\cdot\text{CCl}_3$ radicals from 155a ($E_a(\text{H})$) and the coupling reaction ($E_a(\text{C})$) are different and that $E_a(\text{H}) \gg E_a(\text{C})$. In such a case the chances of coupling reactions are increased relative to the H-abstraction at lower temperatures.

Calculation of rate constants

Scheme 25 summarizes the relevant reactions and the rate constants of interest. The rate constant (k_{Br}) for the reaction of cyclopropylmethyl radical with BrCCl_3 can be expressed as in eq.116, which can be rearranged to eq.117. Under conditions where the



$$[116] \quad \frac{[177] + [180] + [179]}{[176]} = \frac{k_i x [174]}{k_{Br} x [174] [BrCCl_3]}$$

$$[117] \quad k_{Br} = \frac{k_i x [176]}{([177] + [180] + [179]) x [BrCCl_3]}$$

concentration of $BrCCl_3$ remains approximately constant during reaction, the rate constant (k_{Br}) can be calculated from the ratio of the sum of the concentrations ($[177] + [180] + [179]$) of products derived from the radical 174 to the concentration of cyclopropylmethyl bromide [176], and from the rate constant (k_i) for the clock reaction, using eq.117. In the actual rate constant determination, the product concentration terms were substituted by their relative yields from the gc integrator counts (by applying correction for detector responses). The bromotrichloromethane concentration ($[BrCCl_3]$) is taken as the initial concentration of the reagent taken in more than ten-fold stoichiometric excess over that of the radical source, 155a.

The experimental data for the relative product concentrations and the ratio (k_i/k_{Br}) of rate constants determined using eq.117, in the temperature range 253-351 K, are summarized in Table 16.

Rn. #	Method	T, K ^a	Solvent	[155a] ^b (M)	[BrCCl ₃] ^c (M)	[176] ^d [177]+[180]+[179]	k_i/k_{Br} ^e (M)
1	Δ	341.6	C ₆ F ₆	0.159	2.26	1.11	2.04
2	Δ	341.6	C ₆ F ₆	0.159	2.26	1.01	2.24
3	Δ	322.8	C ₆ F ₆	0.159	2.31	1.78	1.30
4	Δ	322.8	CH ₂ Cl ₂	0.051	0.652	0.659	0.989
5	Δ	322.8	CH ₂ Cl ₂	0.051	0.652	0.600	1.09
6	Δ	321.8	C ₆ F ₆	0.185	2.31	1.97	1.17
7	Δ	321.8	C ₆ F ₆	0.217	2.79	2.10	1.33
8	hν	303.0	C ₆ F ₆	0.023	0.682	1.11	0.614
9	hν	303.0	C ₆ F ₆	0.008	0.889	1.61	0.551
10	Δ	302.8	C ₆ F ₆	0.185	2.37	3.58	0.662
11	Δ	302.2	CH ₂ Cl ₂	0.030	0.789	1.51	0.522
12	Δ	302.2	CH ₂ Cl ₂	0.030	0.789	1.52	0.519
13	hν	273.5	CH ₂ Cl ₂	0.051	0.693	2.19	0.316
14	hν	273.5	CH ₂ Cl ₂	0.051	0.693	2.01	0.347
15	hν	273.5	CH ₂ Cl ₂	0.051	0.693	1.99	0.348
16	Δ	273.0	C ₆ F ₆	0.159	2.51	6.80	0.369
17	hν	258.0	C ₆ F ₆	0.030	0.820	6.25	0.131
18	hν	256	C ₆ F ₆ ^f	0.106	1.44	9.99	0.144
19	hν	253	CH ₂ Cl ₂	0.097	1.06	9.55	0.111

^a) $\pm 0.2^\circ$ for $T > 300$ K, $\pm 0.5^\circ$ for $T = 273$ K, and $\pm 1.0^\circ$ for $T < 273$ K. ^b) Initial concentration. ^c) Initial concentration, corrected for volume expansion. ^d) Ratio determined by gas chromatography; each number represents the average value for three injections. The detector response factors for 176 and 177 were indistinguishable; and that for 179 was within 5% of that of 176 and 177 and a correction was not applied. ^e) calculated using eq.117. ^f) CCl₄ (33%) was added with solvent to prevent freezing.

The compounds 176, 177, and 179 were characterized by comparison of their ^1H nmr spectra with those of the authentic samples and also from the gc and/or gc/ms analyses. Details of this are given in the Experimental Section. The relative concentrations of the various products were calculated from their glc peak areas, multiplying them by their relative detector response factors. The detector response factors were calculated by injecting standard mixtures of authentic samples and obtaining relative peak areas per millimol of each compound. It was observed that the detector response factors for 176 and 177 were the same, within experimental errors. The response factor of 179 was within 5% of the response factors of 176 and 177, and a correction was not made. However, for chloroform the detector response was 3.4-fold smaller than those of 176 and 177, and therefore its area count was multiplied by 3.4 to calculate the relative yield.

An Arrhenius plot ($\log(k_i/k_{Br})$ vs. $1/T$) of the kinetic data (Table 16) is given in Fig.4. The Arrhenius expression (eq.118) for the relative rate constant is obtained by the least squares treatment of the data. Substituting $\log(k_i) = 13.31 - 7.26/\theta$ (eq.58) in eq.118, the temperature dependence of k_{Br} can be expressed as eq.119 which yields the rate constant at 25°C as $2 \times 10^8 \text{ M}^{-1} \text{ s}^{-1}$. The above number indicates that the Br abstraction from BrCCl_3 by cyclopropylmethyl radical is one of the fastest radical-molecule reactions. Nevertheless the rate constant, at room temperature, is well below the rate constant (k_d : for a diffusion controlled reaction ($k_d \approx 2 \times 10^9 \text{ M}^{-1} \text{ s}^{-1}$ at 25 °C). Temperature seems to have only a very small effect ($E_a = 2.1 \text{ kcal/mol}$) on the rate constant. A change of solvent: from hexafluorobenzene to methylene chloride resulted in a small increase in rate constant. Since the difference between numbers from the two solvents was marginal, within the range of experimental errors, the whole set of data (Table 16) was used for deriving the Arrhenius expression.

The rate constant for the attack of cyclopropylmethyl radicals on bromotrichloromethane obtained in this experiment can be compared to the gas-phase

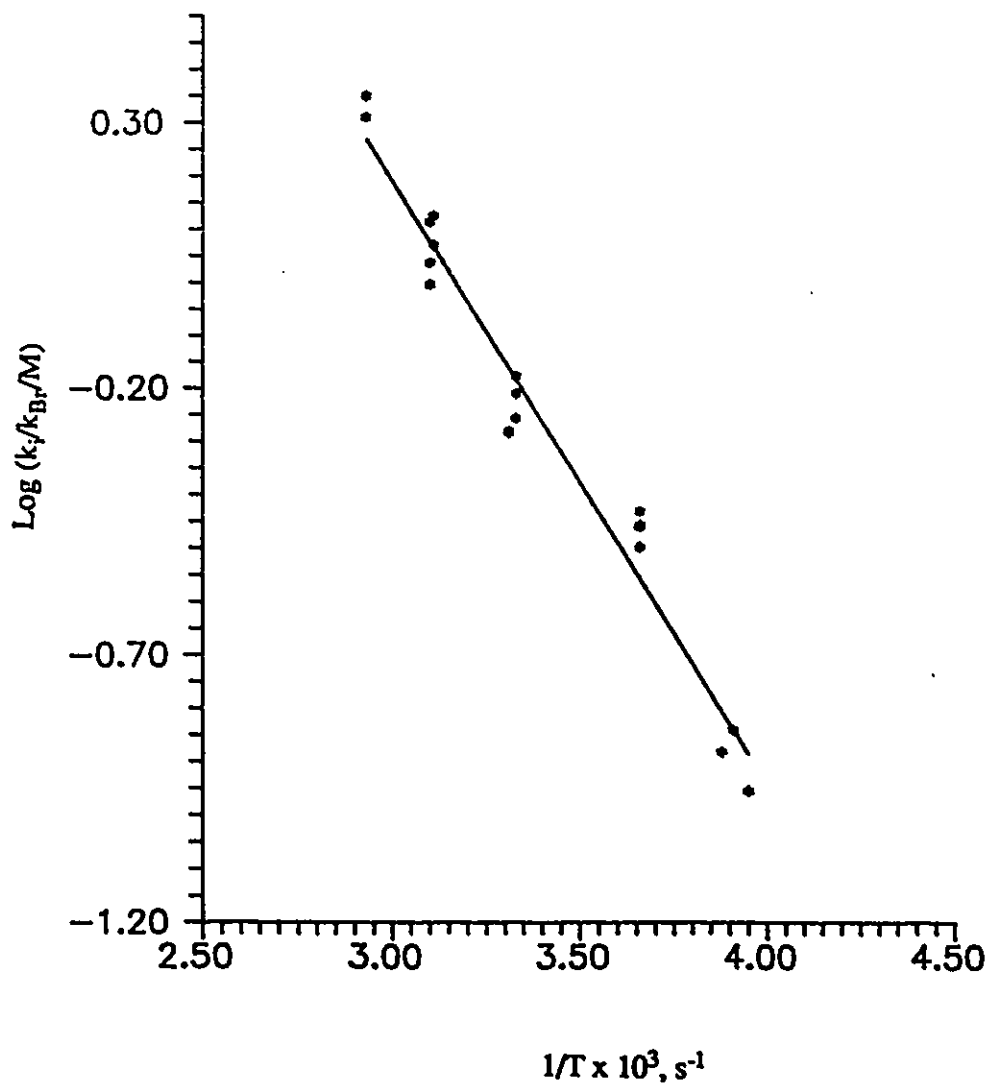
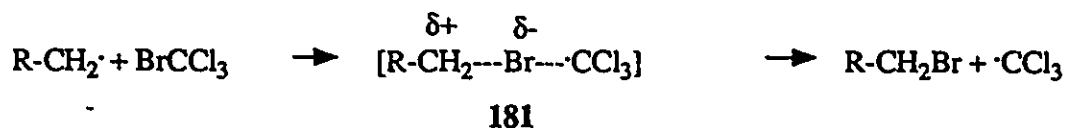


Fig. 4. Arrhenius Plot for the Data in Table 16

$$[118] \quad \log(k/k_{Br}/M) = 3.56 + 5.15/\theta$$

$$[119] \quad \log(k_{Br}/s^{-1}) = 9.75 - 2.11/\theta$$

kinetic data ($k_{Br} = 3.4 \times 10^5 \text{ M}^{-1} \text{ s}^{-1}$ at 25°C) for the bromine abstraction from bromotrichloromethane by methyl radicals.²⁵² Our value ($2 \times 10^8 \text{ M}^{-1} \text{ s}^{-1}$ at 25°C) is almost three orders of magnitude higher. There are no data available, at this stage, for a direct comparison in the solution phase for the same reaction by a primary alkyl radical. A reasonable explanation for the origin of the difference between gas-phase and solution-phase data seems to be the effect of a polar transition state, such as the one shown in 181. This type of polar contribution is known to operate in radical addition and



substitution reactions.²⁶⁰ The stabilization of a polar transition state is more pronounced in the solution-phase than in the gas-phase reactions, and therefore a low activation energy leading to a high rate constant is expected for such a reaction in solution. Moreover, a positive charge on a methyl radical is the least stabilized compared to other homologues, where hyperconjugative and inductive effects contribute to stabilize the charge more readily. When $\text{R} = \text{cyclopropylmethyl}$, the stabilization of the positive charge is even larger because of the non-classical type of interaction by the cyclopropane ring.

The above mentioned transition state stabilization naturally raises the question as to whether cyclopropylmethyl radical can be used as a representative primary alkyl radical

for kinetic studies such as the radical-molecule reaction. If the contribution from the polar stabilization is very high, then it is not possible to employ cyclopropylmethyl radical as a reliable clock.

In order to answer the above question, we have devised a method (see following sections) for the determination of rate constants for bromine abstraction from BrCCl_3 by *n*-butyl (a representative primary alkyl) and phenyl radicals in solution.

b. Rate constants for bromine abstraction from BrCCl_3 by *n*-butyl radicals.

The 'clock' reaction that was chosen for our study is the diffusion-controlled reaction between the radicals of interest and the 1,1,3-tetramethylisoindoline-2-yloxy radical (86). The radicals $\text{R}\cdot$ (where $\text{R} = n\text{-butyl}$) were generated by the thermal decomposition of azocarinols (155d). A mixture of excess 86 and BrCCl_3 were allowed to compete for $\text{R}\cdot$, formed in a chain process given by Scheme 26. The rate constants (k_{Br}) for Br abstraction relative to the rate constants (k_c) for the near diffusion-controlled coupling between 86 and $\text{R}\cdot$ can be calculated from the reaction steps given in Scheme 26.

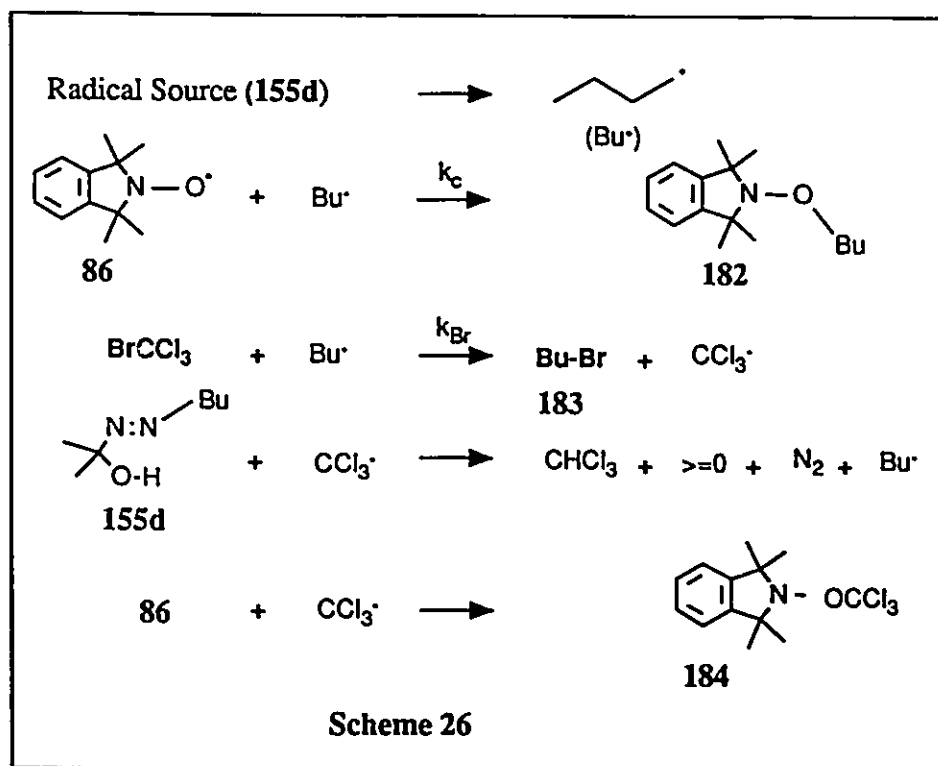
The rate constants (k_{Br}) for the bromine abstraction can be related to the coupling rate constant (k_c) using eq.120,121, knowing the relative concentrations of the coupling product (182) and *n*-butyl bromide (183), under conditions where the known initial concentrations of the nitroxide (86) and bromotrichloromethane remain approximately constant during the reaction.

$$[120] \quad [182]/[183] = (k_c \times [86]) / (k_{\text{Br}} \times [\text{CCl}_3\text{Br}])$$

or

$$[121] \quad k_{\text{Br}} = (k_c \times [86][183]) / ([182][\text{BrCCl}_3])$$

In the actual experiments, the nitroxide 86 and BrCCl_3 were taken in more than



tenfold excess over the azocarbonyl (155d) and therefore the initial concentrations of 86 and BrCCl_3 were used in eq.121 for the calculation of k_{Br} . The coupling rate constants (k_c) were calculated from those for the diffusion control (k_d) and the latter were calculated from the measured viscosities of the reaction medium.¹⁴⁷ Viscosities (η_s) of BrCCl_3 and mixtures of BrCCl_3 and C_6F_6 of appropriate compositions were measured at temperatures ranging from 25-80°C, with a viscometer calibrated with benzene (viscosities η_B) at various temperatures. The viscosities of the BrCCl_3 solutions were then calculated using eq.122, where t is the flow time for a constant volume of the liquid, d the density, and the

$$[122] \quad (\eta_s/\eta_B) = (t_s/t_B)(d_s/d_B)$$

subscripts s and B stand for solution and benzene, respectively. Since the volume change in mixing C_6F_6 and BrCCl_3 was found to be negligible, the densities of the mixtures were

calculated from the densities of the pure solvents. The densities at various temperatures were then estimated by the procedure given in ref.147, assuming the coefficient of cubical expansion (γ) for the solution to be 1.237×10^{-3} , and also assuming ideal behaviour for the solution.

Analysis of products in the reaction mixture obtained by thermolysing a mixture of known concentrations of 86, 155d, and BrCCl_3 could not be made using the ^1H nmr technique because of 86, a paramagnetic species, present in large excess in the reaction medium. Therefore, the progress of this reaction could not be monitored by ^1H nmr analysis. However, the decomposition at 80°C of an approximately 1:1 mixture of a very dilute ($\sim 10^{-2}\text{M}$) solution of azocarinol (155d) and 86 in BrCCl_3 could be followed using ^1H nmr, by monitoring the disappearance of the gem dimethyl peak of the azocarinol and this was used to estimate the minimum time required for the complete decomposition of 155d. Approximately 24 hr was indicated for $>98\%$ conversion at 80°C .

Products from the thermolysis of 155d in media containing both 86 and BrCCl_3 were analyzed for relative product yields by straightforward glc analysis. In addition to acetone and chloroform, the major products that were characterized and identified in the reaction mixture were 1-bromobutane (183) and 2-(1-butoxy)-1,1,3,3-tetramethylisoidoline (182). The product of coupling between 86 and $\text{CCl}_3\cdot$ (184) was eluted late as a broad peak and its presence did not interfere with the analysis. For quantitation of the relative concentrations of 183 and 182, the glc detector responses for these two compounds were determined using authentic materials. It was found that the detector was 3.1 times as sensitive to 182 as to 183.

The rate constants for bromine abstraction from BrCCl_3 by the butyl radical, calculated using eq.121 are given in Table 17. This gives $k_{\text{Br}} = (2.61 \pm 0.38) \times 10^8 \text{ M}^{-1} \text{ s}^{-1}$ at 80°C . The above rate constant reported earlier by us²⁶¹ needs a revision based on the recently published¹⁴⁸ rate constant (k_{T} , see eq.52) for coupling of 5-hexenyl radical with

Table 17. Product ratios and rate constants for 1-butyl radicals (80°C)			
Concentrations of reactants, M ^a		Product ratio ^b [183]/[182]	Rate constants ^c k_{Br} , M ⁻¹ s ⁻¹
[86]	[BrCCl ₃]		
0.848	9.15	1.15	2.24×10^8
0.566	9.44	2.43	3.07×10^8
0.364	9.64	2.96	2.36×10^8
0.283	9.72	4.47	2.75×10^8
Mean (sd)			$(2.61 \pm 0.38) \times 10^8$

^aSolutions of 155d and 86 in BrCCl₃. Initial concentrations of 155d = 0.08-0.02M.

^bEach number comes from separate experiments and is the average of product ratio from at least three gc injections. The actual ratio of gc integrator counts are multiplied by the detector response factor (3.1) to obtain the molar ratio.

^cCalculated from eq.121 using the value of $k_c = 0.2k_d = 2.11 \times 10^9$ M⁻¹s⁻¹. The diffusion controlled rate constant, k_d , was calculated (using eq.95) from the measured viscosity (0.735 centi poise) of the reaction medium.

86. The use of eq.53 gives $k_T = 1.38 \times 10^9$ M⁻¹ s⁻¹ at 80°C. This number is a factor of 1.53 less than what we assumed for k_c based on diffusion-controlled reaction. Substitution of k_T in place of k_c in eq.121 yields the rate constant $k_{Br(Bu)} = (1.72 \pm 0.25) \times 10^8$ M⁻¹s⁻¹ at 80°C. The difference in the rate constants for the Br abstraction by butyl ($k_{Br(Bu)} = 1.72 \times 10^8$ M⁻¹s⁻¹) and cyclopropylmethyl ($k_{Br(Cpm)} = 2.78 \times 10^8$ M⁻¹s⁻¹, calculated from eq.119) radicals at 80 °C seems to indicate that there is a small enhancement of the rate constant for the Br abstraction by cyclopropylmethyl radical, compared to a representative primary alkyl radical like the butyl radical. If one assumes that the pre-exponential factors (A_1 and A_2) for the reaction of cyclopropylmethyl and butyl radicals are the same, the ratio of their reactivities in bromine abstraction from BrCCl₃ can be attributed to the difference in their activation energies E_{a1} and E_{a2} , respectively. From the expression $k_1/k_2 = A_1/A_2 \exp(-(E_{a1} - E_{a2})/RT)$, by substituting for $k_1/k_2 = 1.62$, and $A_1/A_2 = 1$, the difference in the activation energies can be calculated as $E_{a2} - E_{a1} = 0.34$ kcal/mol. This means that the

activation energy for the cyclopropylmethyl radical (2.11 kcal/mol) is lower than that for the butyl radical by 0.34 kcal/mol.

The polar effects in a few similar radical-molecule reactions are worth mentioning. For the Cl abstraction reaction from CHCl_3 , Dutsch and Fischer²⁶² have shown that 1,1-dimethylethyl (*t*-butyl) radical is about six times as reactive as methyl radical. For a polar transition state similar to that in **181**, the positive charge developed at the nucleophilic radical site is more stabilized in the case of attack by *t*-butyl radical, compared to that by the methyl radical. It has been reported by Ingold and co-workers^{259b} that in solution 1-methylcyclopropyl is ten times more reactive than cyclopropyl radical towards CCl_4 . The relative reactivity numbers given above are probably the minimum polar enhancement factors, since those differences are due to the combined polar (rate enhancing) and steric (rate retarding) effects.

An important barrier which makes a comparative study of polar and other effects in many reactions difficult is due to the fact that for a large number of radical-molecule reactions solution-phase kinetic data are non-existent. In some cases where solution-phase data are available, the only comparison that can be made is to similar reactions in the gas-phase. Such comparisons, in many cases, are done with much reservation. However, for many radical reactions the solution-phase and the gas-phase data are in good agreement. Therefore, with a little caution, the following comparisons can be made in terms of polar effects.

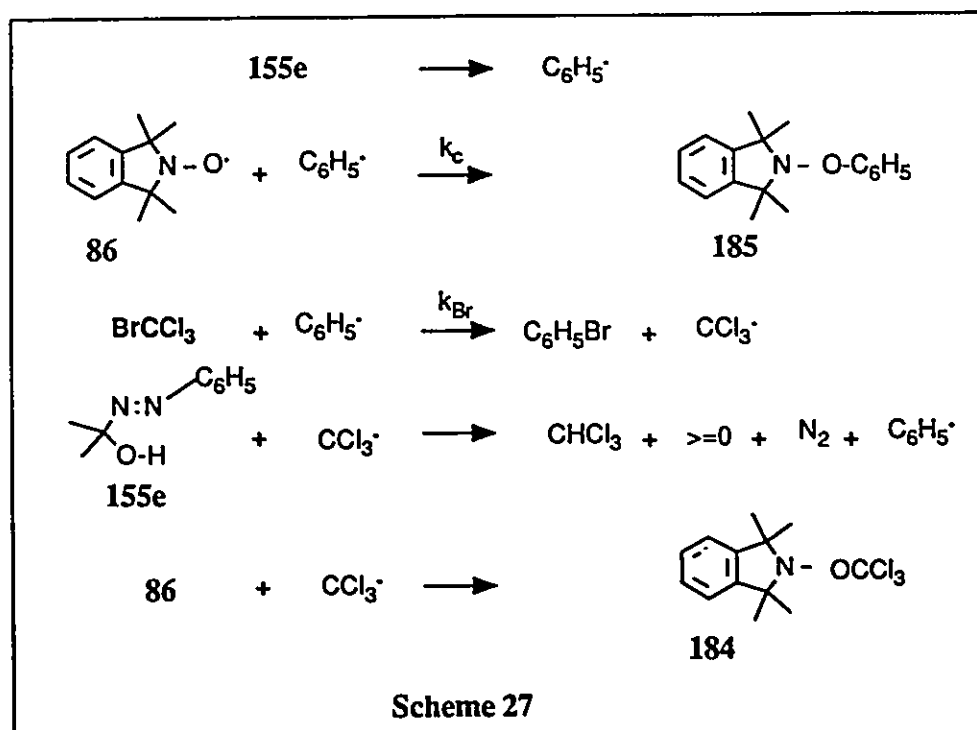
Dutsch and Fischer²⁶² observed that for methyl radicals in the gas-phase the rate constants for Cl abstraction from CHCl_3 and CCl_4 are almost the same ($\approx 17 \text{ M}^{-1} \text{ s}^{-1}$), whereas the rate constant for Cl abstraction by *t*-butyl radical from CHCl_3 ($\approx 10^2 \text{ M}^{-1} \text{ s}^{-1}$) is approximately 400 times smaller than the rate constant for Cl abstraction from CCl_4 by the same radical at room temperature. Once again, a polar transition state stabilization by the *t*-butyl radical, which is greater than that by the methyl radical, is indicated.

For reactions having low activation energies, such as the Br abstraction from BrCCl_3 by alkyl radicals, the polar enhancement factors for various radicals are expected to be small due to the involvement of early transition states. That is exactly what is observed for cyclopropyl and 1-methylcyclopropyl radicals.^{259b} Johnston and Ingold^{259b} showed that 1-methylcyclopropyl is only 1.3 times more reactive than cyclopropyl radical towards BrCCl_3 . (cf. for Cl abstraction from CCl_4 by the same radicals the reactivity ratio is 10). As explained earlier, the above numbers probably reflect only the minimum polar enhancement. For cyclopropylmethyl radical, a larger net enhancement in rate constant compared to a simple primary radical is expected because of the additional conjugative stabilization by the cyclopropane ring on the partially developed cationic center in the transition state (181). Our observation that cyclopropylmethyl radical is about 1.6 times more reactive than butyl radical towards BrCCl_3 is in agreement with the above predictions.

c. Rate constants for Br abstraction from BrCCl_3 by phenyl radicals

The experimental procedure for the determination of rate constants for the attack of phenyl radicals was the same as that for the butyl radicals. A mixture of phenyl azocarbino1 155e and bromotrichloromethane in the presence of excess 86, diluted in some cases with C_6F_6 , was degassed and sealed under vacuum in small tubes and thermolyzed at 80°C . The products of reaction were analyzed by the usual glc technique. The expected reactions are given by Scheme 27.

Analysis of the products of reaction was not straightforward. While it was easy to analyze for bromobenzene, it was not possible to determine the relative yield of the expected coupling product, 2-phenoxy-1,1,3,3-tetramethylisoindoline (185). It is likely that 185 is unstable and undergoes thermolysis, either under the conditions of its formation (80°C) or in the glc column.



To the best of my knowledge, compounds of the type **185** have not yet been reported in the literature. The reason for the instability of **185** is not quite clear at this stage. But if we assume that the PhO-N bond in **185** is similar in strength to the PhO-O bond of an alkyl phenyl peroxide, then the answer is obvious since the latter class of compounds are highly unstable and are not isolable.

Due to the observed instability of **185**, the relative yield of the coupling product was determined from the absolute yields of bromobenzene by glc analysis. The yield was corrected to take into account the fact that in control experiments the yield of bromobenzene was 95%, instead of 100%, from the thermolysis of **155e** in BrCCl_3 , in the absence of **86**. The phenyl moieties that are not accounted for from the corrected yield of bromobenzene are assumed to yield, at least initially, the coupling product, **185**.

A serious error is not expected to result from this determination of product ratio by

difference because in the presence of a large excess of BrCCl_3 and **86** the phenyl radicals are not expected to undergo any major side reactions that can compete with the Br abstraction or coupling with **86**. The ratio of products using different mixtures of **86** and BrCCl_3 were estimated by the above procedure. The rate constants calculated using eq.123, for different initial concentrations of **155e**, **86**, and BrCCl_3 , were in very good agreement. The results are summarized in Table 18.

Table 18. Product ratios and rate constants for phenyl radicals (80°C)				
Concentrations of reactants, M ^a		Product ratio ^b [PhBr]/[185]	Viscosity, ^c cP at 80°C	Rate constants ^d $k_{\text{Br}}, \text{M}^{-1}\text{s}^{-1}$
[86]	[BrCCl ₃]			
1.32	8.47	4.56	0.735	1.50×10^9
0.558	4.79	2.62	0.500	1.18×10^9
0.558	4.79	3.55	0.500	1.30×10^9
0.530	2.07	1.31	0.485	1.13×10^9
0.530	2.07	1.03	0.485	8.80×10^8
0.576	0.588	0.705	0.475 ^e	2.28×10^9
0.576	0.588	0.806	0.475 ^e	2.61×10^9
Mean (sd)				$(1.55 \pm 0.38) \times 10^8$

^aSolutions of **155e**, **86**, and BrCCl_3 in C_6F_6 except for the first entry, where C_6F_6 was absent.

^bThe product ratio was determined from the absolute yield of PhBr; the yield of **185** was determined by difference.

^cViscosities were measured at 77°C, on solvents not containing **86**, **155e**, or products from **155e**. The viscometer was calibrated against CCl_4 and measured viscosities were extrapolated from 77 to 80°C.

^dCalculated from eq. [123], where k_c is derived from k_g , which in turn is derived from the viscosity, see footnote c, Table 17.

^eViscosity of neat C_6F_6 at 80°C.

The rate constant for Br abstraction from BrCCl_3 by phenyl radicals at 80°C is $1.55 \times 10^9 \text{ M}^{-1}\text{s}^{-1}$. This value is very close to the value ($k_{\text{Br}} = 1.7 \times 10^9 \text{ M}^{-1}\text{s}^{-1}$) reported by

Lorand et al,²⁵⁶ for the same reaction at 45°C, considering that the effect of the temperature difference (35°C) corresponds to a rate factor of only 1.5. At 80°C, the rate constant for cyclopropylmethyl radical ($k_{Br} = 2.78 \times 10^8 \text{ M}^{-1}\text{s}^{-1}$) is a factor of 5 less than that for the phenyl radical. The above result is consistent with the fact that phenyl radicals undergo S_H2 reactions faster than primary alkyl radicals. For butyl radicals, the rate constant ($k_{Br(bu)} = 1.72 \times 10^8 \text{ M}^{-1} \text{ s}^{-1}$ at 80 °C) is less than an order of magnitude lower than that of phenyl radicals. The above results indicate that the range of rate constants for various radicals toward CCl_3Br is quite small, and that those rate constants are only about an order of magnitude lower than that of a diffusion-controlled reaction. However, it is observed that there is a small but predictable difference in reactivities for various radicals toward bromotrichloromethane. The observed reactivity is in the order: phenyl > cyclopropylmethyl > butyl radical.

As explained earlier, the only possible explanation for the observed difference in reactivities of the above radicals is the involvement of a polar transition state. The more polarizable cyclopropylmethyl radicals are better stabilizers of polar transition states than the less polarizable butyl and phenyl radicals. It is apparent that the polar enhancement in the case of cyclopropylmethyl radicals is not large enough to make them exceed the inherent greater reactivity of phenyl radicals.

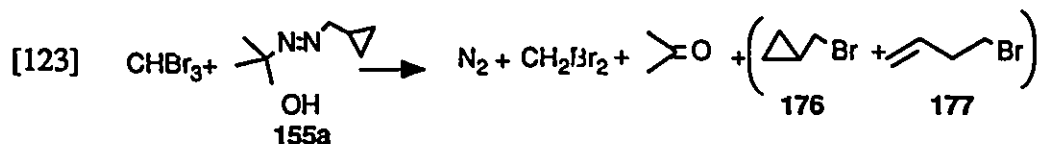
A similar argument based on polar transition state stabilization can be used to accommodate the apparently higher rate constant ($k_{Br} = 2.8 \times 10^9 \text{ M}^{-1}\text{sec}^{-1}$ at 25°C) of cyclopropyl²⁶⁰ radicals relative to that of phenyl²⁵⁶ radicals ($1.55 \times 10^9 \text{ M}^{-1}\text{sec}^{-1}$ at 80°C) towards BrCCl_3 . Cyclopropyl radical is more polarizable than phenyl radical, and therefore a polar transition state can be more stabilized by the cyclopropyl radical than by the phenyl radical. It should also be emphasized that the reactivity numbers for cyclopropyl and phenyl radicals, mentioned above, are based on different methodologies - the rate constant for the former radical was measured by the flash photolysis technique

and the latter by product analysis.

If we assume that for the Br abstraction reactions the pre-exponential factors remain the same for various radicals and that the difference in rate constants for cyclopropylmethyl, phenyl, and butyl radicals at 80 °C arises from a difference in the activation energies, then we are able to calculate approximate Arrhenius expressions for butyl and phenyl radicals based on the Arrhenius expression for the cyclopropylmethyl radical viz. $\log (k_{Br(cpm)}/\text{sec}^{-1}) = 9.75 - 2.11/\theta$ (eq.119). Thus, for butyl and phenyl radicals, the approximate activation energies for the Br abstraction are 2.45 kcal and 1.40 kcal, respectively. However, the questionable assumptions leading to the above activation energies need further investigation.

(ii) Cyclopropylmethyl radical attack on bromoform (CHBr_3) and its rate constant (50 °C)

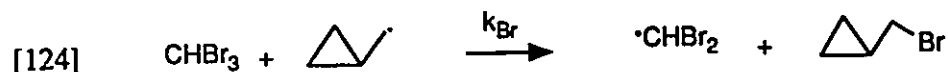
Generation of cyclopropylmethyl radicals by the thermal decomposition of the azocarbino1 155a in CHBr_3 resulted in the formation of products given in eq.123.



The above reaction is similar to the bromotrichloromethane reaction discussed in Section 2.2.2. However, no high molecular weight compounds, similar to that produced by the radical chain addition of bromotrichloromethane on 177 (Scheme 24), was observed in the case of bromoform. In this context, it is reasonable to believe that the intermediate trichloromethyl radical (formed in the case of CCl_3Br) undergoes addition to double bonds much faster than dibromomethyl radical, so that even if any products are formed by

secondary reactions, the amounts are too small to be detected by the gc analysis.

The rate constant (k_{Br}) for the attack of cyclopropylmethyl radicals on bromoform (eq. 124) could then be calculated from eq.125.



$$[125] \quad k_{Br} = \{[176]/[177]\} \times \{k_i/[\text{CHBr}_3]\}$$

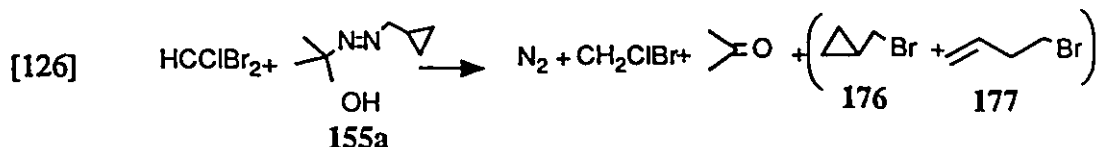
In neat bromoform (11.0M), decomposition of about 0.3M azocarinol resulted in the formation of 176 and 177 in a molar ratio of 0.551 (average of two runs) at 50°C. Using the above data in eq.125, the rate constant for bromine abstraction becomes $k_{Br} = 2.86 \times 10^7 \text{ M}^{-1} \text{ s}^{-1}$ at 50°C (substituting for $k_i = 5.74 \times 10^8$ at 50°C).

The above appears to be the first rate constant reported for a radical attack on bromoform. It is important to note that the rate constant for the attack of cyclopropylmethyl radical, a fairly representative primary alkyl radical, on bromoform is quite high, and that it is an order of magnitude smaller than that for bromotrichloromethane. On a per atom basis, bromoform is 30-fold less reactive than bromotrichloromethane.

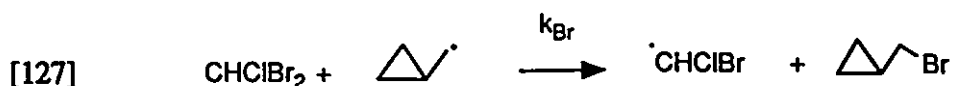
(iii) Rate Constants for the Attack of Cyclopropylmethyl Radicals on Dibromochloromethane.

A procedure similar to that used for the determination of rate constants for bromine abstraction from bromoform (Section 2.2.2b) was used for the title reaction. Decomposition of 155a in neat dibromochloromethane is expected to give the products in

eq.126.



The product ratios [176]/[177] were determined by the usual glc technique and the rate constant for the reaction [127] was calculated using eq.128.



$$[128] \quad k_{\text{Br}} = \{[176]/[177]\} \times \{k_i/[\text{CHClBr}_2]\}$$

When an approximately 0.2M solution of the azocarinol **155a** was decomposed in neat Br_2CHCl (11.4M) at 50°C, the ratio [176]/[177] was found to be 0.213. Substituting this value and also the value for $k_i = 5.74 \times 10^8$ at 50°C in eq.128, gave $k_{\text{Br}} = 1.07 \times 10^7 \text{ M}^{-1} \text{ s}^{-1}$ at 50°C.

Another experiment was conducted for the same reaction at 80°C. In this case, the product ratio [176]/[177] was 0.192 when approximately 0.2M azocarinol (**155a**) was decomposed in neat CHClBr_2 (10.96M). Substituting for $k_i = 1.57 \times 10^9 \text{ M}^{-1} \text{ s}^{-1}$ (at 80°C) in eq.128, the above data gave the rate constant for bromine abstraction at 80°C as $k_{\text{Br}} = 2.75 \times 10^7 \text{ M}^{-1} \text{ s}^{-1}$.

Our observations on the reactions of the three bromo compounds towards cyclopropylmethyl radical can be summarized as follows

- bromotrichloromethane reacts with cyclopropylmethyl radical much faster (more than an order of magnitude) than bromoform and dibromochloromethane.
- the last two compounds have comparable rate constants, though it is observed

that bromoform reacts slightly faster (a factor of 1.3) than dibromochloromethane on a per atom basis.

c) the reactivities of the polyhalobromomethanes seem to be dependant on the number of halogen atoms. Stabilization of the postulated polar transition state, for radical substitution, by electron withdrawing halogen atoms on the substrate is a probable reason for the above observation.

d) the activation energy for the reaction of bromotrichloromethane is very small (2.1 kcal/mol). From the limited available data for bromoform, a low activation energy is indicated for that reaction as well.

In the light of this preliminary study, it is clear that some more studies at various temperatures are needed for CHBr_3 and CHClBr_2 , so as to obtain reliable Arrhenius parameters for the Br abstraction reactions. It is also clear that the study should be extended to other polyhalo bromomethanes as well.

In summary, we have looked at the reactivities of three different radicals (cyclopropylmethyl, butyl, and phenyl radicals) toward bromotrichloromethane, and used cyclopropylmethyl radical as a clock for determining and comparing the rate constants for three bromo compounds (BrCCl_3 , CHBr_3 , and CHClBr_2). It is seen that the reactivities of relatively unhindered carbon-centered radicals such as cyclopropylmethyl, butyl, and phenyl radicals toward BrCCl_3 span a narrow range. The observed low sensitivity of k_{Br} toward radical structure is very striking. The difference in rate constants for the attack of cyclopropylmethyl and butyl radicals on BrCCl_3 is less than a factor of two. The above factor is probably the polar enhancement for cyclopropylmethyl radical relative to a simple primary alkyl radical. It is therefore reasonable to believe that cyclopropylmethyl radical can be used, without serious error, as a clock to estimate rate constants for fast primary radical-molecule reactions in solution.

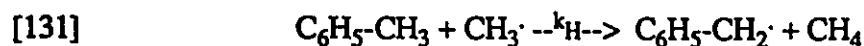
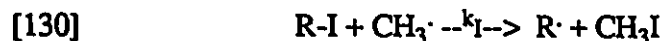
2.2.3. Rate constant(s) for iodine abstraction from iodo compounds by a primary alkyl radical using the cyclopropylmethyl radical clock

There are only a few rate constant data available in the literature for the attack of radicals on iodo compounds, resulting in the iodine atom transfer.^{159,160,256,263} The only absolute rate constant available at the time of our investigation was that for the attack of phenyl radicals on isopropyl iodide (eq 129).²⁵⁶



The rate constant at 45°C for this reaction is reported as $1.1 \times 10^9 \text{ M}^{-1} \text{ s}^{-1}$. The above rate constant is an order of magnitude less than that for the iodine abstraction from molecular iodine (I_2) by phenyl radicals viz. $1.3 \times 10^{10} \text{ M}^{-1} \text{ s}^{-1}$ at 45°C.²⁵⁶

The relative rate constants for the attack of radicals on several iodo compounds are known. For example, Szwarc et.al²⁶³ have reported the rate constants (k_I) for iodine abstraction by methyl radicals from a number of iodo compounds (eq.130) relative to the rate constants (k_H) for the H-abstraction from toluene by methyl radicals (eq.131)



The relative rate constants reported, using the above competition system, for various alkyl iodides (k_I/k_H in brackets) at 65°C are: CH_3I (45), $\text{C}_2\text{H}_5\text{I}$ (180), $(\text{CH}_3)_2\text{CHI}$ (870), $(\text{CH}_3)_3\text{CI}$ (1680), PhCH_2I (7560), CH_2ClI (6400) and CF_3I (20,000). If the rate

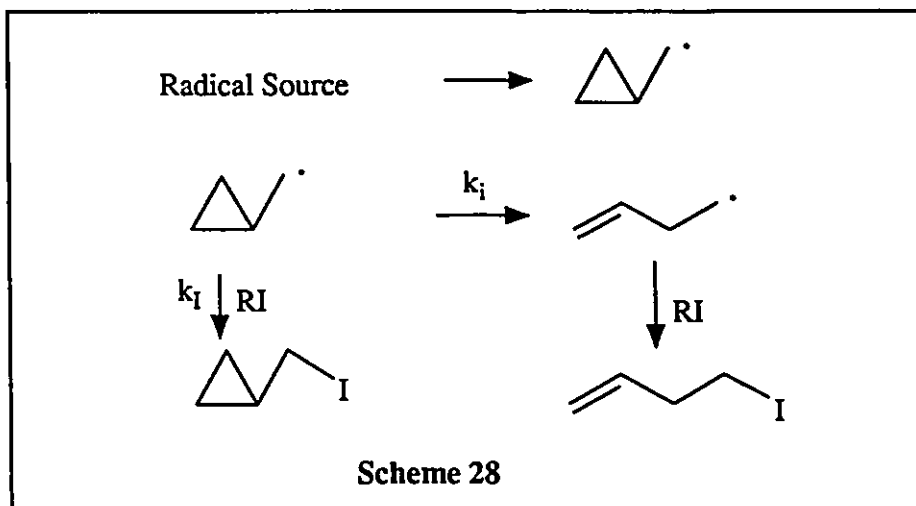
constant for H-abstraction by methyl radicals from toluene is assumed to be $3 \times 10^2 \text{ M}^{-1} \text{ s}^{-1}$,²⁶⁴ then the rate constants for the iodine abstraction by methyl radical from the above listed iodo compounds can be brought to an absolute scale. For example, the iodine abstraction from benzyl iodide can be calculated approximately as $2.3 \times 10^6 \text{ M}^{-1} \text{ s}^{-1}$ and that from CF_3I comes to about $6 \times 10^6 \text{ M}^{-1} \text{ s}^{-1}$ at 65°C . (The above numbers are an order of magnitude smaller than those given in Table 11 of ref.2k, Chapter 2, which resulted from a small arithmetical error. For an explanation see ref. 267).

Danen and Winter¹⁶⁰ reported the rate constants (k_I/k_{Br}) for abstraction of iodine from aliphatic iodides relative to that of the bromine abstraction from BrCCl_3 by phenyl radicals in solution. For the majority of iodo compounds studied, k_I values are 2-5 times smaller than that for the bromine abstraction from bromotrichloromethane by phenyl radicals (see Table 1 of ref.160). However, it is observed that for iodoacetic acid and ethyliodoacetate the iodine abstraction rate constants relative to the Br abstraction are higher; the k_I/k_{Br} values are 1.34 and 1.73, respectively.

Aryl iodides are also known to undergo iodine atom transfer with various aryl radicals.²⁶⁷ However, it seems that there are no rate constants (relative or absolute) available for such processes in solution.

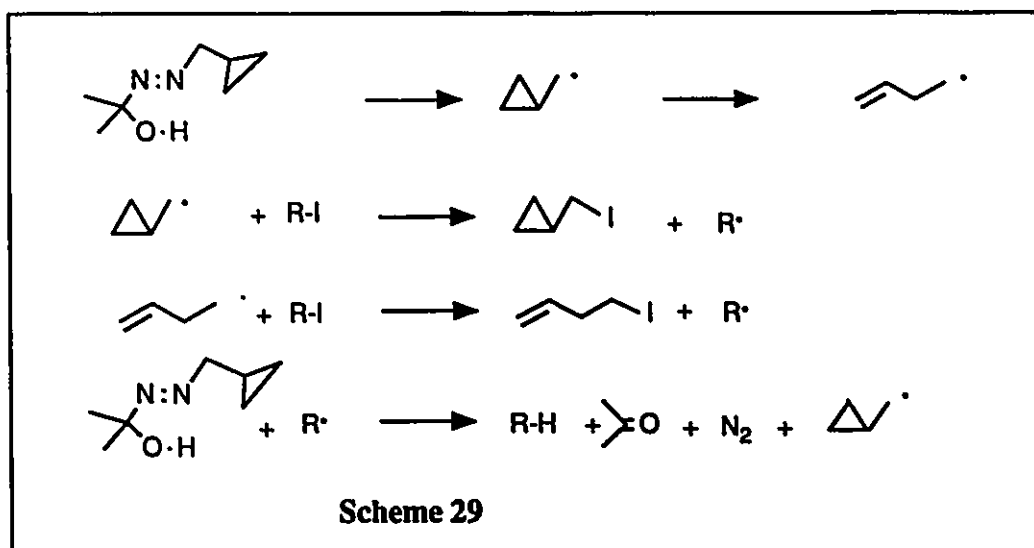
The following few sections deal with our attempts to determine the absolute rate constants for the iodine atom abstraction from a few iodo compounds by a primary alkyl radical- the cyclopropylmethyl radical.

Method: The principle is based on the cyclopropylmethyl radical clock, and its successful application in the determination of rate constants for bromine atom abstraction from bromotrichloromethane has already been described. The same technique has been used in all the iodine abstraction studies. The most important reactions are summarized in Scheme 28.



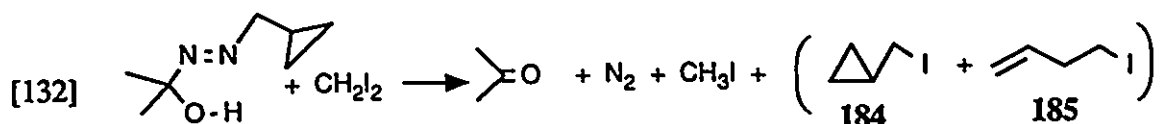
A number of iodo compounds (RI) such as CH_2I_2 , $\text{C}_6\text{H}_5\text{-CH}_2\text{I}$, CH_3I , $(\text{CH}_3)_2\text{CHI}$, $\text{CF}_3\text{CH}_2\text{I}$, and $(\text{CH}_3)_3\text{CI}$ were examined for their reactivity toward cyclopropylmethyl radicals.

The following radical chain mechanism (Scheme 29) is proposed for the decomposition of the azocarbinol **155a** in the presence of an iodo compound, RI.

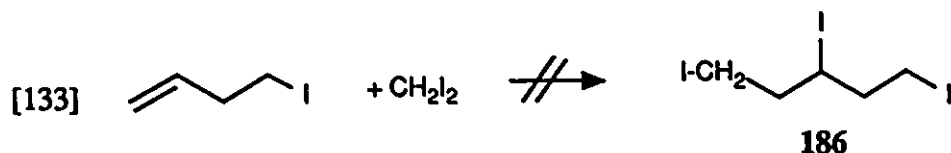


(i) Rate constants for methylene iodide (CH_2I_2)

The azocarinol 155a was allowed to react with excess CH_2I_2 , either in the presence or absence of added solvent CH_2Cl_2 , at various temperatures, after degassing and sealing the solutions in nmr tubes under vacuum. The progress of the reaction was monitored by the disappearance of the gem-dimethyl signal of the azocarinol at about δ 1.5 ppm. The products of reaction were identified either by nmr spectroscopy or by glc analysis. The overall reaction may be written as eq.132.



In addition to acetone and methyl iodide, the only major products registered and identified by glc was the cyclopropylmethyl iodide (184) and 4-iodo-1-butene (185). Very small amounts of a few unidentified products were also indicated from weak glc signals, but the combined area counts for the unidentified peaks ranged from 4 - 9 % of the total area counts for the iodo compounds 184 and 185. It should also be noted that secondary reaction products, such as those observed in the cases of BrCCl_3 and CCl_4 , resulting from the addition of the reagent CH_2I_2 across the double bond of the ring-opened product 185 (eq.133) were not observed. The triiodo compound 186, if present, should have given a gc



signal far later than that for CH_2I_2 ; but no signal after the CH_2I_2 signal was observed.

The rate constants (k_1) for the reaction between cyclopropylmethyl radical and

methylene iodide was calculated by the use of eq.134, under conditions where the CH_2I_2

$$[134] \quad k_I = k_i \times [184] / [185] [\text{CH}_2\text{I}_2]$$

concentration remained constant. Knowing the relative concentration of 184 and 185, at known concentration of CH_2I_2 , k_I can be calculated using the known isomerization rate constant (k_i) for the cyclopropylmethyl radical. The results are summarized in Table 19.

Table 19. Product ratios and rate constants for iodine abstraction from CH_2I_2 by cyclopropylmethyl radicals					
Temp. °C	$[\text{CH}_2\text{I}_2]^a$ (M)	$[184]/[185]^b$	$k_i \times 10^{-8}$ (s^{-1}) ^c	$k_i \times 10^{-7}$ ($\text{M}^{-1}\text{s}^{-1}$) ^d	Mean k_I ($\times 10^7 \text{ M}^{-1}\text{s}^{-1}$)
23	12.35	1.38	0.894	0.999	0.999
44	12.04	0.817	2.02	1.37	1.57
	"	0.926	"	1.55	
	6.02 ^e	0.531	"	1.78	
60	11.82	0.670	3.52	2.00	2.04
	"	0.685	"	2.04	
	"	0.694	"	2.07	
80	11.55	0.412	6.55	2.34	2.74
	"	0.507	"	2.88	
	"	0.500	"	2.84	
	"	0.513	"	2.91	

^aConcentrations of neat CH_2I_2 (corrected for volume expansion) unless otherwise mentioned

^bRelative concentrations of the two products from the relative gc counts, corrected for the detector response factor(1.18) for the two compounds. Each number comes from a separate experiment and is the average of at least 3 injections.

^cThe isomerization rate constant for the cyclopropylmethyl radical calculated using eq.58

^dCalculated using eq.134

^eConcentration in a 1:1 (v/v) mixture of CH_2I_2 and CH_2Cl_2 used as the medium for this reaction

Table 19 reveals that iodine abstractions from methylene iodide by cyclopropylmethyl radicals are very fast; the rate constants for the reaction range from 10^7

$\text{M}^{-1} \text{s}^{-1}$ to $2.7 \times 10^7 \text{ M}^{-1} \text{s}^{-1}$ over a temperature range from 23°C to 80°C . The marginal increase (approximately 3 times) in rate constant over a 57°C temperature range is indicative of a reaction with low activation energy.

Linear regression analysis of the data in Table 19 in which the reciprocal of the absolute temperature ($1/T$) is taken as the X-axis and $\log(k_I)$ value at each temperature is taken as the Y-axis (values are given in Table 20), gave eq.135 with $r = 0.999$. The

Table 20. Data used for linear regression yielding eq.135			
Temp. (K)	$k_I \times 10^{-8}$ ($\text{M}^{-1} \text{s}^{-1}$)	$1/T$ ($\times 10^3$)	$\log(k_I)$
296	1.06	3.378	7.025
317	1.60	3.155	7.204
333	2.00	3.003	7.301
353	2.58	2.283	7.412

Arrhenius plot is given in Fig.5.

$$[135] \log(k_I / \text{M}^{-1} \text{s}^{-1}) = (9.4 \pm 0.2) - (3.2 \pm 0.3)/\theta,$$

The above equation gives $k_I = 1.13 \times 10^7 \text{ M}^{-1}\text{s}^{-1}$ at 25°C . A brief discussion of the significance of such a rate constant (eq.135) for the iodine abstraction reaction in comparison to the rate constant for bromine abstraction from BrCCl_3 by the same radical seems to be appropriate at this stage.

If we recall the rate constants for Br abstraction (k_{Br}) from BrCCl_3 by cyclopropylmethyl radicals (eq.119), it is observed that the rate constants for iodine abstraction from CH_2I_2 (eq.135) by the same radicals are slightly lower due probably to an increase in the activation energy of about 1.1 kcal/mol for the latter reaction, compared to

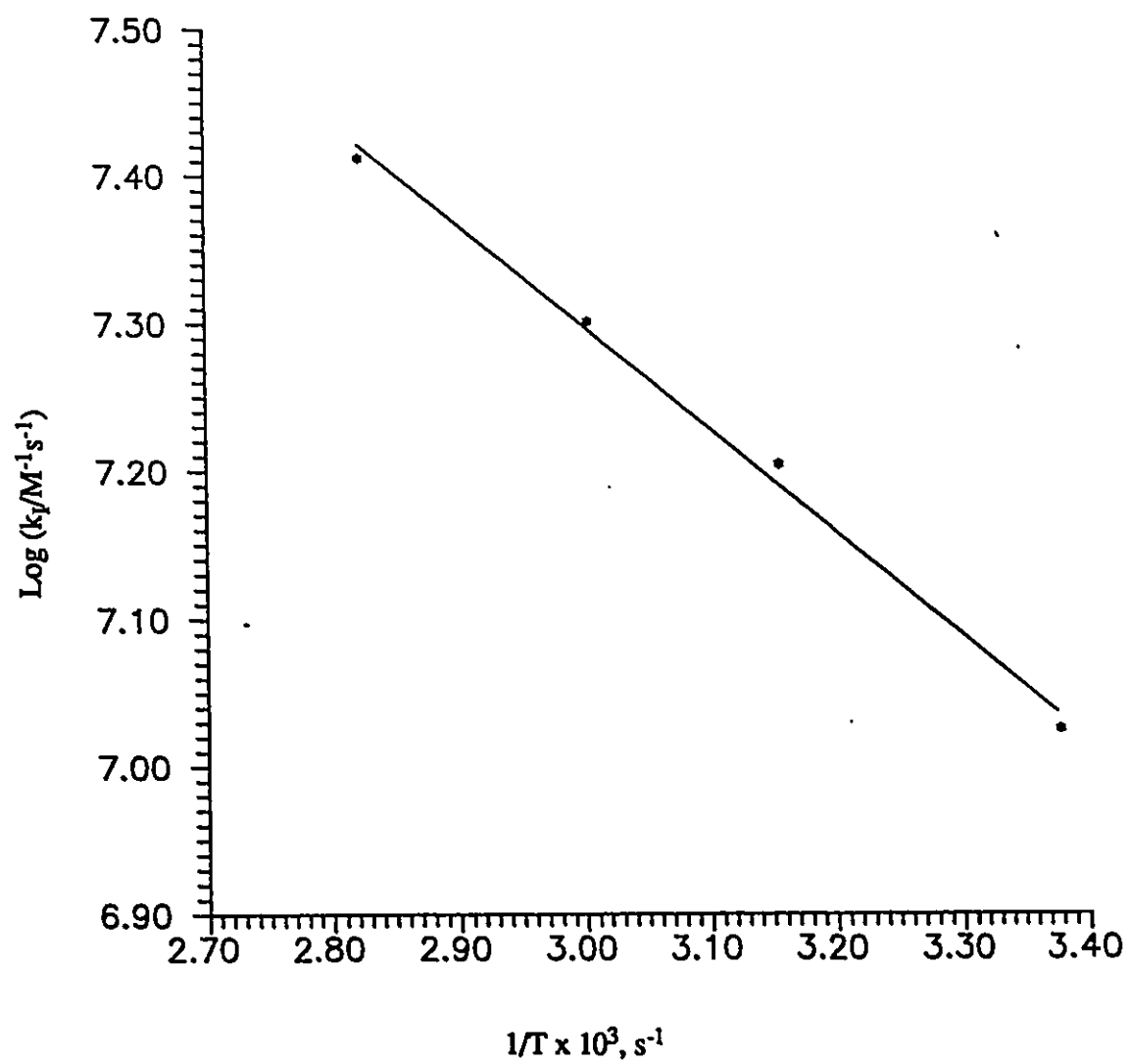


Fig. 5. Arrhenius Plot for the Data in Table 20

the former one. A marginal increase (0.35 in log units) in the preexponential factor for the Br abstraction is also observed. A comparison between the rate constants at 25°C ($k_{\text{Br}} = 1.7 \times 10^8 \text{ M}^{-1} \text{ s}^{-1}$, $k_{\text{I}} = 1.1 \times 10^7$) shows that at room temperature the rate constant for bromine abstraction from BrCCl_3 is 15 times larger than the rate constant for iodine abstraction from CH_2I_2 by cyclopropylmethyl radicals.

Though the rate constants for methyl radical attack on a few alkyl iodides relative to the H-abstraction from toluene are known,²⁶³ similar studies on CH_2I_2 are not found in the literature. However, Szwarc et al.²⁶³ studied a similar compound CH_2ClI , which is reported to have a rate constant 6400 times larger than H-abstraction from toluene by $\text{CH}_3\cdot$ radicals. Assuming that the rate constant for the H-abstraction is $300 \text{ M}^{-1} \text{ s}^{-1}$, the rate constant for iodine abstraction from CH_2ClI can be calculated as $1.8 \times 10^6 \text{ M}^{-1} \text{ s}^{-1}$. Assuming also that the effect of a chlorine atom is approximately equal to that of an iodine atom, CH_2I_2 is expected to have a rate constant approximately twice that for CH_2ClI (i.e. $2 \times 1.8 \times 10^6 = 3.7 \times 10^6 \text{ M}^{-1} \text{ s}^{-1}$), based on the two fold increased probability for iodine abstraction from CH_2I_2 compared to CH_2ClI at 65°C.

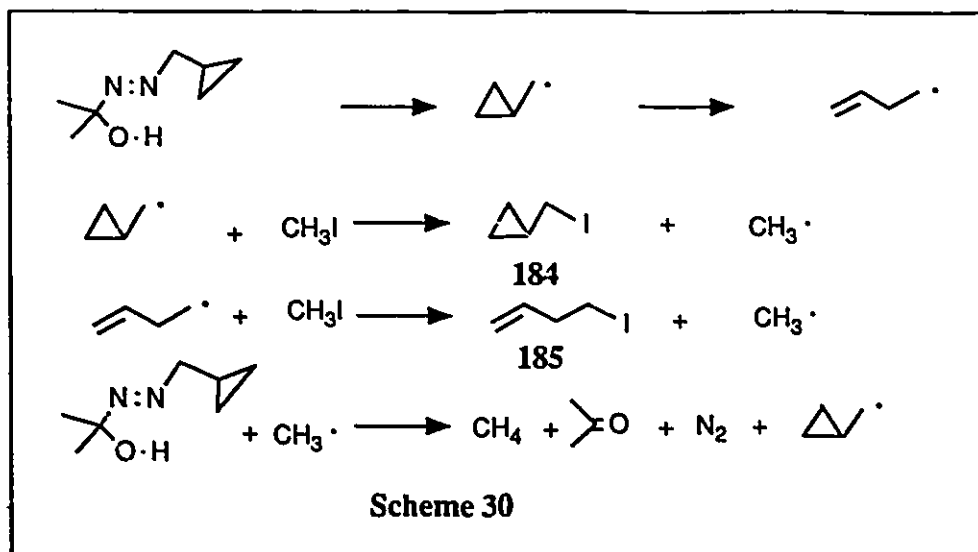
The above predicted rate constant for reaction of methyl with CH_2I_2 is about an order of magnitude smaller than that calculated using eq.135 (ie. $k_{\text{I}} = 5.2 \times 10^7 \text{ M}^{-1} \text{ s}^{-1}$ at 65°C) for the corresponding reaction of cyclopropylmethyl. This increased reactivity for the iodine abstraction by cyclopropylmethyl radical relative to that of the methyl radical could possibly be due to the type of polar contribution postulated earlier in the case of BrCCl_3 .

(ii) Rate constants for methyl iodide

The experimental procedure for the determination of rate constants for the iodine abstraction from CH_3I is similar to that for the methylene iodide described in the previous

section. Degassed and sealed solutions of CH_3I and the azocarbiniol 155a in nmr tubes were thermolysed at different temperatures. The products of reaction were analysed both by nmr and by glc techniques.

The sequence of reactions that follow when the azocarbiniol 155a is decomposed in the presence of CH_3I are analogous to those of CH_2I_2 (previous section) and can be represented by Scheme 30. Formation of methane as a product of reaction was confirmed by the nmr spectral analysis (see Experimental Section for details).



Progress of the reaction could be easily monitored by the disappearance of the nmr signal of the gem-dimethyl group at around 1.5 ppm. A new peak at around 0.1-0.2 ppm was identified as due to CH_4 . Since CH_3I was used as the solvent itself, the formation of acetone could not be confirmed from the nmr spectrum of the reaction mixture because the acetone signal at ~ 2.1 ppm overlapped with the huge signals from CH_3I at ~ 2.0 ppm. No appreciable high field (0.3 - 1.0 ppm) nmr signals characteristic of the cyclopropyl ring protons could be observed in the reaction mixture, indicating that most of the cyclopropylmethyl radicals did ring open before the iodine transfer from CH_3I could

occur.

The identity of cyclopropylmethyl iodide (184) and 3-iodo-1-butene (185) as products of reaction comes from their gas chromatographic retention times and also from the observation that the corresponding peak intensities for the compounds increased when authentic samples of 184 and 185 were co-injected with the reaction mixture. The possibility of signals from impurities overlapping with those of the concerned products 184 and 185 was also checked by the use of the two column technique (see Experimental Section). The use of two different columns gave the same number of major peaks with the same relative peak intensities for products from the same reaction mixture.

For quantitative purposes the ratio of concentrations of 184 and 185 was obtained from their corresponding gc area counts, taking into account the fact that the detector response for 184 is 1.18 times that of 185. The rate constant for the attack of cyclopropylmethyl radical on CH_3I was then calculated using eq.136, where k_i is the

$$[136] \quad k_{i(\text{CH}_3\text{I})} = k_i \times [184] / [185] [\text{CH}_3\text{I}]$$

isomerization rate constant for the cyclopropylmethyl radical and $[\text{CH}_3\text{I}]$ is the initial concentration of methyl iodide, which was taken in very large excess over azocarinol. In all our studies with CH_3I , neat CH_3I was used as the solvent for the azocarinol, and therefore the concentration was calculated from the density, assuming that the azocarinol (<2%) used in reactions has only a negligible effect on the concentration of methyl iodide. However, correction was applied for volume expansion for reactions carried out at various temperatures. The rate constants calculated at two different temperatures for the title reaction are given in Table 21.

It is seen from Table 21 that the rate constants for iodine abstraction from methyl iodide are at least two orders of magnitude lower than those for the bromine abstraction

Table 21. Rate constants for iodine abstraction from CH₃I by cyclopropylmethyl radicals				
Temp. (°C)	[CH ₃ I] ^a (M)	[184]/[185] ^b	k _i × 10 ⁻⁷ (s ⁻¹)	k _i × 10 ^{-5c}
0	15.7	0.102	3.61	2.35
0	15.7	0.099	3.61	2.28
0	15.7	0.178	3.61	4.09
44	15.2	0.107	20.57	14.40

^a Concentrations of neat CH₃I, corrected for volume expansion.

^b Molar ratio of products calculated from gc counts, corrected for differences in detector responses.

Each number represents an average of at least three injections.

^c Rate constants calculated from eq.136.

from BrCCl₃. This probably reflects a substantially higher activation energy needed for the iodine abstraction, compared to the bromine abstraction from bromotrichloromethane.

In most of the experiments, the ratio of concentrations [184]/[185] is approximately 1/10. In studies such as this where the accuracy of the rate constant relies on the accuracy of the relative concentrations of 184 and 185, a ratio of [184]/[185] near unity is the most ideal. Such an ideal situation cannot be achieved in the case of methyl iodide as substrate, because that requires a higher CH₃I concentration (which is impossible since we are already at the limit of its concentration) or a lower k_i. Lower k_i requires lower temperatures which is unfavourable from a practical point of view, since even the thermolysis at 0°C requires more than four weeks for complete decomposition of the azocarinol. Therefore the study at a temperature lower than 0°C was not attempted. The study was mainly done at 0°C, and it is recommended that the rate constants be used only for the order of magnitude comparisons. However, another experiment was conducted at 44°C for the calculation of an approximate activation energy for this reaction. The rate constant at 44°C is 1.44 × 10⁶ M⁻¹ s⁻¹ (Table 21). The above data leads to eq.137, where Θ

= 2.3 RT kcal/mol, as the approximate Arrhenius expression for the iodine abstraction reaction.

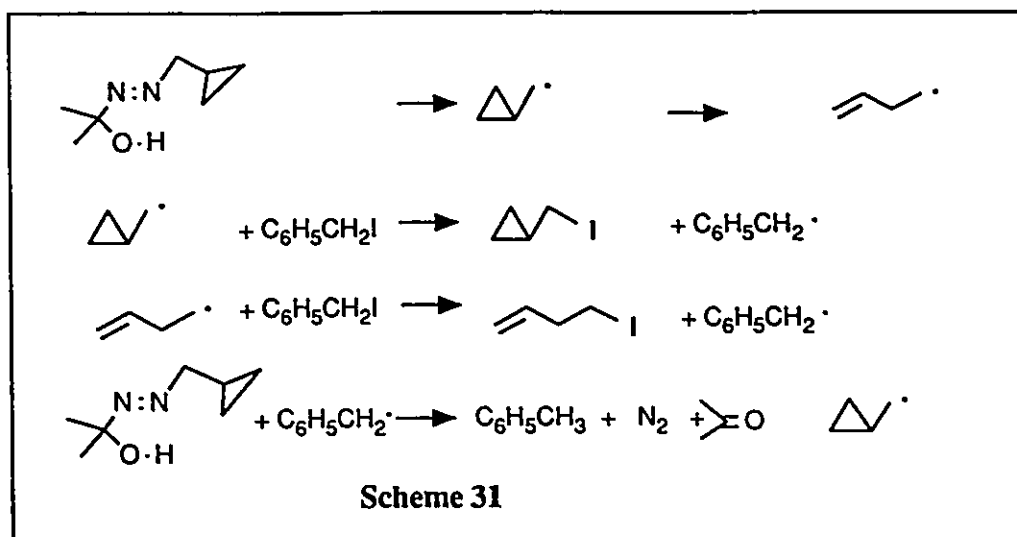
$$[137] \log(k_I / \text{M}^{-1}\text{s}^{-1}) = 10.5 - 6.3/\theta,$$

Eq.137 gives $k_I = 2.6 \times 10^6 \text{ M}^{-1} \text{ s}^{-1}$ at 65°C, which is three orders of magnitude larger than that for the methyl radical attack on CH_3I , calculated from the data given in ref.263. The rate constant at 65°C for the latter reaction is $1.3 \times 10^3 \text{ M}^{-1} \text{ s}^{-1}$. A polar enhancement factor of approximately 10^3 for the attack of cyclopropylmethyl radical, relative to the methyl radical, is probably too large even for a relatively late transition state. One reason for the above difference in reactivity could be that methyl radical is not a good model for a primary alkyl radical. Another reason could be that the experimental pre-exponential factor is slightly larger than what is normally expected ($10^9 \pm 1$) for a simple radical molecule reaction because of the limited number of data points. It is evident that more measurements, done at a few different temperatures inbetween and around those reported are needed for a more reliable temperature dependence of the rate constant and for a more meaningful comparison with other similar iodine abstraction reactions.

(iii) Rate constants for benzyl iodide

The same principle described previously for the determination of iodine abstraction from methyl iodide and methylene iodide was used for the determination of rate constants for iodine abstraction from benzyl iodide by cyclopropylmethyl radicals. The important reactions are summarized in Scheme 31.

Kinetic studies were done at 23°C, 50°C, and 80°C using procedures similar to those described in sections above. Mixtures of 155a and excess benzyl iodide (Bz-I) were



degassed and sealed in nmr tubes and were thermolyzed at particular temperatures by immersing the tubes in constant temperature baths. The products were analyzed by the usual glc and nmr techniques. Details of the procedure are given in the Experimental Section. The rate constant for the title reaction (eq.138) was calculated using eq.139.



[139]
$$k_{I(Bz-I)} = [184] \cdot k_i / [185][Bz-I]$$

The ratios of concentrations, [184]/[185], of the products were determined from the gc peak integrations, corrected for the difference in detector responses. The isomerization rate constants k_i for the cyclopropylmethyl radicals were calculated using eq.58. The benzyl iodide concentration was calculated from its density and was corrected for temperature changes. The results are summarized in Table 22.

Least squares treatment of $1/T$ vs. $\log k_i$ (Table 23) gives the Arrhenius expression for the rate constants (k_i) for iodine abstraction as eq.140, where $\Theta = 2.3RT$ kcal/mol. An

Table 22. Rate constants for iodine abstraction from benzyl iodide by cyclopropylmethyl radicals

Temp. (°C)	[Bz-I] ^a	[184]/[185] ^b	$k_i \times 10^{-8}$ (s ⁻¹)	$k_I \times 10^{-8c}$ (M ⁻¹ s ⁻¹)
23	7.93	4.08	0.894	0.460
50	7.64	3.26	2.51	1.07
50	7.64	2.85	2.51	0.936
50	7.64	2.86	2.51	0.940
80	7.38	1.13	6.55	1.003
80	7.38	1.09	6.55	0.967
80	7.38	1.73	6.55	1.540

^a Concentrations of benzyl iodide calculated from its density at 20°C^b Molar ratio of products calculated from gc counts (see text for details)^c calculated using eq.139**Table 23.** Data used to calculate the Arrhenius expression given in eq.140

Temp. (T, K)	$i/T \times 10^3$	$k_I \times 10^{-8c}$ (M ⁻¹ s ⁻¹)	log(k_I)
296	3.378	0.460	7.663
323	3.096	1.07	8.029
323	3.096	0.936	7.971
323	3.096	0.940	7.973
353	2.833	1.003	8.001
353	2.833	0.967	7.985
353	2.833	1.540	8.188

Arrhenius plot is given in Fig.6.

$$[140] \quad \log(k_I/M^{-1} s^{-1}) = (9.91 \pm 0.78) - (2.96 \pm 1.2)/\theta$$

Eq.140 gives $k_I = 5.0 \times 10^7 M^{-1} s^{-1}$ at 25°C. A comparison of this rate constant with the rate constant for the iodine abstraction from $C_6H_5CH_2I$ by methyl radical (viz. $2.3 \times 10^6 M^{-1} s^{-1}$)²⁶⁸ shows that our value is at least an order of magnitude higher.

The result indicates that iodine abstraction from benzyl iodide is a very fast process: the rate constant is about an order of magnitude higher than that of CH_2I_2 (taking into account a statistical factor of two for the latter), and is about two orders of magnitude higher than the iodine abstraction from methyl iodide by cyclopropylmethyl radicals.

(iv) Rate constants for 1-methylethyl (isopropyl) iodide

Thermal decomposition of 155a in neat isopropyl iodide (more than 20 fold in stoichiometric excess) resulted in the formation of 184 and 185 in addition to propane, acetone, and nitrogen. The important reactions are summarized in Scheme 32.

The rate constant k_I for the title reaction is given by eq.141.

$$[141] \quad k_I = \{[184]/[185]\} \times \{k_2/[(CH_3)_2CHI]\}$$

Under conditions where the concentration of isopropyl iodide remained constant during the reaction, the rate constant k_I could be calculated using eq.142, by determining the relative concentration $[184]/[185]$ of the products and substituting for k_2 and $[(CH_3)_2CHI]$.

In all the experiments neat isopropyl iodide was used as the solvent and therefore

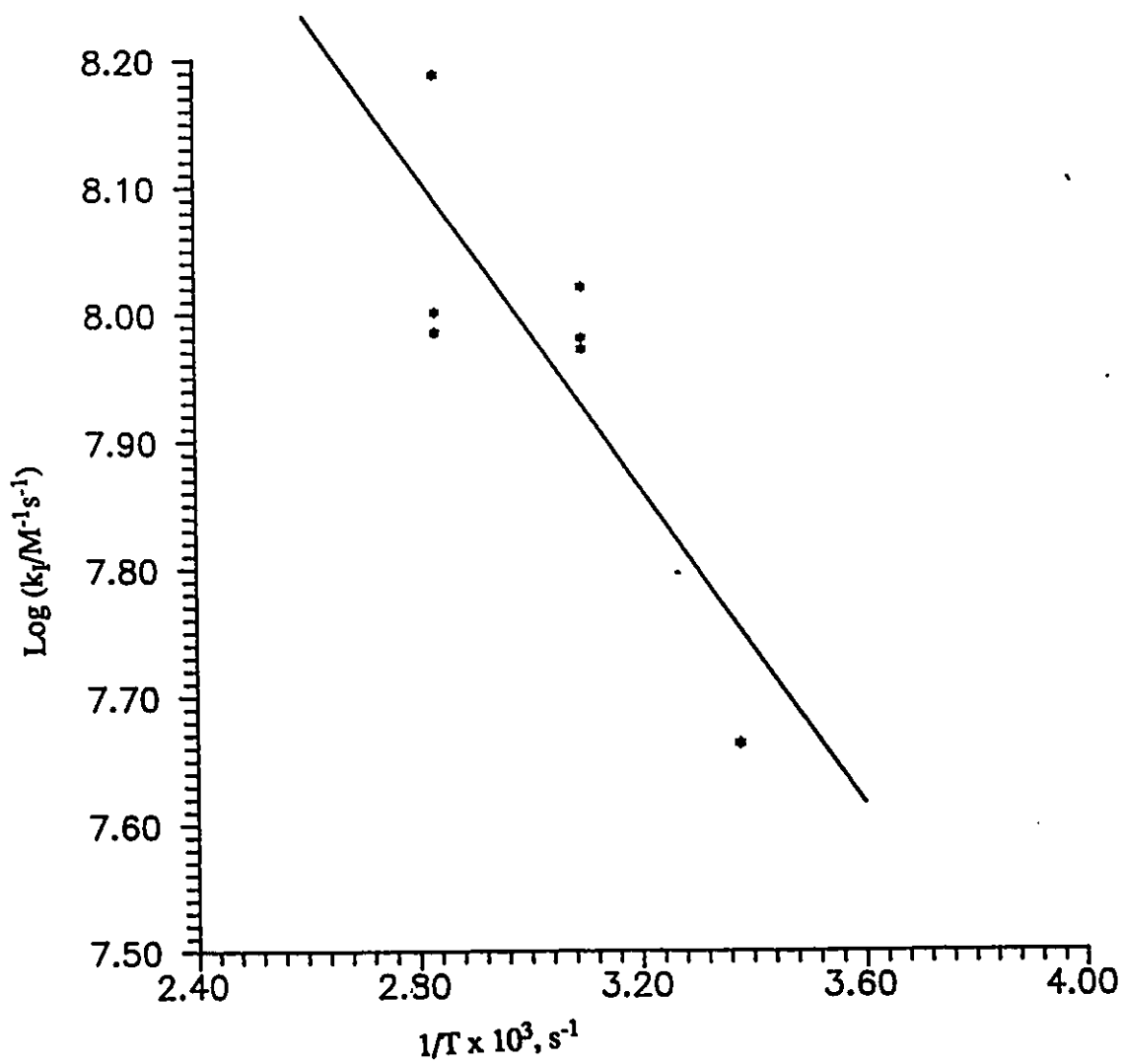
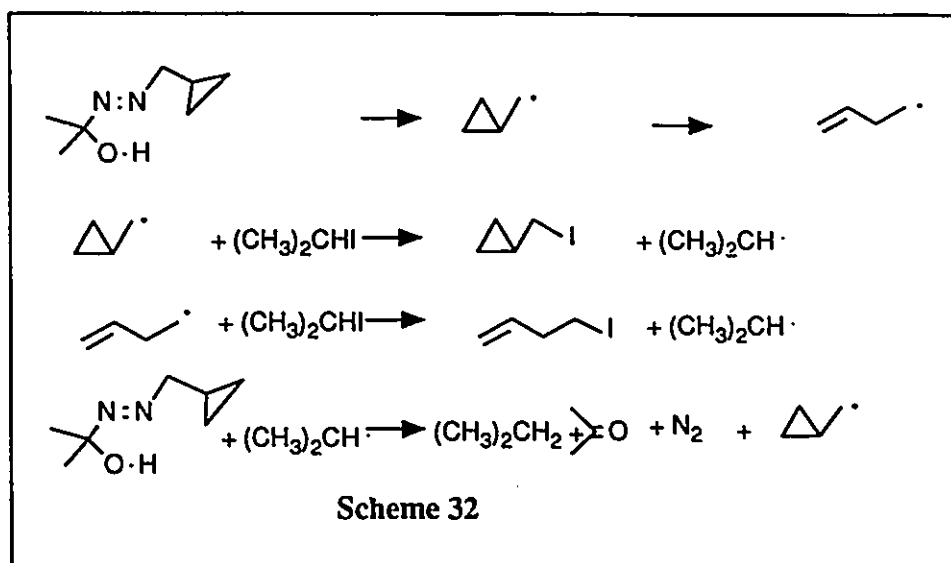


Fig. 6. Arrhenius Plot for the Data in Table 23



its concentration was calculated from its density at 20°C and molecular weight. Correction was applied for volume expansion. The relative concentration of 184 and 185 was estimated as usual by the glc technique. The results are summarized in Table 24.

The rate constants k_I listed in Table 24 are of the right order of magnitude for iodine abstraction reactions, but the actual numbers need further refinement. Errors as large as 50% could be involved because of two reasons. First of all, the isopropyl iodide used as solvent in the reactions has a retention time close to that of the butenyl iodide and therefore, the observed tailing of the solvent peak probably affected the integration of the partially resolved peaks of 184 and 185. Secondly, as explained in a previous section, the accuracy of the product ratio [184]/[185] depends on how close their area counts are; the greater the difference between the numbers, the greater the error. In the case of the isopropyl iodide - cyclopropylmethyl radical reaction, the above area counts for 184 and 185 differ widely. By triangulation of the peaks for 184 and 185 and then manually estimating the relative peak area by cutting and weighing, it was observed that the computer integrations are in agreement with the manual integrations within a 20% error

Table 24. Rate constant for iodine abstraction from isopropyl iodide by cyclopropylmethyl radicals

Temp. (°C)	$[(\text{CH}_3)_2\text{CHI}]^a$ (M)	$[184]/[185]^b$	$k_i \times 10^{-8c}$ (s ⁻¹)	$k_I \times 10^{-6d}$ (M ⁻¹ s ⁻¹)
50	9.66	0.108	2.51	2.81
50	9.66	0.083	2.51	2.16
80	9.33	0.239	6.55	16.78
80	9.33	0.182	6.55	12.68
80	9.33	0.192	6.55	13.48

^a Concentration of neat isopropyl iodide, corrected for volume expansion

^b Ratio determined by glc, corrected for detector responses. Each value is a mean of at least two injections

^c Isomerization rate constant calculated from eq.58

^d Calculated using eq.141

limit. However, the possibility of an impurity which eluted with a retention time close to that of the cyclopropylmethyl iodide, was indicated in a few injections by a small splitting of the signal. This implies that the rate constants in **Table 24** are probably the maximum value at that particular temperature.

In the absence of any rate constant data other than those for iodine abstraction by methyl and phenyl radicals from isopropyl iodide, the present data may be used at least for the order of magnitude comparisons with other radical molecule reactions.

A comparison of our data with the rate constants for iodine abstraction from isopropyl iodide by methyl radicals is possible as follows. The activation energy for the reaction of methyl radical with isopropyl iodide can be calculated from the data by Szwarc et. al.²⁶³ The difference in activation energies for the iodine abstraction from isopropyl

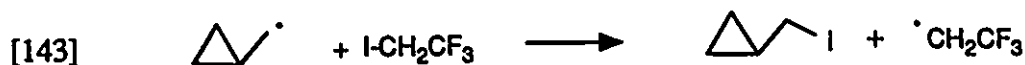
iodide (E_I) and hydrogen abstraction (E_H) from toluene by methyl radicals is $E_I - E_H = -3.4$ kcal/mol.²⁶³ Substituting for $E_H = 9.5$ kcal/mol,²⁶⁴ gives $E_I = 6.1$ kcal/mol. A preexponential factor of 9 ± 1.0 is what is expected for typical iodine abstraction reactions, as described in the previous sections. It follows that the approximate Arrhenius expression for the rate constant for iodine abstraction from isopropyl iodide by methyl radical is given by eq.142, where $\theta = 2.3 RT$ kcal/mol.

$$[142] \log (k_I/M^{-1} s^{-1}) = 9.0 - 6.1/\theta$$

The above expression gives $k_I = 9.4 \times 10^4 M^{-1} s^{-1}$ (at 50°C) and $2.1 \times 10^5 M^{-1} s^{-1}$ (at 80°C). These numbers are considerably smaller than those observed for the reaction of cyclopropylmethyl radicals with isopropyl iodide (see Table 24).

(v) Rate constants for 2,2,2-trifluoroethyl iodide

Decomposition of the azocarbiniol 155a ($\sim 0.25 M$) in neat 2,2,2-trifluoroethyl iodide resulted in the formation of cyclopropylmethyl iodide 184 and butenyl iodide 185. Assuming that the reaction follows the steps given in Scheme 32, where the $(CH_3)_2CHI$ is replaced by CF_3CH_2-I , the rate constant for the reaction [143] can be calculated using eq.144.



$$[144] \quad k_I = ([184]/[185]) \times \{k_f/[CF_3CH_2I]\}$$

The relative concentrations of 184 and 185 were determined by the glc technique. From known initial concentrations of the trifluoroethyl iodide, taken in large excess so that the concentration remains constant, the rate constant k_i is calculated from the product ratios. Thermolysis of a mixture of the azocarbiniol 184 (≈ 0.25 M) in neat trifluoroethyl iodide (9.44 M) at 80 °C gave a ratio $[184]/[185] = 0.0945$. A similar experiment conducted at 50 °C gave a ratio $[184]/[185] = 0.0799$. The combined data are summarized in Table 25.

Table 25. Rate constants for iodine abstraction from 2,2,2-trifluoroethyl iodide by cyclopropylmethyl radicals				
Temp. (°C)	$[\text{CF}_3\text{CH}_2\text{I}]^a$ (M)	$[184]/[185]^b$	$k_i \times 10^{-8c}$ (s ⁻¹)	$k_i \times 10^{-6d}$ (M ⁻¹ s ⁻¹)
50	9.77	0.0799	2.51	2.10
80	9.44	0.0945	6.55	6.56

^a Concentration of 2,2,2-trifluoroethyl iodide, corrected for volume expansion

^b Ratio determined by glc, corrected for detector responses. Each value is a mean of at least two injections

^c Isomerization rate constant calculated from eq.58

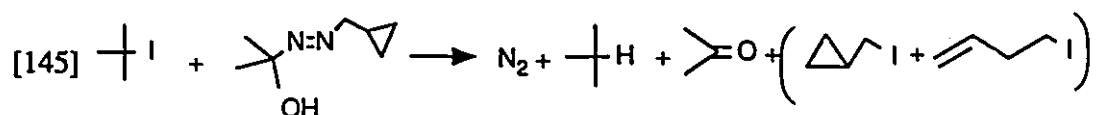
^d Calculated using eq.144

The rate constant for 2,2,2-trifluoroethyl iodide is seen to be of the same order of magnitude as that of isopropyl iodide. On the basis of the proposed polar transition state for radical attacks on alkyl halides, 2,2,2-trifluoroethyl iodide is expected to have a higher rate constant due to the presence of three electron withdrawing fluorine atoms on the beta carbon atom. However, the rate constant at 80°C is seen to be lower than that for isopropyl iodide at the same temperature. It is also interesting to note that the rate constant ($6.56 \times 10^6 \text{ M}^{-1} \text{ s}^{-1}$) is only a factor of 1.7 larger than that ($3.99 \times 10^6 \text{ M}^{-1} \text{ s}^{-1}$) for methyl iodide at

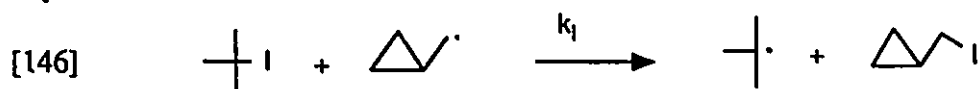
80°C.

(vi) Rate constants for 1,1-dimethylethyl (*t*-butyl) iodide

Thermal decomposition of the azocarbinol 155a in neat 2,2-dimethylethyl iodide (*t*-butyl iodide) resulted in the formation of products given by eq.145, according to reactions similar to those presented in Scheme 32.



The rate constant for the attack of cyclopropyl methyl radical on the *t*-butyl iodide (eq.146) is given by eq.147.



$$[147] \quad k_1 = \{[184]/[185]\} \times \{k_2/[(\text{CH}_3)_3\text{CI}]\}$$

The ratio [184]/[185] obtained by the thermolysis of an approximately 0.2M solution of the azocarbinol in neat *t*-butyl iodide (7.81M, at 80°C) was found to be = 0.774. Substituting also for $k_2 = 6.55 \times 10^8$ (at 80°C) in eq.148, the rate constant k_1 was calculated to be $6.49 \times 10^7 \text{ M}^{-1} \text{ s}^{-1}$. The above number is a factor of four larger than that for isopropyl iodide and is less than a factor of two smaller than that for benzyl iodide at the same temperature.

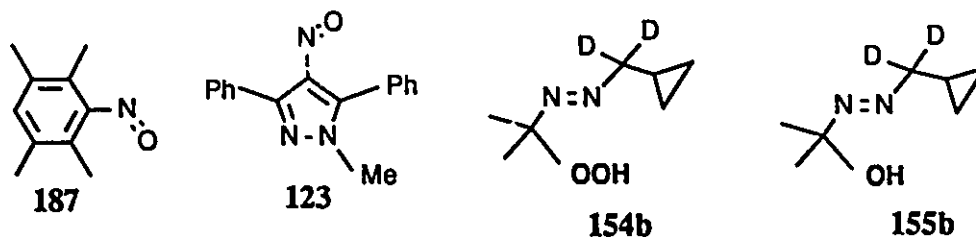
A general comparison can be made of the relative reactivities of various iodo

compounds for attack by cyclopropylmethyl radical from the measured or extrapolated (using Arrhenius expression) rate constants at 80°C. The decreasing order of reactivity is $\text{C}_6\text{H}_5\text{CH}_2\text{I} > (\text{CH}_3)_3\text{CI} > \text{CH}_2\text{I}_2 > (\text{CH}_3)_2\text{CHI} > \text{CF}_3\text{CH}_2\text{I} > \text{CH}_3\text{I}$.

Though we have looked at the rate constants for only a limited number of iodo compounds, the data indicates that the reactions of radicals with iodo compounds are fast and that the rate constants can be conveniently measured using the cyclopropylmethyl radical clock. This work represents a small step forward in an area of radical chemistry which has not been well studied before.

2.2.4. Rate constants for a primary alkyl radical attack on 1-methyl-4-nitroso-3,5-diphenylpyrazole

Nitroso compounds are widely used as spin-traps (see Section 1.4.2d) and the rate constants for spin-trapping by several of these "traps" are known.¹⁹⁹⁻²⁰⁴ 1-Nitroso-2,3,5,6-tetramethyl benzene (nitrosodurene, ND, 187) is known as one of the most efficient nitroso spin-traps having a spin trapping rate constant of $3.9 \times 10^7 \text{ M}^{-1} \text{ s}^{-1}$ at 25°C for a primary alkyl radical.²⁰² Unfortunately this compound is known to dimerize²⁰³ and therefore its use as a kinetic standard for spin trapping requires calculated, rather than measured, concentration of monomer in solution.



In an attempt to prepare new and more efficient nitroso spin traps, Perkins²⁰⁴ synthesized 1-methyl-4-nitroso-3,5-diphenylpyrazole (MNDP, 123) in 1982. This

compound has been shown to be monomeric in benzene solution over a wide range of concentrations.²⁰⁴ This property makes MNDP one of the most useful spin-traps for kinetic studies.

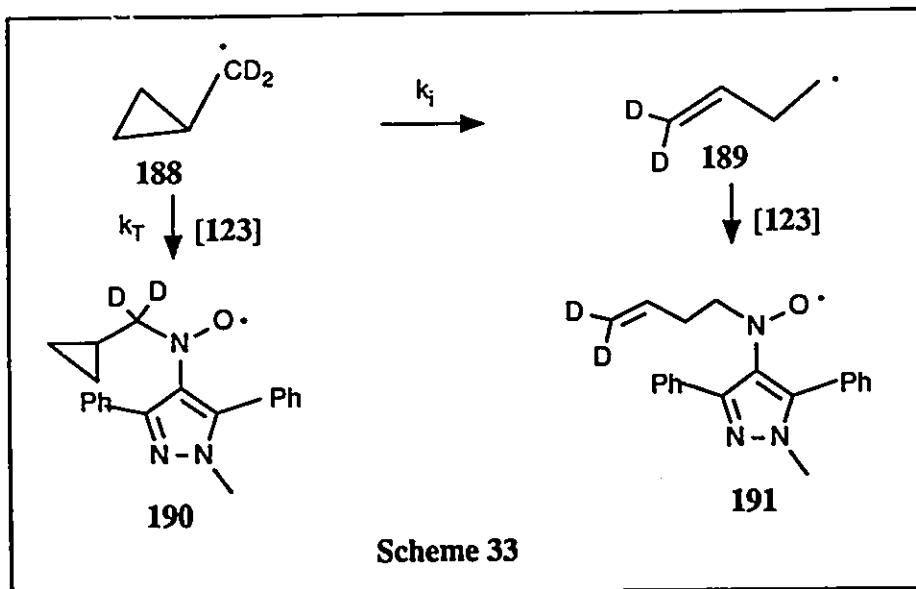
The rate constant at 40°C for attack of undecyl radical on MNDP has been reported by Perkins²⁰⁴ as $1.5 \times 10^7 \text{ M}^{-1} \text{ s}^{-1}$. The above rate constant comes from competition kinetics involving a mixture of MNDP and another spin trap, phenyl-N-t butylnitrone (PNB, $\text{C}_6\text{H}_5\text{CH}=\text{N}(\text{O})\text{C}(\text{CH}_3)_3$), by using $1.3 \times 10^5 \text{ M}^{-1} \text{ s}^{-1}$ as the rate constant for attack by a primary radical on PNB.²⁰² Based on the data given in ref.202, and using the latest value for the 5-hexenyl radical clock ($\log(k_{5\text{-hex}}/\text{M}^{-1} \text{ s}^{-1}) = 10.4 - 6.9/\theta$),¹⁴⁷ one can recalculate the rate constant for attack of a primary radical on PNB as $2.8 \times 10^5 \text{ M}^{-1} \text{ s}^{-1}$. From the above rate constant, the recalculated spin trapping rate constant for MNDP becomes $3.2 \times 10^7 \text{ M}^{-1} \text{ s}^{-1}$.

In order to use MNDP as a more reliable kinetic standard, we decided to determine the rate constant for the cyclopropylmethyl radical attack on MNDP at and near room temperature using the esr technique.

Cyclopropylmethyl radical rearrangement was used as the clock for estimating the spin trapping rate constant (k_T). The principle involves a competition between the isomerization of the deuterium labelled cyclopropylmethyl radical (188), generated from the azohydroperoxide, 154b, and addition to MNDP according to Scheme 32. Because of the difference in the esr spectra of the unrearranged radical adduct 190, and the rearranged radical adduct 191, the relative concentrations of 190 and 191 could be calculated from the esr spectra of mixtures of 190 and 191 formed as products of the reaction.

The rate constant k_T is then calculated using eq.149, from the known concentration of 123 (used in large excess) and the known value of k_i

$$[149] \quad k_T = k_i [190]/[191][123]$$



The success of this technique can be attributed to the fact that the β -H and the β -D hfc's are considerably different ($a_{\beta-D} = 1/6 a_{\beta-H}$). Thus the unrearranged radical **188** gives rise to the product **190** with an esr spectrum consisting of a triplet (1:1:1, due to the α -N, with $a_{\alpha-N} = 12.8$ G) of quintets (1:2:3:2:1, due to two β -D's, with $a_{\beta-D} = 1.5$ G). The rearranged radical adduct **191** gives rise to a triplet (1:1:1, with $a_{\alpha-N} = 12.8$ G) of triplets (1:2:1, due to two β -H's, with $a_{\beta-H} = 9.4$ G). Therefore the ratio $[190]/[191]$ could be easily calculated from the integral of the non-overlapping side signals of **190** and from the total integral of **190** and **191** formed in the same reaction mixture. A representative esr spectrum obtained by thermolysing the radical source (**154b**) in a degassed solution of MNDP in benzene is given in Fig.7.

It was observed that the ratio $[190]/[191]$ remained approximately constant for at least 15 minutes when the esr spectrum was monitored every 3-5 minutes. However, in a few experiments the ratio $[190]/[191]$ was found to increase marginally with time. The reason for this observation is not very clear at this moment. Therefore the ratio $[190]/[191]$

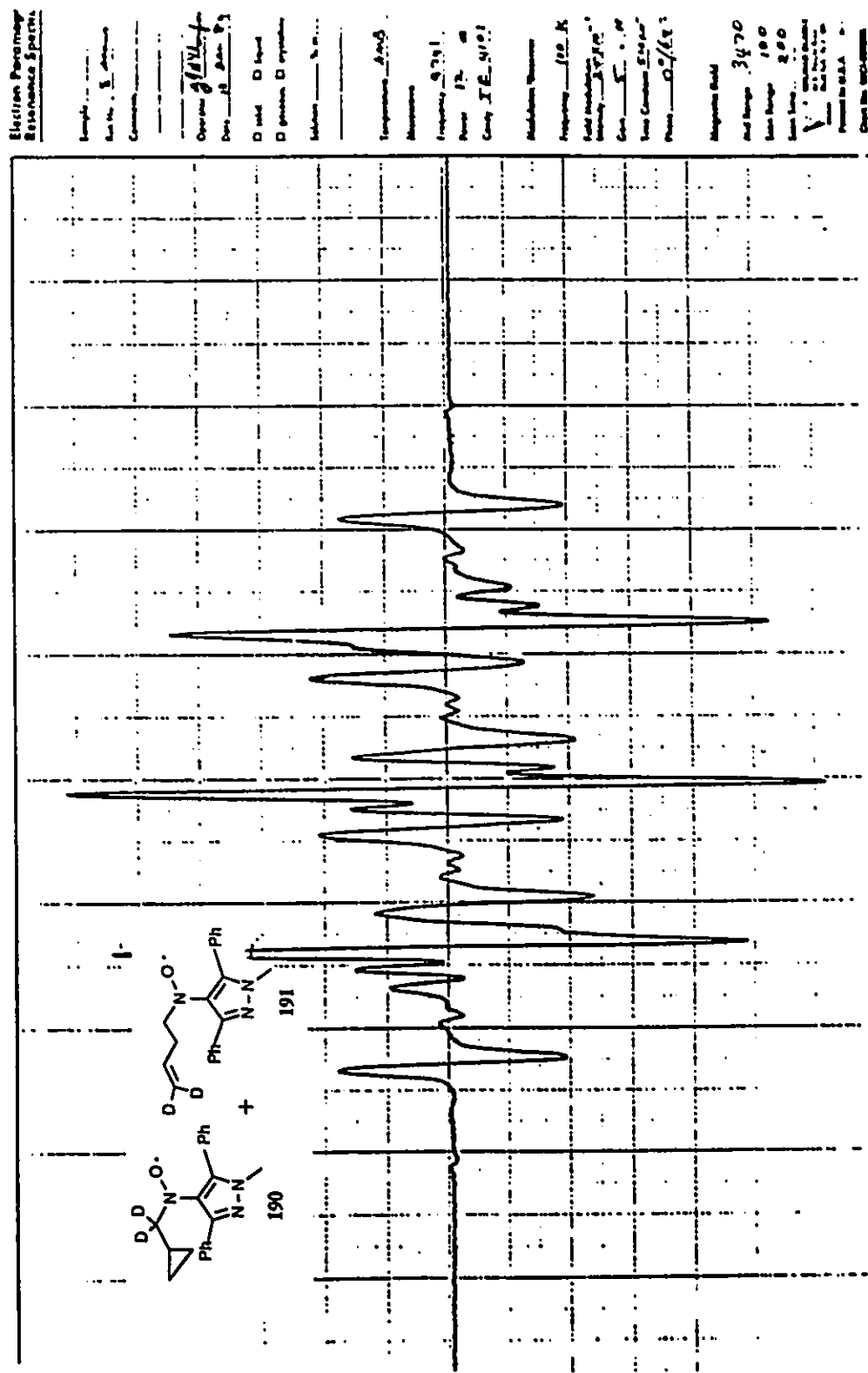


Fig. 7. ESR Spectrum Obtained While Thermolyzing 154b in the Presence of MNDP

was extrapolated to zero time for the rate constant calculation. A few rate constants were calculated from single product ratios, measured immediately after the reaction tubes were set up in the cavity of the esr instrument. The set up time varied from 1 to 3 minutes in most experiments and a change in product ratio is expected to be negligible in such a short period of time. The change in ratio $[190]/[191]$ with time for a few runs is given in Table 26.

Table 26. Change in product ratio $[190]/[191]$ with time					
<u>T = 295 K</u>		<u>T = 303 K</u>		<u>T = 333 K</u>	
Time (min)	$[190]/[191]$	Time (min)	$[190]/[191]$	Time (min)	$[190]/[191]$
0	0.569	0	0.456	0	0.333
3	0.588	5	0.458	5	0.409
15	0.565	10	0.484	10	0.440
		15	0.502		

In our esr experiments we observed a few additional weak signals amounting to about 0.5-3% (calculated from the outside signal intensities of the unknown and of the rearranged radical adduct 191, especially in cases of the 40° and 60° experiments. The signals have a splitting pattern which looked almost like a 1:2:1 triplet (with $a = 11.5$ G) of doublets ($a = 37$ G). This unusual splitting does not correspond to a possible hydroxyl ($\text{OH}\cdot$) radical addition product with MNDP, since a similar nitroxyl radical formed by the addition of t-butoxyl radical to MNDP is reported to give a 1:1:1 triplet esr spectrum with $a_N = 29.9$ G.²⁰⁴

It is known that alkyl azohydroperoxides decompose to alkyl ($\text{R}\cdot$) and hydroxyl ($\text{OH}\cdot$) radicals in solution. If the rate constant for addition of $\text{OH}\cdot$ radicals to a nitroso

"trap" is comparable to that of an $R\cdot$ radical, then for every $R\cdot$ radical added on to the nitroxide, one $OH\cdot$ radical addition product can also be expected. The esr spectrum should then consist of additional signals (triplet of doublet) due to the hydroxyl radical adduct. It should be emphasized at this point that the esr spectra of several alkyl radicals generated from azohydroperoxides in MNDP solutions by Osei-Twum²⁰⁵ in this laboratory did not show any signals from the $OH\cdot$ addition to MNDP; the spectra were very clean and were due only to the alkyl radical addition to the nitroso group.

There were two reasons for choosing the azohydroperoxide (154b), rather than the azocarinol (155b), as the source of the deuterium labelled radical (188) for spin trapping studies. First of all, in our experience, the shelf-life of α -hydroxyalkyl diazenes is much shorter than that of the corresponding α -hydroperoxyalkyl diazenes. Secondly, conversion to the azocarinol and following purification steps cause considerable loss of the valuable labelled radical source. α -Hydroperoxyalkyl diazenes are known to be stable at low temperatures in dilute solutions for long period of time.²⁰⁵

The only assumption involved in the measurement of the rate constant is that MNDP remains monomeric at the working concentrations (≈ 0.95 M) used in our experiments. Perkins²⁰⁴ predicted from its green colour that even in the solid state MNDP remains at least partly monomeric. By measuring the UV absorption at 738 nm ($\epsilon = 92$), Perkins showed that up to 0.03 M, MNDP is 100% monomeric in benzene. In order to see whether or not 123 remains monomeric at higher concentrations as well, we decided to determine the extinction coefficients over a wider range of concentrations. The data obtained at 23 and 40°C are presented in Table 27. It will be seen that within experimental error, the extinction coefficient remains constant. For example, at 40°C, the extinction coefficient remains at around 92 over a concentration ranging two orders of magnitude. Moreover, a change in temperature from 40°C to 23°C has practically no effect on the extinction coefficient. This result clearly excludes the possibility of any

Table 27. Extinction coefficients (ϵ) of 123 in benzene at 40 °C and at 23°C at $\lambda = 738$ nm

[123] ^a	Absorbance, A	l^b (cm)	$\epsilon = A/[123].l$
<u>at 40°C</u>			
0.196	1.811	0.1	92.4
0.0795	0.744	0.1	93.6
0.0318	0.292	0.1	91.8
0.0127	1.188	1.0	93.5
0.00509	0.481	1.0	94.5
0.00203	0.185	1.0	91.1
<u>at 23°C</u>			
0.196	1.874	0.1	95.6
0.0795	0.720	0.1	90.6
0.0318	0.295	0.1	92.8
0.0127	0.112	0.1	88.2

^aConcentration, corrected for tempera changes. ^bPath length of the cell.

appreciable dimer formation in the range of concentrations that were examined.

For technical reasons, we could not carry out the UV measurements at concentrations higher than 0.2 M. However, it was apparent from the general trend that 123 could be monomeric at higher concentrations as well.

Relative concentrations of 190 and 191 and the calculated rate constants for the spin trapping of cyclopropylmethyl radicals by MNDP for the temperature range 10-60 °C

are given in Table 28. Least squares treatment of the data given in Table 28 (the best fit

Table 28. Product ratios and rate data for cyclopropylmethyl radical attack on MNDP				
Temp. (K)	ratio [190]/[191]	[123] ^a	k _i (x 10 ⁻⁷) s ⁻¹	k _T ^b (x 10 ⁻⁷)
283	0.819	0.963	5.63	4.80
293	0.553	0.950	8.50	4.95
295	0.625	0.948	9.20	6.06
295	0.590	0.948	9.20	5.73
298	0.501	0.944	10.3	5.47
300	0.540	0.942	11.2	6.42
313	0.333	0.927	17.9	6.43
313	0.456	0.927	17.9	8.81
333	0.329	0.905	34.6	12.6

^amolar concentration of 123, corrected for volume expansion based on the coefficient of cubical expansion of benzene (see ref.147)

^bin M⁻¹ s⁻¹ units.

line is shown in Fig.8) yields eq.150.

$$[150] \log(k_T / \text{M}^{-1}\text{s}^{-1}) = (10.4 \pm 0.4) - (3.6 \pm 0.5)/\theta$$

The high A-factor indicates that the addition of alkyl radicals to a nitroso spin trap probably involves a loose (or early) transition state. The low activation energy is comparable to those for radical additions to carbon-carbon double bonds. However, it is important to note that the pre exponential factor and the activation energy are considerably larger than those reported by Ingold²⁰³ for 2-methyl-2-nitrosopropane ((CH₃)₃CN=O), viz. A = 10^{8.4} and Ea = 2 kcal/mol. A recalculation of the data by Ingold,²⁰³ using the latest

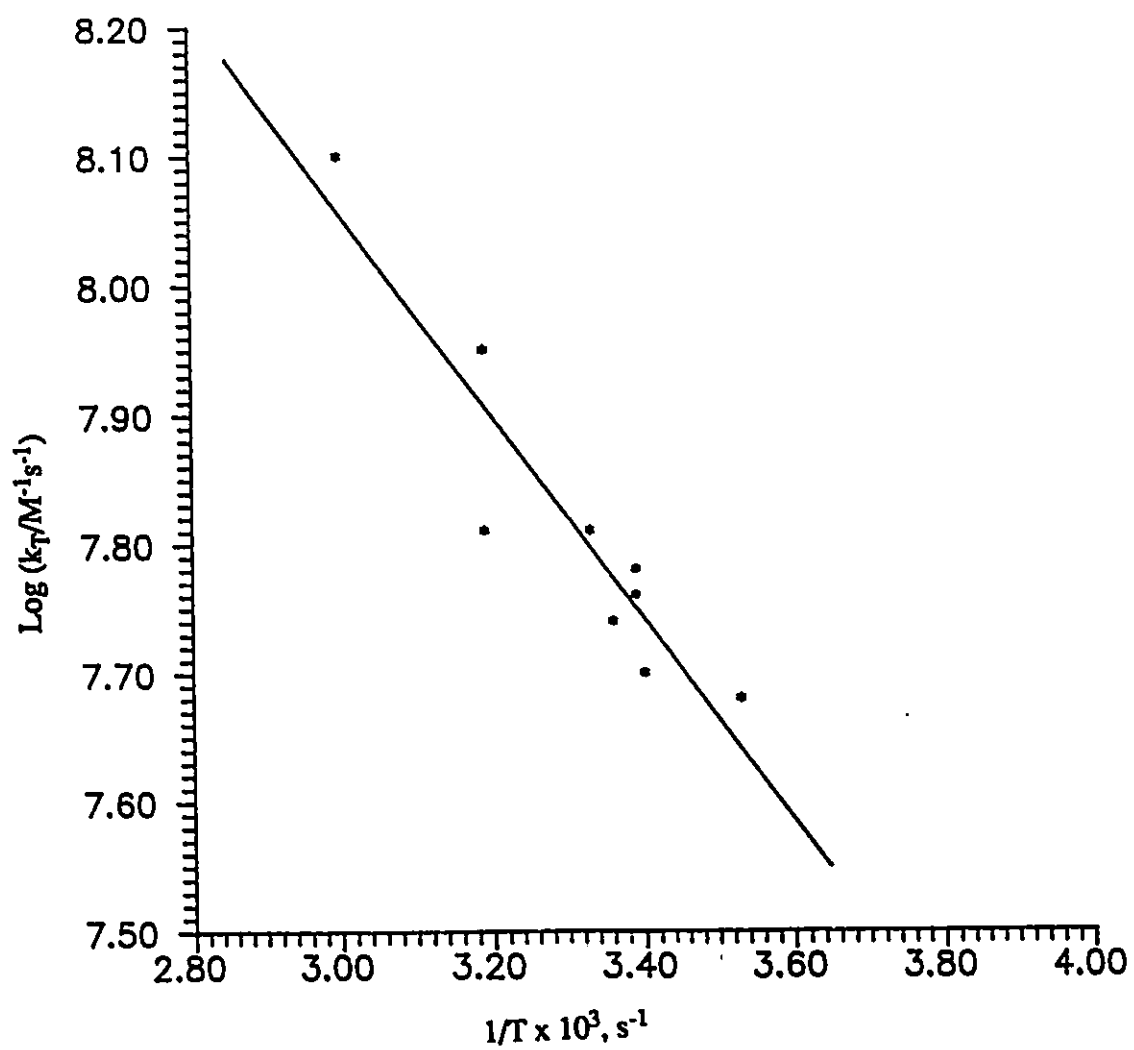


Fig. 8. Arrhenius Plot for the Data in Table 28

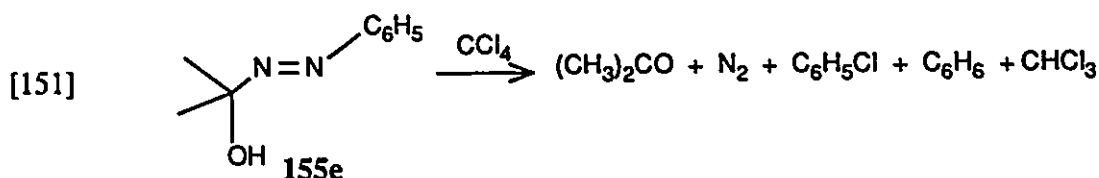
value for the 5-hexenyl radical clock (see Section 1.3.2), gives slightly different numbers: $A = 10^{8.6}$, $E_a = 1.8$ kcal/mol. One can easily assume that these differences are probably due to the structural difference between the two nitroso traps. MNDP contains a conjugated N=O group whereas that in $(\text{CH}_3)_3\text{CN}=\text{O}$ is isolated, and that explains the reason for a higher activation energy for radical attack on MNDP. The bulky *t*-butyl group of 2-methyl-2-nitrosopropane reduces the probability of radical attack on the functional group which naturally reduces the pre-exponential factor. In short, within the limitation of the structural difference between the two spin traps, one can see that there is good agreement between our result and that of Ingold.

From eq.150, the rate constant at 40°C can be calculated as $7.7 \times 10^7 \text{ M}^{-1} \text{ s}^{-1}$. This number is a factor of 2.4 larger than that reported by Perkins.²⁰³ If there is an error in the assumption that **123** is monomeric at 5 times the concentration for which we could measure ϵ , then our number would go further away from agreement with Perkins number for the following reason. If MNDP is partly associated at higher concentrations, then the monomer concentration will be smaller than what was assumed in calculating k_T using eq.149, and therefore the k_T values in Table 27 would be the lower limit for the spin trapping rate constants.

In short, our estimate gives a modest revision for the spin trapping rate constant of this extremely powerful trap. Moreover, since the Arrhenius parameters are known, the use of MNDP can now be extended to kinetic studies over a wide range of temperature.

2.3.0 MECHANISTIC INVESTIGATIONS OF THE DECOMPOSITION OF AZOCARBINOLS

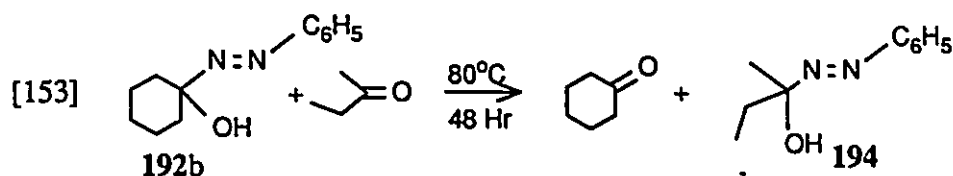
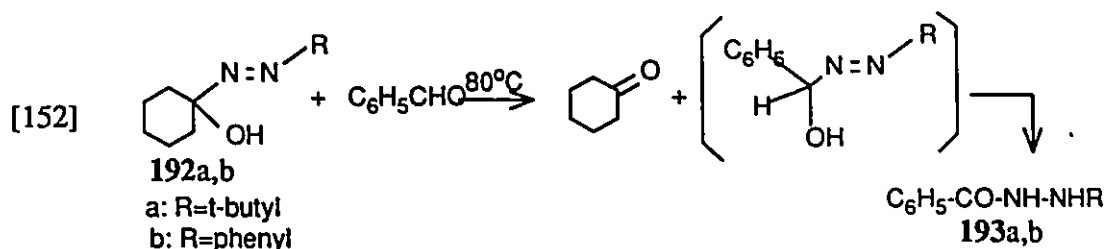
α -Hydroperoxyalkyl diazenes in organic solvents are known to decompose by an induced radical chain mechanism, as has already been explained in the Introduction Section. Several lines of evidence exist for such a mechanism.²³³ One part of the evidence is that the decomposition of the azocarbinol **155e** in carbon tetrachloride at 80°C resulted in the formation of acetone, nitrogen, chlorobenzene, benzene and chloroform as given in eq.151



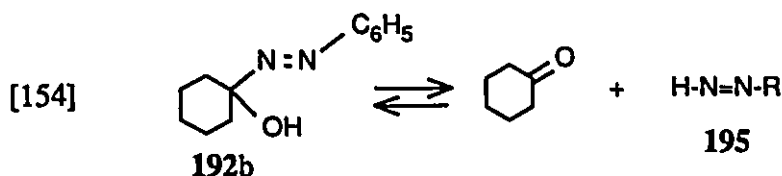
The increase in ratio of $[C_6H_5Cl]/[C_6H_6]$ observed as a consequence of a decrease in concentration of **155e** in CCl_4 was an indication of the involvement of **155e** as H-donor to phenyl radicals in the decomposition process. It is proposed that benzene is formed by the attack of phenyl radicals at the OH group of the azocarbinol **155e** and, therefore, the rate of formation of benzene should be proportional to the azocarbinol concentration.

It was also observed by Warkentin and co-workers²³³ that the rate constant for the decomposition of **155e** in CCl_4 at 80°C ($k_{obs} = 7.76 \times 10^{-4} \text{ s}^{-1}$) was increased by a factor of four in the presence of trace amounts ($\approx 10^{-3} \text{ M}$) of thiophenol, in which case the observed rate constant was $3.2 \times 10^{-3} \text{ s}^{-1}$. Since thiophenols are known as excellent H-atom donors for radicals, the thiophenyl radicals formed in the reaction must be able to initiate a new radical chain, such as the induced decomposition of the azocarbinol, with a greater chain length which accounts for the increased rate constant.

A second mechanism for the decomposition of azocarinols comes from the work of Schulz and Missol.²³⁶ They observed that azocarinols undergo exchange reactions with aldehydes to form hydrazides and with ketones to form new azocarinols. For example, compounds **192a,b** underwent exchange with benzaldehyde to form the

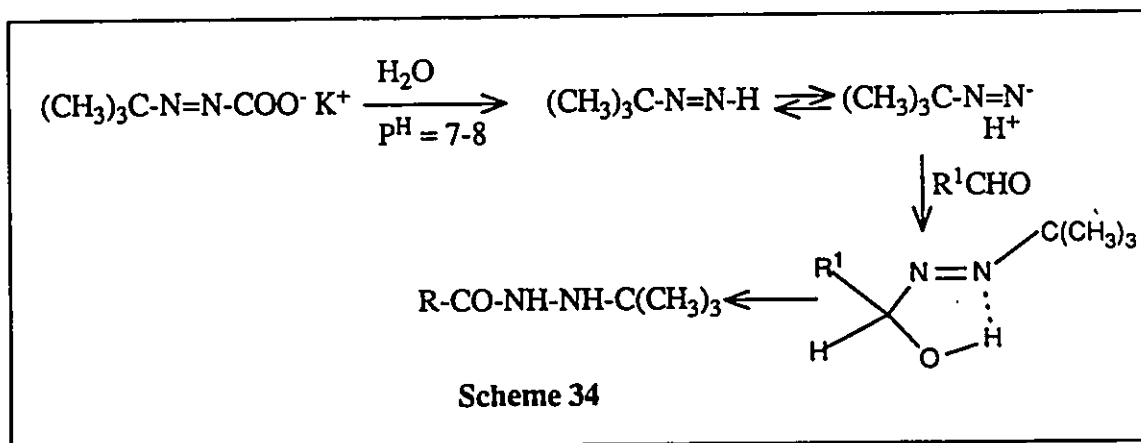


hydrazides **193a,b** (eq.152) in 50% and 60% yields. A similar reaction of **192b** with ethylmethyl ketone resulted in the formation of **194** (eq.153) in excellent (82%) yield. From these observations they concluded that the mechanism for the exchange reaction involves a highly reactive diazene intermediate as is given in eq.154.



Further evidence for a diazene mechanism comes from the works by Hünig and co-workers. It was observed by Hünig and Büttner²³⁵ that diazenes produced independently by the decarboxylation of alkyl diazene carboxylate salts in weakly basic or

neutral aqueous solutions react with aldehydes to form azocarinols which slowly rearrange to the hydrazides according to Scheme 34, where the reaction of *t*-butyl diazene is presented as an example.



According to Freeman and Rathjen, " α -azocarinols might resemble cyanohydrins in that they are adducts of carbonyl compounds and diazenes". Unlike cyanohydrins, however, azocarinols are sensitive to acids and less sensitive to bases.

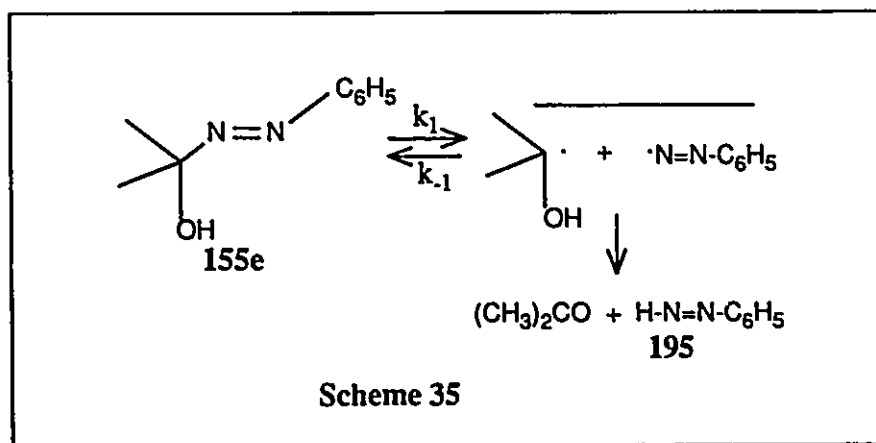
However, Kosower and co-workers,²²⁰ who were able to prepare and characterize phenyl diazene, were unable to observe any nucleophilic attack by phenyl diazene on reactive electrophiles such as benzenesulfonyl chloride or methyl chloroformate in acetonitrile.^{220b} Their conclusion was that phenyl diazene is "non-nucleophilic, as would be expected for azo compounds". The difference in reactivity of diazenes toward electrophiles reported by Hünig^{227,235} and Kosower^{220b} are probably the result of the difference in experimental conditions. Kosower did the experiment in neutral aprotic solvent whereas Hünig's experiment was done in a basic aqueous medium. The implication is that phenyl diazene anion is nucleophilic whereas phenyldiazene is a very poor nucleophile.

Whatever be the implications of the nucleophilic reactions of diazenes, it is

important to consider seriously the possibility of diazene intermediates in the mechanism for the decomposition of α -azocarinols.

The problem that will be addressed in this section of the thesis is whether or not a diazene is involved in the initiation mechanism for the decomposition of azocarinols in non-polar as well as polar aprotic solvents.

There are two major pathways by which diazenes could be formed in the decomposition of azocarinols.²³³ One involves the decomposition via a radical mechanism (Scheme 35) and the other involves an ionic mechanism (Scheme 36).

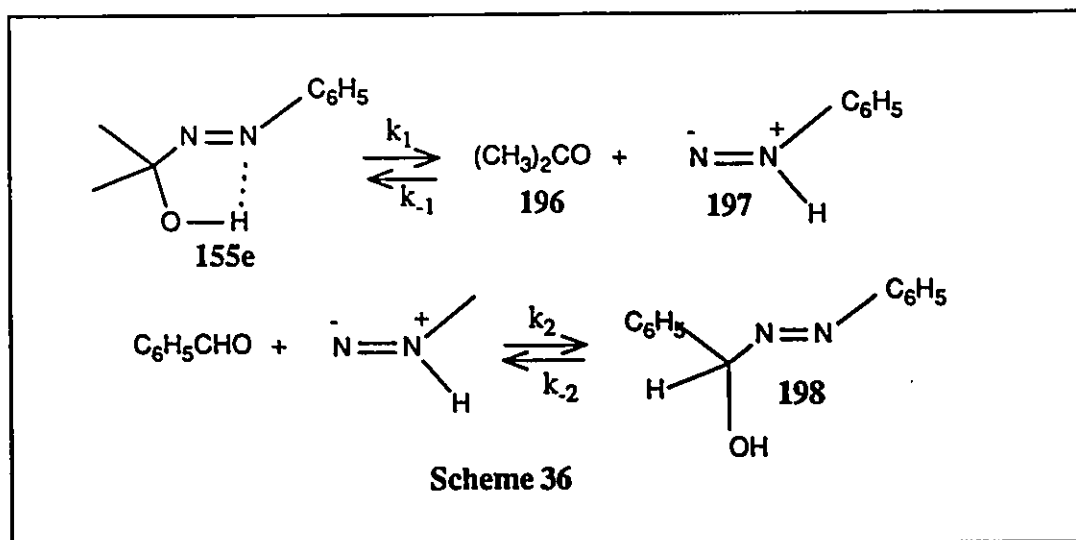


The formation of phenyl diazene (195) by way of a radical mechanism (Scheme 35) was ruled out by Warkentin and co-workers,²³³ based on the fact that if k_1 is assumed to be rate determining then the rate constant for the decomposition of azocarinol 155e should be approximately the same as those of the corresponding -O-methyl or the -O-acetyl compounds. However, the rate constants for the latter compounds were found to be two orders of magnitude smaller. Moreover, they observed that benzaldehyde greatly enhanced the rate constant for the decomposition of 155e. This cannot be explained by the proposed mechanism in Scheme 35.

If one assumes Schultz's mechanism (that is the reversible formation of

phenyldiazene and the carbonyl compound, as in eq.154) for the decomposition of azocarinols, the increased rate constant for the decomposition of 155e in $\text{C}_6\text{H}_5\text{CHO}$ can be thought of as due to the reaction of the diazene with benzaldehyde. Kinetic treatment of the above process predicts a levelling effect at high concentrations of benzaldehyde, but a levelling effect was not observed even with neat benzaldehyde.²³³

Chang, Profetto and Warkentin²³³ looked seriously into an alternate mechanism (Scheme 36), along with other previously postulated mechanisms, for the decomposition of azocarinols. This mechanism involves the reversible formation of acetone and the 1,1-diazene (197).



From the above Scheme, the rate of disappearance of the azocarinol can be expressed as:

$$-\frac{d[155e]}{dt} = k_1[155e] - k_{-1}[196][197]$$

The steady state assumption for 197 gives

$$\frac{-d[197]}{dt} = 0 = k_1[155e] - k_{-1}[196][197] - k_2[C_6H_5CHO][197] + k_{-2}[198]$$

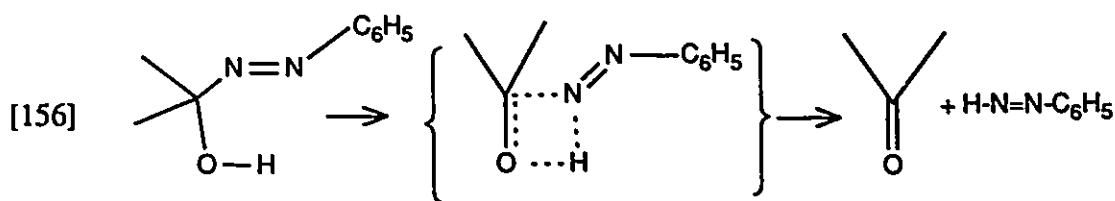
$$\text{or, } [197] = \frac{k_1[155e] + k_{-2}[198]}{k_{-1}[196] + k_2[C_6H_5CHO]}$$

If one assumes that $k_{-2}[198] \ll k_1[155e]$, which is true at least initially when $[198]$ is small, then:

$$\begin{aligned} [155] \quad \frac{-d[155e]}{dt} &= k_1[155e] - k_{-1}[196] \left\{ \frac{k_1[155e]}{k_{-1}[196] + k_2[C_6H_5CHO]} \right\} \\ &= k_1[155e] \left\{ 1 - \frac{k_{-1}[196]}{k_{-1}[196] + k_2[C_6H_5CHO]} \right\} \\ &= k_1[155e] \left\{ \frac{k_2[C_6H_5CHO]}{k_{-1}[196] + k_2[C_6H_5CHO]} \right\} \end{aligned}$$

In order for the disappearance of 155e to be first order in C_6H_5CHO , $k_{-1}[196] \gg k_2[Ph-CHO]$ is required. When the kinetics is done in large excess of PhCHO, $k_{-1}[196]$ should be much less than $k_2[PhCHO]$. Therefore, at high concentrations of aldehyde, the rate constant is expected to be independent of the aldehyde concentration. However, a levelling effect was not obtained and the pseudo-first-order rate constant kept on increasing until the limit of benzaldehyde concentration (9.8 M) was reached. Therefore some sort of direct reaction between benzaldehyde and 155e was suspected.

Even though 1,1-diazeno (197) is proposed as a possible intermediate in the formation of 1,2-diazeno (195),²²⁰ nobody has ever observed such an intermediate and its chemistry is, therefore, uncertain. Probably the rearrangement of the 1,1-diazeno to the 1,2-diazeno is fast, and if that is true one could argue that the reaction of benzaldehyde with azocarbino is via the formation of the 1,2-diazeno as the intermediate. However, the basis for such an argument is weak based on the results of Kosower^{220b} that the 1,2-diazeno is non-nucleophilic. The formation of the 1,2-diazeno directly from the azocarbino through an unfavourable four-membered transition state (eq.156) is very unlikely and therefore can be totally ignored.



In order to obtain a better understanding of the mechanism for decomposition of azocarbino, the following kinetic studies were made.

2.3.1. UV Kinetics

The phenyl azocarbino (155e) has a characteristic absorption at $\lambda_{\text{max}} = 382 \text{ nm}$ (CH_3CN , $\epsilon = 120$) due to the $n \rightarrow \pi^*$ transition. Therefore the rate of disappearance of the azocarbino could be easily followed by UV spectrophotometry.

Degassed solutions of known concentrations of 155e in acetonitrile, in the presence or absence of TEMPO, were placed in the cavity of a UV spectrophotometer. The absorbance (A) was measured at intervals of time. The corrected absorbance ($A_t = A - A_\infty$) at time t was calculated from the observed absorbance (A) and from the absorbance at

infinite time (A_∞). The rate constant k for the disappearance of the azocarinol was then calculated using eq.157. A plot of $\log (A_0/A_t)$ vs t gives a straight line whose slope is $k/2.303$.

$$[157] \quad \log(A_0/A_t) = (k/2.303) t$$

It is observed that in the presence of TEMPO the decomposition of 155e follows first order kinetics. The decomposition was followed at least for three half-lives and the data fit very well for a first order process with rate constant $(1.6 \pm 0.2) \times 10^{-4} \text{ s}^{-1}$. The results are summarized in Table 29. The first column numbers represent the

Table 29. Rate constants for the disappearance of 155e in CH_3CN at 80°C					
#	[155e]	[Tempo]	solvent	mode of reaction	Rate constant $\times 10^5, \text{s}^{-1}$
1	0.0116	0.029	CH_3CN	D ^a	15.5
2	0.0224	0.029	"	D	16.0
3	0.0114	0.029	"	D	17.7
4	0.0090	0.000	"	D	13.2
5	0.0160	0.067	CH_3COCH_3	D	$< 0.350^b$

^a D stands for decomposition leading to radical products

^b this number is calculated as the maximum possible value

corresponding best fit lines presented in Fig.9. The best fit lines (1,2,3) obtained for three separate runs in the presence of TEMPO (125) and the one line (4) obtained for the decomposition in the absence of TEMPO are given in Fig.9.

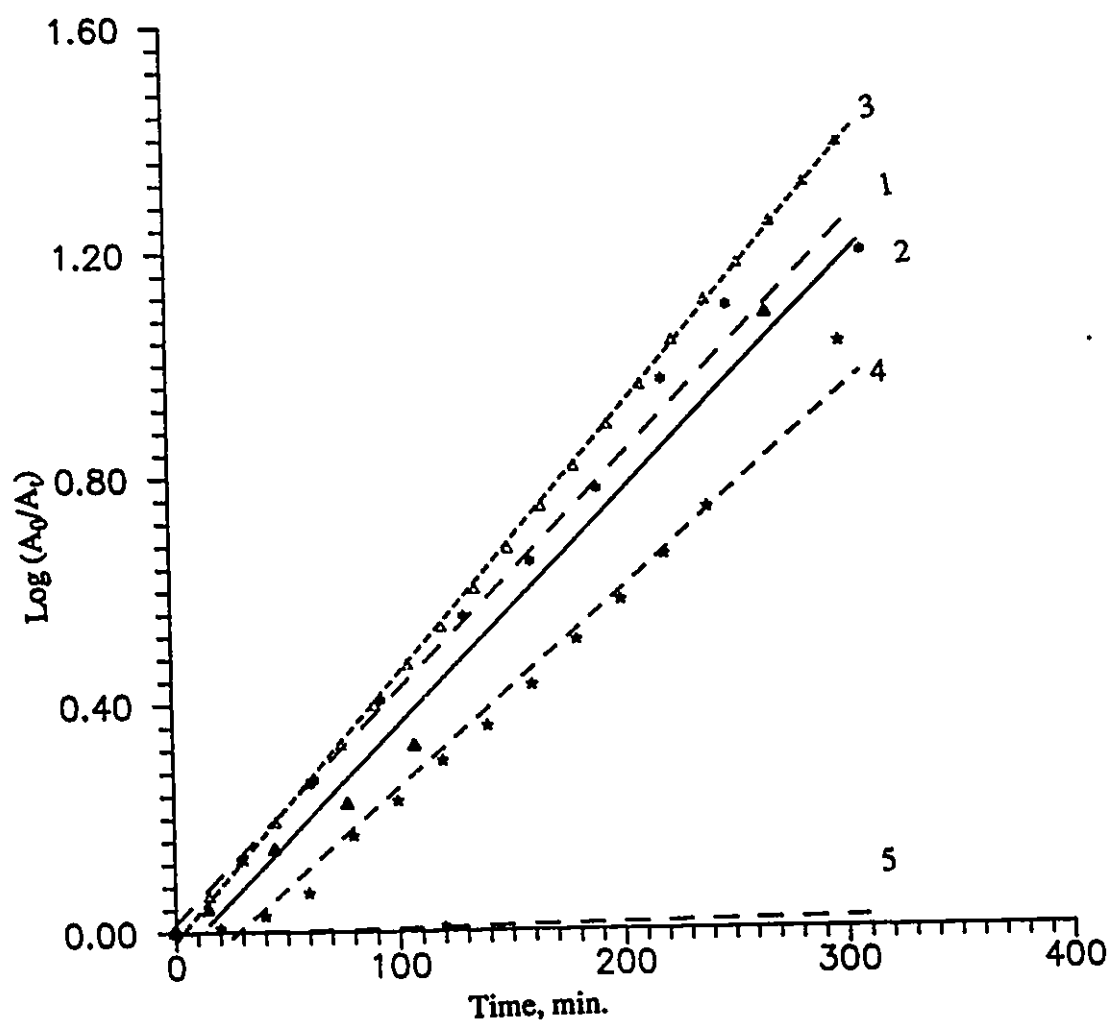


Fig. 9. UV Kinetics of Unimolecular Decomposition of 155e in CH_3CN at 80°C (see full data and individual linear plots in the *Appendix*)

The rate constant for the decomposition ($k = 1.32 \times 10^{-4} \text{ s}^{-1}$) in the absence of TEMPO (see Table 29) is slightly lower than that observed in the presence of TEMPO. One rationale for such an observation is that TEMPO may be inducing the decomposition of the azocarbinol to some extent. Further kinetic studies are necessary to confirm such an induced decomposition.

It is relevant to recall the observation by Warkentin et. al,²³³ that the decomposition of 155e in benzene at 35°C ($k = 4 \times 10^{-6} \text{ s}^{-1}$) was 4-fold reduced ($k = 9.7 \times 10^{-7} \text{ s}^{-1}$) in the presence of TEMPO (0.12M). This result could be explained by assuming that in benzene the azocarbinol decomposes by a radical chain process and TEMPO acts as a radical scavenger. This does not necessarily mean that TEMPO is not capable of inducing azocarbinol decomposition, but it only implies that the rate enhancement, if any, due to the induced decomposition by TEMPO is smaller than the rate retardation by virtue of its radical scavenging ability.

If the above argument holds for the decomposition of the azocarbinol in CH_3CN as well, then we expect at least a four-fold difference in the rate constants in the presence and absence of TEMPO. The fact that the rate constant is approximately the same in solutions with or without TEMPO strongly suggests the possibility that in CH_3CN the involvement of radical chain decomposition is greatly reduced. The result also suggests that the induced decomposition by TEMPO if any, is negligible.

The kinetics of the decomposition of the azocarbinol 155e in acetone was revealing. The first order rate constant for the decomposition of 155e (0.016M) in acetone (13.6M) in the presence of TEMPO (.067M) at 80°C was found to be $\sim 3.5 \times 10^{-6} \text{ s}^{-1}$, which is about 40-fold smaller than that for the decomposition in CH_3CN . The large difference in the rate constants in the two solvents suggests that acetone inhibits the decomposition process. A logical conclusion is that the decomposition takes place according to Scheme 36, in which the initial equilibrium is shifted towards the left in the

presence of excess of acetone. This is also true for the mechanism by which the azocarbinol decomposes reversibly to the ketone and the 1,2-diazene (195) as well.

If one assumes that in the presence of excess acetone the decomposition of azocarbinol occurs mostly by the homolytic cleavage (which is known to be the case with all azo compounds) of a C-N bond, then the observed rate constant ($k = 3.5 \times 10^{-6} \text{ s}^{-1}$) could be the maximum value for the homolytic process at 80°C. The above rate constant compares very well with the rate constant for the decomposition of the O-acetyl derivative of the azocarbinol for which $k = 4.0 \times 10^{-6} \text{ s}^{-1}$ at 80°C (see Section 1.5.2). It also implies that in polar solvents like CH_3CN , the reversible formation of the diazene and acetone (Scheme 36) is more important and the rate constant for the forward process is approximately two orders of magnitude faster than that for the homolytic process.

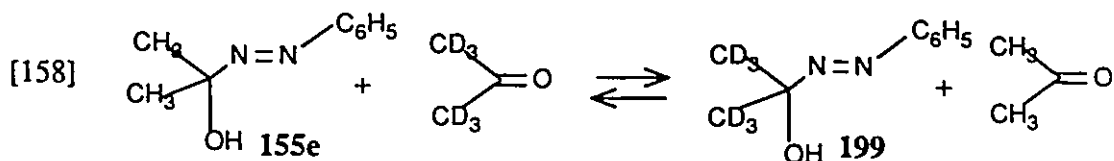
More evidence for the reversibility of the process given in Scheme 36 will be presented in the following section, in which the exchange of acetone- D_6 with the azocarbinol 155e and the kinetic treatment of the exchange process are discussed.

2.3.2 NMR Kinetics

(i) Exchange of acetone- D_6 with the azocarbinol, 155e

The purpose of the following NMR studies was to establish the reversibility of the azocarbinol dissociation as outlined in Scheme 36. If it is true that the initial step in the decomposition of 155e is the reversible formation of acetone and the diazene 197, then by thermolysing 155e in acetone- D_6 one should be able to obtain the exchanged D_6 -labelled azocarbinol 199, as is given in eq.158.

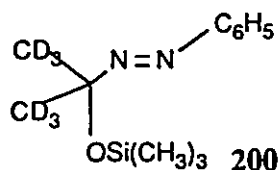
A degassed solution (0.22M) of 155e in acetone- D_6 (13.2M) containing TEMPO (0.19M) was sealed in an NMR tube and was thermolyzed at 80 °C. The NMR spectra were taken at 15 minute intervals to follow the course of the reaction. The gem-dimethyl



signal (at $\delta = 1.47$ ppm) of the azocarinol was found to decrease in intensity and a new signal at $\delta = 2.10$ ppm, apparently due to the acetone formed, was found to increase gradually. The most striking observation was that there was no appreciable change in the phenyl region (which still integrated for 5 ± 0.2 protons, $\delta = 7.5$ to 8 ppm) or in the region for the -OH group ($\delta = 4.95$, broad) which integrated for 0.6 ± 0.1 proton. This observation strongly suggested that acetone- D_6 exchanged with azocarinol at a rate faster than its decomposition to radical products.

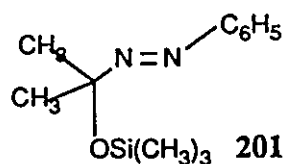
*The reduced -OH signal intensity for the azocarinol in acetone- D_6 can be attributed to small amounts of D_2O , present in acetone- D_6 , which exchanges D for H. The DOH formed by this exchange appeared as a new signal at around 2.6 ppm. The above hypothesis has been confirmed by adding D_2O to an azocarinol solution in acetone- D_6 . The OH signal intensity was found to decrease with time even at room temperature.

After the exchange was more than 90% complete (it took 48 hr at 80 °C), the major product (**199**) of the reaction was characterized by converting it to its stable trimethyl silyl ether **200**. Product **200** gave the same gc retention time as that of an authentic trimethyl silyl ether (**201**) prepared by trimethyl silylation of **155e** (see Experimental Section). GC/MS analysis gave for **200** and **201** the corresponding fragmentation products as shown below:



$$M^+(-15) = 227 \text{ (12\%)}$$

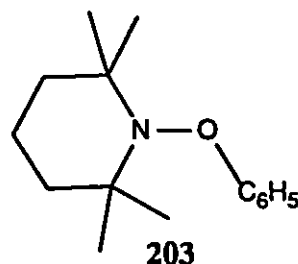
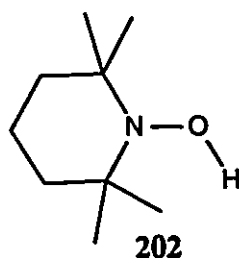
$$M^+(-105) = 137 \text{ (58\%)}$$



$$M^+(-15) = 221 \text{ (12\%)}$$

$$M^+(-105) = 131 \text{ (58\%)}$$

Small amounts of additional products were indicated from the gradual appearance of a few signals at around 1 to 1.3 ppm. There is reason to believe that at least the major signal, at around 1.1 ppm, is due to the four equivalent methyl groups from either of the possible non-radical products (202, 203) resulting from TEMPO, or a mixture of 202 and 203. Our own experience¹⁴⁷ is that compounds of the type 203 (in general with the



functional group, $R_2N-O-Ph$) are highly unstable like those with the function, $R-O-O-Ph$. Therefore, it is assumed that the increase in signal intensity at 1.1 ppm is due only to 202.

The amount of azocarinol decomposed during thermolysis is assumed to be proportional to the increase in the new signal at $\delta = 1.1$ ppm. Therefore it is possible to calculate an approximate rate constant for the decomposition (D) of the azocarinol, assuming that decomposition of one mole of the azocarinol results in the formation of one mole of 202 with twice as much methyl signal as the starting material. On the other hand, if the assumption is wrong, and the new signal at 1.1 ppm is due to both 202 and

203, then the estimated rate constant for decomposition should be reduced by a factor of two. It is important to emphasize that when approximately 67% of the azocarbinol has exchanged with acetone-D₆, less than 4% of the azocarbinol has undergone decomposition.

The data obtained for the rate constants for exchange (E) as well as decomposition (D) for various initial concentrations of the azocarbinol are presented in Table 30. Pairs of data are presented in the Table. The first of each pair (ie. 6a-9a) represents the combined

Table 30. NMR kinetic data on the rate constant for decomposition and exchange reactions					
# ^a	[155e]	[TEMPO]	[acetone-D ₆]	Reaction mode ^b	Rate constant k x 10 ⁵ s
6a	0.223	0.190	13.3	D + E	6.56
6b	0.223	0.190	13.3	D	0.363
7a	0.274	0.158	13.2	D + E	6.21
7b	0.274	0.158	13.2	D	0.382
8a	0.182	0.105	13.4	D + E	5.61
8b	0.182	0.105	13.4	D	0.336
9a	0.091	0.053	13.6	D + E	5.38
9b	0.091	0.053	13.6	D	0.400

^aThese numbers refer to the corresponding best fit lines given in Fig. 10

^bD + E stands for the disappearance of the starting material as a result of both decomposition (D) and exchange with acetone-D₆ reactions (vide infra)

decomposition and exchange (D + E) reactions, and the rate constant is calculated from the increase in signal intensity of acetone (at $\delta = 2.1$ ppm) with time. The second of each pair (ie. 6b-9b) represents the decomposition (D) of the azocarbinol to radical products, and the rate constant for that is calculated from the increase in signal intensity at $\delta = 1.1$

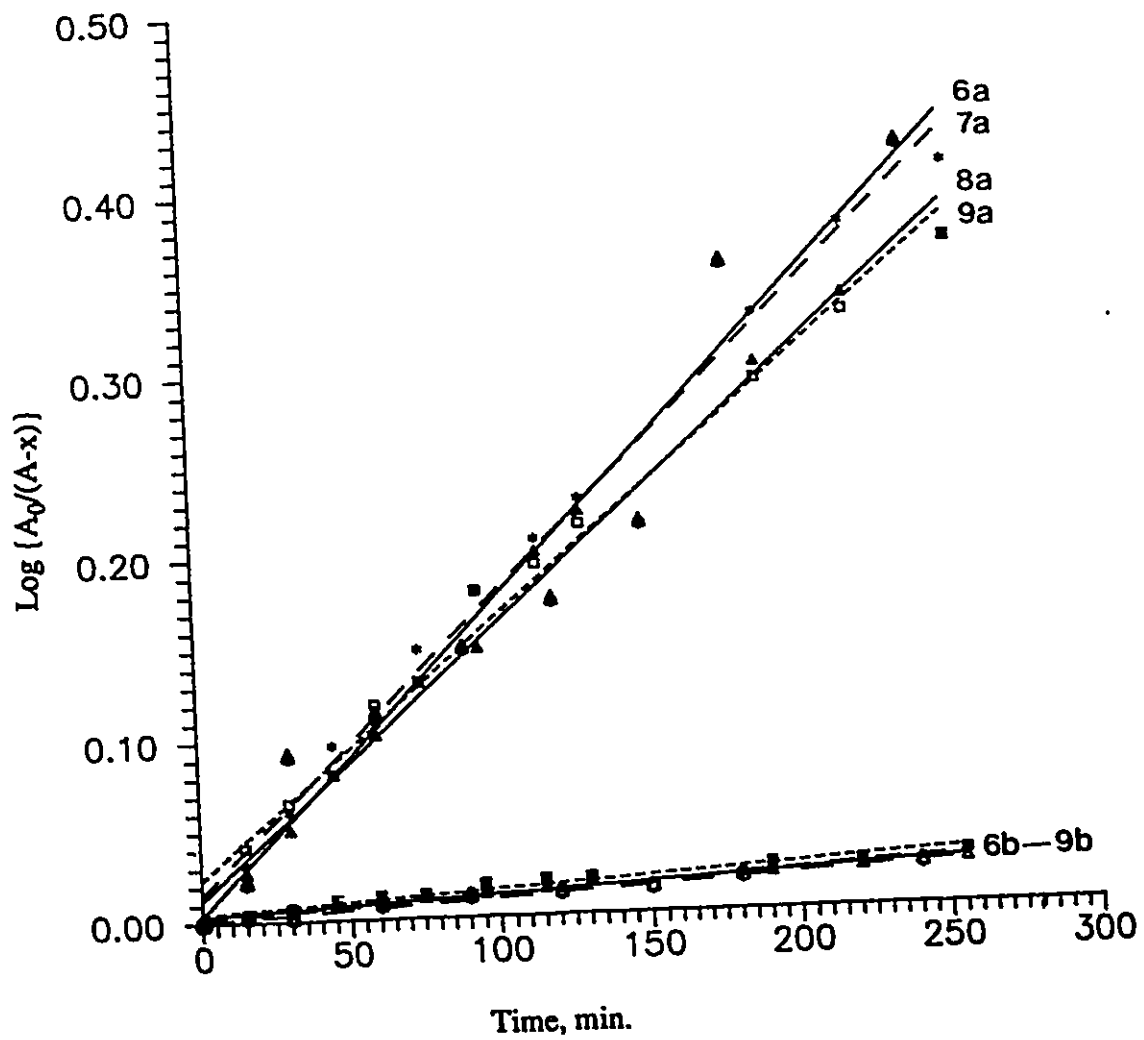


Fig. 10. NMR Kinetics of the Dissociation of 155e in acetone-D₆ at 80°C (see full data and individual linear plots in the *Appendix*)

ppm due to the product **202**, for reasons explained earlier.

Several important observations can be made from the data in Table 30. The most striking observation is that the rate constant for the decomposition of the azocarbinol at 80°C in acetone-D₆ is extremely small ($3.7 \pm 0.2 \times 10^{-6} \text{ s}^{-1}$). This is complementary to the result ($k = 3.5 \times 10^{-6} \text{ s}^{-1}$) obtained from the UV kinetic study of the decomposition of **155e** in the same solvent at the same temperature (see Table 29). The rate constant for the disappearance of the gem-dimethyl signal of **155e** at δ 1.47 ppm is due to the combined decomposition and the exchange reactions. The sum of the pseudo first order rate constants for the exchange (k_E) and the first order rate constant for the decomposition (k_D) together is given as the observed rate constant in the last column for 6a- 9a. An average value for the above rate constant ($k_{\text{obs}} = k_D + k_E$) is estimated as $6.19 \pm 0.57 \times 10^{-5} \text{ s}^{-1}$, from which the pseudo first order rate constant (k_E) for exchange of **155e** with acetone-D₆ at 80°C can be calculated (eq.159). The second order rate constant for the exchange reaction in neat acetone (concentration 13.4 M) becomes $(5.82 \times 10^{-5}) / 13.4 = 4.34 \times 10^{-6} \text{ M}^{-1} \text{ s}^{-1}$.

$$[159] \quad k_E = k_{\text{obs}} - k_D = 6.19 \times 10^{-5} - 3.70 \times 10^{-6} = 5.82 \times 10^{-5} \text{ s}^{-1}$$

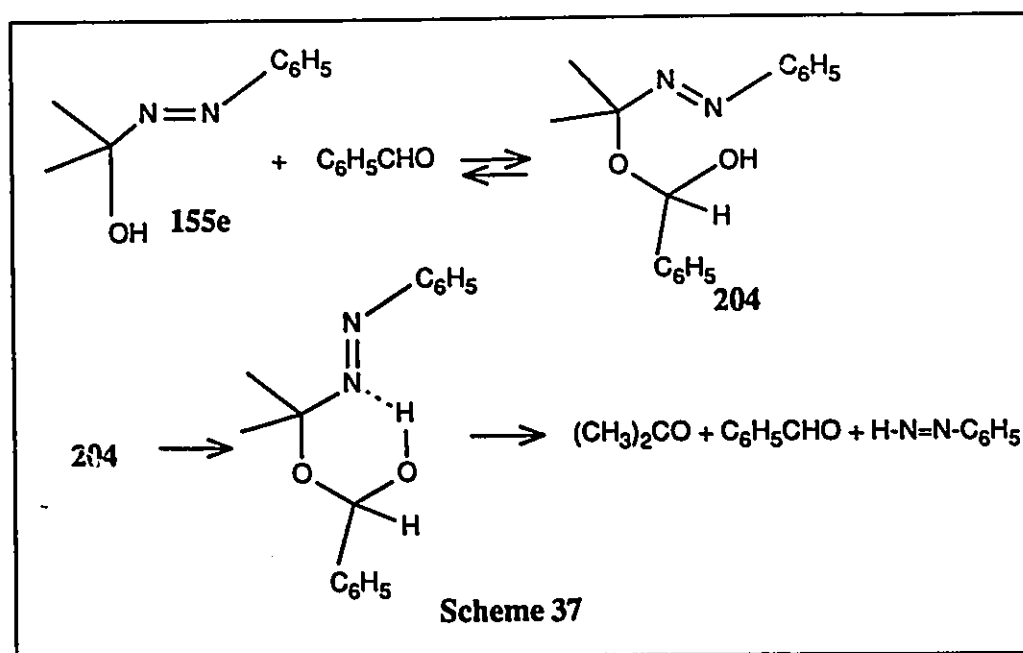
The possibility that the decomposition is second order in **155e** could be ruled out: a three-fold increase in the concentration of **155e** did not alter the decomposition rate constant or the combined rate constant, $k_D + k_E$.

(ii) The influence of aldehydes on the decomposition of **155e**

The next step in the mechanistic investigation was to establish the influence of aldehydes in the decomposition of the azocarbinol. It was already demonstrated by Warkentin et. al.²³³ that benzaldehyde enhances the decomposition of the azocarbinol in

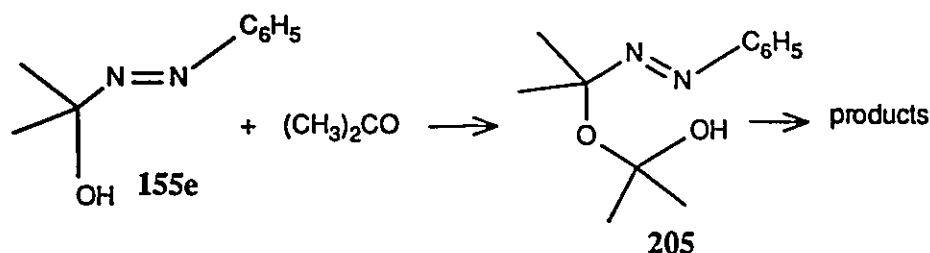
non-polar solvents like benzene. But the observed first order dependence of the decomposition rate constant on the benzaldehyde concentration could not be easily explained. They strongly believed that there is a direct reaction between the azocabinol and the aldehyde probably prior to the decomposition step.

One possible direct reaction is the formation of a hemiacetal **204**. Such an intermediate might decompose fast by a concerted process, such as that shown in Scheme 37.



If the above process is operating, then the question arises as to why acetone does not increase the rate of decomposition by the formation of a hemiketal, **205**. The logical explanation could be that aldehydes react faster than ketones especially when the alcohol group is hindered as in **155e**.

NMR kinetic studies on the influence of benzaldehyde in the presence of TEMPO in acetone- D_6 were carried out. There are two obvious reasons for choosing the above condition for the kinetic studies. First of all, TEMPO is known to inhibit the induced



radical chain decomposition of azocarbinols and, therefore, the observed kinetics is mainly due to reactions presented in Scheme 36. At the same time, the decomposition rate constant ($3.7 \times 10^{-6} \text{ s}^{-1}$) for the azocarbinol in acetone- D_6 in the presence of TEMPO is known. Therefore, any increased rate constant for the decomposition in the presence of benzaldehyde would clearly demonstrate that benzaldehyde is directly involved in the decomposition. The data are summarized in Table 31.

Thermolysis of 155e in 0.19 M benzaldehyde in acetone-D₆ at 80°C gave a rate constant for the combined exchange and decomposition as $k_E + k_D = 8.21 \times 10^{-5} \text{ s}^{-1}$. The rate constant for the decomposition alone, calculated by the procedure described previously, gave $k_D = 1.39 \times 10^{-5} \text{ s}^{-1}$. As already seen, the rate constant for decomposition in acetone-D₆ in the absence of benzaldehyde is $3.7 \times 10^{-6} \text{ s}^{-1}$. Thus, a rate enhancement of 3-fold or more due to the presence of 0.19 M benzaldehyde is indicated. A 3-fold increase in the rate constant for the decomposition in the presence of a low concentration (0.19 M) of benzaldehyde clearly demonstrates some sort of direct reaction.

Since we are dealing with a very complex kinetic process, the rate constants mentioned in the above paragraph are only of qualitative significance. As I have already explained, the decomposition rate constant has been calculated based on the increase in concentration of the radical adduct (202) with TEMPO. It is not easy to distinguish between the radical formation by the homolytic cleavage of the azocarbinol (Scheme 35) and that by the possible decomposition of the 1,2-diazene (195) formed as a result of the

Table 31. Influence of benzaldehyde on the rate constants for exchange and decomposition reactions of the azocarinol, 155e						
# ^a	[155e]	[TEMPO]	[C ₆ H ₅ CHO]	[CD ₃ COCD ₃]	Reaction mode ^b	Rate constant x 10 ⁵ , s ⁻¹
10a	0.089	0.059	0.19	13.2	D + E	8.21
10b	0.089	0.059	0.19	13.2	D	1.39
11a	0.077	0.051	1.39	11.5	D + E	13.80
11b	0.077	0.051	1.39	11.5	D	7.30 ^c
12a	0.119	0.000	0.00	13.6	D + E	8.90
12b	0.119	0.000	0.00	13.6	D	0.27

^aThese numbers refer to the corresponding best fit lines in Fig.11.

^bD + E stands for the disappearance of the starting material as a result of both decomposition (D) and exchange with acetone and with benzaldehyde

^cThe rate constant was calculated for the initial stages of decomposition only (taking the first three points)

rearrangement of the 1,1-diazene (197) intermediate (scheme 36). Therefore, the decomposition rate constant (k_D) can be thought of as the sum of all the rate constants by which radicals are formed under the experimental condition.

In Scheme 36, the rate of disappearance of the azocarinol is mainly due to the rate of exchange with acetone and to reaction with the added benzaldehyde. If we assume that eq.155 is valid for reaction in excess acetone-D₆, then we should expect to get an enhanced rate of disappearance of 155e in the presence of small amounts of benzaldehyde, since the denominator, $k_{-1}[>=O] + k_2[C_6H_5CHO]$, becomes approximately constant, K,

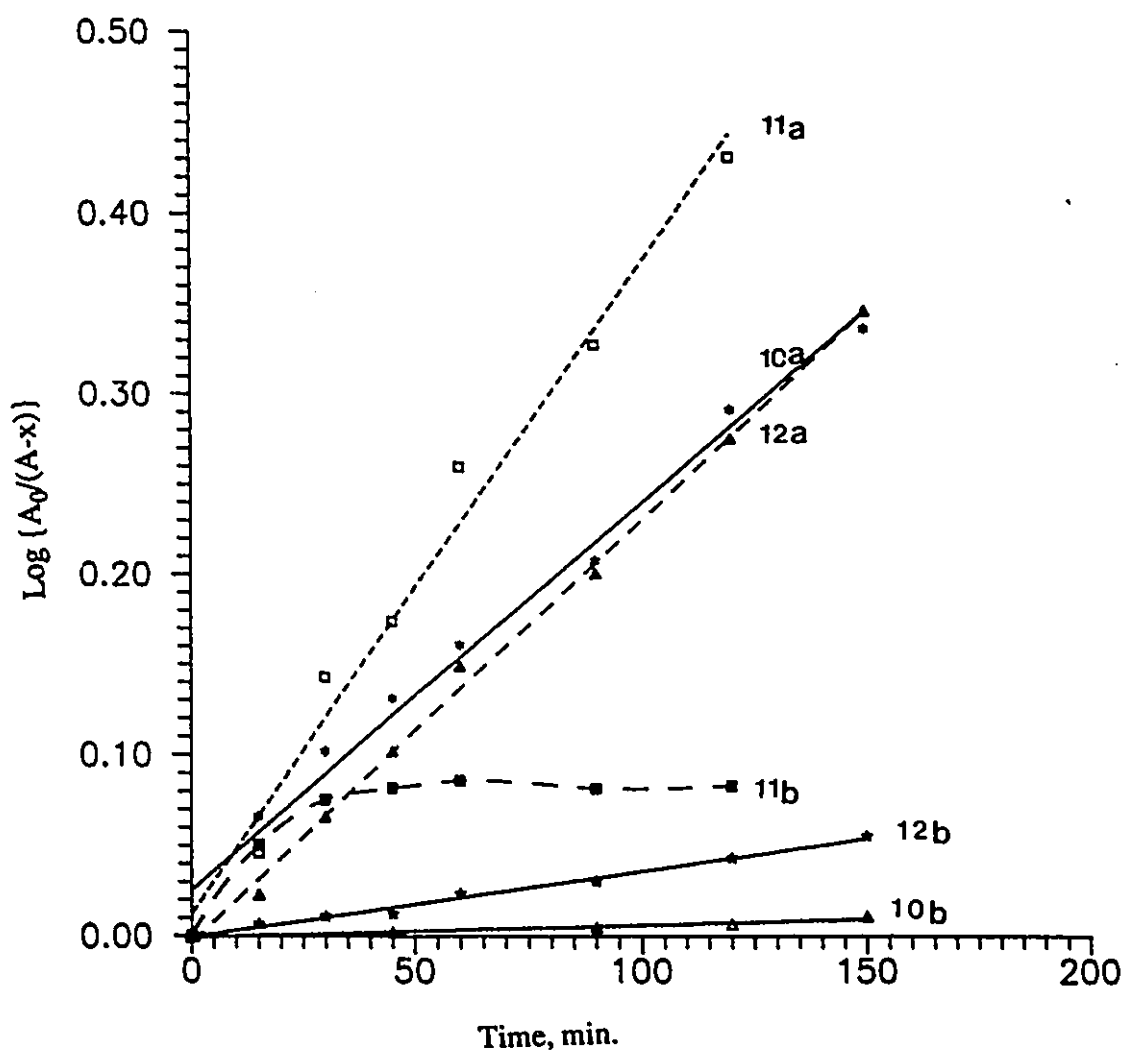


Fig. 11. NMR Kinetics of the Effect of Benzaldehyde on the Dissociation of 155e in Acetone- D_6 at 80°C (see full data and individual linear plots in the *Appendix*)

(assuming that $k_{-1} [>=O] \gg k_2 [C_6H_5CHO]$), and the equation simplifies to eq.160. This is

$$\begin{aligned}
 [160] \quad \frac{-d [155e]}{dt} &= \frac{k_1 [155e] \cdot k_2 [C_6H_5CHO]}{K} \\
 &= K' [155e] [C_6H_5CHO], \text{ where } K' = k_1 k_2 / K
 \end{aligned}$$

not what is observed from the data given in Table 30. If we subtract the rate constant (k_D) for decomposition (leading to radical products) from the corresponding value for the combined $k_E + k_D$, it is easily deduced that the exchange rate constant is practically unaffected by the added aldehyde. Therefore it is clear that the kinetic treatment, as derived from Scheme 36, is not sufficient to explain the influence of benzaldehyde on the rate of exchange reactions.

A closer look at the result in Table 31 reveals that the rate of decomposition has increased from $1.4 \times 10^{-5} \text{ s}^{-1}$ to $7.3 \times 10^{-5} \text{ s}^{-1}$ by a 7-fold increase in the benzaldehyde concentration. If we subtract, from the above rate constants, the rate constant for decomposition ($0.4 \times 10^{-5} \text{ s}^{-1}$) in the absence of any added benzaldehyde, then the increase in first order rate constants in the presence of 0.19 M and 1.39 M benzaldehyde comes to $1 \times 10^{-5} \text{ s}^{-1}$ and $6.9 \times 10^{-5} \text{ s}^{-1}$, respectively. That is, the rate of decomposition is first order in benzaldehyde concentration. The second order rate constant calculated from the above data are 5.2×10^{-5} and $4.9 \times 10^{-5} \text{ M}^{-1} \text{ s}^{-1}$, respectively.

The above results cannot be explained fully by the sequence of reactions represented in Scheme 36. Therefore, the obvious choice is to invoke a direct reaction such as that in Scheme 37, where the direct reaction between the azocarbinol and the aldehyde leads to the formation of the 1,2-diazene, which is known to generate radicals in solution. At the same time, however, the unimolecular decomposition represented by Scheme 36 may also be operating, and the exchange reaction observed even in the

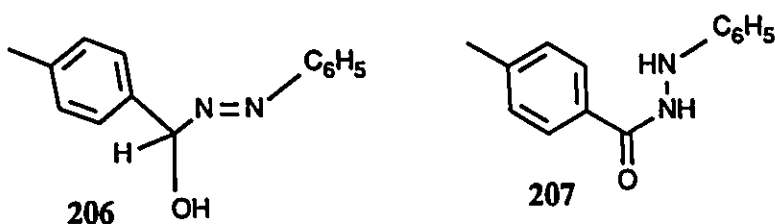
presence of benzaldehyde can be easily explained by such a process. If the above argument can be proved beyond doubt, then the answer to the whole mechanistic problem is very clear. Under neutral conditions, the azocarbinol **155e** decomposes reversibly to acetone and the 1,1-diazene. The reaction between acetone and 1,1-diazene is extremely fast and therefore the steady-state concentration of 1,1-diazene is extremely small, especially in excess of acetone. The 1,1-diazene can rearrange to the 1,2-diazene, which can undergo bimolecular reactions giving phenyl radicals and products derived from them. The fact that the rate of decomposition, as calculated from the radical derived products, is small in acetone- D_6 leads to the conclusion that 1,2-diazene is the major radical source and that its concentration in acetone- D_6 is probably small. In the presence of benzaldehyde, 1,2-diazene is formed from the azocarbinol via the hemiacetal and therefore an increased rate constant is observed for the decomposition.

We are unable to provide any direct evidence for the formation of any hemiacetal of the type **204**. The formation of **204** from **155e** and benzaldehyde is expected to result in a change in the methyl signal region of the NMR spectrum, since the methyl group of **204** is apparently different from the methyl group of **155e**. However, even in the presence of 1.39 M benzaldehyde (in acetone- D_6), the azocarbinol **155e** (0.077M) did not give any new methyl signal in the "gem dimethyl" region. However, it was found that the relatively sharp OH peak of **155e** at δ 4.9 ppm was broadened and was integrated to less than half of a proton in that region. Since there is no other compelling evidence to believe that this reduction in intensity is due to a hemiacetal formation, we attribute this to the probable exchange with D_2O present in acetone- D_6 , which has already been mentioned before.

Another experiment was also conducted to prove whether hemiacetal formation was real or not; but the outcome was not conclusive. A degassed mixture of the azocarbinol and 4-methyl benzaldehyde in benzene- D_6 in an NMR tube was allowed to thermolyze in the cavity of an NMR probe (at $35 \pm 1^\circ C$) and the progress of the reaction

was monitored by taking the NMR spectra at 5 minute intervals. No new signals (except for the one at 2.1 ppm, presumably due to acetone) at or around the aldehyde-methyl region (1.95 ppm, relative to benzene at 7.16 ppm) was visible at least for the first 15 minutes. Another reaction done at a higher temperature (80°C) showed a different pattern. A weak signal at 2.10 ppm present initially in the reaction mixture was found to increase in intensity when the NMR tube was placed in a constant temperature bath at 80°C. The above signal was confirmed as due to acetone, by adding small amount of authentic acetone and observing an increase in the corresponding signal intensity. Thermolysis at 80°C for 15 minutes resulted in 60% decomposition of the azocarbinol. A reduction in intensity for the phenyl protons of the azocarbinol was accompanied by the increase in intensity for a new singlet at 7.16 ppm due to benzene. After 30 minutes of thermolysis at 80°C, there was only 17% of the azocarbinol left undecomposed.

Two weak signals at around 2.12 and 2.15 ppm, amounting to approximately 5% of the aldehyde-methyl signal were also observed. Even though their total intensity remained approximately constant at 5%, their relative intensity changed from 1:1 after 15 minutes to 1:1.3 after 30 minutes at 80°C. The above signals are probably due to the azocarbinol **206** and the hydrazide **207**.



A mixture of 20 μL (~22 mg, .134 mmol) of the azocarbinol and 20 μL (~20.4 mg, .17 mmol) of 4-methyl benzaldehyde in non-degassed benzene- D_6 were allowed to react at room temperature. The rate of decomposition was slow, when compared with the one at 80°C. Only about 28% of the azocarbinol was found to decompose in 10 hr at room

temperature ($22 \pm 2^\circ\text{C}$). Benzene and acetone were the major decomposition products. As in the previous case, two weak signals, very close to but downfield from the methyl signal (δ 1.95 ppm) of the aldehyde at δ 2.15 and δ 2.12 ppm were found to increase with time. When the NMR spectrum of the sample was taken after 20 hr (during which time it was 50% decomposed) the signal at δ 2.15 ppm was integrated to 15% of the methyl signal of tolualdehyde. A new singlet peak observed at 6.35 ppm corresponds well for a CO-NH group, probably of the hydrazide 207.

The failure to observe any hemiacetal intermediate in the reaction mixture does not necessarily imply that such an intermediate is not formed. One possibility is that it is a highly unstable intermediate and that its steady state concentration in solution is very small.

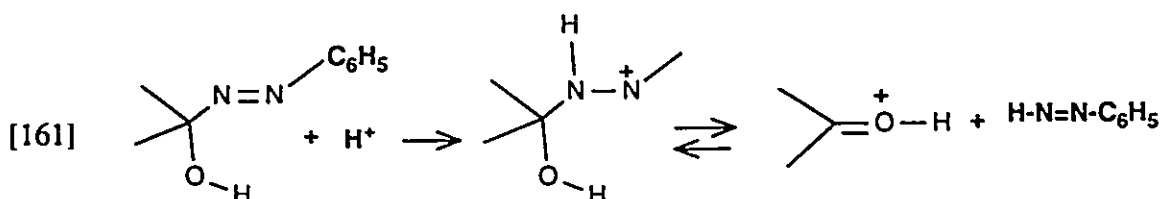
(iii) The influence of acids on the rate of decomposition of 155e.

The effect of small amounts of acids on the rate of decomposition of 155e was also tested. Small amounts of $\text{CF}_3\text{CO}_2\text{H}$ (2 - 4 μL , 0.026 - 0.052 mmol) added to a solution of 155e (~ 11mg, 0.067 mmol) in 0.4 mL of benzene- D_6 greatly enhanced its rate of decomposition even at room temperature ($t_{\frac{1}{2}} = 2$ to 10 min.) In all cases benzene was formed almost quantitatively.

However, the addition of 4 μL (~ 5.92 mg, .052 mmol) of $\text{CF}_3\text{CO}_2\text{H}$ to a solution of 155e (~11 mg, 0.067 mmol) in 0.4 mL acetone- D_6 did not cause any increased rate of decomposition, as judged by the benzene formed in the reaction. A decrease in the methyl signal intensity of 155e was compensated by a corresponding increase in the acetone-methyl signals. The above mentioned process could be easily identified as due to the exchange of acetone- D_6 with 155e, since the signal intensity and also the pattern of the signal in the phenyl region remained identical to the starting azocarbinol spectrum.

It was also surprising to observe that even though the solution was not degassed,

the formation of benzene, a product of decomposition, was extremely slow. The amount of benzene formed in a 10 hr period was less than 5%. If we assume that the function of acid is to increase the rate of formation of 1,2-diazene as given in eq.161, then the fact that



oxygen, which is capable of inducing radical chain decomposition of 1,2-diazene to benzene, did not increase the rate of decomposition of the azocarbonyl suggests that the steady state concentration of the diazene was not increased greatly by the added acid. The reason could be that the rate constant for the backward reaction was also enhanced to the same extent, as the increase in the rate constant for the forward reaction. Or, in other words, the acid acts as a catalyst for both the forward and the backward reactions.

The above experiment strongly suggests that the increased rate constant for the decomposition of the azocarbonyl in acetone-D₆ in the presence of benzaldehyde is not due to any trace amounts of benzoic acid, which could be present as impurity (even though care was taken to make sure that the aldehyde was free from any acid, and the distillation as well as transfer of the aldehyde to the NMR tube prior to sealing was done in an atmosphere of nitrogen). If that was the case, we would only see an increase in the exchange rate constant while the decomposition rate constant remains approximately constant. Therefore it has become more evident that the function of benzaldehyde is to increase the rate of formation of 1,2-diazene.

1.3.3 ESR kinetics

In order to verify the observed influence of benzaldehyde on the rate constant for the decomposition of azocarinols, the following esr kinetic studies were made. The disappearance of the esr signal of TEMPO during thermolysis of the azocarinol 155e in acetone-D₆ or in acetonitrile solvent containing TEMPO was monitored by integrating the esr signal at suitable time intervals. The time taken for the disappearance of half of the esr

Table 32. Half life for the disappearance of TEMPO esr signal by the decomposition of 155e, in the presence and absence of C ₆ H ₅ CHO						
# ^a	[155e]	[TEMPO]	[C ₆ H ₅ CHO]	[Acetone-D ₆]	Reaction mode	t _{1/2} ^a (min)
13	0.068	0.046	0.47	0.47	D ^b	48
14	0.062	0.042	1.28	1.28	D	16
15	0.072	0.048	0.00	13.6	D	> 10 hrs
16	0.088	0.045	0.00	0.00 ^c	D	38

^a Half life for the disappearance of TEMPO, corrected to the nearest whole number

^b D stands for decomposition of the azocarinol leading to radical products

^c The solvent used is acetonitrile

signal intensity (t_{1/2}) was estimated from a plot of % signal intensity vs. time of TEMPO (see Fig.12). Assuming a first order dependence for the disappearance of the esr signal, approximate rate constants were calculated. The data are summarized in Table 32.

The observation from the esr kinetic study is complementary to the results from UV and NMR kinetics. First of all, the UV kinetic study (see Table 29) indicated that the rate constant in acetone is 50 times lower than that in acetonitrile (from entry #3 and #6 of

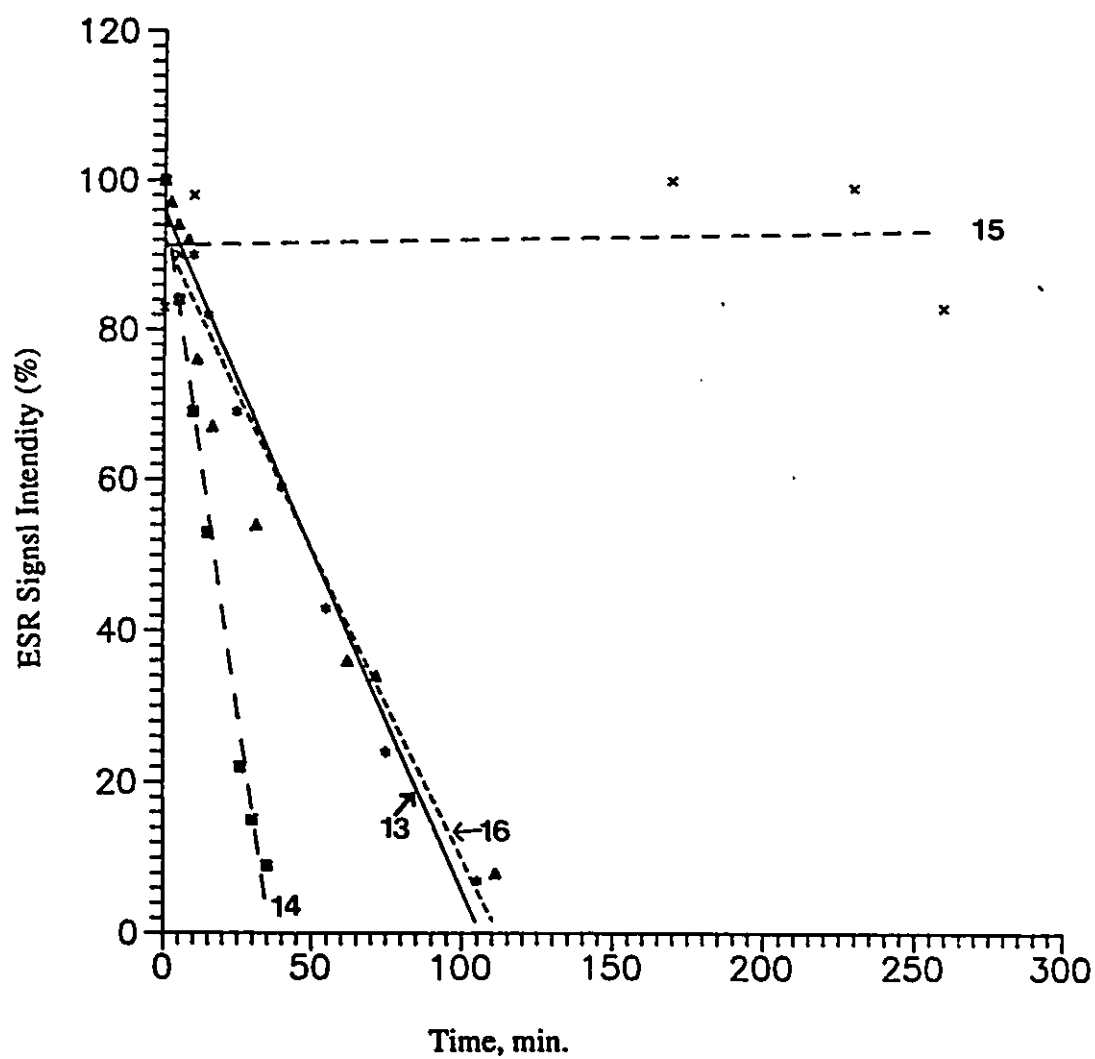


Fig. 12. Kinetics of the Disappearance of TEMPO esr Signal by Decomposition of 155e in Acetone-D₆ in the Presence and in the Absence of Benzaldehyde (see full data and individual linear plots in the *Appendix*)

Table 29). A similar trend is observed in the half lives for the disappearance of the TEMPO signals in the esr experiment (from entry #15 and #16 in Table 31), in which case an increase in half life of greater than 94.7 (3600/38) is indicated in favour of reaction in acetone-D₆. Similarly, a 3-fold reduction in the half life was observed (cf. entry #13 and #14, Table 32) for an approximately 3-fold increase in the benzaldehyde concentration. This is exactly what we observed earlier in the NMR kinetic study.

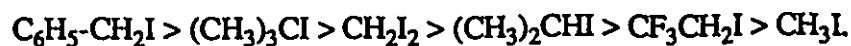
2.4.0 CONCLUSION

The rearrangement of cyclopropylmethyl radical to but-3-enyl radical was used as the 'clock' to determine rate constants for fast bromine and iodine abstraction reactions.

The reactivities of polyhalomethanes such as bromotrichloromethane, bromoform, and dibromochloromethane toward cyclopropylmethyl radical indicate that the reactivity depends on the number of electron-withdrawing substituents and also that the contribution by a more electronegative Cl atom is larger than that by a less electronegative Br atom indicating a possible polar transition state.

The reactivities of cyclopropylmethyl, butyl, and phenyl radicals toward bromotrichloromethane were also determined. It was observed that the reactivities of relatively unhindered radicals such as the above radicals toward BrCCl_3 span only a narrow range.

Cyclopropylmethyl was also found effective for measuring rate constants for iodine abstraction from various iodo compounds. The reactivity order at 80°C for various RI is -



The rate constant for Cl abstraction from CCl_4 was determined using the 5-hexenyl radical clock.

The rate constant for spin-trapping of cyclopropylmethyl radical by 1-methyl-4-nitroso-3,5-diphenyl pyrazole was estimated at various temperatures and the Arrhenius parameters were determined. Application of this useful spin trap is therefore extended.

EXPERIMENTAL

3.0.0. GENERAL

Proton magnetic resonance (^1H nmr) spectra were recorded on either a Varian EM-390, a Bruker WP-80, a Bruker WM-250, or a Bruker AM-500 nmr spectrometer. Tetramethylsilane (TMS) was used as the internal reference in all cases. The solvents used were either hexafluorobenzene or deuteriochloroform (CDCl_3).

The ^{13}C nmr spectra were recorded either on the Bruker WP-80 instrument, a Bruker WM-250, or a Bruker AM-500 nmr spectrometer. CDCl_3 was used as the solvent, except as noted.

Mass spectra (high and low resolution) were recorded on a VG7070 mass spectrometer (VG Micromass, Altricham, U.K.). Samples were introduced through a direct insertion probe system or through a gas chromatographic column via a jet separator. The ion source temperature was 200°C , and the electron energy 70 eV with an emission of 100 μA . The data were acquired and processed with a VG 2035 data system.

Melting points were determined on a Thomas Hoover capillary melting point apparatus and are uncorrected.

UV spectra were recorded on a Hewlett Packard 8451A diode-array spectrophotometer.

Electron spin resonance spectra were recorded on a Bruker ER100D spectrometer equipped with a TE_{102} rectangular cavity and operating normally at a frequency of 9.6 GHz.

The gas chromatographic analysis were done on a Varian VISTA 6000 instrument equipped with an off-column flash injector and a flame ionization detector (FID) at 300°C .

Columns and temperature programs are described under the section on *Product Analysis* below. Semi-preparative GC was performed on a Varian Aerograph A90-P3 instrument with a thermal conductivity detector (TCD) at 300°C and an off column flash injector at 250°C. The column (6 ft x 1/4 in I.D., steel) was packed with 10% OV-17 on Chromosorb W, 80/100 mesh. The carrier gas was helium at a flow rate of 20 mL/min.

Chemicals were purchased from Alrich Chemical Co., (Milwaukee, Wisconsin) and chromatographic materials were obtained from Chromatographic Specialties (Brockville, Ontario).

The chemicals were used without purification, unless otherwise noted. Solvents were mostly glass-distilled and stored, in some cases, over molecular sieves 4A.

3.1.0. SYNTHESIS

Cyclopropylmethyl tosylate

To 14.5 g (0.20 mol) of cyclopropylmethanol was added 42 g (0.22 mol) of p-toluene sulfonyl chloride, with ice-cooling and in an atmosphere of dry N₂. To the cold and well-stirred solution was added dry pyridine (48g, 0.6 mol) over a period of one hr and the resulting solution was kept at 0-5°C for two hr. After overnight storage in the freezer at about -10°C, the reaction mixture was acidified with ice-cold, 10% HCL and extracted three times with ether (50 mL). The combined ether fraction was washed once with 10 mL of saturated solution of NaCl in ice-water. The ether layer was then dried over anhydrous magnesium sulfate and the solvent was evaporated to yield crude cyclopropylmethyl tosylate (31 g, 68.5%).

Cyclopropylmethyl hydrazine (152a)

Cyclopropylmethyl tosylate (11.3 g, 0.05 mol) was added during one hr. to a stirring, ice-cold solution of hydrazine hydrate (50 g, 1 mol) in ethanol (25 mL). The

temperature was then allowed to rise to 20° where it was kept for two hr before it was raised to 40° and kept at that temperature for two hours. The solution was allowed to stand overnight at room temperature before the bulk of the ethanol was taken off with a rotary evaporator. Continuous extraction of the residual liquid with ether for three days, drying of the ether extract with MgSO_4 , and evaporation of the solvent yielded crude cyclopropylmethyl hydrazine (4.0 g, 92%) as a syrupy liquid which was used directly for the next step.

Cyclopropylmethyl hydrazone of acetone (153a)

To crude cyclopropylmethyl hydrazine (4.0g, 0.046 mol) in benzene (20 g, containing 5 g anhydrous potassium carbonate) was added, dropwise and with stirring, 10 g of acetone in 15 min. The resulting mixture was shaken at room temperature in an atmosphere of N_2 for one hour before the temperature was raised to the reflux temperature for another hour. The mixture was cooled and dried over K_2CO_3 . Filtration and evaporation of the solvent left crude hydrazone (3.1 g) as a colourless viscous liquid which was fractionally distilled. Acetone cyclopropylmethyl hydrazone (2.0 g, 35%) boiling at 43-45°C (0.5 Torr) was collected in a small round bottomed flask and was kept glass-stoppered in the fridge, after the air inside the flask had been flushed out with nitrogen.

Butyl hydrazine

1-Bromobutane (13.7 g, 0.1 mol) in 10 mL absolute ethanol was added to a well-stirred solution of hydrazine hydrate (75 g, 1.5 mol) in 25 mL of ethanol at 20°C. The resulting solution was kept stirring at room temperature for 1 hr before the temperature was raised to 40°C where it was kept for another 2 hrs. The solution was extracted continuously with 200 mL of ether for two days, the extract dried over MgSO_4 , filtered, and the solvent evaporated off to yield the crude hydrazine (7.3 g, 83%). The crude

product was used directly for the next step.

Acetone (1-butyl)hydrazone (153d)

Butyl hydrazine (7.0 g, 0.079 mol) was added dropwise, with stirring, to 20 g of acetone in 10 min. The solution was kept stirring, under an atmosphere of nitrogen, for 1 hr before the temperature was raised to the reflux temperature for 1 hr. The mixture was cooled, dried over MgSO_4 (20 g), filtered, rinsed the solid on the filter with 10 mL of dry ether and the solvent was evaporated off to give the crude hydrazone, 153d. Distillation under reduced pressure (1 Torr) gave 153d (9.2 g, 91%) collecting between 40 - 45°C.

Deuterium labelled cyclopropyl methanol, $c\text{-C}_3\text{H}_5\text{-CD}_2\text{OH}$

To a stirred solution of cyclopanecarboxylic acid (8 g, .093 mol) in 150 mL of dry ether (dried over LAH and freshly distilled), under an atmosphere of N_2 , in a Dry Ice-acetone bath, 5g (.119 mol) lithium aluminum deuteride was added in several small portions over a period of 15 min. The mixture was kept stirring at that temperature for 2 hrs before the temperature was slowly raised to 0°C at which it was kept for another hr. Cold water (5 mL) was added drop by drop, with constant stirring, followed by sulfuric acid (2 M) until acidic. The ether layer was separated, and the aqueous phase was extracted with ether (3 x 50 mL). The combined extract was dried over MgSO_4 , and on evaporation yielded 6.3 g (85%) of the title compound which was distilled under reduced pressure (~ 15 Torr). The collected fraction distilled between 50-53°C (5.8 g, 78%) as the pure product.

Deuterium labelled cyclopropylmethyl hydrazine, $c\text{-C}_3\text{H}_5\text{-CD}_2\text{NHNH}_2$ (152b)

A procedure similar to the one used for 152a was followed. First, the tosylate, $c\text{-C}_3\text{H}_5\text{-CD}_2\text{-O-SO}_2\text{-(C}_6\text{H}_4\text{)-Me(p)}$, was prepared from the corresponding alcohol ($c\text{-C}_3\text{H}_5\text{-CD}_2\text{OH}$) by a procedure similar to that for cyclopropylmethyl tosylate. From 5 g

of the alcohol, 13.5 g (87%) of the tosylate was obtained.

The tosylate (13 g, .057 mol) was added slowly to a stirred solution of hydrazine hydrate (60 mL, 1.2 mol) in 25 mL absolute ethanol at 0°C. By following the work up procedure used for 152a, 2.5 g (50%) of the crude hydrazine 152b was obtained, which was used without purification for making the hydrazone 153b.

Deuterium labelled acetone cyclopropylmethyl hydrazone, 153b

Condensation of the hydrazine, 152b (2.5 g, .028 mol) with acetone (10 g) in benzene (20 mL) in presence of anhydrous potassium carbonate (5 g) at room temperature followed by filtration and evaporation of the solvent gave 2.6 g of the crude hydrazone 153b. Fractional distillation under reduced pressure (1 Torr) gave pure hydrazone (1.2 g, 33%) distilling between 46-48°C.

Acetone phenylhydrazone

Phenylhydrazine hydrochloride (20 g, .138 mol) was placed in a 500 mL round bottomed flask containing 150 mL of ether and 25 g of anhydrous potassium carbonate. Acetone (15.8 g, 0.27 mol) was added to the mixture, in an atmosphere of nitrogen, followed by dropwise addition of 10 mL of water. After the initial vigorous reaction was over, the solution was refluxed for 3 hrs. The mixture was dried over K_2CO_3 (30 g), filtered, and the residue on the filter was rinsed with 2 x 25 mL dry ether. Distillation of the solvent, under nitrogen, gave a pale yellow liquid which was distilled under reduced pressure (1.5 Torr) The collected fraction (12 g, 59%) distilled between 91-92°C as a pale yellow liquid.

Autoxidation of hydrazones (153a-e) to α -hydroperoxydiazenes (154a-e)

Solutions of hydrazones (153a-e) in benzene or in petroleum ether are autoxidized rapidly to α -hydroperoxydiazenes in presence of air or oxygen. All the

α -hydroperoxydiazines (155a-e) in the present study were prepared by the same procedure, which is documented below for the autoxidation of acetone cyclopropylmethyl hydrazone.

Cyclopropylmethyl [1-hydroperoxy-1-methylethyl] diazene (154a)

Acetone cyclopropylmethyl hydrazone (0.5 g, 4.0 mmol) in dry petroleum ether (20 mL, b.p. 40-60°C), cooled in ice and stirred, was exposed to oxygen in a gas system fitted with a gas burette and a mercury manometer. When the uptake of oxygen ceased, the completion of reaction was checked by taking the NMR spectrum of an aliquot, freed from solvent. The two methyl singlets for the hydrazone had completely disappeared. The entire solution was stored in the freezer at -30 °C. The purity of the sample, checked by iodometric titration, was 99.9%

Reduction of α -hydroperoxydiazines (154a-e) to α -hydroxydiazines (155a-e)

α -Hydroperoxydiazines are conveniently reduced to the corresponding hydroxy diazenes by the use of triphenylphosphine (Ph_3P) in petroleum ether or in hexane solvent. This method offers a clean system from which the reduction product can be easily isolated in very good yield. A typical procedure is given below for the cyclopropylmethyl system.

Cyclopropylmethyl [1-hydroxy-1-methylethyl] diazene (155a)

An aliquot containing 2.4 mmol of 154a in petroleum ether was added slowly to a solution of triphenyl phosphine (0.70g, 2.7 mmol) in 12 mL of petroleum ether, cooled to 0-5°C in ice-water. The flask was then kept at ca -5°C overnight, and the precipitated Ph_3PO was filtered off and the solvent distilled off using a rotary evaporator at 20°C. The crude residue was subjected to bulb-to-bulb distillation under high vacuum, from a bulb at room temperature to a receiver in liquid nitrogen. The first fraction was the petroleum ether. The second fraction distilling at 10^{-2} Torr was collected as a colourless oil (0.23 g, 67%).

N-Benzylphthalimide (157)

A method similar to that given in the literature²⁶⁹ was used for the synthesis of 157.

Phthalimide (147 g, 1.0 mol) and anhydrous K_2CO_3 (88 g, 0.6 mol) were ground well in a mortar and the mixture was added to benzyl chloride (253 g, 2 mol) in a 2 litre round bottom flask. The mixture was refluxed for four hours in an oil bath at 190-200°C, after which the excess benzyl chloride was removed by steam distillation. On cooling, the whole solution solidified. The solid was broken into pieces, filtered, washed several times with water until free from carbonate, washed with 200 mL of 60% ethanol and dried. The crude product weighed 180 g (75%), m.p. 100-105°C. About 100 g of this material was used for recrystallization from glacial acetic acid, which gave 70 g of white crystalline solid m.p. 108-111°C. A second recrystallization from the same solvent yielded 52 g. of the *N*-benzylphthalimide which was dried under high vacuum (0.2 Torr) at 40°C. The melting point of this material was 114-115°C (lit. ²⁶⁹, 116°C).

N-benzyl-1,1,3,3-tetramethylisoindoline (158)

A slight modification of a procedure reported by Solomon et. al²⁴⁵ was used.

A solution of methyl Grignard reagent was prepared from methyl iodide (170 g, 1.2 mol) and magnesium turnings (30.5 g, 1.25 mol) in dry ether (600 mL), under N_2 atmosphere. The solution was concentrated by slow distillation of ether under N_2 , until the internal temperature rose to 80°C. About 400 mL of ether had been distilled out. The solution was cooled to 60°C, and 200 mL of toluene was added to it. With vigorous stirring, a solution of *N*-benzyl phthalimide (47.5 gm, 0.2 mol) in 300 mL of toluene was added to the solution at such a rate as to maintain a temperature of 60-65°C. When the addition was complete, the solvent was distilled slowly from the mixture until the temperature reached 108-111°C. The solution was kept refluxing at this temperature for 14

hrs. It was then concentrated to about 200 mL by further solvent distillation, 300 mL of light petroleum ether was added, and the resulting slurry was filtered through celite. The residue was washed with petroleum ether (4 X 100 mL). The combined filtrate, initially yellow in colour, was left open in a wide mouthed filter flask and kept stirring for 2 hr. During this time the solution turned purple in colour and a fluffy purple-coloured material was precipitated. It was kept stirring for one more hour and the solution was filtered through celite again, when a pale yellow solution was obtained. The solution was concentrated on a rotary evaporator, during which time the solution turned purple-brown and finally a thick, brown liquid was obtained (30 g). The residue was dissolved in a minimum quantity of petroleum ether and transferred onto a short column (6") of basic alumina (60 gm) of activity 1, and the column was eluted with petroleum ether. The very pale yellow solution obtained on evaporation gave 22 g (42%) of a pale yellow solid, which on analysis by gc (Column #2, Program #2; see Section on *Product Analysis* below) gave two peaks, one at retention time 17.9 min (81.5%) and another at 19.1 min (18.5%), which were later identified as 158 and 159, respectively. Recrystallisation of this sample once from methanol gave a white crystalline solid, which by gc analysis was found to contain ca 3% of 159 and 97% of 158. A second recrystallisation from methanol gave 158 (6.2 g, m.p. 62-62.5°C), which was found to be 99.8% pure by gc analysis. Concentration of the mother liquor by further evaporation of solvent gave another crop of white crystals (5.1 g), which was >99% pure. The spectral data matched with those reported.²⁴⁵

1,1,3,3-Tetramethylisoindoline (160)

A solution of N-benzyl-1,1,3,3-tetramethylisoindoline (5 g, 18.9 mmol) in glacial acetic acid (100 mL) was taken in a hydrogenation bottle, 1 g of Pd/C was added to it and the solution was kept for hydrogenation at 30 lb/in², for four hours. The solution was filtered and the solvents were distilled off under reduced pressure, at about 30-40°C. About 4 g of a pale yellow liquid was left behind. Crystallization, induced by blowing N₂

gas onto the surface while cooling, gave colorless flaky crystals of **160** (crude). The crystals were dissolved in 20 ml of water and the solution was made alkaline (pH 9) with 10% NaOH. The organic materials were extracted with ether (3 X 50 ml). The combined organic layer was dried over anhydrous MgSO_4 (2 hr), filtered and the filtrate was evaporated to give **160** as colourless crystals (3.1 g, 94%). Gc analysis showed that it was 99% pure; m.p. 35-37°C, (lit.²⁴⁵, 36-38°C from MeOH).

1,1,3,3-Tetramethylisoindolin-2-yloxyl(161)

A solution of 1,1,3,3-tetramethylisoindoline (3 g, 17.1 mmol) was prepared in a mixture of methanol (30 mL) and acetonitrile (2.4mL). Sodium bicarbonate (1.2 g, 14.8 mmol), sodium tungstate (0.18 g, 0.55 mmol), and 30% aqueous hydrogen peroxide (7 mL, 62 mmol) were added to it. The resulting mixture was kept stirring at room temperature and progress of the reaction was monitored by gc. The solution, stirred for 36 hr was found to contain the final product **161** in more than 99% yield by gc analysis. The reaction mixture was diluted with 29 mL of distilled water and the organic materials were extracted with light petroleum ether (3 X 75 mL). The combined extract was dried over MgSO_4 (5g, 6 hrs), filtered, and the solvent was evaporated off. Product **161** was obtained as yellow, spongy, needle-shaped crystals (3.2g, 97%). Recrystallisation from light petroleum ether gave long needle-shaped crystals, m.p. 127-128°C. The compound was found to be 99.8% pure by gc analysis. The spectral data were identical with those reported.²⁴⁵

Iodometric Titration

The purity of α -hydroperoxy diazene (**154a**) was determined by iodometric titration.

A sample of **154a** was freed from petroleum ether (solvent) by blowing N_2 through the solution at 0-5°C. A small amount of **154a** (14.45 mg, 9.15×10^{-5} mol) was accurately

weighed into an iodine-flask. Cold methanol (5 ml) was added into it followed by a small piece of Dry Ice, to expel oxygen. Freshly prepared saturated KI solution (2 mL) and glacial acetic acid (10mL) containing FeCl_3 (ca 0.003%) were added, and the flask was kept stoppered, in the dark, for 10 min. The iodine liberated was diluted with 25 mL of water and was titrated using 0.01 M $\text{Na}_2\text{S}_2\text{O}_3$ solution to the starch end point. From the volume of $\text{Na}_2\text{S}_2\text{O}_3$ used (18.2 ml, 18.3 ml), the purity of the hydroperoxide was calculated (>99%).

3,5-Dibromo-1,1,1-trichloropentane (179)

4-Bromo-1-butene (2.7 g, 0.017 mol), benzoyl peroxide (0.2g, 0.8mmol) and bromotrichloromethane (5.0g, 0.025 mol) were heated in a sealed evacuated tube at 80°C for 4 days. The ^1H nmr spectrum of the resulting solution was nearly free from vinyl proton signals. The product was isolated from a portion of the reaction mixture by preparative tlc (silica gel-60, F_{251} , 1 mm thick, on glass) with petroleum ether (80 parts) and ether (20 parts) as the solvent system. The pure product had $R_f = 0.46$ on silica gel-60 (0.2mm, on plastic), with the same solvent system; ^1H nmr (CDCl_3 , 500 MHz) δ : 2.38 (m, 1H), 2.59 (m, 1H), 3.23 (dd, 1H), 3.52 (dd, 1H), 3.59 (m, 2H), 4.53(m, 1H); ms (ei) m/z : 338, 336, 334, 332, 330(M^+); 301, 299, 297, 295 ($\text{M}^+ - \text{Cl}$); 263, 261, 259 ($\text{M}^+ - 2\text{Cl}$); 255, 253, 251 ($\text{M}^+ - \text{Br}$); 221, 219, 217, 215 ($\text{M}^+ - \text{Br} - \text{Cl}$); 111, 109 ($\text{C}_2\text{H}_4\text{Br}^+$); 77, 75 ($\text{C}_3\text{H}_4\text{Cl}^+$); 40 (100%, C_3H_4^+).

Mixed azine of acetone and cyclopropanecarboxaldehyde

A solution of cyclopropanecarboxaldehyde and acetone hydrazone (1:1) in CCl_4 at room temperature was examined periodically by ^1H nmr spectroscopy. When the aldehyde signal was no longer visible, solid potassium carbonate was added and the supernatant solution was passed through a short column of magnesium sulfate. Evaporation of most of the solvent and chromatography on a rotating disk (Chromatotron apparatus) gave

fractions containing the unsymmetric azine contaminated with symmetric aldazine. The latter was obtained in pure form by preparative tlc (Al_2O_3 on plastic), permitting assignment of the gc signals from the mixture of azines and the assignment of ^1H nmr signals of the mixture. For the mixed azine, ^1H nmr (CDCl_3) δ : 0.67-1.08 (m, 2H, CH_2), 1.53-1.92 (m, 1H, CH), 2.00 (s, 3H, CH_3), 2.03 (s, 3H, CH_3), 7.18 (d, $j = 8$ Hz, $\text{CH}=\text{N}$); gc (conditions: Column 1, Program 1, in *Product Analysis* below) retention time 25.3 min. For the symmetric aldazine, ^1H nmr (CDCl_3) δ : 0.67-1.08 (m, 4H), 1.53-1.92 (m, 2H), 7.35 (d, $J = 8$ Hz, 2H); gc retention time 28.9 min.

2-(1-Butoxy)-1,1,3,3-tetramethylisoindoline (182)

This product of coupling between 86 and butyl radical was prepared by thermolysis of 155d in hexafluorobenzene containing 86. The product 182 was separated from other products of reaction by preparative tlc on silica gel (1 mm) coated glass plates using petroleum ether containing 10% (v/v) ether. The fraction thus obtained was further purified by chromatography on a rotating, alumina coated plate (Chromatotron apparatus) using petroleum ether; ^1H nmr (CDCl_3 , 90 MHz) δ : 0.89 (t, 3H), 1.20-2.67 (m, 16H), 3.8S (t, 2H), 6.96-7.32 (m, 4H); ^{13}C nmr (CDCl_3 , 62.90 MHz) δ : 14.23, 19.92, 23-31 (broad signal for the four methyl groups), 31.67, 67.32, 77.38, 121.61, 127.25, 145.59; ms (ei) m/z : 247 (M^+), 232 ($\text{M}^+ - \text{CH}_3$), 100%, 176 (90%).

3.2.0. THERMOLYSIS

Thermolysis of 155a in polyhalomethanes and in alkyl iodides

Solutions of known quantities (5-10 mg) of 155a in suitable volumes (0.3-0.5 mL) of the halo alkane (or a known concentration of the haloalkane in solvents such as hexafluorobenzene) were mixed in nmr tubes before they were degassed, by two or more freeze-pump-thaw cycles, and sealed under vacuum (10^{-1} - 10^{-3} Torr). The tubes were then

immersed in constant temperature baths for as long as necessary (1-30 days, depending on temperature and nature of the reaction medium) to decompose all of the starting material. The products were then analysed by gc-fid, gc-ms, and nmr. Thermolysis of 155a in bromotrichloromethane, given below, is typical.

Thermolysis of 155a in bromotrichloromethane

Stock solutions of BrCCl_3 in C_6F_6 or in CH_2Cl_2 were prepared. Solutions for thermolysis were prepared by measuring the appropriate volumes of the stock solutions with small pipettes or syringes into nmr tubes, sealed to ground glass joints, and containing known quantities (5-10 mg) of 155a. The contents were freed from dissolved gases prior to sealing by means of several freeze-pump-thaw cycles, care being taken to warm the sample gently, and only until melting was complete. A sealed tube was then heated until starting material could not be detected in the ^1H nmr spectrum. Thermal decompositions at 0°C and 30°C were complete in 10 days and 4 days, respectively. At higher temperatures, 2 days was sufficient.

Thermolysis of 155d and 155e in BrCCl_3 containing 86

Solutions of these substrates and 86 in BrCCl_3 , with or without C_6F_6 , were prepared in volumetric flasks and portions were transferred into small Pyrex tubes for freeze-pump-thaw degassing prior to sealing. The tubes were then placed in a thermostated bath at $80 \pm 0.2^\circ\text{C}$ for four days before they were cut open for gc analysis. The completion of the reaction, or the progress of the reaction, could not be monitored by nmr spectroscopy, because of the paramagnetic species 86. However, from our previous experience¹⁴⁷ that at 89°C complete decomposition of 155a in hexafluorobenzene containing 80 was achieved in two days, four days at 80°C should be more than sufficient for complete thermolysis.

3.3.0. PHOTOLYSIS

Photolysis of 155a in presence of BrCCl₃

Diazenes 155a (10-15 mg) was dissolved in a solution of BrCCl₃ in C₆F₆ or CH₂Cl₂ in nmr tubes. The tubes were sealed after freeze-pump-thaw cycles and were transferred to a quartz Dewar flask containing the thermostating fluid and a magnetic stirring bar. Photolyses with 300nm light were carried out with a Rayonet apparatus. The photolyses were interrupted frequently to check the progress of reaction by nmr spectroscopy and to adjust the temperature so as to maintain a $\pm 1^\circ\text{C}$ or better range. Photolyses were complete (¹H nmr) in 2-3 hrs.

Photolysis of 155c in CCl₄

A solution of 155c (43.0 mg) in carbon tetrachloride was prepared in 1 mL volumetric flask, and shaken for uniform concentration. 300 μL of the solution was transferred to each of three nmr tubes. The tubes were sealed after freeze-pump-thaw cycles under vacuum. Photolysis was carried out in a Rayonet apparatus in exactly the same way as described above for thermolysis in BrCCl₃. Photolysis was complete in 3 hrs.

3.4.0. PRODUCT ANALYSIS

Gas chromatographic analyses were done on a Varian Vista 6000 gc, with a flame ionization detector and an off column flash injector, interfaced to a Varian Vista 402 data processor. The detector temperature was set at 300°C and the injector temperature, 220°C. The carrier gas (N₂) flow rate was 10 mL/min, unless otherwise specified. Different columns and temperature programs used are given below.

Column 1: 8 ft x 1/8 in. glass column packed with OV-17 (3%) on Chromosorb P (AW,

100/120 mesh)

Column 2: 5 ft x 1/8 in. glass column packed with Carbowax 20M (5%) on Chromosorb P (AW, 100/120 mesh)

Column 3: 10 ft x 1/8 in. glass column packed with Carbowax (10%) on Chromosorb P (AW, 100/120 mesh)

Column 4: 7 ft x 1/8 in. glass column packed with OV-17 (3%) on Chromosorb P (AW, 100/120 mesh)

Column 5: 5 ft x 1/8 in. glass column packed with OV-101 (5%) on Chromosorb P (AW, 100/120 mesh)

Program 1: 35°C for 15 min, 10°C/min to 210°C, hold time 15 min.

Program 2: 40°C for 3 min, 5°C/min to 220°C, hold time 10 min.

Program 3: 35°C for 10 min, 10°C/min to 250°C, hold time 15 min.

Specific columns and programs used for the quantitation of products from reactions of CCl_4 with 155c (Column 2, Program 2) and BrCCl_3 with 155a, 155d, and 155e (Column 1, Program 1), and the retention times of important products have been reported.^{147,257}

The products of reactions of iodo compounds, except those from CH_2I_2 , with 155a were analysed using Column 5, Program 3. Retention times (min, in brackets) of starting materials and products in the order of elution are: acetone (2.0), CH_3I (2.5), $\text{CF}_3\text{CH}_2\text{I}$ (3.5), $(\text{CH}_3)_2\text{CHI}$ (10.2), $\text{C}_6\text{H}_5\text{CH}_3$ (14.46), 185 (15.30), 184 (16.73), $\text{C}_6\text{H}_5\text{CH}_2\text{I}$ (25.1).

The products of reaction of CH_2I_2 with 155a were analysed using Column 4, Program 3. The order of elution of components of the mixture (retention time in brackets) was: acetone, co-eluting with CH_2Cl_2 and CH_3I (2.2), 185 (14.10), 184 (16.07), CH_2I_2 (20.3).

The products of reaction of CHClBr_2 with 155a were analysed using Column 5,

Program 3, which gave the following order of elution: CH_2ClBr (not confirmed, 4.70), 177 (10.94), 176 (13.95), CHClBr_2 (16.0).

The reaction mixture from thermolysis of 155a with CHBr_3 was analyzed using Column 4, Program 3. The order of elution of components (rt in brackets) was: acetone (2.0), 177 (7.52) 176 (11.91), CHBr_3 (18.90).

3.5.0. NMR Kinetics.

Stock solutions of TEMPO was prepared in acetone- D_6 . Portions of this solution were syringed into nmr tubes containing known amounts of the azocarinol 155e and other reagents (eg. benzaldehyde) prior to sealing the nmr tube under vacuum (0.1-0.2 Torr). A typical experiment follows.

TEMPO (29.75 mg) was dissolved in 1 mL of acetone- D_6 . The resulting solution (0.30 mL, 0.19 M) was syringed into an nmr tube through a disposable pipette with a drawn capillary end through which 10 μL (11.0 mg) of the azocarinol 155e had already been syringed in. The tube was then sealed after two freeze-pump-thaw cycles under vacuum (0.01 Torr). After thawing and thoroughly mixing the contents, the nmr spectrum was taken as quickly as possible and the tube was then placed in a thermostated bath at 80 (± 0.1) $^\circ\text{C}$. The kinetics of the process was monitored from the decrease in intensity of the nmr signal at δ 1.47 ppm (the gem-dimethyl signal of 155e) by taking the spectrum at 15, 30, and 60 min intervals to a total of 240 min. During this time 64% of the starting material was found to undergo dissociation. The new signal formed at 1.1 ppm, assumed to be due to the radical addition product with TEMPO (*vide infra*) was also integrated, for each time interval, and the rate constant for the homolytic process was calculated from it.

3.6.0. UV Kinetics

Solution (2-3 mL) of known concentration of the azocarbinol 155e in acetonitrile (or in acetone), with or without added TEMPO, were transferred by syringe into a quartz uv cell (10 mm path length) which was sealed on to a 4 inch long pyrex tube with a ground glass joint. The tube was sealed after degassing the solution by freeze-pump-thaw cycles, under vacuum (.01 Torr). The cell was then placed in the cavity of the uv instrument, with a built in thermostatable cavity. Water at 80°C was used as the thermostating fluid. The absorbance (A) at 382 nm was measured at suitable intervals of time. The corrected absorbance $A_t = A - A_\infty$, where A_∞ is the absorbance at infinite time, at time t is related to the absorbance at t=0, ie A_0 , by the expression $\log (A_0/A_t) = (k/2.303)t$, where k is the rate constant for the disappearance of the starting material. The plot of $\log (A_0/A_t)$ vs. t gave a straight line, and the rate constant (k) for the disappearance of the azocarbinol was calculated from its slope = $k/2.303$.

3.7.0. SPIN TRAPPING

A solution of 123 (0.963 M) in benzene was prepared in a 10 mL volumetric flask. Small volumes of this solution were transferred by syringe into vials containing known amounts of solvent-free, deuterium-labelled cyclopropylmethyl radical source, 154b. After mixing, the solutions were transferred into quartz tubes before they were degassed and sealed under vacuum. The tubes were then placed in the previously thermostated cavity of the esr spectrometer. The esr spectrum of the radical adducts were recorded at small intervals of time. The ratio of the cyclopropylmethyl and the butenyl radical adducts were then calculated. Integrating the non-overlapping outside signal of the butenyl adduct (191), which gives rise to a 1:2:1 triplet of a 1:1:1 triplet (vide infra), and subtracting twelve times this value (corresponding to the total intensity due to 191) from the total integral for all the signals from 190 and 191 gives the integral corresponding to 190.

4.0.0.

APPENDIX: RAW KINETIC DATA FOR THE FIRST ORDER PLOTS IN FIG.9-12.

Kinetic data^a for the decomposition of **155e** (0.0116 M) in CH₃CN in presence of TEMPO
(0.029 M) at 80°C (Best fit line #1, Fig.9)

Time t (min)	Absorbance $A_t = A_0 - A_{\infty}$	$\log (A_0/A_t)^b$
0.00	1.06	0.000
30	0.789	0.126
63	0.570	0.267
93	0.414	0.406
130	0.295	0.553
160	0.237	0.648
190	0.171	0.775
220	0.114	0.966
250	0.084	1.097
310	0.068	1.191

^aKinetic data obtained by measurement of UV absorbance at $\lambda = 382$ nm.

^bRate constant calculated from this data is $1.6 \times 10^{-4} \text{ s}^{-1}$.

Kinetic data^a for the decomposition of 155e (0.0116 M) in CH₃CN in presence of TEMPO
(0.029 M) at 80°C (Best fit line #2, Fig.9)

Time t (min)	Absorbance $A_t = A_0 - A_\infty$	$\log (A_0/A_t)^b$
0	2.15	0.000
15	1.97	0.039
45	1.54	0.145
78	1.28	0.224
108	1.02	0.325
268	0.17	1.080

^aKinetic data obtained by measurement of UV absorbance at $\lambda = 382$ nm.

^bRate constant calculated from this data is $1.6 \times 10^{-4} \text{ s}^{-1}$.

Kinetic data^a for the decomposition of 155e (0.0114 M) in CH₃CN in presence of TEMPO
(0.029 M) at 80°C (Best fit line #3, Fig.9)

Time	Absorbance	log (A ₀ /A _t) ^b
t (min)	A _t = A ₀ -A _∞	
0	1.09	0.000
15	0.939	0.064
30	0.807	0.129
45	0.694	0.195
60	0.595	0.262
75	0.510	0.329
90	0.435	0.398
105	0.369	0.464
120	0.317	0.535
135	0.272	0.602
150	0.231	0.672
165	0.196	0.744
180	0.167	0.814
195	0.141	0.887
210	0.120	0.957
225	0.100	1.036
300	0.045	1.383

^aKinetic data obtained by measurement of UV absorbance at $\lambda = 382$ nm.

^bRate constant calculated from this data is $1.7 \times 10^{-4} \text{ s}^{-1}$.

Kinetic data^a for the decomposition of 155e (0.009 M) in CH₃CN in the absence of
TEMPO at 80°C (Best fit line #4, Fig.9)

Time t (min)	Absorbance $A_t = A_0 - A_\infty$	$\log (A_0/A_t)^b$
0	0.64	0.00
20	0.63	0.01
40	0.60	0.03
60	0.54	0.07
80	0.43	0.17
100	0.37	0.23
120	0.32	0.30
140	0.28	0.36
160	0.24	0.43
180	0.20	0.51
200	0.17	0.58
220	0.14	0.66
240	0.12	0.74
300	0.067	1.03

^aKinetic data obtained by measurement of UV absorbance at $\lambda = 382$ nm.

^bRate constant calculated from this data is $1.3 \times 10^{-4} \text{ s}^{-1}$.

Kinetic data^a for the dissociation of 155e (0.223 M) in CD₃COCD₃ in presence of TEMPO
(0.190 M) at 80°C (Best fit lines #6a & #6b, Fig.10)

Time	% 155e ^b		% 155e ^d	
t (min)	(A-x)	log{A ₀ /(A-x)} ^c	(A-x ₁)	log{A ₀ /(A-x ₁)} ^c
0	100	0.000	100	0.0000
15	95	0.022	99.4	0.0026
30	81	0.092	99.6	0.0017
60	77	0.114	98.2	0.0079
90	76	0.119	97.4	0.0114
120	67	0.173	97.2	0.0123
150	61	0.215	96.9	0.0136
180	44	0.357	95.9	0.0182
240	38	0.420	94.9	0.0230

^aKinetic data obtained by measurement of the nmr signal intensity of acetone (vide infra).

^bStarting material (initially 100%) remaining in solution at time t

^cThe pseudo-first-order rate constant calculated from this data is $6.56 \times 10^{-5} \text{ s}^{-1}$.

^dPercentage of the azocarinol (as starting material 155e and as the exchanged product 199) remaining in solution at time t. This is obtained by subtracting from the initial starting material (100%) the amount (mole %) of the radical adduct with TEMPO at time t.

^eRate constant calculated from this data is $3.63 \times 10^{-6} \text{ s}^{-1}$.

Kinetic data^a for the dissociation of **155e** (0.274 M) in CD₃COCD₃ in presence of TEMPO
(0.158 M) at 80°C (Best fit lines #7a & #7b, Fig.10)

Time	% 155e ^b		% 155e ^d	
t (min)	(A-x)	log{A ₀ /(A-x)} ^c	(A-x ₁)	log{A ₀ /(A-x ₁)} ^c
0	100	0.000	100	0.000
15	93	0.032	99.5	0.002
30	87	0.060	99.0	0.004
45	80	0.097	98.5	0.007
60	78	0.108	98.0	0.009
75	71	0.149	97.5	0.011
95	66	0.181	97.0	0.013
115	62	0.208	96.5	0.015
130	59	0.229	96.0	0.018
190	47	0.328	95.5	0.020
220	42	0.377	95.0	0.022
225	39	0.409	94.2	0.027

^aKinetic data obtained by measurement of the nmr signal intensity of acetone (vide infra).

^bStarting material (initially 100%) remaining in solution at time t

^cThe pseudo-first-order rate constant calculated from this data is $6.21 \times 10^{-5} \text{ s}^{-1}$.

^dPercentage of the azocarinol (as starting material **155e** and as the exchanged product **199**) remaining in solution at time t. This is obtained by subtracting from the initial starting material (100%) the amount (mole %) of the radical adduct with TEMPO at time t.

^eRate constant calculated from this data is $3.82 \times 10^{-6} \text{ s}^{-1}$.

Kinetic data^a for the dissociation of 155e (0.182 M) in CD₃COCD₃ in presence of TEMPO
(0.105 M) at 80°C (Best fit lines #8a & #8b,

Fig.10)

Time	% 155e ^b		% 155e ^d	
t (min)	(A-x)	$\log\{A_0/(A-x)\}^c$	(A-x ₁)	$\log\{A_0/(A-x_1)\}^c$
0	100	0.000	100	0.000
15	94	0.027	99.0	0.004
30	89	0.051	98.5	0.007
45	83	0.081	98.0	0.009
60	79	0.102	98.0	0.009
75	74	0.131	97.5	0.011
95	71	0.149	97.0	0.013
115	63	0.201	96.5	0.015
130	60	0.222	96.0	0.018
190	50	0.301	95.5	0.020
220	46	0.337	95.0	0.022
255	43	0.366	94.5	0.025

^aKinetic data obtained by measurement of the nmr signal intensity of acetone (vide infra).

^bStarting material (initially 100%) remaining in solution at time t

^cThe pseudo-first-order rate constant calculated from this data is $5.61 \times 10^{-5} \text{ s}^{-1}$.

^dPercentage of the azocarinols (see text for details) remaining in solution at time t. This is obtained by subtracting from the initial starting material (100%) the amount (mole %) of the radical adduct with TEMPO at time t.

^eRate constant calculated from this data is $3.36 \times 10^{-6} \text{ s}^{-1}$.

Kinetic data^a for the dissociation of **155e** (0.091 M) in CD₃COCD₃ in presence of TEMPO (0.053 M) at 80°C (Best fit lines #9a & #9b, Fig.10)

Time	% 155e ^b		% 155e ^d	
t (min)	(A-x)	log{A ₀ /(A-x)} ^c	(A-x ₁)	log{A ₀ /(A-x ₁)} ^c
0	100	0.000	100	0.000
15	91	0.041	99.0	0.004
30	86	0.065	98.5	0.007
45	83	0.081	97.5	0.011
60	76	0.119	97.0	0.013
75	74	0.131	97.0	0.013
95	66	0.180	96.0	0.018
115	64	0.194	95.5	0.020
130	61	0.215	95.5	0.020
190	51	0.292	94.5	0.025
220	47	0.328	94.5	0.025
255	43	0.367	93.5	0.029

^aKinetic data obtained by measurement of the nmr signal intensity of acetone (vide infra).

^bStarting material (initially 100%) remaining in solution at time t

^cThe pseudo-first-order rate constant calculated from this data is $5.38 \times 10^{-5} \text{ s}^{-1}$.

^dPercentage of the azocarinol (as starting material **155e** and as the exchanged product **199**) remaining in solution at time t. This is obtained by subtracting from the initial starting material (100%) the amount (mole %) of the radical adduct with TEMPO at time t.

^eRate constant calculated from this data is $4.00 \times 10^{-6} \text{ s}^{-1}$.

Kinetic data^a for the dissociation of **155e** (0.089 M) in CD₃COCD₃ in presence of TEMPO (0.059 M) and benzaldehyde (0.19 M) at 80°C (Best fit lines #10a & #10b, Fig.11)

Time	% 155e ^b		% 155e ^d	
t (min)	(A-x)	log{A ₀ /(A-x)} ^c	(A-x ₁)	log{A ₀ /(A-x ₁)} ^c
0	100	0.000	100	0.000
5	86	0.006	98.5	0.0066
30	79	0.102	97.5	0.0110
45	74	0.131	97.2	0.0123
60	69	0.161	94.7	0.0237
90	62	0.208	93.2	0.0306
120	51	0.292	90.5	0.0434
150	46	0.337	88.0	0.0555

^aKinetic data obtained by measurement of the nmr signal intensity of acetone (vide infra).

^bStarting material (initially 100%) remaining in solution at time t

^cThe pseudo-first-order rate constant calculated from this data is $8.21 \times 10^{-5} \text{ s}^{-1}$.

^dPercentage of the azocarinol (as starting material **155e** and as the exchanged product **199**) remaining in solution at time t. This is obtained by subtracting from the initial starting material (100%) the amount (mole %) of the radical adduct with TEMPO at time t.

^eRate constant calculated from this data is $1.39 \times 10^{-5} \text{ s}^{-1}$.

Kinetic data^a for the dissociation of 155e (0.077 M) in CD₃COCD₃ in presence of TEMPO (0.051 M) and benzaldehyde (1.39 M) at 80°C (Best fit lines #11a & #11b, Fig.11)

Time	% 155e ^b		% 155e ^d	
t (min)	(A-x)	$\log\{A_0/(A-x)\}^c$	(A-x ₁)	$\log\{A_0/(A-x_1)\}^c$
0	100	0.000	100	0.000
15	90	0.046	89	0.051
30	72	0.143	84	0.076
45	67	0.174	82.8	0.082
60	55	0.260	82.0	0.086
90	47	0.328	82.8	0.082
120	37	0.432	82.5	0.084

^aKinetic data obtained by measurement of the nmr signal intensity of acetone (vide infra).

^bStarting material (initially 100%) remaining in solution at time t

^cThe pseudo-first-order rate constant calculated from this data is $1.38 \times 10^{-4} \text{ s}^{-1}$.

^dPercentage of the azocarinol (as starting material 155e and as the exchanged product 199) remaining in solution at time t. This is obtained by subtracting from the initial starting material (100%) the amount (mole %) of the radical adduct with TEMPO at time t.

^eRate constant calculated from this data is $7.30 \times 10^{-5} \text{ s}^{-1}$.

Kinetic data^a for the dissociation of 155e (0.119 M) in CD₃COCD₃ in the absence of TEMPO and benzaldehyde (1.39 M) at 80°C (Best fit lines #11a & #11b, Fig.11)

Time	% 155e ^b		% 155e ^d	
t (min)	(A-x)	log{A ₀ /(A-x)} ^c	(A-x ₁)	log{A ₀ /(A-x ₁)} ^c
0	100	0.000	100	0.000
15	94	0.027	--	--
30	86	0.066	--	--
45	79	0.102	99.5	0.002
60	71	0.149	--	--
90	63	0.200	98.9	0.005
120	53	0.275	98.5	0.006
150	45	0.347	97.5	0.011

^aKinetic data obtained by measurement of the nmr signal intensity of acetone (vide infra).

^bStarting material (initially 100%) remaining in solution at time t

^cThe pseudo-first-order rate constant calculated from this data is $1.38 \times 10^{-4} \text{ s}^{-1}$.

^dPercentage of the azocarinol (as starting material 155e and as the exchanged product 199) remaining in solution at time t. This is obtained by subtracting from the initial starting material (100%) the amount (mole %) of the radical adduct with TEMPO at time t.

^eRate constant calculated from this data is $7.30 \times 10^{-5} \text{ s}^{-1}$.

Kinetic data for the disappearance of the esr signal intensity of TEMPO (0.046 M) in CD_3COCD_3 by thermal decomposition of 155e (0.068 M) in presence of benzaldehyde (0.47 M) at 80°C (Best fit line #13 in Fig.12)

Time	% TEMPO	Time	% TEMPO
0	100	60	71
15	94	90	63
30	86	120	53
45	79	150	45

Kinetic data for the disappearance of the esr signal intensity of TEMPO (0.042 M) in CD_3COCD_3 by thermal decomposition of 155e (0.062 M) in presence of benzaldehyde at 80°C (Best fit line #14 in

Fig.12)

Time	% TEMPO	Time	% TEMPO
0	100	26	22
5	84	30	15
10	69	35	9
15	53		

Kinetic data for the disappearance of the esr signal intensity of TEMPO (0.046 M) in CD_3COCD_3 by thermal decomposition of 155e (0.068 M) at 80°C (Best fit line #15 in Fig.12)

Time	% TEMPO	Time	% TEMPO
0	83	120	100
5	90	230	99
10	98	260	83

Kinetic data for the disappearance of the esr signal intensity of TEMPO (0.045 M) in CH_3CN by thermal decomposition of 155e (0.088 M) at 80°C (Best fit line #16 in Fig.12)

Time	% TEMPO	Time	% TEMPO
0	100	16	67
2	97	31	54
4	94	62	36
8	92	45	34
11	76	111	08

REFERENCES

1. (a) Gomberg, M. *J. Am. Chem. Soc.* **1900**, *22*, 757.; *Ber.* **1900**, *33*, 3150.
2. (a) Waters, W. A. *The Chemistry of Free Radicals*; Reinhold: New York, 1954. (b) Steacie, E. W. R. *Atomic and Free Radical Reactions*; Reinhold: New York, 1954. (c) Leffler, J. E. *The Reactive Intermediates of Organic Chemistry*; Interscience: New York, 1956. (d) Walling, C. *Free Radicals In Solution*; Wiley: New York, 1957. (e) Trotman-Dickenson, A. F. *Free Radicals*; Mathuen: London, 1959. (f) Stirling, C. J. M. *Radicals in Organic Chemistry*; Oldbourne: London, 1965. (g) Pryor, W. A. *Free Radicals*; McGraw-Hill: New York, 1966. (h) Forrester, A. R.; Hay, J. M.; Thomson, R. H. *Organic Chemistry of Stable Free Radicals*; Academic Press: London, 1968. (i) Huyser, E. S. *Free Radical Chain Reactions*; Wiley: New York, 1970. (j) Beckwith, A. L. J. in *Essays on Free Radical Chemistry*; Chem. Soc. Spec. Publ. No. 24, 1970. (k) *Free Radicals*; Kochi, J. K., Ed.; Wiley-Interscience: New York, 1973; Vol. I, II. (l) *Organic Free Radicals*; Pryor, W. A., Ed.; Symposium Series 69; *Am. Chem. Soc.*: Washington, D. C., 1978. (m) Davies, D. I.; Parrott, M. J. *Free Radicals in Organic Synthesis. Reactivity and Structure Concept in Organic Chemistry*, Vol. 7; Springer-Verlag: Berlin - Heidelberg, 1979. (n) Nonhebel, D. C.; Tedder, J. M.; Walton, J. C. *Radicals*; Cambridge University Press, 1979. (o) *Substituent Effects in Radical Chemistry*; Viehe, H. G., Janousek, Z., Merenyi, R., Eds.; Reidel: Dordrecht, 1986.
3. Gomberg, M.; Cone, L. H. *Ber.* **1906**, *39*, 3286.
4. Gomberg, M. *Chem. Rev.* **1925**, *1*, 91, and references therein.
5. (a) Goldschmidt, S.; Renn, K. *Ber.* **1922**, *55*, 628. (b) Goldschmidt, S; Graef, F. *Ber.* **1928**, *61*, 1858.
6. (a) Goldschmidt, S; Wolffhardt, E.; Drimmer, I.; Nathan, S. *Annalen* **1924**, *437*, 194. (b) Goldschmidt, S; Bader, J. *Annalen* **1929**, *473*, 137.
7. Paneth, F.; Hofeditz, W. *Ber.* **1929**, *62*, 1335.

8. Rice, F. O.; Herzfeld, K. F. *J. Am. Chem. Soc.* **1934**, *56*, 284.
9. Hey, D. H.; Waters, W. A. *Chem Rev.* **1937**, *21*, 169.
10. Kharasch, M. S.; Engelmann, H.; Mayo, F. R. *J. Org. Chem.* **1937**, *2*, 288.
12. Flory, P. J. *J. Am. Chem. Soc.* **1937**, *59*, 241.
13. For various examples see ref. 2(g); Chapter 5, and ref. 2(i); Chapter 1.
14. (a) Ref. 2(g); Chapter 7. (b) Griller, D.; Ingold, K.U. *Acc. Chem. Res.* **1980**, *13*, 193, 317.
15. (a) *Radical Reaction Rates in Liquids*; Fisher, H., Ed.; Springer Verlag: West Berlin. 1983-85; Landolt-Börnstein, New Ser., Vols. II/13a-e, and references cited therein. (b) Ingold, K. U. In ref. 2 (k), Vol. I, p 37.
16. Giese, B. In *Radicals in Organic Synthesis: Formation of Carbon-Carbon Bonds*; Baldwin, J. E. Ed.; Pergamon: Oxford, 1986, and references therein.
17. Giese, B. *Angew. Chem. Int. Ed., Engl.* **1985**, 553.
18. Hart, D. J. *Science* (Washington, D. C.) **1984**, *223*, 883.
19. Stork, G. In *Current Trends in Organic Synthesis*; Nozaki, H., Ed.; Pergamon: New York, 1983; p.359
20. (a) Bachi, M. D.; Frolow, F.; Hoornaert, C. *J. Org. Chem.* **1983**, *48*, 1841. (b) Bachi, M. D.; Bosch, E. *Tetrahedron Lett.* **1986**, *27*, 641.
21. Büchi, G.; Wüest, H. *J. Org. Chem.* **1979**, *44*, 546.
22. Bakuzis, P.; Campos, O. S.; Bakuzis, M. L. F. *J. Org. Chem.* **1979**, *44*, 546.
23. (a) Chuang, C. P.; Hart, D. J. *J. Org. Chem.* **1983**, *48*, 1782. (b) Burnett, D. A.; Choi, J. K. Hart, D. J.; Tsai, Y. M. *J. Am. Chem. Soc.* **1984**, *106*, 8201. (c) Hart, D. J.; Huang, H. C. *Tetrahedron Lett.* **1985**, *26*, 3746. (d) Choi, J. K.; Hart, D. J. *Tetrahedron* **1985**, *41*, 3959.
24. Stork, G.; Mook, R. *J. Am. Chem. Soc.* **1983**, *105*, 3721. (b) Stork, G.; Baine, N. H. *J. Am. Chem. Soc.* **1982**, *104*, 2321. (c) Stork, G.; Willird, P. G. *J. Am. Chem. Soc.* **1977**, *99*, 7067. (d) Stork, G.; Mook, R.; Biller, S. A.; Rychnovsky, S. D. *J. Am. Chem. Soc.*

- 1983, *105*, 3741. (e) Stork, G.; Baine, N. H. *Tetrahedron Lett.* 1985, *26*, 5927.
25. Beckwith, A. L. J.; Roberts, D. H.; Schiesser, C. H.; Wallner, A. *Tetrahedron Lett.* 1985, *26*, 3349.
 26. (a) Curran, D. P.; Rakiewicz, D. M. *Tetrahedron* 1985, *41*, 3943. (b) Curran, D. P.; Chen, M. H. *Tetrahedron Lett.* 1985, *26*, 4991 (c) Curran, D. P.; Kuo, S. C. *J. Am. Chem. Soc.* 1986, *108*, 1106.
 27. Ladlow, M.; Pattenden, G. *Tetrahedron Lett.* 1984, *25*, 4317.
 28. Leonard, W. R.; Livinghouse, T. *Tetrahedron Lett.* 1985, *26*, 6431.
 29. Corey, E. J.; Shih, C.; Shih, N. Y.; Shimoji, K. *Tetrahedron Lett.* 1984, *25*, 5013
 30. Ono, N.; Miyake, H.; Kamimura, A.; Hamamoto, I.; Tamura, R.; Kaji, A. *Tetrahedron* 1985, *41*, 4013.
 31. Beckwith, A. L. J.; Ingold, K. U. In "*Rearrangements in Ground and Excited States*"; deMayo, P., Ed.; Academic Press: New York, 1980; Vol.1, p 161.
 32. Surzur, J. M. In "*Reactive Intermediates*"; Abramovitch, R. A., Ed.; Plenum Press: New York, 1982; Vol.2, p 121.
 33. (a) Kerr, J. A.; Parsonage, M. J. *Evaluated Kinetic Data on Gas Phase Reactions*; Butterworths: London, 1976 and references therein. (b) "*Handbook of Bimolecular and Termolecular Gas Reactions*"; Kerr, J. A., Moss, S. J., Eds.; CRC: Boca Raton, 1981; Vol. I, II. (c) Ross, A. B.; Neta, P. *Rate Constants for Reactions of Aliphatic Radicals in Solution*; National Bureau of Standards; Washington, DC, 1952; NSRDS-NBS 70.
 34. Fischer, H. In ref. 2 (k), Vol. II; p 435
 35. Griller, D.; Ingold, K.U. *Acc. Chem. Res.* 1980, *13*, 317 and references therein.
 36. Fischer, H.; Paul, H. *Acc. Chem. Res.* 1987, *20*, 200 and references therein.
 37. Chemically induced dynamic nuclear polarization (CIDNP),³⁸ chemically induced dynamic electron polarization (CIDEP),³⁹ muon-spin rotation (μ SR) spectroscopy,⁴⁰ and electron spin resonance (esr) spectroscopy are the most commonly used

techniques.

38. For details, see (a) *Chemically Induced Magnetic Polarization*; Leply, A. R.; Closs, G. L., Eds.; Wiley: New York, 1973. (b) Ward, H. R. In ref 2k, p 239. (c) Kaptein, R. *Adv. Free Radical Chem.* 1975, 5, 319. (d) Closs, G. L.; Miller, R. J.; Redwine, O. D. *Acc. Chem Res.* 1985, 18, 196.
39. Fessenden, R. W.; Schuler, J. J. *Chem. Phys.* 1963, 39, 2147.
40. (a) Schenck, A. *Muon Spin Rotation Spectroscopy: Principles and Applications in Solid State Physics*; Hilger: London, 1985. (b) Roduner, E.; Fischer, H. *Chem. Phys.* 1981, 54, 261
41. For details of esr spectroscopy, see (a) Carrington, A. *Quart. Rev.* 1963, 17, 67. (b) Assenheim, H. M. *Introduction to Electron Spin Resonance*; Plenum: New York, 1967. (c) Wertz, J. E.; Bolton, J. R. *Electron Spin Resonance: Elementary Theory and Practical Applications*; McGraw-Hill: New York, 1972. (d) Kochi, J. K. *Adv. Free Radical Chem.* 1975, 5, 189.
42. (a) Livingston, R.; Zeldes, H. *J. Chem. Phys.* 1966, 44, 1245 (b) Kochi, J. K.; Krusic, P. J. In ref 2j, p 147.
43. (a) Norman, R. O. C.; West, P. R. *J. Chem Soc. (B)*, 1969, 389. (b) Norman, R. O. C. In ref 2j, p 117.
44. (a) Perkins, M. J. *Adv. Free Radical Chem.* 1980, 17, 1 and references therein. (b) Iwamura, M.; Inamoto, N. *Bull. Chem Soc. Jap.* 1967, 40, 702, 703. (c) Janzen, E. G. *Acc. Chem. Res.* 1971, 4, 31.
45. Bielski, B. H. J.; Gebicki, J. M. *Atlas of Electron Spin Resonance Spectra*; Academic Press: New York, 1967.
46. Surzur, J.-M. In *Reactive Intermediates*; Abramovitch, R. A., Ed.; Plenum: New York, 1982; Vol. 2, p 121.
47. Walling, C. In *Molecular Rearrangements*; de Mayo, P., Ed.; Wiley: New York, 1963; Part I, p 182.

48. Beckwith, A. L. J. In ref. 2j, p 239.
49. Beckwith, A. L. J.; Ingold, K. U. In *Rearrangements in Ground and Excited States*; Mayr, H. Ed.; Academic Press: New York, 1980; Chapter 4.
50. Wilt, J. W. In ref. 2k, Vol. I, p 418.
51. Beckwith, A. L. J. *Tetrahedron* **1981**, 3083.
52. Urry, W. H.; Kharasch, M. S. *J. Am. Chem. Soc.* **1944**, 66, 1438.
53. (a) Rüchardt, C. *Chem. Ber.* **1961**, 94, 2599. (b) Rüchardt, C.; Trautwein, H. *Chem. Ber.* **1965**, 98, 2478.
54. (a) Wilt, J. W.; Schneider, C. A. *J. Org. Chem.* **1961**, 26, 4196. (b) Wilt, J. W.; Phillips, B. H. *ibid.* **1960**, 25, 891. (c) Wilt, J. W.; Zawadzki, J. F.; Schultenover, D. G. *ibid.* **1966**, 31, 876.
55. Maillard, B.; Ingold, K. U. *J. Am. Chem. Soc.* **1976**, 98, 1244, 4692.
56. Brunton, G.; McBay, H. C.; Ingold, K. U. *J. Am. Chem. Soc.* **1977**, 99, 4447.
57. Beckwith, A. L. J.; Thomas, C. B. *J. Chem. Soc., Perkins II* **1973**, 861.
58. Poutsma, M. L.; Ibarbia, P. A. *Tetrahedron Lett.* **1972**, 3309.
59. Franz, J. A.; Burrows, R. D.; Camaioni, D. M. *J. Am. Chem. Soc.* **1984**, 106, 3964.
60. Johnston, L. J.; Luszyk, J.; Wayner, D. D. M.; Abeywickreyma, A. N.; Beckwith, A. L. J.; Scaiano, J. C.; Ingold, K. U. *J. Am. Chem. Soc.* **1985**, 107, 4594.
61. Lindsay, D. A.; Luszyk, J.; Ingold, K. U. *J. Am. Chem. Soc.* **1984**, 106, 7087.
62. Slauch, L. H. *J. Am. Chem. Soc.* **1959**, 81, 2262.
63. Bartlett, P. D.; Cotman, J. D. Jr. *J. Am. Chem. Soc.* **1950**, 72, 3095.
64. Curtin, D. Y.; Kauer, J. C. *J. Org. Chem.* **1960**, 25, 880.
65. Rüchardt, C.; Trautwein, H. *Chem. Ber.* **1965**, 98, 2478.
66. Ref. 49, p 172 and references therein.
67. Montgomery, L. K.; Matt, J. W. *J. Am. Chem. Soc.* **1967**, 89, 923.
68. Montgomery, L. K.; Matt, J. W. *J. Am. Chem. Soc.* **1967**, 89, 3050.
69. Montgomery, L. K.; Matt, J. W. *J. Am. Chem. Soc.* **1967**, 89, 6556.

70. Friedrich, E. C.; Holmstead, R. L. *J. Org. Chem.* **1971**, *36*, 971.
71. Friedrich, E. C.; Holmstead, R. L. *J. Org. Chem.* **1972**, *37*, 2550.
72. Friedrich, E. C.; Holmstead, R. L. *J. Org. Chem.* **1972**, *37*, 2546.
73. Effio, A.; Griller, D.; Ingold, K. U.; Beckwith, A. L. J.; Serelis, A. K. *J. Am. Chem. Soc.* **1980**, *102*, 1734.
74. Ingold, K. U.; Warkentin, J. *Can. J. Chem.* **1980**, *58*, 348.
75. Slaugh, L. H. *J. Am. Chem. Soc.* **1965**, *87*, 1522.
76. Halgren, T. A.; Howden, M. E. H.; Medof, M. E.; Roberts, J. D. *J. Am. Chem. Soc.* **1967**, *89*, 3051.
77. Nishinaga, A.; Nakamura, K.; Matsuura, T. *Tetrahedron Lett.* **1978**, 3557.
78. For comprehensive reviews see ref. 31, 32, 50, and 51.
79. Beckwith, A. L. J. *Tetrahedron* **1985**, *41*, 3941.
80. Kochi, J. K.; Bethea, T. W. *J. Org. Chem.* **1968**, *33*, 75.
81. (a) Lamb, R. C.; Ayers, P. W.; Toney, M. K. *J. Am. Chem. Soc.* **1963**, *85*, 3483. (b) Lamb, R. C.; Ayers, P. W.; Toney, M. K.; Garst, J. F. *J. Am. Chem. Soc.* **1966**, *88*, 4261.
82. Julia, M. *Acc. Chem. Res.* **1971**, *4*, 389 and references therein.
83. Julia, M. *Pure Appl. Chem.* **1974**, *40*, 553.
84. (a) Julia, M.; Maumy, M. *Bull. Soc. Chim. Fr.* **1969**, 2415, 2427. (b) Julia, M.; Maumy, M. *Bull. Soc. Chim. Fr.* **1968**, 1603.
85. Capon, B.; Rees, C. W. *Annual Reports.* **1964**, *61*, 261 .
86. Capon, B. *Quart. Rev.* **1964**, *18* , 45.
87. Beckwith, A. L. J.; Moad, G. J. *Chem. Comm.* **1974**, 472.
88. Struble, D. L.; Beckwith, A. L. J.; Green, G. E. *Tetrahedron Lett.* **1968**, 3701.
89. (a) Fumimcto, H.; Yamabe, S.; Minato, T.; Fukuji, K. *J. Am. Chem. Soc.* **1972**, *94*, 9205. (b) Dewar, M. J. S.; Olivella, S. *J. Am. Chem. Soc.* **1978**, *100*, 5291. (c) Hoyland, J. R. *Theor. Chim. Acta.* **1971**, *22*, 229.

90. Hamann, S. D.; Pompe, A.; Solomon, D. H.; Spurling, T. H. *Aust. J. Chem.* **1975**, *29*, 1975.
91. Walling, C.; Cioffari, A. *J. Am. Chem. Soc.* **1972**, *94*, 6059.
92. (a) Beckwith, A. L. J.; Blair, I. A.; Phillipou, G. *Tetrahedron Lett.* **1974**, 2251. (b) Beckwith, A. L. J.; Schiesser, C. H.; *Tetrahedron*. **1985**, *41*, 3925.
93. Julia, M.; Descoins, C.; Baillarge, M.; Jacquet, B.; Uguen, D.; Groeger, F.A. *Tetrahedron*. **1975**, *31*, 1737.
94. Beckwith, A. L. J.; Easton, C. J.; Serelis, A. K. *J. Chem. Soc. Chem. Commun.* **1980**, 482.
95. Shono, T.; Nishiguchi, I.; Ohmizu, H.; Mitani, M. *J. Am. Chem. Soc.* **1978**, *100*, 545.
96. (a) Beckwith A. L. J.; Serelis, A. K. *J. Am. Chem. Soc.* **1980**, *102*, 1734. (b) Beckwith, A. L. J.; *Tetrahedron* **1981**, *37*, 3073.
97. Beckwith, A. L. J.; Phillipou, G.; Serelis, A. K. *Tetrahedron Lett.* **1981**, 2811.
98. Surzur, J. M.; Bertrand, M. P.; Nougier, *Tetrahedron Lett.* **1969**, 4197.
99. Gilbert, B. C.; Holmer, R. G. G.; Laue, H. A. H.; Norman, R. O. C. *J. Chem. Soc. Perkin Trans. 2*. **1976**, 1047.
100. Nicolaou, K. C.; Gasic, G. P.; Barnette, W. E. *Angew. Chem., Int. Ed. Engl.* **1968**, *17*, 293.
101. Stella, L.; Tordo, L.; Surzur, J. M. *Tetrahedron Lett.* **1970**, 3107.
102. Maeda, Y.; Ingold, K. U. *J. Am. Chem. Soc.* **1980**, *102*, 328.
103. Surzur, J. M.; Crozet, M. P.; Dupey, C. *Tetrahedron Lett.* **1971**, 2035.
104. (a) Beckwith, A. L. J.; O'Shea, D. M.; Gerba, S.; Westwood, S. W. *J. Chem. Soc. Chem. Comm.* **1987**, 666. (b) Beckwith, A. L. J.; O'Shea, D. M.; Westwood, S. W. *J. Am. Chem. Soc.* **1988**, *110*, 2565.
105. Beckwith, A. L. J.; Wang, S. F.; Warkentin, J. *J. Am. Chem. Soc.* **1987**, *109*, 5289.
106. Schuster, D. I.; Roberts, J. D. *J. Org. Chem.* **1962**, *27*, 51.
107. Benson, S. W. *Thermochemical Kinetics*, 2nd Ed.; Wiley: New York, 1976.

108. Groves, J. T.; Ma, K. W. *J. Am. Chem. Soc.* **1974**, *96*, 6527.
109. Detty, M. R.; Paquette, L. H. *J. Org. Chem.* **1978**, *43*, 118.
110. Stein, S. E.; Rabinovich, B. S. *J. Phys. Chem.* **1975**, *79*, 191.
111. Walsh, R. *Int. J. Chem. Kinet.* **1970**, *2*, 71, 75.
112. Cordichi, D.; Balsi, R. D. *Can. J. Chem.* **1969**, *47*, 2601.
113. Itzel, H.; Fischer, H. *Helv. Chim. Acta.* **1976**, *59*, 880.
114. Dobbs, A. J.; Gilbert, B. C.; Laue, H. A. H.; Norman, R. O. C. *J. Chem. Soc. Perkin Trans. 2.* **1976**, 1044.
115. Kochi, J. K.; Krusic, P. J.; Eaton, D. R. *J. Am. Chem. Soc.* **1969**, *91*, 1877, 1879.
116. Maillard, B.; Forrest, D.; Ingold, K. U. *J. Am. Chem. Soc.* **1976**, *98*, 7024.
117. Danen, W. C. *J. Am. Chem. Soc.* **1972**, *94*, 4835.
118. Stock, L. M.; Young, P. E. *J. Am. Chem. Soc.* **1972**, *94*, 7686.
119. Effio, A.; Griller, D.; Ingold, K. U. *J. Am. Chem. Soc.* **1980**, *102*, 1734.
120. Newcomb, M.; Glenn, A. G.; Williams, W. G. *J. Org. Chem.* **1989**, *54*, 2675.
121. Beckwith, A. L. J.; Phillipou, G. *Aust. J. Chem.* **1976**, *29*, 123.
122. Davies, A. G.; Muggleton, B. *J. Chem. Soc. Perkin Trans. II.* **1976**, 502.
123. Danen, W. C.; West, C. T. *J. Am. Chem. Soc.* **1974**, *96*, 2447 and references therein.
124. (a) DePuy, C. H.; Jones, H. L.; Gibson, D. H. *J. Am. Chem. Soc.* **1968**, *90*, 5306. (b) *ibid*, **1972**, *94*, 3924.
125. Maeda, Y.; Ingold, K. U. *J. Am. Chem. Soc.* **1980**, *102*, 328.
126. Griller, D.; Ingold, K. U. *Acc. Chem. Res.* **1980**, *13*, 317.
127. Robinson, P. J.; Holbrook, K. A. *Unimolecular Radical Reactions*; Wiley: New York, **1972**; Chapter 7.
128. Griller, D.; Ingold, K. U. *Acc. Chem. Res.* **1980**, *13*, 193.
129. Adamic, K.; Bowman, D. F.; Gillan, T.; Ingold, K. U. *J. Am. Chem. Soc.* **1971**, *93*, 902.
130. Davies, A. G.; Griller, D.; Ingold, K. U. *Angew. Chem., Int. Ed. Engl.* **1971**, *10*, 738.

131. Calvert, J. G.; Pitts, J. N. *Photochemistry*; Wiley: New York, 1976; p 625-627.
132. For an example see: Lal, D.; Husband, S.; Ingold, K. U. *J. Am. Chem. Soc.* **1974**, *96*, 6355.
133. Schuh, H.; Fischer, H. *Int. J. Chem. Kinet.* **1976**, *8*, 341.
134. Carlsson, D. J.; Ingold, K. U. *J. Am. Chem. Soc.* **1968**, *90*, 7047.
135. Walling, C.; Cooley, J. H. Ponaras, A. A.; Racah, E. J. *J. Am. Chem. Soc.* **1966**, *88*, 5361.
136. Howard, J. A.; Tong, S. B. *Can. J. Chem.* **1979**, *57*, 2755.
137. Schmid, P.; Ingold, K. U. *J. Am. Chem. Soc.* **1978**, *100*, 2493.
138. Maeda, Y.; Schmid, P.; Ingold, K. U. *J. Chem. Soc. Chem. Comm.* **1978**, 525.
139. Jewell, D. R.; Mathew, L.; Warkentin, J. *Can. J. Chem.* **1987**, *65*, 311.
140. Lakhani, C.; Mathew, L.; Warkentin, J. *Can. J. Chem.* **1987**, *65*, 1748.
141. Lal, D.; Griller, D.; Husband, S.; Ingold, K. U. *J. Am. Chem. Soc.* **1974**, *96*, 6355.
142. Schmid, P.; Griller, D.; Ingold, K. U. *Int. J. Chem. Kinet.* **1979**, *11*, 333.
143. Chatgililoglu, C.; Ingold, K. U.; Scaiano, J. C. *J. Am. Chem. Soc.* **1981**, *103*, 7739.
144. Cristol, S. J.; Barbour, R. V. *J. Am. Chem. Soc.* **1968**, *90*, 2832.
145. Maillard, B.; Forrest, D.; Ingold, K. U. *J. Am. Chem. Soc.* **1976**, *98*, 7024.
146. For details see ref.147.
147. Mathew, L.; Warkentin, J. *J. Am. Chem. Soc.* **1986**, *108*, 7981.
148. Beckwith, A. L. J.; Bowry, V. W.; Moad, G. *J. Org. Chem.* **1988**, *53*, 1632.
149. Newcomb, M.; Glenn, A. G. *J. Am. Chem. Soc.* **1989**, *111*, 275.
150. Barton, D. H.; Crich, D.; Motherwell, W. B. *Tetrahedron* **1985**, *41*, 3901.
151. Ingold, K. U.; Luszyk, J.; Maillard, B.; Walton, J. C. *Tetrahedron Lett.* **1988**, *29*, 917.
152. Newcomb, M.; Park, S. -U. *J. Am. Chem. Soc.* **1986**, *108*, 4132.
153. Newcomb, M.; Glenn, A. G.; Williams, W. G. *J. Org. Chem.* **1989**, *54*, 2675.
154. Franz, J. A.; Bushaw, B. A.; Alnajjar, M. S. *J. Am. Chem. Soc.* **1989**, *111*, 268.

155. Beckwith, A. L. J.; Bowry, V. W. *J. Org. Chem.* 1989, 54, 2681.
156. For a comprehensive review see: Russell, G. A. In ref.2k; Chapter 7, and references cited therein.
157. Howard, J. A.; Ingold, K. U. *Can. J. Chem.* 1966, 44, 1119.
158. Burton, G. W.; Ingold, K. U. *Acc. Chem. Res.* 1986, 19, 194.
159. Danen, W. C.; Saunders, D. G. *J. Am. Chem. Soc.* 1969, 91, 5924.
160. Danen, W. C.; Winter, R. L. *J. Am. Chem. Soc.* 1971, 93, 716.
161. Benson, S. W. *Thermochemical Kinetics*; Wiley: New York, 1968; p 56.
162. Ingold, K. U. In ref.2k; p 69.
163. Evans, M. G.; Polanyi, M. *Trans. Faraday Soc.* 1938, 34, 11.
164. Semenov, N. N. *Some Problems in Chemical Kinetics and Reactivity*; Princeton University Press: New Jersey, 1958.
165. Benson, S. W.; DeMore, W. B. *Ann. Rev. Phys. Chem.* 1965, 16, 397.
166. Johnston, H. S. *Adv. Chem. Phys.* 1960, 3, 131.
167. Benson, S. W.; Bose, A. N. *J. Chem. Phys.* 1963, 39, 3463.
168. Zavitsas, A. A. *J. Am. Chem. Soc.* 1972, 94, 2779.
169. Morse, R. M. *Phys. Rev.* 1929, 34, 57.
170. Johnston, L. J.; Luszyk, J.; Wayner, D. D. M.; Abeywickreyma, A. N.; Beckwith, A. L. J.; Scaiano, J. C.; Ingold, K. U. *J. Am. Chem. Soc.* 1985, 107, 4594.
171. Edwards, F. G.; Mayo, F. R. *J. Am. Chem. Soc.* 1950, 72, 1265.
172. (a) Bridger, R. F; Russell, G. A. *J. Am. Chem. Soc.* 1964, 85, 3754. (b) Pryor, W. A.; Smith, K.; Echols, J. T. (Jr.); Fuller, J. L. *J. Org. Chem.* 1972, 36, 1753.
173. From Table 12-2 and Table 12-4 of ref.2i, and references therein.
174. Afanas'ev, I. B.; Mamontova, I. V. *J. Org. Chem. (USSR)*, 1971, 7, 691.
175. Afanas'ev, I. B.; Mamontova, I. V. ; Samokhvalov, G. I. *J. Org. Chem. (USSR)*, 1971, 7, 462.
176. Afanas'ev, I. B.; Safronenko, E. D. *J. Org. Chem. (USSR)*, 1971, 7, 457; Table 2.

177. For comprehensive reviews see: (a) ref. 2i; Chapter 4, 5. (b) ref. 156. (c) Poutsma, M. L. In ref. 2k; Vol. II, Chapter 15. (d) Howard, J. A. *Reviews of Chemical Intermediates* **1984**, *5*, 1.
178. Kharasch, M. S.; Gladstone, M. T. *J. Am. Chem. Soc.* **1943**, *65*, 15.
179. Hammett, L. P. *Chem. Rev.* **1935**, *17*, 125.
180. Pearson, R. E.; Martin, J. C. *J. Am. Chem. Soc.* **1963**, *85*, 3142.
181. Russell, G. A. *J. Org. Chem.* **1958**, *23*, 1407.
182. Russell, G. A.; Williamson, R. C. (Jr.) *J. Am. Chem. Soc.* **1964**, *86*, 2357.
183. Howard, J. A.; Ingold, K. U.; Symmonds, M. *Can. J. Chem.*, **1968**, *46*, 1017.
184. Sakurai, H.; Hosomi, A. *J. Am. Chem. Soc.* **1967**, *89*, 458.
185. Huyser, E. S. *J. Am. Chem. Soc.* **1960**, *82*, 392, 394.
186. For comprehensive reviews, see: (a) ref.2d. (b) ref.2i. (c) Abell, P. I. In ref.2k, p 63. (d) Giese, B. *Angew. Chem., Int. Ed. Engl.* **1983**, *22*, 753.
187. Starks, C. M. *Free Radical Telomerization*; Academic Press: New York, 1974.
188. Several examples can be seen in ref.186a-e, and references therein.
189. For a review on "The Factors Influencing Reactivity and Selectivity in Radical Substitution and Addition Reactions", see: Tedder, J. M. *Angew. Chem., Int. Ed. Engl.* **1982**, *21*, 401.
190. (a) Goering, H. L.; Abell, P. I.; Aycock, B. F. *J. Am. Chem. Soc.* **1952**, *74*, 3588. (b) Goering, H. L.; Larsen, D. W. *J. Am. Chem. Soc.* **1959**, *81*, 5937.
191. Skell, F. S.; Woodworth, R. C. *J. Am. Chem. Soc.* **1955**, *77*, 4638.
192. Cited in ref.2i, p201.
193. Kharasch, M. S.; Friedlander, H. N. *J. Org. Chem.* **1949**, *14*, 239.
194. Osborne, C. L.; Van Auken, T. V.; Trecker, D. J. *J. Am. Chem. Soc.* **1968**, *90*, 5806.
195. Trecker, D. J.; Henry, J. P. *J. Am. Chem. Soc.* **1963**, *85*, 3204.
196. Cristol, S. J.; Brindell, G. D.; Reeder, J. A. *J. Am. Chem. Soc.* **1958**, *80*, 635.
197. Dowbenko, R. *Tetrahedron* **1964**, *20*, 1843.

198. Traynham, J. G.; Hsieh, H. H. *J. Org. Chem.* **1973**, *38*, 868.
199. Janzen, E. G.; Evans, C. A. *J. Am. Chem. Soc.* **1973**, *95*, 8205.
200. Janzen, E. G.; Evans, C. A. *J. Am. Chem. Soc.* **1975**, *97*, 205.
201. Schmid, P.; Ingold, K. U. *J. Am. Chem. Soc.* **1977**, *99*, 6434.
202. Schmid, P.; Ingold, K. U. *J. Am. Chem. Soc.* **1978**, *100*, 2493.
203. Maeda, Y.; Ingold, K. U. *J. Am. Chem. Soc.* **1979**, *101*, 4975.
204. Kaur, H.; Perkins, M. J. *Can. J. Chem.* **1982**, *60*, 1587.
205. Osei-Twum, E. *Ph. D. Thesis*; McMaster University, 1985.
206. Gibian, M. J.; Corley, R. C. *Chem. Rev.* **1973**, *5*, 441.
207. North, A. M. *Quart. Rev. (London)* **1966**, *20*, 421.
208. McLaughlin, E. *Trans. Farad. Soc.* **1959**, *55*, 28.
209. Calvert, J.G.; Pitts, J. N. *Photochemistry*; Wiley: New York **1966**, p 625-629
210. Ingold, K. U. In ref.2k, p 39-40.
211. For several radical coupling reactions and their rate constants, see: (a) Ingold, K. U. In ref.2k, p 40-57 and leading references therein. (b) Watts, G. B.; Ingold, K. U. *J. Am. Chem. Soc.* **1972**, *94*, 491. (c) Weiner, S. A.; Hammond, G. S. *J. Am. Chem. Soc.* **1969**, *91*, 986. (d) Weiner, S. A. *J. Am. Chem. Soc.* **1972**, *94*, 581.
212. For a comprehensive survey of these rate constants, see: Ingold, K. U. In ref.15, Vol.13c, pp 181-200.
213. Chatgililoglu, C.; Ingold, K. U.; Scaiano, J. C. *J. Am. Chem. Soc.* **1981**, *103*, 7739.
214. Chateaneuf, J.; Lusztyk, J.; Ingold, K. U. *J. Org. Chem.* **1988**, *53*, 1629.
215. Huang, P. C.; Kosower, E. M. *J. Am. Chem. Soc.* **1968**, *90*, 2362.
216. (a) "*The Chemistry of Hydrazo, Azo, and Azoxy Groups*"; Patai, S. Ed.; Wiley: New York, 1975. (b) Meier, H.; Zeller, K. P. *Angew. Chem., Int. Ed. Engl.* **1977**, *16*, 835. (c) Engel, P. S. *Chem. Rev.* **1980**, *80*, 99.
217. Kosower, E. M.; Huang, P. C. *J. Am. Chem. Soc.* **1965**, *87*, 4646.
218. Widman, O. *Ber.* **1895**, *28*, 1925.

219. Chattaway, F. D. *J. Chem. Soc.* **1907**, 1323.
220. (a) Huang, P. C.; Kosower, E. M. *J. Am. Chem. Soc.* **1968**, *90*, 2354. (b) Huang, P. C.; Kosower, E. M. *J. Am. Chem. Soc.* **1968**, *90*, 2367. (c) Kosower, E. M.; Huang, P. C.; Tsuji, T. *J. Am. Chem. Soc.* **1969**, *91*, 2325.
221. (a) Huang, P. C.; Kosower, E. M. *J. Am. Chem. Soc.* **1967**, *89*, 3911. (b) Tsuji, T., Kosower, E. M. *J. Am. Chem. Soc.* **1971**, *93*, 1992.
222. (a) Tsuji, T., Kosower, E. M. *J. Am. Chem. Soc.* **1969**, *91*, 3375. (b) Tsuji, T., Kosower, E. M. *J. Am. Chem. Soc.* **1971**, *93*, 1999.
223. Smith, M. R.; Hillhouse, G. L. *J. Am. Chem. Soc.* **1988**, *110*, 4066.
224. Schmitz, E.; Ohme, R.; Schramm, S. *Angew. Chem., Int. Ed. Engl.* **1963**, *2*, 157.
225. (a) Freeman, J. P.; Rathjen, C. P. *Chem. Comm.* **1969**, 538. (b) Freeman, J. P.; Rathjen, C. P. *J. Org. Chem.* **1972**, *37*, 1686.
226. (a) Knittel, P.; Warkentin, J. *Can. J. Chem.* **1975**, *53*, 2275. (b) Knittel, P. Warkentin, J. *Can. J. Chem.* **1976**, *54*, 1341.
227. Hünig, S.; Büttner, G. *Angew. Chem., Int. Ed. Engl.* **1964**, *8*, 451.
228. Southwick, P. L.; Latif, N.; Klijanowicz, J.; O'Connor, J. G. *Tetrahedron Lett.* **1970**, 1767.
229. Hünig, S.; Cramer, J. *Angew. Chem., Int. Ed. Engl.* **1968**, *7*, 943.
230. (a) Yeung, D. W. K.; Warkentin, J. *Can. J. Chem.* **1976**, *54*, 1345, 1349. (b) *ibid* **1980**, *58*, 2386.
231. MacLeay, R. E.; *U. S. Patent*: 4,086,224; April 25, 1978.
232. Nazran, A. S.; Warkentin, J. *J. Am. Chem. Soc.* **1981**, *103*, 236.
233. Chang, Y. M.; Profetto, R.; Warkentin, J. *J. Am. Chem. Soc.* **1981**, *103*, 7189.
234. Yeung, D. W. K. *Ph.D. Thesis*; McMaster University, 1977.
235. (a) Büttner, G.; Hünig, S. *Chem. Ber.* **1971**, *104*, 1104. (b) Büttner, G.; Cramer, J.; Hünig, S. *Chem. Ber.* **1971**, *104*, 1118.
236. Schulz, M.; Missol, U. *Zeit. Chem.* **1974**, *14*, 265.

237. MacLeay, R. E.; Sheppard, C. S. *U. S. Patent*: 4,010,152; March 1, 1977.
238. Dixon, D. W.; Barbush, M. J. *Org. Chem.* **1985**, *50*, 3194.
239. (a) Landis, M. E.; Lindsey, R. L.; Watson, W. H. *J. Org. Chem.* **1980**, *45*, 525. (b) Baumstark, A. L.; Pilcher, R. S. *J. Org. Chem.* **1982**, *47*, 1141.
240. (a) For a review on several oxidation reactions using α -azohydroperoxides, see: Baumstark, A. L. *Bioorg. Chem.* **1986**, *14*, 326. (b) Baumstark, A. L.; Vasquez, P. C. *J. Org. Chem.* **1983**, *48*, 65.
241. (a) Tezuka, T.; Iwaki, M. *Tetrahedron Lett.* **1983**, *24*, 3109. (b) Tezuka, T.; Iwaki, M. *J. Chem. Soc. Perkin Trans. I*, **1984**, 2057.
242. Baumstark, A. L.; Vasquez, P. C. *J. Org. Chem.* **1987**, *52*, 1939 and references therein.
243. (a) Tezuka, T.; Narita, N.; Ando, W.; Oae, S. *J. Am. Chem. Soc.* **1981**, *103*, 3045. (b) Grant, R. D.; Rizzardo, E.; Solomon, D. H. *J. Chem. Soc. Perkin II*, **1985**, 379.
244. (a) Osei-Twum, E. Y.; McCallion, D.; Nazran, A. S.; Panicucci, R.; Risbood, P. A.; Warkentin, J. *J. Org. Chem.* **1984**, *49*, 336. (b) Osei-Twum, E. Y.; Warkentin, J. *J. Org. Chem.* **1985**, *50*, 4725.
245. Griffiths, P. G.; Moad, G.; Rizzardo, E.; Solomon, D. H.; *Aust. J. Chem.* **1983**, *36*, 397.
246. Heidenbluth, K.; Tonjes, H.; Scheffler, R. *J. Prakt. Chem.* **1965**, *30*, 204. (*Chem. Abstr.* **1966**, *64*, 8122f)
247. Currie, J.; Sidebottom, H.; Tedder, J. *Int. J. Chem. Kinet.* **1974**, *6*, 481.
248. Katz, M. G.; Horowitz, A.; Rajbach, L. A. *Int. J. Chem. Kinet.* **1975**, *7*, 183.
249. Matheson, I.; Tedder, J.; Sidebottom, H. *Int. J. Chem. Kinet.* **1983**, *15*, 905.
250. Frith, P. G.; McLauchlan, K. A. *J. Chem. Soc. Farad. Trans. II*, **1976**, *72*, 87.
251. Paul, H. *Int. J. Chem. Kinet.* **1979**, *11*, 511.
252. Macken, K. V.; Sidebottom, H. *Int. J. Chem. Kinet.* **1979**, *11*, 511.
253. Matheson, I.; Tedder, J.; Sidebottom, H. *Int. J. Chem. Kinet.* **1982**, *14*, 1037.

254. Lindsay, D. A.; Luszyk, K.; Ingold, K. *J. Am. Chem. Soc.* **1984**, *106*, 7087.
255. Hawari, J. A.; Davis, S.; Engel, P. S.; Gilbert, B. C.; Griller, D. *J. Am. Chem. Soc.* **1985**, *107*, 4721.
256. Kryger, R. G.; Lorand, J. P.; Steven, N. R.; Herron, N. R. *J. Am. Chem. Soc.* **1977**, *99*, 7589.
257. The reaction was photo-initiated.
258. Most of the work were done in collaboration with Jewell, D. R., who did most of the thermolysis experiments.
259. (a) Johnston, L. J.; Scaiano, J. C.; Ingold, K. U. *J. Am. Chem. Soc.* **1984**, *106*, 4877.
(b) Johnston, L. J.; Ingold, K. U. *J. Am. Chem. Soc.* **1986**, *108*, 2343.
260. A similar transition state has already been postulated²⁵⁵ for alkyl radical attacks on CCl_4
261. Mathew, L.; Warkentin, J. *Can. J. Chem.* **1988**, *66*, 11.
262. Dutsch, H. -R, Fischer, H. *Int. J. Chem. Kinet.* **1981**, *13*, 527.
263. Evans, F. W.; Fox, R. J.; Szwarc, M. *J. Am. Chem. Soc.* **1960**, *82*, 6414.
264. Based on the data used by Ingold, K. U. in ref.2k, Chapter 2.
265. Bunnett, J. F.; Wamser, C. C. *J. Am. Chem. Soc.* **1966**, *88*, 5534.
266. Correction for thermal expansion applied as mentioned in ref.147.
267. Ingold, K. U. in ref.2k, Chapter 2, Table 11 reported a value $2.3 \times 10^7 \text{ M}^{-1} \text{ s}^{-1}$ which resulted from a small arithmetical error. The relative rate constant k_I/k_H , where k_H is the rate constant for H-abstraction by methyl radical from toluene is 7560.²⁶⁴ Multiplying this number by the assumed value for $k_H = 3 \times 10^2$ at 65°C gives $k_I = 2.3 \times 10^6 \text{ M}^{-1} \text{ s}^{-1}$.
268. Cher, M.; Hollingsworth, C. S.; Scissilio, F. *J. Phys. Chem.* **1966**, *70*, 877.
269. Ref.2k, Table 6, p 74.
270. "Organic Synthesis", Coll. Vol.II; 1943, p 83.